VOL. 463 NO. 1 JANUARY 20, 1989

NAL OF HROMATOGRAPHY

RNATIONAL JOURNAL ON CHROMATOGRAPHY, ELECTROPHORESIS AND RELATED METHODS

ELSEVIER

JOURNAL OF CHROMATOGRAPHY

Scope. The *Journal of Chromatography* publishes papers on all aspects of chromatography, electrophoresis and related methods. Contributions consist mainly of research papers dealing with chromatographic theory, instrumental development and their applications. The section *Biomedical Applications*, which is under separate editorship, deals with the following aspects: developments in and applications of chromatographic and electrophoretic techniques related to clinical diagnosis or alterations during medical treatment; screening and profiling of body fluids or tissues with special reference to metabolic disorders; results from basic medical research with direct consequences in clinical practice; drug level monitoring and pharmacokinetic studies; clinical toxicology; analytical studies in occupational medicine.

Submission of Papers. Papers in English, French and German may be submitted, in three copies. Manuscripts should be submitted to: The Editor of *Journal of Chromatography*, P.O. Box 681, 1000 AR Amsterdam, The Netherlands, or to: The Editor of *Journal of Chromatography, Biomedical Applications*, P.O. Box 681, 1000 AR Amsterdam, The Netherlands. Review articles are invited or proposed by letter to the Editors. An outline of the proposed review should first be forwarded to the Editors for preliminary discussion prior to preparation. Submission of an article is understood to imply that the article is original and unpublished and is not being considered for publication elsewhere. For copyright regulations, see below.

Subscription Orders. Subscription orders should be sent to: Elsevier Science Publishers B.V., P.O. Box 211, 1000 AE Amsterdam, The Netherlands, Tel. 5803 911, Telex 18582 ESPA NL. The *Journal of Chromatography* and the *Biomedical Applications* section can be subscribed to separately.

Publication. The *Journal of Chromatography* (incl. *Biomedical Applications*) has 37 volumes in 1989. The subscription prices for 1989 are:

J. Chromatogr. + *Biomed. Appl.* (Vols. 461–497):
Dfl. 6475.00 plus Dfl. 999.00 (p.p.h.) (total *ca.* US$ 3933.75)

J. Chromatogr. only (Vols. 461–486):
Dfl. 5200.00 plus Dfl. 702.00 (p.p.h.) (total *ca.* US$ 3106.25)

Biomed. Appl. only (Vols. 487–497):
Dfl. 2200.00 plus Dfl. 297.00 (p.p.h.) (total *ca.* US$ 1314.25).

Our p.p.h. (postage, package and handling) charge includes surface delivery of all issues, except to subscribers in Argentina, Australia, Brasil, Canada, China, Hong Kong, India, Israel, Malaysia, Mexico, New Zealand, Pakistan, Singapore, South Africa, South Korea, Taiwan, Thailand and the U.S.A. who receive all issues by air delivery (S.A.L. — Surface Air Lifted) at no extra cost. For Japan, air delivery requires 50% additional charge; for all other countries airmail and S.A.L. charges are available upon request. Back volumes of the *Journal of Chromatography* (Vols. 1–460)are available at Dfl. 230.00 (plus postage). Claims for missing issues will be honoured, free of charge, within three months after publication of the issue. Customers in the U.S.A. and Canada wishing information on this and other Elsevier journals, please contact Journal Information Center, Elsevier Science Publishing Co. Inc., 655 Avenue of the Americas, New York, NY 10010. Tel. (212) 989-5800.

Abstracts/Contents Lists published in Analytical Abstracts, ASCA, Biochemical Abstracts, Biological Abstracts, Chemical Abstracts, Chemical Titles, Chromatography Abstracts, Current Contents/Physical, Chemical & Earth Sciences, Current Contents/Life Sciences, Deep-Sea Research/Part B: Oceanographic Literature Review, Excerpta Medica, Index Medicus, Mass Spectrometry Bulletin, PASCAL-CNRS, Referativnyi Zhurnal and Science Citation Index.

See inside back cover for Publication Schedule, Information for Authors and information on Advertisements.

0021-9673/89/$03.50

Printed in The Netherlands

CONTENTS

(Abstracts/Contents Lists published in Analytical Abstracts, ASCA, Biochemical Abstracts, Biological Abstracts, Chemical Abstracts, Chemical Titles, Chromatography Abstracts, Current Contents/Physical, Chemical & Earth Sciences, Current Contents/Life Sciences, Deep-Sea Research/Part B: Oceanographic Literature Review, Excerpta Medica, Index Medicus, Mass Spectrometry Bulletin, PASCAL-CNRS, Referativnyi Zhurnal and Science Citation Index)

(Continued overleaf)

Notes

In articles with more than one author, the name of the author to whom correspondence should be addressed is indicated in the article heading by a 6-pointed asterisk (*)

JOURNAL OF CHROMATOGRAPHY

VOL. 463 (1989)

JOURNAL *of* CHROMATOGRAPHY

INTERNATIONAL JOURNAL ON CHROMATOGRAPHY,
ELECTROPHORESIS AND RELATED METHODS

ELSEVIER
AMSTERDAM — OXFORD — NEW YORK — TOKYO

0021-9673/89/$03.50

Printed in The Netherlands

Journal of Chromatography, 463 (1989) 1–20
Elsevier Science Publishers B.V., Amsterdam — Printed in The Netherlands

CHROM. 21 026

ALGORITHMS TO CORRECT GRADIENT SCAN AND TRANSFER RULE PREDICTIONS OF ISOCRATIC RETENTION IN REVERSED-PHASE LIQUID CHROMATOGRAPHY

DAVE P. HERMAN, HUGO A. H. BILLIET* and LEO DE GALAN
Department of Analytical Chemistry, Delft University of Technology, de Vries van Heystplantsoen 2, 2628 RZ Delft (The Netherlands)
(First received March 8th, 1988; revised manuscript received September 7th, 1988)

SUMMARY

An efficient means of predicting solute retention in the three common binary eluents used in reversed-phase liquid chromatography is to pre-analyse the sample using an exploratory methanol–water gradient scan and thereafter calculate isoeluotropic acetonitrile–water and tetrahydrofuran–water compositions via a simple set of transfer rule equations. However, for some samples the single gradient scan and transfer rule equations fail to yield accurate estimates of k' values in these eluents. In this paper a procedure is described by which these occasionally errant initial predictions can be readily corrected by (1) combining the gradient scan data, T_r', with the first measured isocratic methanol–water retention data, k', and (2) combining the results of this extended gradient–isocratic procedure with a new, re-evaluated set of transfer rule equations. A step-by-step procedure is proposed by which these correction algorithms may be invoked in a logical manner to define rapidly the limits of the mobile phase search area in an eluent optimization procedure.

INTRODUCTION

Optimization of eluent composition is often the most time-consuming step in the analysis of complex mixtures by reversed-phase liquid chromatography. The four most commonly used selectivity-adjusting solvents for reversed-phase liquid chromatography are methanol, acetonitrile, tetrahydrofuran (THF) and, of course, water. The major steps involved in determining what combination of these four solvents (and in what relative concentrations) will best separate a specific mixture include defining a suitable range of mobile phase compositions over which to search for the eluent optimum, acquiring retention data adequately spanning the chosen range, analysing these data via one of several different methodologies and, finally, from this analysis, calculating the optimum mobile phase composition. In this paper we shall concentrate on the first step in this sequence. Specifically, we wish to discuss methods for rapidly and accurately predicting solute retention behaviour in binary eluents for the purpose of selecting starting conditions for eluent optimization in reversed-phase liquid chromatography.

0021-9673/89/$03.50

An increasingly accepted method for estimating the isocratic retention of any solute molecule in the three common binary eluents methanol–water, acetonitrile–water and THF–water is first to pre-analyse the sample using an exploratory methanol–water gradient scan. From measured retention times under gradient elution conditions, capacity factors (k') in methanol–water eluents under isocratic conditions can be estimated[1]. It is then up to the analyst to select that methanol–water composition which yields an adequate degree of retention for all sample components, *i.e.*, where the least and most retained solutes fall within an acceptable range (*e.g.*, $1 \leqslant k' \leqslant 10$). A means by which to select this k' range based on the component number and the polarity range of the mixture was described previously[2]. The acetonitrile–water and THF–water concentrations which are predicted to yield chromatograms exhibiting the same range of k' values, that is, which are predicted to be iso-eluotropic with the previously selected binary reference methanol–water composition, can be calculated using simple "transfer rule" equations[1]. A detailed description of the origin and utility of these gradient scan and transfer rule procedures are presented in the Theory and Results and Discussion sections.

Although the isocratic retention behaviour of many solutes can be accurately predicted from the gradient scan and transfer rule equations, for some solutes large deviations between predicted and experimentally measured k' values have been observed[3]. The purpose of this study was to determine the source(s) of these discrepancies, if and when they occur, and to develop a means by which these occasionally errant first predictions can be readily corrected in an efficient stepwise manner. Most important, from the analyst's point of view, the correction procedures were designed such that the number of additional required experiments is a minimum.

THEORY

Determination of isocratic retention from gradient elution scans

Theoretical models have been published that allow the interconversion of isocratic and gradient elution data for solutes subjected to linear gradients[4–6]. For those solutes exhibiting a linear relationship between $\ln k'$ and eluent volume fraction, φ, the following simple equations relate the gradient net retention time, T_r'(the retention time under gradient conditions minus the column void time), to isocratic and experimental parameters:

$$T_r' = 1/Sb \ln [1 + Sbt_0k'(\varphi_i)] \tag{1}$$

for $T_r' \leqslant T_G$, and

$$T_r' = k'(\varphi_f)t_0 + 1/Sb[k'(\varphi_f)/k'(\varphi_i) - 1] + T_G \tag{2}$$

for $T_r' > T_G$. In these equations, and in all equations to follow, S is the positive slope of the $\ln k'$ *vs.* φ plot, φ_i and φ_f designate the initial and final volume fractions of binary eluent during the gradient scan, T_G is the time of the gradient program, b is the rate of change of eluent composition with time $[(\varphi_f - \varphi_i)/T_G]$ and t_0 is the column void time. In most instances, all solutes will elute before the end of the gradient programme such that only eqn. 1 need be considered. Hence, if we experimentally determine the slope

and intercept of a solute's ln k' *vs.* φ plot, we can directly calculate via eqn. 1 or 2 the solute's retention time when subjected to a $\varphi_i \rightarrow \varphi_f$ linear gradient in T_G min.

The reverse process, in which one measures experimentally the gradient retention time and desires to predict isocratic retention from this single measurement, requires that we have some pre-knowledge of the relationship between the slope and the intercept of the solute's ln k' *vs.* φ plot. In the absence of this information we are confronted with the problem of trying to solve a single equation with two unknowns, namely, S and $k'(\varphi_i)$. Fortunately, in the methanol–water eluent system most solutes exhibit an approximately linear relationship between the slopes, S_m, and intercepts, ln k'_0, of their ln k' *vs.* φ_m plots[7,8]. From a study of the slope–intercept relationships for a large number of solutes representing many different functional groups, the following equation was derived[8]:

$$S_m = 2.86 + 0.77 \ln k'_0 \tag{3}$$

By substituting eqn. 3 into eqns. 1 and 2, we can derive a new set of equations where isocratic retention data *in the methanol–water eluent system* can be unambiguously predicted from gradient elution data:

$$T_r' = 1/S_m b \ln (1 + S_m b t_0 \exp\{[(1 - 0.77\varphi_i)S_m - 2.86]/0.77\}) \tag{4}$$

and

$$T_r' = t_0 \exp\{[(1 - 0.77\varphi_f)S_m - 2.86]/0.77 + T_G + 1/S_m b\,[\exp(S_m\varphi_i - S_m\varphi_f) - 1]\} \tag{5}$$

These equations are the basis of the method proposed by Schoenmakers *et al.*[1] for predicting isocratic retention from a *single* standard gradient scan. It should be recognized, however, that several implicit simplifying assumptions have been made in the derivation of the T_r'–S_m relationships expressed by eqns. 4 and 5. Several non-ideal processes (instrumental and chromatographic) which are unique to gradient elution chromatography can violate these assumptions and thereby lead to errors in calculated S_m values from gradient elution data. Quarry *et al.*[9,10] described the many non-ideal processes that may occur within the column or originate from the gradient equipment and, in some instances, they derived expressions to correct gradient elution data for these non-ideal effects. In this paper we shall concern ourselves only with those effects which have the potential to degrade the ability of eqns. 4 and 5 to predict isocratic retention behaviour from a preliminary gradient elution experiment. The major non-ideal processes which may occur are (in increasing order of importance):

(1) solvent demixing caused by preferential adsorption of methanol by the non-polar stationary phase;

(2) gradient delay as a result of the finite extra-column volume between the pump heads and the column inlet, which in turn causes pre-elution of solutes before the gradient has reached the top of the column;

(3) gradient profile distortion due to dispersion in gradient mixers, pulse dampers, connecting tubing, etc., which can cause the gradient programme to become non-linear;

(4) variations in flow-rate, F, (and therefore also t_0) owing to the volume loss incurred on mixing neat methanol and neat water during the course of the gradient;

(5) non-linearity of the solute's $\ln k'$–φ_m function over the range of eluent volume fractions scanned during the gradient;

(6) deviation of a specific solute from the linear slope *vs.* intercept relationship expressed by eqn. 3.

It should be noted that, of these potential error sources, only the last two are totally specific to the physical and chemical properties of the solute. The first four non-ideal processes, which are relatively small by comparison, can either be made negligible by proper selection of experimental conditions or can be completely eliminated using quantitative expressions to correct experimental T_r' values for the specific effect. We shall now briefly discuss each of these effects in turn.

In a detailed analysis of the solvent demixing effect, Quarry *et al.*[10] developed a model for the quantitative change in eluent volume fraction due to preferential uptake of methanol by the stationary phase. They concluded that the difference in actual φ_m from the ideal gradient profile value of φ_m, caused by solvent demixing, is proportional to s/V_G, where s is the total surface area of sorbent within the column and V_G is the gradient volume ($V_G = T_G F$). Clearly, relatively high flow-rates and long gradient times are desirable so as to minimize this effect. Fortunately, on a typical analytical reversed-phase liquid chromatography column with a total surface area of around 500 m^2, gradient volumes in excess of 20 ml will be sufficient to render this effect negligible.

Gradient delay will have a sizeable effect on observed T_r' values only for those chromatographic systems which have large extra-column volumes, $V_{p\rightarrow c}$, between the pump head(s) and the column inlet. Pre-elution of sample mixtures with $V_{p\rightarrow c}$ ml of eluent at fixed composition φ_i will cause the experimental T_r' values to be greater than those calculated by eqns. 4 and 5. One may correct for this effect by either employing a quantitative correction factor[4,9] or by delaying the injection of sample until the gradient arrives at the column inlet. We prefer the latter method owing to its ease of implementation and for the additional reasons discussed below with reference to gradient distortion effects.

In addition to the gradient delay effect, the finite and, in some instances, non-trivial pump-to-column extra-column volume, $V_{p\rightarrow c}$, can cause substantial distortions of the actual gradient profile that reaches the column inlet. The primary source of this gradient distortion is the gradient mixer. The most frequently observed distortion of a linear gradient programme is that in which the eluent composition at the column inlet varies linearly with time at compositions near the mid-point of the gradient programme, but deviates from linearity at the eluent extremes (*e.g.*, at $\varphi_m < 0.1$ and $\varphi_m > 0.9$ when performing a $\varphi_m = 0 \rightarrow 1$ linear gradient). The magnitudes of these deviations have been evaluated by Quarry *et al.* (see Table I in ref. 10) and shown to be proportional to V_M/V_G (V_M is the effective volume of the gradient mixer). From the tabulated data provided in that paper, we conclude that V_M/V_G must be less than 0.08 in order for an imposed linear gradient between $\varphi_m = 0$ and 1 to produce an eluent profile which is effectively linear ($\Delta\varphi_m < 0.005$) between $\varphi_m = 0.1$ and 0.95. A particularly simple, yet effective, means of eliminating gradient distortion is to perform a gradient scan of large V_G between 0 and 100% methanol and delay the injection of the sample until 10% methanol reaches the column inlet. In this manner,

most solutes will be eluted only during that part of the gradient which varies linearly with time. Thus, under these experimental conditions, the gradient linearity assumption implicit in eqns. 4 and 5 is obeyed.

The major source of variations in eluent flow-rate (and hence likewise t_0) during the course of a gradient scan is due to the non-ideal mixing behaviour of methanol–water mixtures. This is not the case for low-pressure gradient devices where the mobile phase is first mixed and then pumped. The volume loss incurred on mixing the two neat solvents varies with the mixing ratio, φ_m. The volume of a methanol–water mixture relative to the sum of the volumes of the two neat solvents (V_m/V^{neat}) is related to φ_m according to the empirical equation

$$V_m/V^{neat} = 0.130\varphi_m^3 - 0.059\varphi_m^2 - 0.071\varphi_m + 1 \quad (6)$$

From this equation we see that V_m/V^{neat} initially decreases with increasing φ_m, reaches a minimum of 0.964 at $\varphi_m = 0.6$ and thereafter increases until it reaches a value of 1 again at $\varphi_m = 1.0$. Hence, the mobile phase linear flow velocity can vary up to 3.6% during the course of a 0–100% methanol–water gradient experiment. Such relatively small deviations in linear flow velocity (and therefore also t_0) can in some instances cause large errors in estimated S_m values from preliminary gradient elution data. This is readily understood when one realizes that all of the gradient elution equations above ($T_r' = f\{S\}$) were derived assuming that t_0 remains constant. This effect therefore needs to be quantitatively accounted for if the derived gradient equations are to remain analytically valid. We correct the observed net retention times of each solute for the effects of varying flow-rate by substituting for t_0 in the gradient equations the following average void times:

$$\overline{t_0} = L/\overline{U} \quad (7)$$

where L is column length and $\bar{U}$ is the displacement weighted integrated average linear flow-rate of each solute, given by the expression

$$\bar{U} = \frac{\int_0^L u(z)/[1 + k'(z)]dz}{\int_0^L 1/[1 + k'(z)]dz} \quad (8)$$

where z is the relative displacement of the solute down the column and $k'(z)$ and $u(z)$ represent the capacity factor and the instantaneous linear flow-rate, respectively, at the moment the solute reaches position z in the column. In eqn. 8 $u(z)$ can be calculated as

$$u(z) = \frac{L}{t_0^{neat}}(C_1\varphi_p^3 + C_2\varphi_p^2 + C_3\varphi_p + C_4) \quad (9)$$

where C_1–C_4 are the regression coefficients given in eqn. 6, t_0^{neat} is the column void time at the flow-rates delivered by the pump(s) when pumping either neat methanol or neat water as eluent and φ_p is the volume fraction of eluent at the pump head. φ_p written as a function of z is given by

$$\varphi_p = \varphi_i + b\left\{1/S_m b \ln\left[1 + S_m b\left(\frac{z}{u_0^{neat}}\right)k'(\varphi_i)\right] + \frac{z}{u_0^{neat}}\right\} + b\tau_{p\rightarrow c} \quad (10)$$

where u_0^{neat} is simply L/t_0^{neat} and $\tau_{p\rightarrow c}$ is the pump-to-column delay time ($\tau_{p\rightarrow c} = V_{p\rightarrow c}/F$). Finally, we express k' as a function of z using the following equation:

$$k'(z) = \exp\left\{\ln(k_0') - S_m\varphi_i - \ln\left[1 + S_m b\left(\frac{z}{u_0^{neat}}\right)k'(\varphi_i)\right]\right\} \quad (11)$$

After substituting eqns. 8–11 into eqn. 7, we can calculate $\overline{t_0}$ by numerical integration. The variation in net retention time due to non-ideal mixing of methanol–water mixtures, $\Delta T_{r_{nim}}$, is thus equal to the difference in calculated T_r' values from eqn. 4 or 5, whichever is appropriate, using $t_0 = \overline{t_0}$ and $t_0 = t_0^{neat}$. $\Delta T_{r_{nim}}$ is a solute-dependent correction factor which is a measure of the extent to which non-ideal mixing causes eqns. 4 and 5 to underestimate T_r' when S_m is known, or overestimate S_m when T_r' is known. Having discussed the four instrumental sources for non-ideality, we now turn our attention to the two solute-dependent factors that may have a much greater influence.

Implicit in the mathematics of eqns. 4 and 5 is the assumption that isocratic $\ln k'$ values vary linearly with φ_m. Over a limited range of methanol–water compositions (specifically, those where $1 \leqslant k' \leqslant 10$), the $\ln k'$–φ_m function of most solutes is indeed linear. However, it is generally recognized that most solutes do exhibit some degree of $\ln k'$–φ_m curvature when considering the full range of eluent compositions under which they will probably elute during the course of a standard gradient scan. Under such conditions it may become necessary to express the functional dependence of $\ln k'$ on φ_m as a second-order polynomial of the form

$$\ln k' = a\varphi_m^2 + b\varphi_m + c \quad (12)$$

In order to evaluate the extent to which $\ln k'$–φ_m non-linearity affects the ability of eqns. 4 and 5 to predict T_r' when S_m is known (or predict S_m when T_r' is known), we have performed many computational gradient scans wherein the isocratic retention behaviour of 32 solutes was modelled according to eqn. 12. The retention data used for this purpose can be found in ref. 11. T_r' values were calculated by numerical integration for each of the 32 solutes under the assumed experimental conditions of $\varphi_i = 0.1$, $\varphi_f = 1.0$, $t_0 = 2.08$ min and $T_G = 30$ min. The same computational procedure was again performed after having fitted the experimental isocratic retention data between capacity factors of 1 and 10 to a first-order log-linear polynomial rather than eqn. 12 as was done above. The difference in corresponding calculated T_r' values ($\ln k'$ quadratic in φ_m rather than linear) were statistically evaluated and the average deviation in T_r' due to $\ln k'$ curvature, $\Delta T_{r_{curv}}$, was found to be 0.16 min ($\sigma = 0.076$). Thus, one

concludes that the average curvature of the ln k'–φ_m function of an "average" solute causes the retention times of gradient scan analysed solutes to be greater by 0.16 min than would be predicted from our gradient equations which assume log-linearity. As a first-order approximation, experimental gradient retention times can be corrected for non-log-linearity by simply subtracting 0.16 min from all experimentally determined T_r' values. By applying this "average" correction factor, all the gradient elution T_r'–S_m relationships listed above become statistically more valid. Furthermore, constraints on the isocratic k' values (between 1 and 10) and the newly defined "standard" gradient (see Results and discussion section) have a minimizing influence on the correction.

By far the largest source of error responsible for discrepancies between actual and calculated values of S_m via eqns. 4 and 5 is the assumption that the linear relationship between the slopes and intercepts of all ln k'–φ_m plots is rigorously described by eqn. 3 for *all* solutes. Inspection of the original 32 solute data set from which eqn. 3 was derived (see Fig. 3 in ref. 8) reveals that slopes and intercepts are not perfectly correlated, but rather are slightly scattered about the line of eqn. 3 with a correlation coefficient of 0.98. As a result, the uncertainty (standard deviation) in the intercept of the S_m–ln k_0' plot, σ_p, is fairly large ($\sigma_p = \sigma S_m = 0.34$). As will be shown later, for other solutes not among the original 32, the difference between the S_m values calculated via eqn. 3 and true actual values can be much larger ($\Delta S_m \gg 2\sigma_p$). In order to correct eqns. 4 and 5 for those solutes not following the slope–ln k_0' relationship of eqn. 3, we must replace the approximation of eqn. 3 with an exact relationship. By performing one methanol–water isocratic experiment and measuring k' for each of the mixture's j solutes, $k'_{meas,j}$, at volume fractions φ_{meas}, exact relationships between S_m and ln k_0' become known when these data are combined with information from the initial gradient run. They are

$$S_j = \ln k'_{0j}/\varphi_{meas} - \ln k'_{meas,j}/\varphi_{meas} \tag{13}$$

Substituting eqn. 13 (in lieu of eqn. 3) into eqns. 1 and 2 leads to the following equalities which accurately express the $T_r' - S_m$ relationship for *any* solute:

$$T_{r_j}' = 1/S_j b \ln [1 + S_j b t_0 \exp (\ln k'_{meas,j} + S_j \varphi_{meas} - S_j \varphi_i)] \tag{14}$$

$$T_{r_j}' = t_0 \exp (\ln k'_{meas,j} + S_j \varphi_{meas} - S_j \varphi_f) + 1/S_j b \exp (S_j \varphi_i - S_j \varphi_f - 1) + T_G \tag{15}$$

Eqns. 14 and 15 thus provide a means for accurately predicting isocratic S_m values (from which k'–φ_m functions are readily calculated) for any solute by combining the retention results of a linear gradient scan with those of a single isocratic experiment. Proof will be given in Table II.

Determination of iso-eluotropic binary eluents

After having selected the methanol–water eluotropic strength, φ_m^*, which produces a chromatogram in which all solutes of the mixture fall within a suitable range of k' values, there remains the problem of predicting retention in the two remaining binary eluents, acetonitrile–water and THF–water. Calculation of equivalent eluotropic strength (relative to φ_m^*) for these two binary modifiers can be

performed using the "solvent polarity scale" first described by Snyder[12]. All binary eluents with equivalent solvent polarity are to a first approximation assumed to be iso-eluotropic. The expression given by Snyder for calculating the solvent polarity index of a binary solvent mixture is

$$P'_{mix} = \varphi_A P'_A + \varphi_B P'_B \quad (16)$$

where φ_A and φ_B are the volume fractions of solvents A and B and P'_A and P'_B are the polarity index values of the pure solvents. P' values reported for neat water, methanol, acetonitrile and THF are 9.0, 6.6, 6.2 and 4.2, respectively.

An alternative approach for obtaining the compositions of iso-eluotropic binaries is that taken by Schoenmakers *et al.*[1]. Based on the detailed isocratic retention behaviour of a set of 32 solutes in all three binary eluents, transfer rule equations relating iso-eluotropic acetonitrile–water and THF–water volume fractions, φ_{ACN} and φ_{THF}, to specified binary reference methanol–water volume fractions, φ^*_m, were derived. They are as follows:

$$\varphi_{ACN} = 0.32\varphi^{*2}_m + 0.57\varphi^*_m \quad (17)$$

$$\varphi_{THF} = 0.66\varphi^*_m \quad (18)$$

Eqns. 17 and 18 represent an *average* of the eluent transfer behaviours of each of the solutes of the data set considered. The scatter about these average predicted values is fairly large such that large deviations between predicted and actual iso-eluotropic volume fractions are observed in practice. Therefore, these equations provide only a "first best guess" prediction of equivalent eluotropic strength among the three binary eluents. A re-evaluation of these transfer rule equations and a new algorithm for correcting these first predicted iso-eluotropic φ_{ACN} and φ_{THF} volume fractions if in error is described below.

EXPERIMENTAL

All gradient elution and isocratic experiments in Tables I and II were performed on equipment consisting of a Model 1090 liquid chromatograph, a 3392A integrator and a 100 × 2.1 mm I.D. Hypersil ODS (5 μm) analytical column, all from Hewlett-Packard (Waldbronn, F.R.G.).

The isocratic elution data in Table IV were collected on equipment from Waters Assoc. (Milford, MA, U.S.A.) and consisted of an M6000 pump, a Model 440 UV detector and a 100 × 8 mm I.D. Nova-Pak C_{18} Radial-Pak (5 μm) analytical column.

HPLC-grade methanol, acetonitrile and tetrahydrofuran were obtained from Rathburn (Walkerburn, U.K.). Distilled, deionized, organic-free water was prepared in-house using a Milli-Q water-purification system (Millipore, Molsheim, France).

RESULTS AND DISCUSSION

Rapid evaluation of isocratic retention behaviour using the combined gradient–isocratic method

A convenient way for estimating isocratic methanol–water retention behaviour is to run a "standard" gradient as proposed by Schoenmakers *et al.*[1] (*i.e.*, a 0 → 100% methanol linear gradient, T_G = 15 min, t_0 = 125 s). From the experimentally determined net retention time of each solute, an estimate of the slope (eqn. 4 or 5) and intercept (eqn. 3) of each solute's $\ln k'$–φ_m function is calculable; however, as described above, serious errors can be introduced.

Of the six non-ideal processes listed above, the first three may be effectively eliminated/minimized by simple adaptation of "standard" experimental conditions. We now recommend that the gradient time should be extended from T_G = 15 to 30 min. Solvent demixing and gradient distortion can be minimized in this way.

Errors in predicted isocratic retention behaviour (S_m and $\ln k_0$) can be further minimized by increasing the initial effective eluent composition of the gradient programme from φ_i = 0 to 0.1. In this way, the often very non-linear $\ln k'$–φ_m behaviour of many solutes at $\varphi_m < 0.1$ can be avoided.

We now recommend the following instrument settings as the new standard conditions for the preliminary gradient scan: 10 → 100% methanol linear gradient, T_G = 30 min, t_0 = 2 min; the sample injection is delayed until that moment when the volume fraction methanol–water at the column inlet equals 0.1. This injection delay time can be determined using an UV-active tracer.

In the Theory section we described how to correct gradient elution data for the non-ideal effects of varying flow-rate (eqns. 7–11), $\ln k'$–φ_m non-linearity (subtraction of 0.16 min from all experimental T_r' values) and non-perfectly correlated $\ln k'$–φ_m slopes and intercepts (eqns. 13–15). Hence from the preceding discussions one should reasonably conclude that isocratic retention behaviour can be accurately and unambiguously determined by performing at most two chromatographic experiments (one gradient scan followed by one isocratic run) after having applied all of the correction procedures described above. Unfortunately, some ambiguities remain such that the analyst may be required in some rare instances to perform a second isocratic experiment.

The reason for the potential failure of the combined gradient–isocratic method to predict isocratic retention behaviour becomes readily apparent if we plot T_r' as a function of S_m according to eqns. 14 and 15 for solutes exhibiting a wide range of hydrophobicities. For example, in Fig. 1 the relationship between T_r' and S_m is shown for a set of seven hypothetical solutes having isocratic $k'_{meas,j}$ values of 1, 2, 3, ..., 15 at φ_{meas} = 0.5 and analysed utilizing an effective 10 → 100% methanol linear gradient, T_G = 30 min, t_0 = 2.08 min.

These plots show that for solutes with intermediate k' values (3–7) the measured T_r' values can be nearly independent of S_m (between S_m = 7 and 20) and, in some instances, can even lead to two analytical solutions for S_m. Hence for some solutes a double value problem exists for which we are unable to determine which one of the two calculated roots correctly describes the slope of the $\ln k'$–φ_m function. Fortunately, this will not often be the case when using the combined gradient–isocratic procedure for the purpose of selecting starting conditions for eluent optimization.

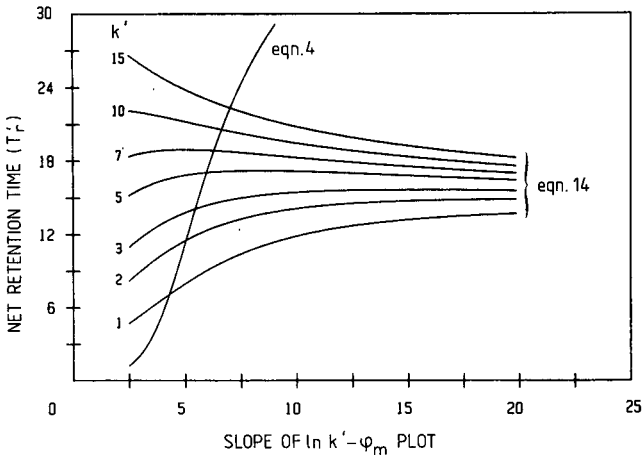

Fig. 1. Plots of gradient scan net retention time as a function of ln k'–φ_m slope according to eqns. 4 and 14 for seven hypothetical solutes exhibiting isocratic k' values of 1, 2, 3, ..., 15 at $\varphi_m = 0.5$. Assumed conditions: 0.1 → 1.0 linear methanol–water gradient in 30 min, $t_0 = 2.08$ min.

Also plotted in Fig. 1 is T_r' as a function of S_m according to eqns. 4 and 5 for those ideal solutes obeying the S_m–ln k'_0 linear relationship in eqn. 3. Unlike the case considered above where the S_m–ln k'_0 relationship is determined experimentally by performing a single isocratic experiment and S_m is calculated via eqn. 14 or 15, the eqn. 4 or 5 solution for S_m will be unique and independent of solute hydrophobicity at any measured T_r' value. Although eqns. 4 and 5 will always lead to unique solutions for S_m, the error in these calculated values can be unacceptably large owing to the inadequacy of the eqn. 3 approximation. An efficient and therefore recommended approach for accurately predicting the isocratic retention behaviour of the least and most retained solutes in a mixture is the following:

(1) perform the standard *effective* 10 → 100% methanol linear gradient scan and apply eqns. 3–5 to obtain a first estimate of isocratic retention behaviour (ln k'–φ_m);

(2) from the results of the preliminary gradient scan, select an eluent composition, φ_m, in which the k' values of the least and most retained solutes span a suitable range and perform an isocratic experiment at this volume fraction;

(3) combine the isocratic retention results of step 2 with the gradient scan retention results of step 1 and use eqns. 13–15 to determine accurately the ln k'–φ_m function of these two limiting solutes. From these functions, choose a suitable binary reference methanol–water composition, φ_m^*. If a double value solution for S_m is found, a second isocratic experiment must be run so as to allow S_m to be determined unambiguously.

In order to demonstrate the ability of the combined gradient–isocratic method to predict accurately the isocratic retention behaviour for solutes known to deviate strongly from the idealized S_m–ln k'_0 relationship of eqn. 3, a six-component mixture was subjected to a 9.3 → 100% methanol–water linear gradient, $T_G = 30.27$ min, $t_0 = 2.03$ min. The absolute retention times of all solutes were recorded and are given

TABLE I

DATA DERIVED FROM THE STANDARD GRADIENT AND THE FIRST ISOCRATIC BINARY METHANOL–WATER COMPOSITION OF SIX SOLUTES

Gradient conditions: 9.3 to 100% methanol in 30.27 min, t_0^{neat} = 2.03 min, $\tau_{p\to c}$ = 0.61.

No.	*Solute*	*Gradient scan data*				*Isocratic data:* k'_{meas} *(*φ_m *= 0.48)*
		T_r	T_r' $(T_r - t_0^{neat})$	$T_r' - \Delta T_{r_{curv}}$	$T_r' - \Delta T_{r_{curv}} - \Delta T_{r_{nim}}$	
1	Benzaldehyde	12.54	10.51	10.35	10.16	1.37
2	Benzyl alcohol	15.19	13.16	13.00	12.79	2.22
3	*m*-Dinitrobenzene	16.54	14.51	14.35	14.12	3.06
4	Dimethyl phthalate	17.36	15.33	15.17	14.93	3.12
5	Prednisone	19.03	17.00	16.84	16.60	5.26
6	Hydrocortisone	20.14	18.11	17.95	17.76	7.62

in the first data column of Table I. The last three data columns list the uncorrected net retention times ($T_r - t_0^{neat}$), net retention times corrected for ln k'–φ_m curvature ($\Delta T_{r_{curv}}$) and net retention times corrected for the effect of flow-rate variation due to non-ideal mixing of methanol and water ($\Delta T_{r_{nim}}$), respectively. The calculation of uncorrected net retention times and retention times corrected for ln k'–φ_m curvature are straightforward and simply require subtracting t_0^{neat} and 0.16 min, respectively, from all absolute retention time values. However, calculation of the correction factors $\Delta T_{r_{nim}}$ is more complex because of the need to know the S_m and $k'(\varphi_i)$ values for each individual solute in advance (see eqns. 10 and 11). As a first estimate of these values, one can use the eqn. 3–5 solution for S_m and ln k'_0 where the initial corrected net retention time used in the calculation is $T_r' - \Delta T_{r_{curv}}$. The additional correction term $\Delta T_{r_{nim}}$ can then be calculated using eqns. 7–11 and the procedure repeated until $\Delta T_{r_{nim}}$ converges to a constant value. In practice, it is found that only one iteration is required. As can be seen from the data in Table I, $\Delta T_{r_{nim}}$ values are solute dependent, and for the solutes studied vary between 0.19 and 0.24 min. From this single gradient scan, an isocratic eluent of 48% methanol in water was predicted from eqns. 3 and 4 to yield a chromatogram in which the k' values of the least and most retained solutes span a suitable range, specifically k' = 1–10. The k' values actually found for this isocratic run are listed in the last data column in Table I. Ultimately, of course, these single isocratic k' values allow us to use the combined gradient–isocratic procedure (eqns. 13–15) to verify or improve our estimates of $S_{m,j}$ and ln $(k'_0)_j$.

Fig. 2 shows plots of gradient scan net retention times as a function of S_m (eqn. 14) for the six solutes listed in Table I. Also plotted is T_r' as a function of S_m using the approximation relationship of eqn. 4. The dashed lines represent the T_r'–S_m function for solutes for which the S_m–ln k'_0 relationship is given not by eqn. 3 but rather by $S_m = 2.86 + 0.77\ln k'_0 \pm 2\sigma_p$, where $\sigma_p = 0.34$ is the scatter about the eqn. 3 line observed by Schoenmakers *et al.*[8]. The area between the two dashed lines therefore represents the 95% confidence interval range of potential S_m values for any solute which exhibits a gradient scan net retention time of T_r'. The dotted points in Fig. 2 are the points at which corrected T_r' values ($T_r' - \Delta T_{r_{curv}} - \Delta T_{r_{nim}}$) intersect the corresponding T_r'–S_m curve for each of the six solutes. Except for solute 3, we see that

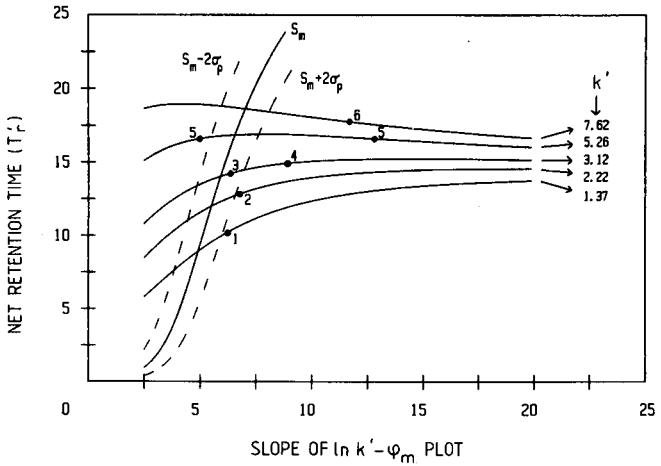

Fig. 2. As Fig. 1, except that T_r' *versus* S_m plots were generated for the six real solutes listed in Table I whose isocratic k' values at $\varphi_m = 0.48$ were measured to be 1.37, 2.22, 3.06, 3.12, 5.26 and 7.62, respectively. Points 1–6 indicate the location where the experimentally determined gradient scan T_r' values (corrected) intersect the T_r'–S_m plot for each solute. For an explanation of the dashed lines at $S_m \pm 2\sigma_p$, see the text. Gradient scan conditions: 0.093 → 1.0 linear methanol–water gradient in 30.27 min, $t_0 = 2.03$ min. Column: 100 × 2.1 mm I.D. Hypersil ODS (5 μm).

all S_m values calculated via eqn. 14 fall outside this 95% confidence interval range. We should warn the reader at this point that the retention behaviour of these particular solutes is not typical, but rather we have deliberately selected these solutes because of their non-ideal behaviour with respect to the correlation between the slopes and intercepts of their ln k'–φ_m plots. These solutes thus serve well to demonstrate the extent to which the combined gradient–isocratic procedure can correct errant first predictions of isocratic retention behaviour obtained via the single gradient scan approach.

Table II gives the S_m values calculated via the original gradient scan procedure

TABLE II

DETERMINATION OF LN k'–φ_m SLOPES FOLLOWING THE SINGLE GRADIENT SCAN AND THE COMBINED GRADIENT SCAN–ISOCRATIC ALGORITHMS

Experimental conditions: 9.3 to 100% methanol in water in 30.27 min, $t_0^{meat} = 2.03$ min.

Solute	*Slope calculated via original gradient scan procedure (WOC)**	*Slope calculated via original gradient scan procedure (WC)**	*Slope calculated via gradient–isocratic procedure (WC)**	*Experimentally determined slope from many isocratic experiments*
Benzaldehyde	5.22	5.15	6.14	6.45
Benzyl alcohol	5.74	5.66	6.65	7.03
m-Dinitrobenzene	6.02	5.94	6.26	6.56
Dimethyl phthalate	6.20	6.11	8.79	9.57
Prednisone	6.60	6.50	4.90, 12.77	12.09
Hydrocortisone	6.88	6.78	11.56	12.20

* WC and WOC designate *W*ith and *W*ith*O*ut *C*orrecting gradient scan retention times for the effects of ln k' curvature ($\Delta T_{r_{curv}}$) and non-ideal methanol–water mixing ($\Delta T_{r_{mix}}$).

(eqn. 4) and via the combined gradient–isocratic procedure (eqn. 14). In addition, a separate and independent set of isocratic experiments were performed in order to determine exact S_m values for each of the six solutes studied. These exact values, with which all other calculated S_m values should be compared, are given in the fourth data column in Table II. The first two columns list the S_m values calculated from eqn. 4 using uncorrected net retention times ($T_r - t_0^{neat}$) and using corrected T_r' values ($T_r - \Delta T_{r_{curv}} - \Delta T_{r_{nim}}$), respectively. Except for solute 3 (*m*-dinitrobenzene), in both instances large discrepancies between calculated and true values are observed (compare columns 1 and 2 with column 4). On the other hand, S_m values determined via the combined gradient–isocratic procedure with T_r' correction (column 3) are seen to be in much more reasonable agreement with the true values listed in column 4. A single anomaly occurs in the case of solute 5 (prednisone). As can be seen in Fig. 2, for this particular solute two analytical solutions of S_m are found from eqn. 14. In this single instance, a second isocratic experiment would be needed in order to determine which of the two solutions is indeed correct.

The major conclusion to be drawn from these experimental data is that by combining the results of the first isocratic experiment with the retention data of the preliminary gradient scan, greatly improved estimates of isocratic retention behaviour (S_m and $\ln k_0'$) are indeed obtained relative to the single gradient scan procedure first proposed by Schoenmakers *et al.*[1] for those solutes not closely adhering to the slope–intercept relationship of eqn. 3. An accurate determination of these values is the critical first step in selecting the three limiting iso-eluotropic binary eluent compositions, methanol–water, acetonitrile–water and THF–water, which will serve to define the limits of the parameter space searched during the course of either a ternary or quaternary eluent optimization procedure.

Accurate determination of iso-eluotropic compositions by extension/modification of the existing transfer rule equations

For many solutes, the transfer rule eqns. 17 and 18 fail to yield sufficiently accurate predictions of the acetonitrile–water and THF–water compositions having the same overall retention as a specified binary reference methanol–water eluent[3]. This result is not surprising when one realizes that these transfer rule equations were derived by comparing the retention behaviour of a limited set of 32 *non-structurally related* solutes in each of the three binary eluent systems[1]. Specifically, the transfer rule equations were derived by fitting the retention data of each solute in each eluent system to a log-quadratic function of the form of eqn. 12. From these quadratic equations iso-eluotropic eluents were calculated at all binary reference methanol–water compositions for each solute of the data set. A plot of iso-eluotropic φ_{THF} *versus* φ_m^* calculated in this manner is shown in Fig. 3A, where each curve represents one of the 32 solutes. Transfer rule eqn. 18 was obtained by fitting the best straight line with zero intercept through the data. The intercept of these plots must be exactly zero because the origin in the plot represents 100% water in both eluent systems considered.

Of particular concern is the observation that the curves in Fig. 3A are highly scattered such that errors in iso-eluotropic THF–water compositions predicted by eqn. 18 will be substantial and are likely to occur often. More important, at least for the discussion to follow, is the observation that virtually none of the solutes exhibit φ_{THF} *versus* φ_m^* curves tending towards the origin. For this reason, we decided to re-evaluate

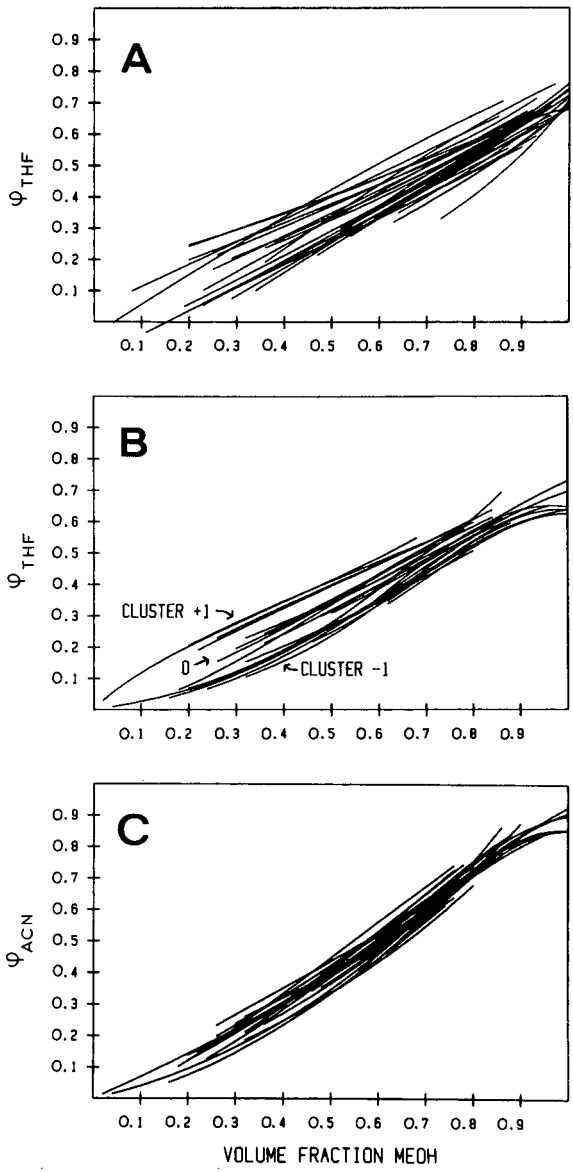

Fig. 3. Plots of iso-eluotropic THF–water and acetonitrile–water volume fractions relative to binary reference methanol–water compositions for the 32 solutes listed in ref. 1. Plot A (for THF) was obtained following the procedure in ref. 1 where all isocratic k'–φ data were fitted to eqn. 12. Plots B (THF) and C (acetonitrile) were derived making use of eqn. 19.

the retention data by forcing the ln k'–φ_{eluent} data for each solute to come to a common intercept at 100% water for each of the three eluent systems *prior* to calculating iso-eluotropic compositions rather than *after* calculating these compositions as done previously. For example, Fig. 4 shows ln k'–φ_{eluent} experimental data for dimethyl

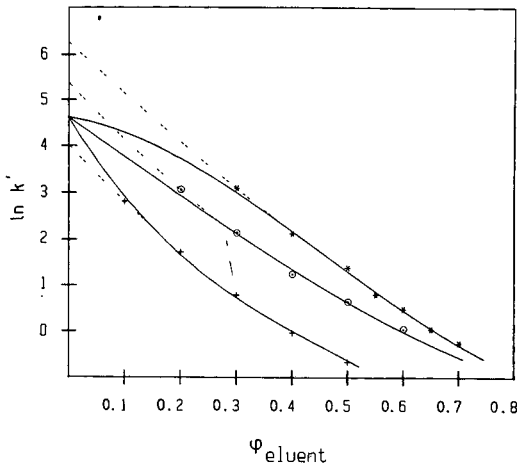

Fig. 4. Dependence of ln k' for dimethyl phthalate on eluent composition in the three binary eluents methanol–water (*), acetonitrile–water (⊙) and THF–water (+). The dashed lines were obtained by regression fitting of eqn. 12. The solid curves were obtained by regression fitting of eqn. 19 where the intercept at $\varphi_{\text{eluent}} = 0$ is forced to be in common. Column: 100 × 8 mm I.D. Nova-Pak C_{18}, Radial-Pak (5 μm).

phthalate in the three binary eluents. Also plotted are quadratic regression equations (eqn. 12) fitted independently to the experimental data of each eluent and third-order log-linear polynomial equations of the form

$$\ln k' = a\varphi^3_{\text{eluent}} + b\varphi^2_{\text{eluent}} + c\varphi_{\text{eluent}} + d \tag{19}$$

which have also been fitted to the experimental data but where all three regression equations are forced to come to a common intercept at $\varphi_{\text{eluent}} = 0$; the value of d in eqn. 19 is the same for all three modifiers but different if only quadratic fittings were used. It is clear that quadratic log-linear polynomials are not sufficiently flexible to describe adequately solute retention at eluent compositions near $\varphi_{\text{eluent}} = 0.0$. Therefore, we chose to fit the ln k' data for each solute of the original data set to eqn. 19 by an iterative multilinear least-squares method and from these equations to calculate iso-eluotropic THF–water and methanol–water volume fractions. Plots of φ_{THF} *versus* φ^*_{m} evaluated in this slightly different manner are given in Fig. 3B. Although these curves exhibit a great deal of scatter about a central tendency, the data indicate that real solutes tend to cluster into one of three groups for which the intra-group scatter is significantly lower. The clustering has no relation to molecular functional groups. Therefore, rather than attempt to represent all of the data with a single transfer rule equation, we have fitted a simple third-order polynomial with zero intercept through each of the three data clusters in Fig. 3B. The fitting function was of the form

$$\varphi_x = a\varphi^{*3}_{\text{m}} + b\varphi^{*2}_{\text{m}} + c\varphi^*_{\text{m}} \tag{20}$$

where x can represent either THF or ACN. The coefficients a, b and c for each of the three data clusters indicated in Fig. 3B are given in Table III. For a totally unknown

TABLE III

COEFFICIENTS OF THE NEW EMPIRICAL TRANSFER RULE EQUATIONS (SEE EQN. 20) RELATING ISO-ELUOTROPIC ACETONITRILE–WATER AND THF–WATER BINARY ELUENTS TO USER-SPECIFIED BINARY REFERENCE METHANOL–WATER ELUENT COMPOSITIONS

Eluent	*Cluster*	*a*	*b*	*c*
THF–water	0	−0.420	0.702	0.423
	+1	0.574	−0.906	1.118
	−1	−0.906	1.597	−0.036
Acetonitrile–water	0σ	−0.490	0.953	0.447
	+4σ	−0.568	0.799	0.751
	−4σ	−0.412	1.108	0.143

solute we have no way of predicting in advance into which of the three clusters its φ_{THF} *versus* φ^*_m function will fall. For this reason we have no choice but to choose the central cluster (cluster 0) as the first best estimate of the iso-eluotropic THF–water volume fraction. Thus, we now propose the use of

$$\varphi_{THF} = -0.420\varphi^{*3}_m + 0.702\varphi^{*2}_m + 0.423\varphi^*_m \quad (21)$$

as the new transfer rule equation in place of eqn. 18.

A similar re-evaluation of the transfer rule equation relating acetonitrile–water to methanol–water was carried out in a similar manner and the iso-eluotropic φ_{ACN} *versus* φ^*_m curves are plotted in Fig. 3C. For this eluent system pair no obvious clustering of solute type is observed. In view of this more ideal transfer behaviour, a single third-order polynomial of the form of eqn. 20 was fitted through all of the data. The coefficients *a*, *b* and *c* are also reported in Table III (refer to the 0σ values). Therefore, we now propose that eqn. 22 be used in place of eqn. 17 for calculating iso-eluotropic acetonitrile–water compositions:

$$\varphi_{ACN} = -0.490\varphi^{*3}_m + 0.953\varphi^{*2}_m + 0.447\varphi^*_m \quad (22)$$

Also reported in Table III are the coefficients of the regression equations (eqn. 20) fitted through the data points φ^*_m, $\varphi_{ACN}+4\sigma$ and φ^*_m, $\varphi_{ACN}-4\sigma$, where σ is the standard deviation in φ_{ACN} at each φ^*_m value. In the discussion to follow, the transfer behaviour of solutes between acetonitrile–water and methanol–water will be treated as if real solutes distributed themselves among three data clusters, *i.e.*, between 0σ, +4σ and −4σ. We justify the creation of two "artificial" data clusters at +4σ and −4σ based on the following reasoning. First is the observation that a few solutes have recently been found (not part of the original 32 solute data set) which exhibit both positive and negative deviations in φ_{ACN} which fall outside the 99.9 confidence interval range of values represented in Fig. 3C (*i.e.*, at values greater than $\pm 3.7\sigma$). Also, because of the requirement that all φ_{ACN} *versus* φ^*_m plots must pass through the origin, solutes whose true iso-eluotropic φ_{ACN} values differ significantly in the positive (negative) sense from eqn. 22 will have φ_{ACN} *versus* φ^*_m plots whose instantaneous

slopes, $d\varphi_{ACN}/d\varphi^*_m$, are substantially larger (smaller) than those calculated from eqn. 22. The importance of the derivative functions $d\varphi_{THF}/d\varphi^*_m$ and $d\varphi_{ACN}/d\varphi^*_m$ will become clear shortly.

We now address the problem of how to correct eqns. 21 and 22 if and when they fail to predict correctly, within acceptable error limits, iso-eluotropic THF–water and acetonitrile–water volume fractions relative to a specified binary reference methanol–water composition. Specifically, we wish to know how much to change the eluent composition, φ_x, predicted by eqn. 21 or 22 if a specific experimentally determined capacity factor, k'_x, in eluent φ_x differs significantly from its capacity factor, k'^*_m, in the binary reference methanol–water eluent, φ^*_m. To calculate the change in φ_x required to shift k'_x to the desired value k'^*_m, we simply multiply the change in methanol–water composition required to shift k'_x to k'^*_m [given by $(\ln k'_x - \ln k'^*_m)/S_m$] by the derivative function $d\varphi_x/d\varphi^*_m$ evaluated at φ^*_m. Therefore, to a good first approximation, by combining the isocratic retention data of the first acetonitrile–water or THF–water chromatogram with gradient scan determined values of S_m, φ^*_m, and k'^*_m in the methanol–water eluent system, a more accurate prediction of iso-eluotropic eluent, φ'_x, can be calculated according to the equation

$$\varphi'_x = \varphi_x + d\varphi_x/d\varphi^*_m(\ln k'_x - \ln k'^*_m)/S_m \tag{23}$$

where the derivative $d\varphi_x/d\varphi^*_m$ is first evaluated at φ^*_m using eqn. 21 or 22. This first calculated value of φ'_x is then used to determine the relative placement of the solute under consideration among the three φ_x *versus* φ^*_m data clusters and, from this, a new weighted average derivative is calculated. For example, assume for THF–water that it is found that our first estimate of φ'_{THF} falls between the φ_{THF} value calculated using the cluster 0 coefficients in Table III and φ_{THF} evaluated using cluster -1 coefficients. In this instance we would calculate the derivatives $d\varphi_x/d\varphi^*_m$ from both cluster 0 and cluster -1 equations and then use an average derivative weighted according to the relative distance of φ'_{THF} between the two clusters to calculate a new φ'_{THF} value from eqn. 23. This new φ'_{THF} is then used to calculate a new weighted average derivative and the iteration procedure continued until φ'_{THF} converges to a constant value. In practice it is found that two iterations are usually sufficient.

In order to test the validity of the eqn. 23 iteration procedure we have collected isocratic retention data for five solutes at several binary reference methanol–water compositions, φ^*_m, and at acetonitrile–water and THF–water compositions predicted to be iso-eluotropic with φ^*_m according to eqns. 17, 18 and 21–23. The k' values of the five solutes studied in these supposedly iso-eluotropic eluents are given in Table IV.

Of the five solutes listed, the two steroids prednisone and hydrocortisone are of particular interest because they both exhibit very non-ideal eluent transfer behaviour. For example, from Table IV it is seen that k' for hydrocortisone in 40% methanol was measured to be 9.7. The volume fractions acetonitrile–water predicted to be iso-eluotropic with $\varphi^*_m = 0.4$ according to eqn. 17 and 22 are 0.279 and 0.300, respectively. The respective k' values at these two eluent compositions were measured and found to be 2.7 and 1.9. Clearly, estimates of iso-eluotropic acetonitrile–water composition from eqns. 17 and 22 are grossly in error for this particular solute such that the capacity factors obtained in these solvents differ from the desired target value of 9.7 by a factor of nearly four.

TABLE IV

CAPACITY FACTORS MEASURED IN BINARY ELUENTS PREDICTED VIA THE INDICATED EQUATIONS TO BE ISO-ELUOTROPIC

The values in parentheses refer to the φ_{ACN} or φ_{THF} volume fractions at which the k' values were measured.

Solute	*Binary reference*		*Acetonitrile–water*			*THF–water*		
	Methanol φ_m^*	*k' at* φ_m^*	*k' (eqn. 17)*	*k' (eqn. 22)*	*k' (eqn. 23)*	*k' (eqn. 18)*	*k' (eqn. 21)*	*k' (eqn. 23)*
Benzaldehyde	0.15	6.5	5.5 (.093)	5.9 (.087)	6.6 (.077)	3.2 (.099)	3.7 (.078)	5.1 (.036)
	0.20	4.7	3.8 (.127)	4.0 (.124)	4.8 (.106)	2.5 (.132)	2.9 (.109)	4.0 (.068)
	0.30	2.5	2.0 (.200)	1.8 (.207)	2.6 (.166)	1.6 (.198)	1.8 (.179)	2.3 (.142)
Benzyl alcohol	0.20	9.0	9.5 (.127)	9.7 (.124)	9.0 (.133)	5.1 (.132)	5.9 (.109)	7.4 (.074)
	0.30	4.5	5.2 (.200)	4.9 (.207)	4.5 (.218)	3.3 (.198)	3.8 (.179)	4.3 (.160)
	0.40	2.3	2.9 (.279)	2.6 (.300)	2.4 (.313)	2.2 (.264)	2.3 (.255)	2.3 (.254)
m-Dinitrobenzene	0.20	10.6	18.9 (.127)	19.4 (.124)	8.7 (.223)	19.3 (.132)	22.6 (.109)	10.8 (.211)
	0.40	3.1	5.6 (.279)	4.8 (.300)	2.7 (.379)	7.1 (.264)	7.6 (.255)	3.3 (.353)
	0.50	1.7	2.9 (.365)	2.3 (.401)	1.5 (.454)	4.0 (.330)	3.9 (.335)	1.7 (.423)
Prednisone	0.40	9.9	2.5 (.279)	1.7 (.300)	14.9 (.178)	1.6 (.264)	1.8 (.255)	10.9 (.139)
	0.45	5.4	1.2 (.321)	0.7 (.350)	10.3 (.199)	1.1 (.297)	1.1 (.294)	5.1 (.183)
	0.50	3.0	0.5 (.365)	0.3 (.401)	7.6 (.216)	0.8 (.330)	0.8 (.335)	2.3 (.234)
Hydrocortisone	0.40	9.7	2.7 (.279)	1.9 (.300)	14.6 (.181)	1.8 (.264)	2.0 (.255)	10.3 (.144)
	0.45	5.3	1.3 (.321)	0.8 (.350)	10.2 (.202)	1.3 (.297)	1.3 (.294)	4.9 (.189)
	0.50	3.1	0.6 (.365)	0.3 (.401)	7.8 (.217)	0.9 (.330)	0.9 (.335)	2.4 (.241)

When the single retention datum at $\varphi_{ACN} = 0.3$ is combined according to eqn. 23 with known S_m, φ_m^* and $k_m'^*$ values to give 0.181 as the new corrected estimate of iso-eluotropic acetonitrile, and k' at this eluent composition is measured, we obtain $k' = 14.6$. Although the difference between $k' = 14.6$ and 9.7 is significant, in some applications errors of this magnitude may be tolerable. If a further refinement in iso-eluotropic acetonitrile–water composition is desired one may of course use the now known k' values at the first predicted eluent composition, $\varphi_{ACN} = 0.300$, and at the eqn. 23-corrected eluent composition, $\varphi_{ACN} = 0.181$, to construct a simple $\ln k'$–φ_{ACN} plot from which to calculate a better estimate of iso-eluotropic φ_{ACN}. However, when considering the transfer behaviour of the five solutes in Table IV as a whole, we observe that the eqn. 23 iteration procedure described above does in most instances predict iso-eluotropic acetonitrile–water and THF–water compositions with sufficient accuracy such that additional isocratic experiments in these two eluents need not be performed. From these data we can therefore conclude that the limiting acetonitrile–water and THF–water compositions most suitable for use in a ternary or quaternary eluent optimization procedure can be accurately determined for most mixtures from the results of only one isocratic experiment in each eluent (*i.e.*, from eqn. 23).

GLOSSARY OF TERMS

b	steepness of the gradient $(\varphi_f - \varphi_i)/T_G$
C_1–C_4	regression coefficients in eqn. 9
F	flow through the column
k'	chromatographic capacity factor
k'_0	capacity factor of a solute in 100% water
$k'_{meas,j}$	isocratically measured capacity factors of j solutes at φ_{meas} (a known isocratic methanol–water eluent)
L	column length
$\ln k'$	natural logarithm of the capacity factor
P'_{mix}	Snyder's solvent polarity index of a binary mixture
P'_A,P'_B	Snyder's solvent polarity index for solvents A and B
S	positive slope of the $\ln k'$–φ plot
s	total surface area of sorbent within the column
S_m	positive slope of the $\ln k'$–φ plot for a certain solute in the methanol–water
THF	tetrahydrofuran
T_G	gradient duration time
T'_r	net retention time under gradient conditions
t_0	column void time
t_0^{neat}	column void time at the flow-rates delivered by the pump(s) when pumping either neat methanol or water
$\bar{U}$	displacement weighted integrated average linear flow-rate
U_0^{neat}	L/t_0^{neat}
V_G	gradient volume; $V_G = T_G F$
V_m	volume of methanol
V_M	effective volume of the gradient mixer
V^{neat}	resulting volume when mixing the two neat solvents methanol and water
$V_{p\rightarrow c}$	volume between the pump head(s) and the column

z relative displacement of the solute down the column
$\Delta T_{r_{nim}}$ variation in net retention time due to non-ideal mixing of methanol–water mixtures
$\Delta T_{r_{curv}}$ deviation in T_r' due to ln k' curvature
σ_p standard deviation of the intercept of the S_m–ln k_0 plot
$\tau_{p\rightarrow c}$ pump to column delay time
φ volume fraction of organic component in the eluent
φ_f final volume fraction of organic component
φ_{ACN} volume fraction of acetonitrile
φ_i initial volume fraction of organic component
φ_m volume fraction of methanol
φ_m^* selected methanol–water isocratic eluent after the gradient run and corrections
φ_{THF} volume fraction of tetrahydrofuran
φ_p volume fraction of organic component in the eluent at the pump head
φ_x volume fraction of tetrahydrofuran or acetonitrile
φ_x' corrected volume fraction of tetrahydrofuran or acetonitrile

ACKNOWLEDGEMENT

The financial support of Millipore Waters Chromatography Division, Milford, MA, U.S.A., throughout the course of this work is gratefully acknowledged.

REFERENCES

1 P. J. Schoenmakers, H. A. H. Billiet and L. de Galan, *J. Chromatogr.*, 205 (1981) 13.
2 D. P. Herman, H. A. H. Billiet and L. de Galan, *Anal. Chem.*, 58 (1986) 2999.
3 P. R. Haddad and S. Sekulic, *J. Chromatogr.*, 392 (1987) 65.
4 P. J. Schoenmakers, H. A. H. Billiet, R. Tijssen and L. de Galan, *J. Chromatogr.*, 149 (1978) 519.
5 L. R. Snyder, J. W. Dolan and J. R. Gant, *J. Chromatogr.*, 165 (1979) 3.
6 M. A. Quarry, R. L. Grob and L. R. Snyder, *Anal. Chem.*, 58 (1986) 907.
7 H. A. Cooper and R. J. Hurtubise, *J. Chromatogr.*, 360 (1986) 313.
8 P. J. Schoenmakers, H. A. H. Billiet and L. de Galan, *J. Chromatogr.*, 185 (1979) 179.
9 M. A. Quarry, R. L. Grob and L. R. Snyder, *J. Chromatogr.*, 285 (1984) 1.
10 M. A. Quarry, R. L. Grob and L. R. Snyder, *J. Chromatogr.*, 285 (1984) 19.
11 P. J. Schoenmakers, H. A. H. Billiet and L. de Galan, *J. Chromatogr.*, 218 (1981) 261.
12 L. R. Snyder, *J. Chromatogr.*, 92 (1974) 223.

Journal of Chromatography, 463 (1989) 21–37
Elsevier Science Publishers B.V., Amsterdam — Printed in The Netherlands

CHROM. 21 011

RE-EVALUATION OF THE SOLVENT TRIANGLE AND COMPARISON TO SOLVATOCHROMIC BASED SCALES OF SOLVENT STRENGTH AND SELECTIVITY

SARAH C. RUTAN*
Department of Chemistry, Virginia Commonwealth University, Richmond, VA 23284 (U.S.A.)
PETER W. CARR, WON JO CHEONG and JUNG HAG PARK*
Department of Chemistry, University of Minnesota, Minneapolis, MN 55455 (U.S.A.)
and
LLOYD R. SNYDER
L. C. Resources, Inc., 26 Silverwood Court, Orinda, CA 94563 (U.S.A.)
(First received June 22nd, 1988; revised manuscript received September 28th, 1988)

SUMMARY

The principal thrust of this work is to explore the validity of the major assumptions made in developing the solvent triangle and to examine the relationship between the selectivity parameters derived from the solvent triangle and independently determined, solvatochromically based measures of dipolarity, hydrogen bond acidity, and basicity. It is shown that the original solvent triangle classification scheme is only slightly modified by the use of a much more rigorous correction for the behavior of a reference alkane. These results are based on new experimental measurements of the gas–liquid partition coefficients of Rohrschneiders' probe solutes and a set of alkanes (*n*-pentane–*n*-octane). More fundamentally we have shown that the original selectivity parameters based of the properties of ethanol, dioxane and nitromethane are all lumped parameters composed of dipolar, hydrogen bond acidity and hydrogen bond basicity terms. Perhaps most importantly the original probe solutes used to develop the solvent triangle are shown to be inefficient choices in terms of their ability to discriminate between similar solvents. This is an important limitation in that the primary use of the solvent triangle has been for the optimization of selectivity and the classification of phases.

INTRODUCTION

A qualitative and quantitative understanding of the nature and strength of solute–solvent interactions is obviously important in chromatography. A major goal of many studies has been the development of schemes for classifying solvents to facilitate the selection of an optimum mobile phase for use in liquid chromatography.

* Present address: Department of Chemistry, Yeung Nam University, Gyongsan 632, Seoul, Korea.

0021-9673/89/$03.50

Similarly, the classification of stationary phases in gas chromatography requires the use of a set of probe solutes that explore different types of physicochemical interactions with the stationary phase. Accordingly, many approaches have been developed for separating the contributions of dipolarity, hydrogen bond acidity (HBA) and hydrogen bond basicity (HBD) to the overall solvent strength. Intuitively, any two phases that are similar in all three of the above properties should behave similarly in terms of their retention properties. The Snyder solvent triangle approach has been used very widely in chromatography[1,2]. In contrast, in chemical engineering, the separation of the cohesive energy density (solubility parameters) into similar types of terms has received considerable attention[3,4], most recently by Thomas and Eckert[5]. The solubility parameter approach has also been used extensively in chromatography[6,7]. A third approach, the use of the phenomenon of solvatochromism, in conjunction with linear solvation energy relationships (LSER), is widely used by physical organic chemists to rationalize, correlate and predict the effect of solvent on the rates and equilibria of chemical reactions[8–10]. This last approach has also been used to unravel the role of specific chemical processes in gas–liquid and liquid–liquid partitioning[8,11,12].

Several of the studies described above made extensive use of Rohrschneider's gas–liquid partition data for six prototypical solutes (octane, toluene, nitromethane, ethanol, dioxane and 2-butanone) in 81 common liquids[13]. The approach taken by Snyder is based entirely on this data set. In Snyder's approach, the P' polarity scale is a global or overall measure of solvent strength that is a composite of all types of solute–solvent interactions, except for dispersive interactions. Other workers have used the Rohrschneider data set to test their models[11]. Recently many of the above data have been redetermined by a methodology which circumvents most of the shortcomings and assumptions inherent in Rohrschneider's measurements[14]. In addition, the gas–liquid partition coefficients of a set of alkanes in the same solvents have been measured[15].

The purpose of this paper is to examine, in light of this new data, two of the approaches used to classify and quantify solvent properties. The first method is the solvent triangle and P' scale[1,2]. The second approach is that of Kamlet and Taft[8], in which gas–liquid partition coefficients are correlated with the solvatochromic scales describing solvent dipolarity–polarizability (π^*), hydrogen bond acidity (α) and basicity (β). In this study, we employ an additional term to account for solvent reorganization effects in self-associating solvents[16]. In addition, we have evaluated the suitability of each of these two methods for ranking and classifying solvents, and discuss appropriate modifications to these solvent strength scales and classification methods.

THEORY

P' polarity scale

Snyder's approach[1,2] is based on the assumption that the dispersive interactions and cavity formation contributions can be eliminated from the partition coefficient by first multiplying the partition coefficient by the solvent molar volume, V_s, as shown in eqn. 1, and then referencing this quantity to that which would result for a hypothetical alkane with the same molar volume as the solute,

$$\log K'_{i,s} = \log(K_{i,s}V_s) \quad (1)$$

$$\log K''_{i,s} = \log K'_{i,s} - (V_i/163) \log(K_{0,s}V_s) \quad (2)$$

Here $K_{i,s}$ is the gas–liquid partition coefficient of solute i in solvent s, V_s is the solvent molar volume, $K_{0,s}$ is the gas–liquid partition coefficient for octane in solvent s, and V_i is the molar volume of the probe solute. The term 163 is the molar volume of octane. In the absence of measured values for the partition coefficients for a series of n-alkanes, the above correction is the best available expedient. The accuracy of this approach, however, is entirely contingent upon the validity of Snyder's assumption that the intercept of a plot of the log of the partition coefficient for the n-alkanes *vs.* the molar volume (V_{alkane}) is insignificant.

In Snyder's approach, the $\log K''_{i,s}$ value given in eqn. 2 was then modified by subtracting the average of the $\log K''_{i,s}$ values for the ith solute in the solvents hexane, cyclohexane, and isooctane ($\log K''_{i,\text{hci}}$) as shown in eqn. 3

$$P'x_i = \log K''_{i,s} - \log K''_{i,\text{hci}} \quad (3)$$

The calculations described by eqns. 1–3 were done using ethanol ($P'x_e$), p-dioxane ($P'x_d$) and nitromethane ($P'x_n$) as solutes, where the following condition holds

$$1 = x_e + x_d + x_n \quad (4)$$

Snyder suggested that x_e, x_d and x_n should be measures of the solvent hydrogen bond basicity, the solvent hydrogen bond acidity and the solvent dipolarity, respectively.

Poppe and Slaats[17] proposed two modifications to the approach described above. First, they suggested that a Flory–Huggins correction factor be included in eqn. 1 to account for the entropic contribution to the partition coefficient due to differences in molecular size. The net effect of this correction is to arithmetically completely eliminate the dependence on the molar volume of the solvent introduced in eqn. 1, so that the final equation for $P'x_i$ becomes

$$P'x_i = \log K_{i,s} - (V_i/163) \log K_{0,s} - \log K_{i,\text{hci}} + (V_0/163) \log K_{0,\text{hci}} \quad (5)$$

In general, the magnitude of the Flory–Huggins factor is relatively small for molecules with similar sizes. The second correction proposed by these authors involves an improvement in the estimate of the contribution from a hypothetical n-alkane with the same molar volume as the solute, so that the expression for $P'x_i$ then becomes

$$P'x_i = \log K_{i,s} - (V_i/163) \log K_{0,s} - \log K_{i,\text{hci}} + \\ + (V_0/163) \log K_{0,\text{hci}} + (\beta_{\text{hci}} - \beta_s)[1 - (V_i/163)] \quad (6)$$

where β_s is a term which takes into account the fact that a plot of $\log K_{\text{alkane},s}$ *vs.* V_{alkane} may have a non-zero intercept. These authors found that the Flory–Huggins correction (equivalent to the omission of the original V_s correction) produced $P'x_i$ values for the non-polar alkane solvents that were virtually independent of the solvent. More importantly, changes in the P' values and the x_e, x_d and x_n factors were negligible

in terms of the solvent classification scheme[17]. These authors were unable to evaluate the proposed correction given in eqn. 6, due to the difficulty in estimating the β_s values.

Recently, gas–liquid partition coefficient data for a series of alkanes in the Rohrschneider solvents have become available[15]. These data permit the estimation of the contribution from a non-zero intercept. In all solvents studied, the data for at least four *n*-alkanes (pentane to octane) give rise to precise linear relationships of the following form,

$$\log K_{\text{alkane},s} = m_s V_{\text{alkane}} + b_s \tag{7}$$

where m_s and b_s are the solvent dependent slope and intercept, respectively. In addition, limited data for a few of the solvents studied here show linear behavior with carbon number and hard core volume down to a carbon number of two, although the relationship with molar volume is not as linear[18]. It can therefore be argued that the solute volume parameter used in eqn. 7 should be a molecular hard core volume (*e.g.*, based on the Bondi-group contribution method[19]), rather than a molar volume as is employed here. This was investigated briefly, however the approach, although quantitatively different, showed no changes in the final classification scheme.

If the linear extrapolation given by eqn. 7 is assumed to be valid, and the V_s correction introduced in eqn. 1 is omitted, as is suggested by the theoretical work of Ben-Naim[18], the following expression for $P'x_i$ is obtained

$$P'x_i = \log K_{i,s} - m_s V_i - b_s - \log K_{i,\text{hci}} + m_{\text{hci}} V_i + b_{\text{hci}} \tag{8}$$

This approach is somewhat different from that proposed by Poppe and Slaats as given in eqn. 6.

Correlation with solvatochromic parameters

A second solvent characterization scheme has been reported by Kamlet *et al.*[8] that is similar to the approach described above; it is based on a dissection of the partition coefficient into contributions from solvent dipolarity, hydrogen bond basicity and hydrogen bond acidity. Here, the partition coefficient data were corrected for dispersion and cavity formation by referencing to an alkane of similar size to the solute. These values were then correlated with the solvatochromic scales. The parameters π^*, α, β and δ are the solvatochromic parameters describing the solvent dipolarity–polarizability, hydrogen bond acidity, hydrogen bond basicity, and the polarizability correction factor, respectively. These solvent parameters were then used as linear energy parameters in an LSER. For aliphatic solvents, the correlation takes the form

$$\log K_{i,s} - \log K_{\text{alkane},s} = SP_0 + s\pi^* + a\alpha + b\beta \tag{9}$$

or alternatively (in aromatic and polyhalogenated solvents), to correct for differences in the polarizability contribution (δ) to π^*

$$\log K_{i,s} - \log K_{\text{alkane},s} = SP_0 + s\pi^* + d\delta + a\alpha + b\beta \tag{10}$$

where δ is 0 for non-chlorinated, aliphatic solvents, 0.5 for polychlorinated, aliphatic solvents, and 1.0 for aromatic solvents. Here, SP_0 is the solute dependent intercept, which corresponds to the corrected log K value for a solvent with zero values for π^*, α, β and δ (*i.e.*, cyclohexane). The coefficients s, a, b and d are the solute dependent coefficients which can be determined from multiple linear regression; these coefficients should describe the solute dipolarity–polarizability, hydrogen bond basicity, hydrogen bond acidity, and the contribution from the polarizability correction factor for the solute, respectively.

In the work of Kamlet *et al.*[8] ethane was used as the reference alkane solute for ethanol and nitromethane, propane the reference for 2-butanone and *p*-dioxane, and butane the reference for toluene. A similar analysis of the newer experimental results has been carried out, using the Hildebrand solubility parameter to estimate the relative contribution of the cavity formation step[20].

In this work, instead of referencing with respect to an alkane with similar size, the gas–liquid partition coefficients are referenced with respect to a hypothetical alkane with a molar volume equal to the solute molar volume, obtained from the regression results calculated using eqn. 7. The appropriate equation for the examination of the selectivity parameters in terms of the solvatochromic parameters can then be given as

$$P'x_i = SP_0 + s\pi^* + d\delta + a\alpha + b\beta \tag{11}$$

Since the terms involving the averages of the solvent characteristics for hexane, cyclohexane, and isooctane (hci) in eqn. 8 are constants, the correlation given by eqn. 11 differs from that given in eqn. 10 by a constant. In this work, all correlations are based on the product $P'x_i$, rather than x_i, since this should yield coefficients which can be interpreted based on known solute properties, and is consistent with an analysis of the units involved (energy), whereas the x_i values are normalized, dimensionless quantities.

Recent work has demonstrated that an additional term must be added to eqn. 11 to adequately model the gas–liquid partition behavior for the wide range of solvents employed here[16]. An additional parameter, $\alpha\beta$, which is the product of the solvent hydrogen bond basicity and acidity, is included to give the following equation

$$P'x_i = SP_0 + s\pi^* + d\delta + a\alpha + b\beta + h\alpha\beta \tag{12}$$

This term is required to account for the additional reorganization of self-associating solvents which occurs when the solute is capable of hydrogen bonding.

EXPERIMENTAL

Data for 65 solvents were evaluated in the reassessment of Snyder's P' scale. In this case, only those solvents for which gas–liquid partition coefficients were available for octane, ethanol, *p*-dioxane and nitromethane were included in the data set. For those solvents for which data were not determined in the more recent study[14], values from the original Rohrschneider set[13] were used, so that each of the 65 solvents was characterized by four gas–liquid partition coefficient values. In addition, data for *n*-alkane solutes were available for 58 of these solvents[15]. A list of these solvents is given in Table I.

TABLE I

RE-EVALUATION OF P' AND x_i VALUES*

Solvent	P'	x_e	x_d	x_n
Hexane**	−0.14			
Decane**	0.06			
Hexadecane**	0.20			
Isooctane**	−0.03			
Squalane**	0.44			
Cyclohexane**	0.17			
Triethylamine	2.19	0.66	0.08	0.26
Carbon disulfide	1.07	0.22	0.39	0.39
Diethyl ether	3.15	0.53	0.13	0.34
Dibutyl ether	1.65	0.48	0.14	0.38
Diisopropyl ether	1.83	0.51	0.10	0.39
Tetrahydrofuran	4.28	0.41	0.19	0.40
p-Dioxane	5.27	0.37	0.23	0.40
Bis-2-ethoxyethyl ether	4.13	0.38	0.20	0.42
2-Butanone	4.62	0.36	0.20	0.43
Cyclohexanone	4.72	0.37	0.21	0.41
Ethyl acetate	4.24	0.36	0.22	0.42
Acetonitrile	5.64	0.33	0.25	0.42
Butyronitrile	4.60	0.35	0.23	0.42
Nonanenitrile	3.66	0.36	0.22	0.42
Pentadecanenitrile	2.84	0.36	0.21	0.43
N,N-Dimethylformamide	6.31	0.40	0.21	0.39
N,N-Dimethylacetamide	6.45	0.41	0.20	0.38
Hexamethylphosphoramide	7.10	0.47	0.16	0.37
γ-Butyrolactone	6.27	0.34	0.26	0.40
N-Methylpyrrolidone	6.45	0.41	0.21	0.39
Nitromethane	5.78	0.29	0.30	0.41
Dimethylsulfoxide	7.29	0.40	0.22	0.37
Benzene	3.19	0.27	0.28	0.45
Toluene	2.68	0.28	0.27	0.45
p-Xylene	2.55	0.28	0.26	0.45
Acetophenone	4.95	0.35	0.25	0.40
Ethoxybenzene	3.34	0.30	0.27	0.43
Benzonitrile	4.77	0.32	0.26	0.41
Nitrobenzene	4.74	0.29	0.29	0.43
Pyridine	5.53	0.42	0.22	0.36
2-Picoline	5.15	0.44	0.20	0.36
Anisole	3.87	0.30	0.28	0.42
Methylene chloride	4.29	0.27	0.33	0.40
Chloroform	4.31	0.31	0.35	0.34
Carbon tetrachloride	1.56	0.26	0.40	0.34
Methylene iodide	4.31	0.28	0.37	0.35
Fluorobenzene	3.03	0.26	0.29	0.44
Chlorobenzene	3.02	0.27	0.30	0.43
Bromobenzene	3.14	0.28	0.31	0.42
Ethanol	4.40	0.52	0.19	0.29
Propanol	4.13	0.54	0.19	0.27
Butanol	4.11	0.54	0.18	0.28
Octanol	3.23	0.58	0.17	0.25
Isopropanol	3.92	0.57	0.17	0.26
tert.-Butanol	4.03	0.56	0.20	0.24

TABLE I (*continued*)

Solvent	P'	x_e	x_d	x_n
Isopentanol	3.46	0.58	0.17	0.25
Methoxy ethanol	5.71	0.41	0.22	0.36
Benzyl alcohol	6.06	0.40	0.29	0.31
Trifluoroethanol	7.55	0.40	0.33	0.27
Hexafluoroisopropanol	8.68	0.45	0.27	0.27
Aniline	6.31	0.33	0.31	0.36
Acetic acid	6.13	0.41	0.30	0.30
Perfluorohexane**	−0.84			
Nitroethane***				
Ethylene glycol***				
Diethylene glycol***				
m-Cresol***				
Benzyl ether***				
2,6-Lutidine***				
Iodobenzene***				

* These values were calculated using eqn. 8, based on the linear correlation of the *n*-alkane partition coefficients.

** This solvent has a value for P' which is too small to obtain reliable x_e, x_d and x_n values.

*** Data for the partition coefficients for the *n*-alkane solutes in these solvents were not available, so P', x_e, x_d and x_n values based on eqn. 8 could not be calculated.

Data for 44 solvents were used in the calculation of the coefficients for the solvatochromic regression equations. These solvents were chosen based on the availability of π^*, α and β values for these liquids. These solvents, along with the corresponding values for π^*, α and β[21] are given in Table II. All multiple linear regression results were obtained using the Kalman filter, a recursive, least-squares algorithm[22,23]. The regression program was written in Pascal, and run on an IBM PC compatible computer with an 8087 coprocessor and 384K of memory.

RESULTS AND DISCUSSION

P' polarity scale

Snyder's P' values and the selectivity parameters, x_e, x_d and x_n were reevaluated using the new partition coefficient data for the Rohrschneider solvents. Three different calculation approaches based on eqns. 3, 5 and 8 were employed. As will be demonstrated, there were few significant differences in the resulting classification scheme. For 57 of 65 solvents considered by Snyder given in Table I[1], the newer experimental partition coefficient values are used to compute new P' values via eqn. 3 (the original approach used by Snyder). The following regression equation was obtained for the correlation of the new P'values (P'_{new}) based on eqn. 3, with the original values reported by Snyder (P'_{old}).

$$P'_{new} = (0.921 \pm 0.017)\, P'_{old} + (0.040 \pm 0.073) \qquad (13)$$
$$r^2 = 0.983 \qquad s = 0.236 \qquad n = 57$$

The value for the slope (0.921) in eqn. 13 is explained by the fact that the P'_{old} values

TABLE II

SOLVENT SOLVATOCHROMIC PARAMETERS*

Solvent	π^*	α	β
Pentane	−0.08	0	0
Hexane	−0.04	0	0
Heptane	−0.02	0	0
Decane	0.03	0	0
Hexadecane	0.08	0	0
Isooctane	−0.04	0	0
Cyclohexane	0	0	0
Triethylamine	0.14	0	0.71
Diethyl ether	0.27	0	0.47
Dibutyl ether	0.24	0	0.46
Diisopropyl ether	0.27	0	0.49
Tetrahydrofuran	0.58	0	0.55
p-Dioxane	0.55	0	0.37
Acetone	0.71	0.08	0.48
2-Butanone	0.67	0.06	0.48
Cyclohexanone	0.76	0	0.53
Ethyl acetate	0.55	0	0.45
Acetonitrile	0.75	0.19	0.31
N,N-Dimethylformamide	0.88	0	0.69
N,N-Dimethylacetamide	0.88	0	0.76
Hexamethylphosphoramide	0.87	0	1.01
γ-Butyrolactone	0.87	0	0.49
Nitromethane	0.85	0.22	0.25
Dimethylsulfoxide	1.00	0	0.76
Benzene	0.59	0	0.10
Toluene	0.55	0	0.11
p-Xylene	0.51	0	0.12
Acetophenone	0.90	0	0.49
Benzonitrile	0.90	0	0.41
Nitrobenzene	1.01	0	0.39
Pyridine	0.87	0	0.64
Anisole	0.73	0	0.22
Methylene chloride	0.82	0.30	0
Chloroform	0.58	0.44	0
Carbon tetrachloride	0.28	0	0
Ethylene chloride	0.81	0	0
Fluorobenzene	0.62	0	0.07
Chlorobenzene	0.71	0	0.07
Bromobenzene	0.79	0	0.06
Methanol	0.60	0.93	0.62
Ethanol	0.54	0.83	0.77
Butanol	0.47	0.79	0.88
Isopropanol	0.48	0.76	0.95
tert.-Butanol	0.40	0.68	1.01

* Solvatochromic parameters from ref. 21.

were multiplied by 1.1 before tabulation. The intercept is not significantly different from zero. These data are shown in Fig. 1. There are five solvents for which the absolute discrepancy between the P' scale based on the new and old Rohrschneider

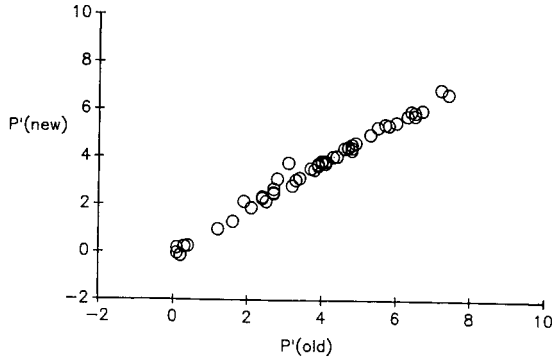

Fig. 1. Plot of new P' values calculated using eqn. 3 *vs.* the original values reported by Snyder in ref. 1.

data is greater than ± 0.3: diethylene glycol, ethylene glycol, triethylamine, methylene chloride and ethyl ether. The discrepancy in the values for the glycols is not surprising; these solvents are very viscous, and the difficulty of making accurate gas–liquid partition coefficient determinations on them has been previously noted[14]. The value for the partition coefficient for *p*-dioxane in methylene chloride in Rohrschneider's original data set is also in error[14]. In general, the new and old values for the x_e, x_d and x_n selectivity scales are in agreement within ± 0.03.

The most marked deviations for the Snyder selectivity parameters were observed for triethylamine and methylene chloride, which were not correctly classified in the original solvent triangle, and for chloroform. The original solvent triangle is shown in 2, where the changes for these three solvents are indicated. These modifications, which

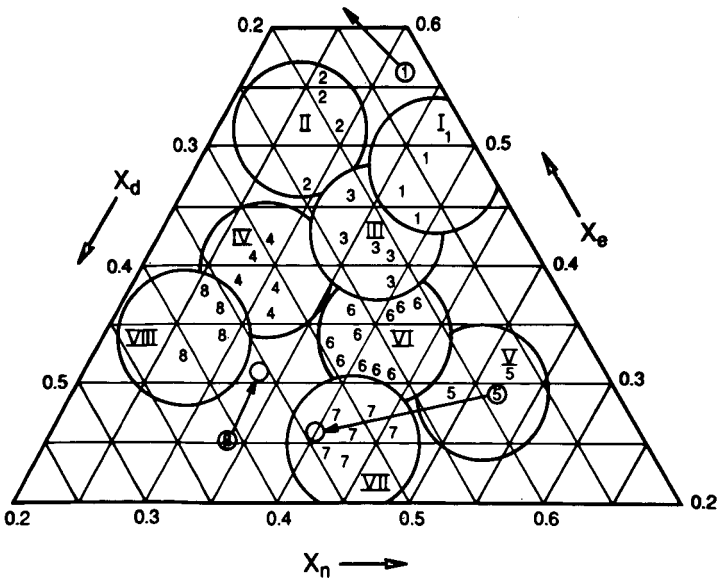

Fig. 2. Original solvent triangle, with modifications for triethylamine (1), methylene chloride (5), and chloroform (8). Reproduced from *J. Chromatogr. Sci.* (ref. 1) by permission of Preston Publications, A Division of Preston Industries, Inc.

result from the use of the new data, are consistent with the known chemistry of these compounds. For example, triethylamine (1), a good hydrogen bond acceptor (β = 0.71), is shifted toward the basic corner of the triangle, methylene chloride (5), a slightly acidic compound, is shifted away from ethylene chloride towards the acidic corner of the triangle, and chloroform, a moderately strong hydrogen bond donor (α = 0.44) is shifted closer to group VIII which consists of the strong hydrogen bond acids, fluoroalkanols, water and *m*-cresol.

The two alternate formulations (Poppe's and our own) used for calculation of the P' values are given by eqns. 5 and 8. It is difficult to evaluate the merits of the modified scales relative to Snyder's original approach (eqn. 3), since there were not very many differences between the three methods. The calculations based on eqns. 3 and 8 (the original approach, and the method proposed here) gave a range of P' values within the homologous series of *n*-alkane solvents, while the method based on eqn. 5 (Poppe's approach) gave essentially identical P' values for all of the alkanes. Since we cannot completely account for dispersion interactions and solute dipole–solvent induced dipole interactions, it appears that eqns. 3 and 8 give more realistic estimates of the relative P' values for these compounds. In addition, carbon disulfide, benzene and carbon tetrachloride, which are non-polar, non-hydrogen bonding solvents, all yield P' values significantly larger than those of the alkanes using all methods. These P' values presumably reflect larger dipole–induced dipole interactions between the polar solutes and these non-polar, but highly polarizable solvents.

In general, the differences between the x_e, x_d, and x_n values for the three different approaches used for computation of the x_i values were small, and did not appear to provide any insight as to whether any of the three approaches is superior. For all three calculation methods, the x_i values within the homologous series were consistent with the original observations; the x_i values were similar within a given series, except that the first few members of the series tended to have slightly different values relative to the rest of the series.

There can be no "true" or unique ranking for any single parameter solvent strength scale, such as the P' scale, since the scale will depend on differences in the relative contributions of dispersion, dipole–dipole, dipole–induced dipole, and hydrogen bonding interactions, which must be solute dependent[24]. From this point, we assume that the method based on subtracting out the contribution due to a hypothetical alkane of identical size to the probe solute is the most appropriate approach (eqn. 8). This is consistent with the observations described above, since we expect that there will be at least some small variations of P' within the *n*-alkane solvent set due to variations in induced dipole interactions (a 0.34 variation in P' between hexane and hexadecane was observed). This is true of other solvent strength scales as well, including the π^* solvatochromic scale and the scales based on the cohesive energy density[3].

The following regression equation was obtained for the correlation of the P' values obtained using eqn. 8 (based on the correction calculated from a hypothetical *n*-alkane), with the original values reported by Snyder (P'_{old}).

$$P' = (0.994 \pm 0.025)\, P'_{old} + (0.06 \pm 0.11) \qquad (14)$$
$$r^2 = 0.970 \quad s = 0.341 \quad n = 50$$

Only 50 solvents were used here, since data for the *n*-alkane solutes for the last seven of the solvents listed in Table I were not measured[15]. The slope obtained in this comparison is close to one, as opposed to the value of 0.921 given in eqn. 13. This is due to the omission of the volume correction introduced in eqn. 1. The intercept is not significantly different from zero. The final values for P' and the selectivity parameters, x_e, x_d and x_n using eqn. 8 are given in Table I.

As mentioned earlier, there is also very good agreement between the original x_i values reported by Snyder, and those calculated using eqn. 8, shown in Table I. This implies that many of the observations made by Snyder in the original reports are valid for these values as well. The values in Table I show tight clustering of the x_i values with in the homologous series (the alkylnitriles and the *n*-alcohols). However, if comparisons are made between classes, some confusion can arise. For example, if it is assumed, as Snyder proposed, the values for x_d indicate the relative solvent hydrogen bond acidity, the x_d for benzene (a non-acidic compound, $\alpha = 0$) should be less than that for ethanol ($\alpha = 0.33$). In fact, the x_d for benzene is 0.28 and the x_d for ethanol is 0.19. Similar inconsistencies can be found throughout Table I. It was these inconsistencies which led us to investigate the correlation of the $P'x_i$ values with the solvatochromic parameters.

Correlation with solvatochromic parameters

Snyder originally proposed, as described in the Theory section, that x_e, x_d and x_n should describe the hydrogen bond basicity of the solvent, the hydrogen bond acidity of the solvent, and the dipolarity of the solvent, respectively. If this were true, then x_e, x_d and x_n should correlate strongly with β, α and π^*, respectively. As Fig. 3 demonstrates, there is disappointingly little correlation of the selectivity factors with the individual solvatochromic parameters.

We realized first that the descriptor which relates to these solvatochromic parameters should be $P'x_i$, rather than x_i, as seen by inspection of the derivation leading to eqn. 12. However, there was little change in the quality of the correlation with the solvatochromic parameters with this modification. Next, multiple linear regression was used to evaluate the relationship between the $P'x_i$ values for 2-butanone, ethanol, toluene, *p*-dioxane, and nitromethane and the solvatochromic parameters, π^*, α and β. All correlations were based on eqn. 12, and the regression results are given in Table III. All solutes were sensitive to the solvent dipolarity–polarizability, with the strongest dependence observed for nitromethane, as expected based on it's π^* and bond dipole moment[10]. The s coefficient for nitromethane was 2.29, as compared to 1.65 for 2-butanone, 1.44 for *p*-dioxane, 1.32 for ethanol, and 0.97 for toluene. These coefficients were correlated with the π^* values for these solutes, as shown in Table IV. A moderate dependence on solvent α was observed for 2-butanone, ethanol, and *p*-dioxane, while a weaker dependence was observed for toluene and nitromethane. These coefficient values are again consistent with the values for solute β, as given in Table IV. In addition, a strong dependence on solvent β was observed for ethanol ($b = 1.88$), and a weaker dependence on solvent β ($b = 0.55$) was observed for nitromethane. The values for solute α are consistent with these observations. Fig. 4 shows plots of the $P'x_i$ values *vs.* the $P'x_i$ values predicted from the regression calculation.

These results indicate that the assumption that of the three solutes ethanol is the

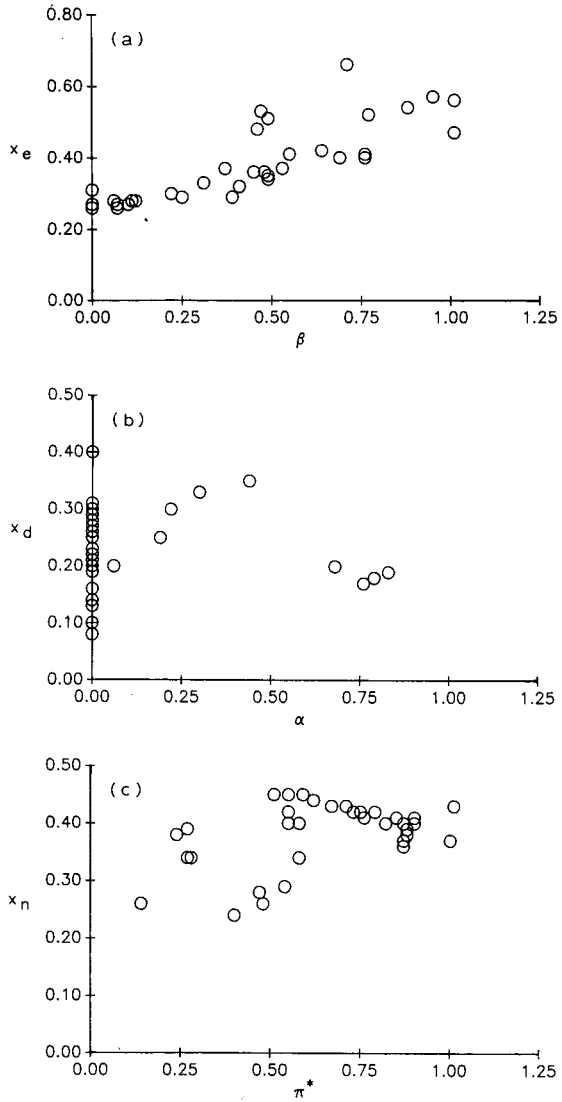

Fig. 3. (a) x_e *vs.* β; (b) x_d *vs.* α; (c) x_n *vs.* π^*. Snyder selectivity parameters are given in Table I.

main probe of solvent basicity is correct, however, the assumption that x_n is the main indicator of solvent dipolarity is incorrect, as all three solutes have appreciable dipolar interactions with the solvents. In addition, sensitivity to solvent hydrogen bond acidity is split approximately equally between ethanol and dioxane, with a small contribution from x_n.

Based on the observations described above, one can predict that the most basic solvents should lie at the top of the triangle, the most acidic solvents should lie towards the left edge of the triangle, and the polar solvents might be found almost anywhere in

TABLE III

MULTIPLE LINEAR REGRESSION RESULTS

Solute	*Regression coefficients**						*Standard error of the fit*
	s	*d*	*a*	*b*	*h*	SP_0	
2-Butanone	1.65 (0.06)	−0.18 (0.05)	0.89 (0.24)	−**	−0.79 (0.28)	−0.18 (0.04)	0.103
Ethanol	1.32 (0.15)	−0.24 (0.10)	1.31 (0.38)	1.88 (0.17)	−1.59 (0.24)	0.00 (0.06)	0.173
Toluene	0.97 (0.03)	−0.13 (0.02)	0.13 (0.09)	−**	−0.54 (0.11)	0.01 (0.02)	0.053
p-Dioxane	1.44 (0.06)	−0.06 (0.05)	1.07 (0.18)	−**	−1.14 (0.23)	0.02 (0.04)	0.110
Nitromethane	2.29 (0.13)	−0.34 (0.08)	0.49 (0.27)	0.55 (0.14)	−1.27 (0.39)	0.04 (0.05)	0.138

* Standard deviations of the coefficients are given in parenthesis. Eqn. 12 is the regression equation employed.

** These coefficients were found to be not significantly different from zero and were omitted in the final fit.

the triangle. This can be seen in Fig. 2, where the basic groups (I, ethers; II, alkanols) are found at the top of the triangle, the most acidic groups (II, alkanols; IV, glycols, acetic acid, benzyl alcohol; VIII fluoroalkanols) are located near the left edge of the triangle, and the most polar groups (III, sulfoxides, amides, pyridines; VI, ketones, nitriles, esters; V, ethylene chloride) are located in the center and somewhat towards the right corner of the triangle. In addition, since all solutes show some indication of solvent dipolarity, this indicates that the triangle should not allow very strong discrimination between solvents of differing dipolarity.

TABLE IV

SOLUTE SOLVATOCHROMIC PARAMETERS

From refs. 21 and 31.

Solute	π^*	α	β
2-Butanone	0.67	0.02	0.48
Ethanol	0.54	0.33	0.45
Toluene	0.42*	0	0.11
p-Dioxane	0.55	0	0.37
Nitromethane	0.85	0.12	0.25

* This value is modified by a $-d\delta$ correction term.

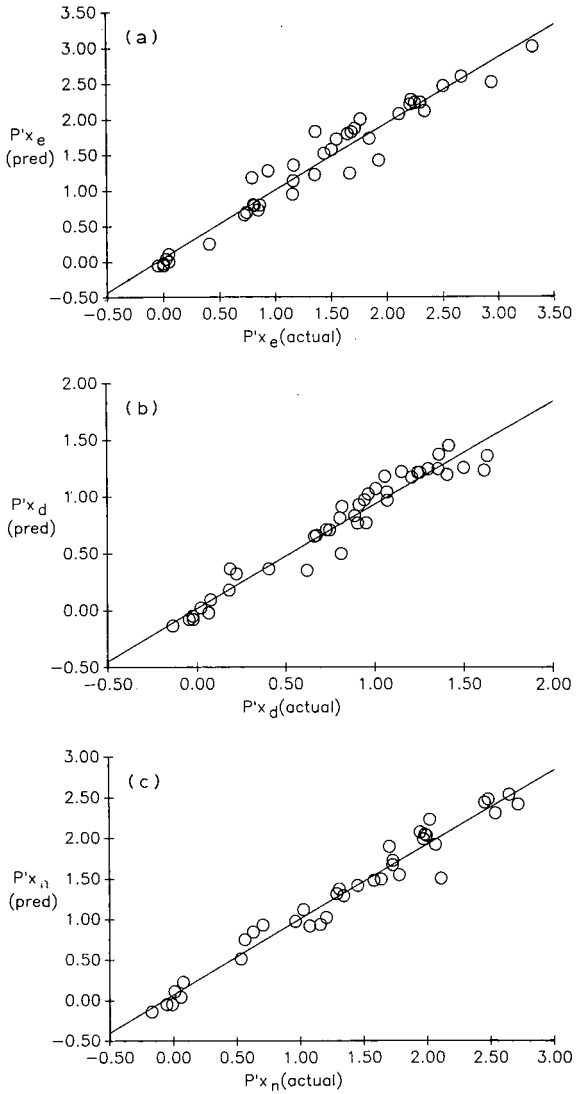

Fig. 4. (a) $P'x_e$ (pred) *vs.* $P'x_e$. (b) $P'x_d$ (pred) *vs.* $P'x_d$. (c) $P'x_n$ (pred) *vs.* $P'x_n$. All predicted values calculated using eqn. 12 and the regression results tabulated in Table III.

CONCLUSIONS

The above solvatochromic correlation results impact upon the use of the x_e, x_d and x_n selectivity parameters generated in Snyder's approach. As can be seen from the coefficients given in Table IV, the x_e values reflect a composite of solvent dipolarity–polarizability, hydrogen bond basicity, and hydrogen bond acidity, the x_d values reflect a composite of solvent dipolarity and solvent acidity, and the x_n values reflect

predominately solvent dipolarity, with small contributions from hydrogen bond basicity and acidity.

While the solvent triangle does allow classification on the basis of these three characteristics, it appears that knowledge of the solvatochromic parameters should permit the selection of more appropriate probe solutes for the development of a solvent triangle with better ability to allow discrimination between solvents. For example, triethylamine ($\pi^* = 0.14$, $\alpha = 0$, $\beta = 0.71$), a very basic, but relatively non-polar compound, and trifluoroethanol ($\pi^* = 0.73$, $\alpha = 1.51$, $\beta = 0$), a strongly acidic compound might be more suitable probe solutes. Selection of probe solutes such as these, based on information theory principles[25], should permit the development of a solvent triangle which allows for better distinction between the solvent classes.

Another limitation to the classification ability of the solvent triangle is the lack of an explicit selectivity parameter describing dispersive interactions. The work of Meyer and co-workers[26–29] clearly shows that dispersive interactions predominate over all other interactions in organic solvents. Although the alkane correction reduces the dependence of the x_i factors on dispersion, residual variations in dispersive interactions undoubtably contribute to the observed x_i factors.

One could also envision a triangle based directly on the solvatochromic π^*, α and β scales, however, this requires an arbitrary normalization and probably would not yield a triangle with high discriminating power, since so many of the common solvents have low hydrogen bond acidity. A better approach, which could be based directly on the solvatochromic parameters, would be to develop a classification scheme using cluster analysis methods[30]. In this case, solvents would be determined to be in the same solvent class when the π^*, α and β values of the solvents are similar.

The above results demonstrate several points of interest to chromatographers seeking better methods for classifying solvents. First, the redetermination of the Rohrschneider gas–liquid partition coefficients has been found to change the P' scale and selectivity triangle in only a few instances. An improved method of calculation of the $P'x_e$, $P'x_d$ and $P'x_n$ based on newly determined partition coefficients for the *n*-alkanes in the Rohrschneider solvents has been examined, and determined to give similar values to the original approach. In addition, the values for $P'x_e$, $P'x_d$ and $P'x_n$, have been rationalized in terms of their correlations with the π^*, α and β solvatochromic parameters. Finally, some suggestions for improvements in solvent classification methods based on the Snyder selectivities and the solvatochromic parameters have been proposed.

ACKNOWLEDGEMENTS

This research was supported by the National Science Foundation with Grant no. CHE-8616097 and with funds from the Petroleum Research Fund, administered by the American Chemical Society to the University of Minnesota.

GLOSSARY

$K_{i,s}$ gas–liquid partition coefficient of solute i in solvent s
V_s molar volume of solvent s
V_i molar volume of solute i

x_i selectivity parameter
P' polarity parameter
β_s correction factor for non-zero slope of a plot of log K for n-alkanes in solvent s *vs.* solvent molar volume (Poppe's approach)
π^* solvatochromic dipolarity–polarizability parameter
α solvatochromic hydrogen bond acidity parameter
β solvatochromic hydrogen bond basicity parameter
δ solvatochromic polarizability correction parameter
s coefficient for π^* parameter
d coefficient for δ parameter
a coefficient for α parameter
b coefficient for β parameter
m_s slope of plot of log K for n-alkanes in solvent s *vs.* solvent molar volume
b_s intercept of plot of log K for n-alkanes in solvent s *vs.* solvent molar volume

Subscripts

o octane
hci average value for the solvents hexane, cyclohexane, and isooctane
e ethanol
d p-dioxane
n nitromethane
s solvent
i solute

REFERENCES

1 L. R. Snyder, *J. Chromatogr. Sci.*, 16 (1978) 223.
2 L. R. Snyder, *J. Chromatogr.*, 92 (1974) 223.
3 C. M. Hansen, *J. Paint Technol.*, 39 (1967) 505.
4 A. F. M. Barton, *CRC Handbook of Solubility Parameters and Other Cohesion Parameters*, CRC Press, Boca Raton, FL, 1983.
5 E. R. Thomas and C. A. Eckert, *Ind. Eng. Chem. Process Des. Dev.*, 23 (1984) 194.
6 R. Tijssen, H. A. H. Billiet and P. J. Schoenmakers, *J. Chromatogr.*, 122 (1976) 185.
7 B. L. Karger, L. R. Snyder and C. Eon, *J. Chromatogr.*, 125 (1976) 71.
8 M. J. Kamlet, R. W. Taft, P. W. Carr and M. H. Abraham, *J. Chem. Soc., Faraday Trans. I*, 78 (1982) 1689.
9 C. Reichardt, *Solvent Effects in Organic Chemistry*, Verlag Chemie, Weiheim, 1979.
10 M. J. Kamlet, J. L. M. Abboud and R. W. Taft, in R. W. Taft (Editor), *Progress in Physical Organic Chemistry*, Vol. 13, Wiley, New York, 1980, pp. 485–630.
11 P. W. Carr, *J. Chromatogr.*, 194 (1980) 105.
12 C. R. Yonker and R. D. Smith, *J. Phys. Chem.*, 92 (1988) 2374.
13 L. Rohrschneider, *Anal. Chem.*, 45 (1973) 1241.
14 J. H. Park, A. Hussam, P. Couasnon, D. Fritz and P. W. Carr, *Anal. Chem.*, 59 (1987) 1970.
15 W. J. Cheong and P. W. Carr, *Anal. Chem.*, (1988) in preparation.
16 S. C. Rutan, P. W. Carr and R. W. Taft, *J. Phys. Chem.*, (1988) in press.
17 H. Poppe and E. H. Slaats, *Chromatographia*, 14 (1981) 89.
18 A. Ben-Naim, *J. Phys. Chem.*, 82 (1978) 792.
19 A. Bondi, *Physical Properties of Molecular Crystals, Liquids and Glasses*, Wiley, New York, 1968, pp. 453–469.
20 J. H. Park, P. W. Carr and S. C. Rutan, *J. Chromatogr.*, (1988) in preparation.
21 M. J. Kamlet, J. L. M. Abboud, M. H. Abraham and R. W. Taft, *J. Org. Chem.*, 48 (1983) 2877.
22 S. D. Brown, *Anal. Chim. Acta*, 181 (1986) 1.

23 S. C. Rutan, *J. Chemomet.*, 1 (1987) 7.
24 P. Shah, H. Na and L. B. Rogers, *J. Chromatogr.*, 329 (1985) 5.
25 K. Eckschlager and V. Stepanek, *Information Theory as Applied to Chemical Analysis*, Wiley, New York, 1979.
26 E. F. Meyer and R. E. Wagner, *J. Phys. Chem.*, 70 (1966) 3162.
27 E. F. Meyer, T. A. Renner and K. S. Stec, *J. Phys. Chem.*, 75 (1971) 642.
28 E. F. Meyer and C. A. Holtz, *J. Chem. Eng. Data*, 21 (1976) 274.
29 E. F. Meyer, M. J. Awe and R. E. Wagner, *J. Chem. Eng. Data*, 25 (1980) 371.
30 M. Chastrette, M. Rajzmann, M. Chanon and K. F. Purcell, *J. Am. Chem. Soc.*, 107 (1985) 1.
31 R. W. Taft, unpublished results, June 1988.

Journal of Chromatography, 463 (1989) 39–49
Elsevier Science Publishers B.V., Amsterdam — Printed in The Netherlands

CHROM. 21 038

THE SEPARATION PROCESS IN ISOTACHOPHORESIS

I. A 32-CHANNEL ULTRAVIOLET-PHOTOMETRIC ZONE DETECTOR

TAKESHI HIROKAWA*, KIYOSHI NAKAHARA and YOSHIYUKI KISO
Applied Physics and Chemistry, Faculty of Engineering, Hiroshima University, Shitami, Saijo, Higashi-hiroshima 724 (Japan)

(First received March 23rd, 1988; revised manuscript received September 12th, 1988)

SUMMARY

Multichannel ultraviolet (UV)-photometric zone detector was made in order to study the separation process in isotachophoresis. Thirty-two photometric cells with photodiode detectors were arrayed along the separation tube at intervals of *ca.* 5 mm (16.6 cm per 32 channels). Quartz optical fibres were used to pass UV light from a deuterium lamp to the tube. The detection limit of picric acid was *ca.* 10 pmol. The time resolution achieved in this system, a single cycle to scan the 32 detectors, was *ca.* 0.25 s by the use of an electrical scanning method, and it was sufficiently high to trace the variation of the zone lengths accurately. Using the apparatus, the separation process in binary mixtures [4,5-dihydroxy-3-(*p*-sulphophenylazo)-2,7-naphthalene-disulphonic acid and monochloroacetic acid, and monochloroacetic acid and picric acid] was measured and the boundary velocities and the resolution time were evaluated.

INTRODUCTION

A computer simulation of the isotachophoretic steady state[1] can be applied to the estimation of the optimum separation condition[2]. We have demonstrated the utility of this technique in practical analysis of many ionic substances. Simulated quantitative and qualitative indices have been tabulated for 287 anions[3]. However, the information obtained by steady state simulation is limited to the static properties of the separated zones[3,4]. In order to study the dynamics of separation, the simulation of the isotachophoretic transient state is inevitable. The resulting resolution time of the samples provides the criterion for the separation under the electrolyte and apparatus conditions used.

The resolution time for samples in isotachophoresis is closely related to the velocities of the mixed zone boundaries as extensively discussed by Mikkers *et al.*[5,6]. However the velocities have not been measured yet even for binary mixtures and all discussions concerning the dynamic features of isotachophoresis were based on the resulting resolution time. Moreover the fundamental problem of whether the progression of the mixed zone boundaries can be described by linear functions of time has not been solved.

0021-9673/89/$03.50

As detailed in the following paper, some different transient state models can be formulated. To obtain knowledge concerning the validity of these models, a zone scanning analyzer is indispensable to observe both the resolution time and the boundary velocity and to compare them with the theoretical estimates. For this purpose the time resolution of the analyzer must be sufficiently high for accurate observation of the separation process. Schumacher[7,8] reported a multichannel isotachophoretic analyzer equipped with an equidistant array of 256 detection electrodes (total length = *ca.* 10 cm) for observation of the potential gradient profile of the transient zones. Although Thormann *et al.*[8,9] studied the separation process of some organic acids using this system, the resolution time and boundary velocities were not reported.

In the apparatus reported[7,8], complex electronic circuits were necessary to isolate potential gradient detector signals from high voltage. Considering the convenience of construction, we designed a 32-channel UV photometric detection system. And an electrical scanning method was used to improve the time resolution instead of a mechanical scanning method[7,8].

In this paper we report the design and the detection limit of the UV detection system. The abilities to observe the resolution time and the velocity of the zone boundaries are also discussed for binary mixtures.

EXPERIMENTAL

Apparatus

Fig. 1 shows a schematic diagram of the UV-multichannel detection system. The length of the UV-photocell arrays to be scanned was 16.6 cm and the interval of

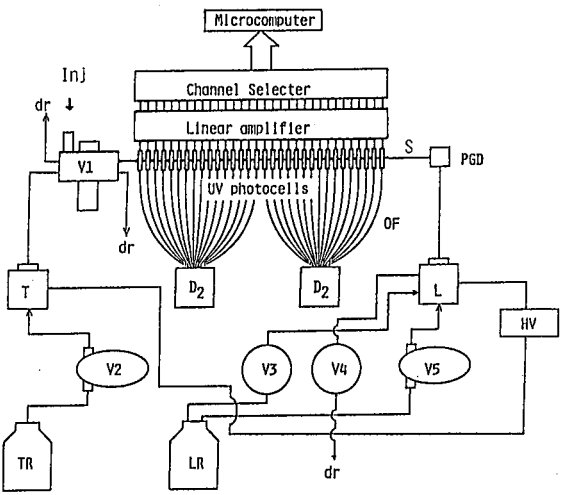

Fig. 1. Schematic diagram of isotachophoretic analyzer with 32-channel UV-photometric zone detector. S = PTFE separating tube; D_2 = D_2 lamp with power supply; OF = quartz optical fibres; L = leading electrode compartment; T = terminating electrode compartment; Inj = injection port; LR and TR = leading and terminating electrolyte reservoirs; V1–V5 = valves to fill or to drain the electrolytes; dr = drain; PGD = potential gradient detector; HV = high voltage power supply.

photocells was *ca.* 5 mm. The length of the photocell array was determined such that the transient state could be observed during 40 min under conditions where the leading ion was 5 m*M* Cl^- and the migration current was 50 μA.

A narrow-bore migrating tube penetrated the centre of 32 photocells, which were made of black acrylic resin (20 × 20 × 3 mm). The separating tube was made of PTFE and the I.D. and O.D. were 0.5 mm and 1 mm. The tube was irradiated by UV light from quartz optical fibres (OF in Fig. 1). The core and clad diameters were 0.8 mm and 1.1 mm, respectively. The fibres were set at right angles to the separating tube. The transmitted UV light was led to short-cut optical fibres (*ca.* 10 mm in length) plugged into the cell. Therefore the slit width of each photocell can be regarded as *ca.* 1 mm. At the end of the fibres were placed detection elements. The elements used were Model S1227-16BQ silicone photodiodes (15 × 2.7 × 2 mm) Hamamatsu, Japan. Each photodiode was equipped with a head amplifier using LF356N and LM741CN operational amplifiers.

The UV-light source was two Hamamatsu D_2 lamps (Model L1626, D_2 in Fig. 1) set separately in a box equipped with a cooling fan. The lamps were driven by an independent power supply (Hamamatsu Model C1518). The UV light from each D_2 lamp was led to 16 optical fibres through an UV-glass filter (Toshiba Glass, Tokyo, Japan, Model D33S, λ_{max} = 330 nm).

To obtain high time resolution, an electrical channel selector using analogue switches was utilized for scanning the UV signals from the head amplifiers. This was in contrast to the mechanical scanning of the electrodes in the multichannel detection system reported by Schumacher *et al.*[7,8]. By the control of a microcomputer system through an RS-232C line, the selector scanned the 32 detectors and the signal detected at each channel were successively acquired through an analogue-to-digital converter and subsequently stored in the 2MB random access memory (a RAM disk system) of the microcomputer. The use of the RAM disk system is important for rapid data acquisition. A single cycle to scan the 32 detectors per 16 cm, namely the time resolution of the system, was 243.2 ms. The rate-determining step was the transfer of the channel selection signal through the RS-232C line (9600 Baud). The time resolution was considerably improved in comparison with the previous multichannel analyzer[7,8] where it took *ca.* 30 s to scan the 255 detectors per 10 cm (data acquisition, 60 ms · 255; moving back to the first channel, 14 s).

Usually the number of data acquired was 5000–7000 per channel. After the acquisition was completed, the data in the RAM disk were transferred to a floppy disk. The data were evolved and analyzed to obtain the boundary velocities as discussed in a subsequent section. Since the levels of the acquired signals from each detector were different, they were normalized appropriately by multiplying factors.

Except for the detection system, the parts used were those of a commercial isotachophoretic analyzer (Model IP-1B, Shimadzu, Kyoto, Japan). The power supply was from a Shimadzu IP-2A. The distance from the injection port to the first photocell was about 16 cm. A potential gradient detector (PGD in Fig. 1) was placed at the end of the migrating tube, 5 cm from the 32nd photocell.

Samples

The samples were 4,5-dihydroxy-3-(*p*-sulphophenylazo)-2,7-naphthalene disulphonic acid (SPADNS), picric acid (PIC) and monochloroacetic acid (MCA). Except

for MCA, these samples absorb visible and ultraviolet light. The sodium salt of SPADNS was obtained from Dojin (Kitakyusyu, Japan) in the most pure form. The others were obtained from Tokyo Kasei (extra pure grade). Stock sample solutions (*ca.* 10 m*M*) were prepared by dissolving them in distilled water without further purification.

Operational electrolyte system

The concentration of the sample to be separated is closely related with that of the leading ion. For the SPADNS and MCA (1:1) system, the leading electrolyte was 10 m*M* hydrochloric acid. The pH was adjusted to 3.6 by adding β-alanine. For the MCA and PIC (1:1) system, the difference between the UV absorption of the mixed zone and that of the PIC zone was small when the 10 m*M* leading electrolyte was used, therefore in this case a 5 m*M* leading electrolyte was used for accurate boundary observation. The 2.5 m*M* leading electrolyte was used only for the sensitivity evaluation of PIC. The pH measurements were carried using a Model F7ss expanded pH meter (Horiba, Tokyo, Japan).

The terminator was 10 m*M* caproic acid. The sample solution was injected into the terminating electrolyte near the boundary between the leading and the terminating electrolytes.

Hydroxypropylcellulose (HPC, 0.2%) (Tokyo Kasei, Tokyo, Japan) was added to the leading and terminating electrolytes to suppress electroendosmosis. The viscosity of the 2% aqueous solution is 1000–4000 cP at 20°C according to the specification. The reproducibility of the observed boundary velocity was not so good when the HPC concentration was low, *e.g.*, 0.02%. The other cause of this was temperature variation. Although the apparatus was set in a thermostatted room (25°C), the experimental errors of a few percent could not be reduced.

The data processing was carried by the use of Model PC9801E and PC9801VX microcomputers (NEC, Tokyo, Japan). A Model DXY-980 (Roland DG, Tokyo, Japan) was used to plot the evolved pherograms.

RESULTS AND DISCUSSION

Sensitivity evaluation

Isotachopherograms of picric acid were obtained to estimate the practical detection limit of the system used by varying the injected amount in the range of 16 pmol–5 nmol (injected volume 1–5 μl). The concentration of the leading ion was 2.5 m*M*. Fig. 2 shows the observed UV response at 1–31 channels (interval: two channel) together with the blank test. The abscissa scale is the time of migration and the ordinate scale is the observed UV absorption. The position of baselines shows the distance of each UV photocell from the sample injection port. Apparently, 16 pmol picric acid were detected.

Arlinger[10] discussed the resolution and detection limits of isotachophoresis using an UV detector. The capillary diameter was 0.45 mm and the slit width of the detector was chosen as 0.2 mm. When a leading electrolyte of 0.5 m*M* hydrochloric acid–1 m*M* histidine was used (pH 5.98, 0.01% Triton X-100), the detection limit of adenosine triphosphate ion was 1 pmol. This result is comparable with that of the present work considering the difference in the leading ion concentrations.

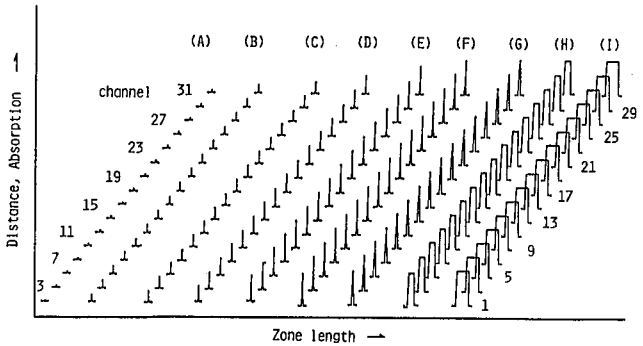

Fig. 2. Detection limit of picric acid by the use of the 32-channel UV-photometric detector. The position of the baselines shows the distance of the photocell from the sample injection port. (A) Blank test; (B) 15.7, (C) 39.2, (D) 62.7, (E) 157, (F) 313, (G) 627, (H) 2507 and (I) 5013 pmol. The leading ion was 2.5 m*M* hydrochloric acid (pH 3.6, buffer = β-alanine). The terminator was 10 m*M* caproic acid. The migration current was 24.5 μA. The I.D. of the separation tube was 0.54 mm.

Quantitative analysis in isotachophoresis using an UV detector can be achieved by analyzing the width of the zones in the case when the zone length is sufficiently larger than the slit width, *e.g.*, 5 nmol, (I) in Fig. 2. However, when the zone length is similar to or smaller than the width, the UV absorption band observed will have a quasi-Gaussian shape. As discussed by Svoboda and Vacík[11], in such a case the peak height is useful for determination; a linear relationship holds between the relative photometric height and the amount of sample injected.

The peak area can be utilized similarly instead of the peak height. Fig. 3 shows the relationship between the observed peak area in arbitrary units and the amount of picric acid. The gradient of the plots over *ca.* 1 nmol was different from that below *ca.* 1 nmol. According to our simulation, the zone length of 1 nmol picric acid is 3.2 mm under the electrolyte condition used. The length was three times as large as the clad diameter of the optical fibres used.

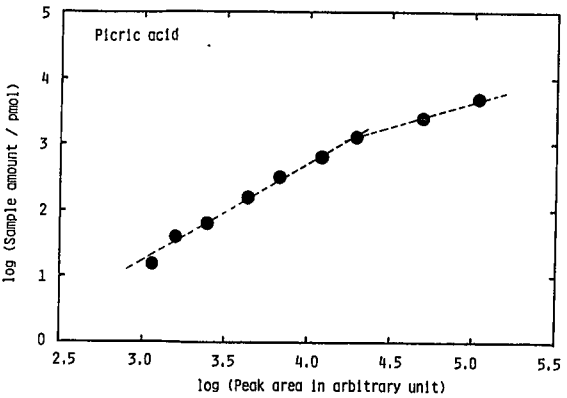

Fig. 3. The UV peak area in arbitrary units *vs.* sample amount of picric acid. The sample amount was varied from 15.7 to 5013 pmol. For the operational system, see Fig. 2.

The detection limit of picric acid is probably *ca.* 10 pmol. By the use of digital data processing, and if necessary appropriate UV-transparent spacers, the detection limit in isotachophoresis is probably comparable with those of high-performance liquid chromatography (HPLC) and capillary zone electrophoresis.

Separation process of the binary mixtures

Under the electrolyte condition used, the samples were detected in the order of SPADNS, MCA and PIC. To measure the separation process as ideally as possible, it is preferable to sandwich the sample solution by the leading and the terminating electrolytes at the initial stage. However, in this work the sample was injected into the terminating electrolyte near the interface of the leading and terminating electrolytes by use of a micro-syringe. Although the partial mixing of the sample solution and the terminating electrolyte was indispensable, no mixed zone between the sample and the terminator was observed. When the sample solution was injected into the leading electrolyte, however, the formation of a mixed zone of the leading ion and the most mobile sample ion was frequently observed.

Fig. 4 shows the evolution of a transient isotachopherogram of SPADNS and MCA, where the mixed zone of the leading ion and SPADNS was seen. The number of data used for the evolution was 3500 per channel. Before starting migration, in this particular case, the injected sample zone was forced to move toward the terminating electrolyte compartment. In Fig. 4, the boundaries between the terminating and the

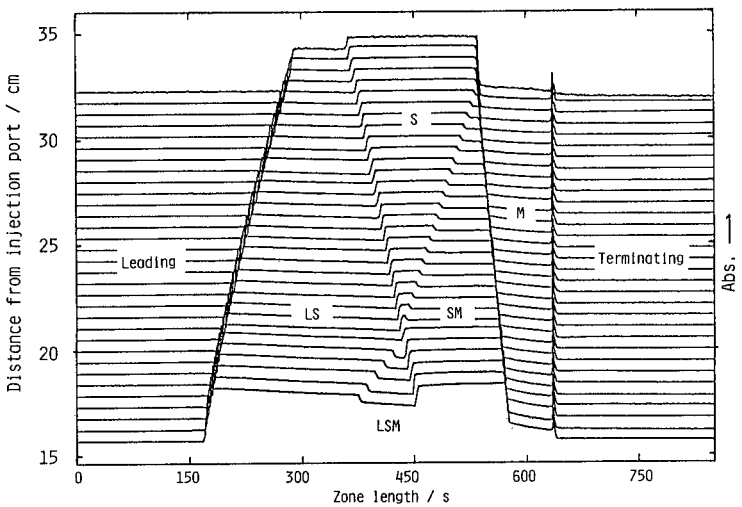

Fig. 4. Transient isotachopherogram of SPADNS and monochloroacetic acid observed by the use of the 32-channel UV-photometric detector. The injected sample zone was pushed toward the terminating electrolyte compartment. The position of baselines of the UV absorption shows the distance of the photocell from the sample injection port. The observed boundaries between the terminating and the preceding MCA zones were rearranged at the same abscissa position. Samples: 5 m*M* SPADNS(S); 5 m*M* monochloroacetic acid (M), 10 μl. LS, LSM and SM denote the mixed zones formed among the leading ions(L), SPADNS(S) and monochloroacetate ions(M). The leading electrolyte was 1 m*M* hydrochloric acid and the pH was adjusted to 3.6 (buffer β-alanine). The terminating electrolyte was 10 m*M* caproic acid. The migration current was 98.4 μA. The I.D. of the separation tube was 0.51 mm.

preceding MCA zones were rearranged at the same abscissa position to demonstrate clearly the change in the individual zone length at the transient state. This procedure correponds to the situation of 100% counterflow of the solvent. Considering the fact that the UV absorption was due to SPADNS and the concentrations in each zones were different from each other and all of the width-decreasing zones were mixed zones, the different zone found in Fig. 4 can easily be assigned as shown. Besides the mixed zone of the leading ion (Cl^-) and SPADNS(LS) and that of SPADNS and MCA(SM), a mixed zone of all of them (LSM) was seen. However that of the terminating ion (caproate) and MCA not observed.

Fig. 5 shows the transient isotachopherograms of a 1:1 mixture of SPADNS and MCA obtained under the usual conditions. The number of data used for the evolution was 1200 per channel. The boundaries between the terminating and the preceding PIC zones were rearranged at the same abscissa position. A small amount of PIC was added to the mixture to distinguish the terminating zone. The sample concentration was 1.25 m*M*. The sample amounts were (A) 40, (B) 50 and (C) 60 nmol. The mixed zone observed was due to SPADNS and MCA. The small peak adjacent to the terminating zone was due to the absorption of PIC. The zone imposed by the peak and the mixed zone (SM), the width of which was increasing, is that of MCA(M). It is apparent from Fig. 5A that the progression of the boundaries can be expressed by linear functions with respect to time. The boundary velocity of S/SM was smaller than the isotachophoretic velocity, V_{IP}, and that of SM/M was larger than V_{IP}. The time-based zone lengths of the whole sample zones were almost constant during detection. After the mixed zones were diminished, the zone lengths of the separated samples were constant.

In order to determine the boundary-detected time and subsequently the boundary velocity, the observed UV signals were differentiated with respect to time and the positive and negative peaks of the differentiated signals were searched. Table

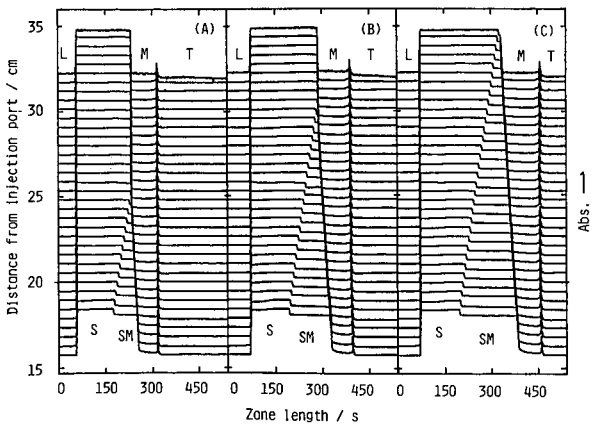

Fig. 5. Transient isotachopherogram of SPADNS(S) and monochloroacetic acid(M) observed by the use of the 32-channel UV-photometric detector. The sample concentration was 1.25 m*M* and the amounts were (A) 40, (B) 50 and (C) 60 nmol. SM = Mixed zone; L, T = the leading and terminating zones. For the operational system, see Fig. 4.

TABLE I

THE DETECTOR POSITION, BOUNDARY-DETECTED TIME AND TIME-BASED ZONE LENGTH FOR THE SPADNS AND MONOCHLOROACETIC ACID (1:1) SYSTEM

Operational system: leading electrolyte, 10 m*M* hydrochloric acid–*β*-alanine (pH 3.60). Current: 98.4 *μ*A. Diameter of the separation tube: 0.51 mm. Sample concentration: 1.25 m*M*. Sample amounts: each 40 nmol. –, Did not exist; ?, the exact boundary positions could not be estimated.

Detector position		*Boundary-detected time (s)*					*Overall zone length (s)*
No.	*mm*	*L/S*	*S/SM*	*S/M*	*SM/M*	*M/T*	
1	0	470.8	586.4	–	665.2	726.7	256.0
2	5.4	486.8	606.5	–	679.5	741.8	255.0
3	10.5	502.4	626.5	–	693.6	758.4	256.0
4	15.9	519.0	647.7	–	709.0	774.7	255.7
5	21.2	535.0	667.9	–	723.6	791.0	256.0
6	26.5	551.8	689.0	–	738.6	808.0	256.2
7	31.8	567.9	708.7	–	753.5	823.6	255.7
8	37.1	584.2	730.0	–	768.3	840.4	256.2
9	42.4	600.2	750.3	–	783.2	856.2	256.0
10	47.4	615.8	769.3	–	797.3	872.2	256.4
11	53.0	632.8	791.2	–	812.6	889.0	256.2
12	58.5	649.9	812.1	–	827.9	905.3	255.5
13	63.9	665.9	833.3	–	843.0	922.1	256.2
14	69.1	682.5	853.7	–	857.8	938.9	256.4
15	74.6	699.2	?	?	?	955.2	256.0
16	79.9	716.0	(173.7)*	889.7	(81.8)**	971.5	255.5
17	85.3	732.8	(173.7)	906.5	(81.5)	988.0	255.2
18	90.8	749.6	(173.7)	923.3	(81.0)	1004.3	254.7
19	96.1	766.4	(173.7)	940.1	(81.3)	1021.4	255.0
20	101.4	782.7	(173.5)	956.2	(81.8)	1038.0	255.2
21	106.9	799.5	(173.5)	973.0	(81.8)	1054.7	255.2
22	112.3	816.0	(173.7)	989.7	(82.0)	1071.7	255.7
23	117.8	832.8	(173.7)	1006.5	(81.8)	1088.3	255.5
24	123.1	848.9	(174.0)	1022.8	(81.8)	1104.6	255.7
25	128.4	865.7	(173.7)	1039.4	(81.8)	1121.1	255.5
26	133.6	881.7	(173.7)	1055.5	(82.0)	1137.4	255.7
27	138.9	898.0	(173.7)	1071.7	(81.8)	1153.5	255.5
28	144.2	914.6	(173.7)	1088.3	(81.5)	1170.0	255.2
29	149.6	930.6	(173.7)	1104.3	(81.8)	1186.1	255.5
30	154.8	947.2	(173.5)	1120.6	(82.0)	1202.6	255.5
31	160.2	963.5	(173.7)	1137.2	(81.8)	1218.9	255.5
32	165.5	979.5	(174.0)	1153.5	(82.0)	1235.5	256.0

* Zone length(s) of SPADNS.
** Zone length(s) of MCA.

I summarizes the boundary-detected time at each detector after starting the separation of SPADNS and MCA for the 40-nmol case. The boundary velocities can be evaluated by the least-squares method on the basis of these numerical data.

The resolution time, t_{res}, of a binary mixture (components A and B, effective mobility of A larger than that of B) can be expressed as follows[5]

$$t_{res} = l_A/(V_{IP} - V_{A/AB}) \quad (1)$$

TABLE II

OBSERVED BOUNDARY FUNCTIONS FOR THE SPADNS–MONOCHLOROACETIC ACID (1:1) SYSTEM AND THE RESOLUTION TIME

For the operational system, see Table I. V = Boundary velocity (mm s^{-1}) · 10. D = The observed intercepts of the boundary functions; the first detector position is the frame of reference. D_0 = The intercepts; the initial position of the leading electrolyte observed is the frame of reference. t_{res} = Resolution time.

	Sample amount (nmol)								
	40			*50*			*60*		
	V	*D*	D_0	*V*	*D*	D_0	*V*	*D*	D_0
L/S	3.246	−152.5	0	3.250	−158.6	0	3.224	−157.3	0
S/SM	2.583	−151.4	1.1	2.607	−158.1	0.5	2.582	−157.3	0
S/M	3.246	−209.0	−56.5	3.297	−232.8	−74.2	–	–	
SM/M	3.579	−237.9	−85.4	3.616	−267.5	−108.9	3.579	−284.7	−127.4
M/T	3.249	−235.8	−83.3	3.287	−264.8	−106.2	3.238	−280.8	−122.2
t_{res}(s)		868			1007			1222	

where l_A is the zone length of the component A at the steady state, V_{IP} the isotachophoretic velocity and $V_{A/AB}$ the boundary velocity of A/AB. Eqn. 1 can be rewritten in terms of the time-based zone length of component A, t_A

$$t_{res} = t_A/(1 - V_{R,A/AB}) \quad (2)$$

where $V_{R,A/AB}$ is the velocity ratio to V_{IP}. If t_A cannot be observed as in Fig. 5C, t_{res} can be obtained by solving simultaneous functions expressing the progression of the boundaries A/AB and AB/B. In the present study t_{res} was obtained by this method. The boundary functions and the observed t_{res} for the SPADNS and MCA system are shown in Table II. The distance between the injection port and the first detector was *ca.* 16 cm

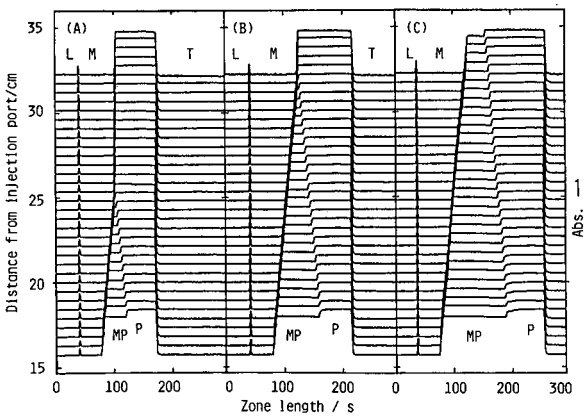

Fig. 6. Transient isotachopherogram of monochloroacetic acid and picric acid observed by the use of the 32-channel UV-photometric detector. The sample concentration was 5 m*M* and the amounts were (A) 15, (B) 20 and (C) 25 nmol. The leading electrolyte was 5 m*M* hydrochloric acid and the pH was adjusted to 3.6 (buffer β-alanine). The terminating electrolyte was 10 m*M* caproic acid. The migration current was 49.2 μA. The I.D. of the separation tube was 0.51 mm.

in this case, however the observed values were not consistent as shown. This shows that the initial sample zone moved slightly when it was connected with the leading electrolyte by the valve V1 in Fig. 1. The probable error of t_{res} was within 20–30 s.

Fig. 6 shows the observed transient isotachopherogram of MCA and PIC on varying the sample amounts. The number of data used for the evolution was 1200 per channel. Small amounts of SPADNS were added to the mixture to distinguish the

TABLE III

DETECTOR POSITION, BOUNDARY-DETECTED TIME AND TIME-BASED ZONE LENGTH FOR THE MONOCHLOROACETIC ACID AND PICRIC ACID (1:1) SYSTEM

Operational system: leading electrolyte, 5m*M* hydrochloric acid–*β*-alanine (pH 3.60). Current: 49.2 *μ*A. Diameter of the separation tube: 0.51 mm. Sample concentration: 4.6 m*M*. Sample amounts: each 15 nmol. –, Does not exist; ?, the exact boundary positions could not be estimated.

Detector position		*Boundary-detected time (s)*					*Overall zone length (s)*
No.	*mm*	*L/M*	*M/MP*	*M/P*	*MP/P*	*P/T*	
1	0	505.5	543.6	–	586.1	636.9	131.4
2	5.4	522.3	561.9	–	601.7	653.8	131.4
3	10.5	539.0	580.3	–	617.1	670.6	131.6
4	15.9	556.6	599.3	–	633.5	688.2	131.6
5	21.2	573.9	617.6	–	648.6	705.5	131.6
6	26.5	591.2	636.9	–	665.2	722.6	131.4
7	31.8	608.1	655.2	–	680.6	739.5	131.4
8	37.1	625.4	674.8	–	696.7	757.1	131.6
9	42.4	642.8	692.6	–	712.1	773.7	130.9
10	47.4	659.1	710.7	–	727.0	790.0	130.9
11	53.0	677.0	729.7	–	743.1	807.6	130.7
12	58.5	695.0	748.8	–	759.0	825.7	130.7
13	63.9	712.1	767.1	–	774.7	842.5	130.4
14	69.1	728.7	786.1	–	790.5	859.9	131.1
15	74.6	746.3	?	?	?	877.7	131.4
16	79.9	763.4	(59.3)*	822.8	(71.8)**	894.6	131.1
17	85.3	781.0	(59.6)	840.6	(71.6)	912.1	131.1
18	90.8	798.1	(59.8)	857.9	(71.8)	929.7	131.6
19	96.1	815.7	(59.8)	875.5	(72.5)	948.0	132.4
20	101.4	833.0	(60.1)	893.1	(71.8)	964.9	131.9
21	106.9	850.1	(60.6)	910.7	(72.5)	983.2	133.1
22	112.3	867.2	(60.8)	928.0	(72.8)	1000.8	133.6
23	117.8	885.0	(60.8)	945.8	(72.5)	1018.4	133.3
24	123.1	902.4	(61.1)	963.4	(72.0)	1035.5	133.1
25	128.4	919.5	(61.5)	981.0	(72.3)	1053.3	133.8
26	133.6	936.1	(61.8)	997.9	(72.3)	1070.2	134.1
27	138.9	953.4	(61.8)	1015.2	(72.5)	1087.7	134.3
28	144.2	970.8	(62.0)	1032.8	(72.0)	1104.8	134.1
29	149.6	988.3	(61.5)	1049.9	(72.3)	1122.2	133.8
30	154.8	1005.2	(62.0)	1067.2	(71.8)	1139.0	133.8
31	160.2	1023.3	(61.5)	1084.8	(71.6)	1156.4	133.1
32	165.5	1039.9	(62.3)	1102.1	(71.3)	1173.5	133.6

* Zone length (s) of MCA.
** Zone length (s) of PIC.

TABLE IV

OBSERVED BOUNDARY FUNCTIONS FOR THE MONOCHLOROACETIC ACID AND PICRIC ACID (1:1) SYSTEM AND THE RESOLUTION TIME

For the operational system, see Table III. For the definition of symbols, see Table II.

	Sample amount (nmol)								
	40			*50*			*60*		
	V	*D*	D_0	*V*	*D*	D_0	*V*	*D*	D_0
L/M	3.099	−156.7	0	3.101	−157.0	0	3.104	−162.6	0
M/MP	2.847	−154.8	1.9	2.859	−156.0	1.0	2.857	−160.7	1.9
M/P	3.063	−172.1	−15.4	3.051	−176.8	−19.8	–	–	–
MP/P	3.380	−198.2	−41.5	3.368	−210.4	−53.4	3.333	−225.9	−65.2
P/T	3.081	−196.0	−39.3	3.079	−209.0	−52.0	3.076	−168.8	−66.9
t_{res}		814			1069			1370	

leading zone. The sample concentration was 5 m*M* and the pH of the solution was 3.03. The sample amounts were (A) 15, (B) 20 and (C) 25 nmol. Table III shows the boundary-detected time in the separation process of the 15-nmol mixture. The boundary functions and the observed t_{res} for the MCA and PIC system are shown in Table IV. The resolution time needed for the MCA/PIC system is twice as large as that of the SPADNS/MCA system. This is because the mobility difference between MCA and PIC is smaller than that between SPADNS and MCA. The effective mobilities $\bar{m}$, at the steady state were $48 \cdot 10^{-5}$, $35 \cdot 10^{-5}$ and $29 \cdot 10^{-5}$ $cm^2\ V^{-1}\ s^{-1}$.

Thus the present apparatus is very useful for the study of the transient state, although the samples are restricted. Namely, in the two-component system, at least one of the samples must be UV-absorptive. A detailed discussion of factors affecting the boundary velocities and the resolution time will be reported in the following paper.

ACKNOWLEDGEMENTS

T. H. thanks the Ministry of Education, Science, and Culture of Japan for support of the part of this work under a Grant-in-Aid for Scientific Research (No. 61540423). The authors thank Fujikura Densen Co. for supplying the quartz optical fibres. They are also grateful for the helpful suggestions made by the referee, Dr. F. M. Everaerts (Eindhoven University of Technology, The Netherlands).

REFERENCES

1 F. M. Everaerts, J. L. Beckers and Th. P. E. M. Verheggen, *Isotachophoresis*, Elsevier, Amsterdam, 1976.
2 T. Hirokawa and Y. Kiso, *J. Chromatogr.*, 257 (1983) 197.
3 T. Hirokawa, M. Nishino, N. Aoki, Y. Kiso, Y. Sawamoto, T. Yagi and J.-I. Akiyama, *J. Chromatogr.*, 271 (1983) D1.
4 T. Hirokawa and Y. Kiso, *J. Chromatogr.*, 260 (1983) 225.
5 F. E. P. Mikkers, F. M. Everaerts and J. A. F. Peek, *J. Chromatogr.*, 168 (1979) 293.
6 F. E. P. Mikkers, F. M. Everaerts and J. A. F. Peek, *J. Chromatogr.*, 168 (1979) 317.
7 E. Schumacher, in F. M. Everaerts (Editor), *Analytical Isotachophoresis*, Elsevier, Amsterdam, 1981.
8 W. Thormann, D. Arn and E. Schumacher, *Electrophoresis*, 5 (1984) 323.
9 W. Thormann, D. Arn and E. Schumacher, *Electrophoresis*, 6 (1985) 10.
10 L. Arlinger, *J. Chromatogr.*, 91 (1974) 785.
11 M. Svoboda and J. Vacík, *J. Chromatogr.*, 119 (1975) 539.

Journal of Chromatography, 463 (1989) 51–71
Elsevier Science Publishers B.V., Amsterdam — Printed in The Netherlands

CHROM. 21 039

THE SEPARATION PROCESS IN ISOTACHOPHORESIS

II. BINARY MIXTURES AND TRANSIENT STATE MODELS

TAKESHI HIROKAWA*, KIYOSHI NAKAHARA and YOSHIYUKI KISO
Applied Physics and Chemistry, Faculty of Engineering, Hiroshima University, Shitami, Saijo, Higashi-hiroshima 724 (Japan)
(First received March 23rd, 1988; revised manuscript received September 12th, 1988)

SUMMARY

By the use of a multichannel ultraviolet-photometric zone detector, the separation processes in binary mixtures (monochloroacetic acid and picric acid, 4,5-dihydroxy-3-(*p*-sulphophenylazo)-2,7-naphthalenedisulphonic acid and monochloroacetic acid) were measured to obtain information about how the transient state is affected by the properties of the sample solution, such as the pH (pH_S), the concentration and the ratio of the constituent concentrations. It was found that the velocity of the mixed zone boundaries and the resolution time, t_{res}, of the binary systems were dependent on these properties to a considerable extent as previously reported for the chlorate–formate system by different authors. Some theoretical models are discussed to simulate the transient state. It is concluded by simulations that pH_S varies considerably at the initial stage of migration due to the influence of the buffer ion from the leading zone, namely the pH of the actually solution interfacing with the mixed zone formed is different from pH_S. The properties of the mixed zone are dependent not only on those of the sample but also on those of the leading zone. A good agreement was obtained between the observed and simulated t_{res} by considering this pH change.

INTRODUCTION

In order to study the dynamics of isotachophoretic separation, we constructed a 32-channel UV-photometric detection system and the design and the performance were reported in the preceeding paper[1]. The time to scan the 32 detectors per 16.5 cm was *ca.* 0.25 s and the high resolution allowed the accurate determination of the boundary velocities and the resolution time in the transient state.

Several studies have been reported concerning the analysis of the transient state. Brouwer and Postema[2] proposed a separation diagram and showed that the sample introduces a transient system of homogeneous zones which are finally reduced to the zones containing only one component of the sample. Vacik and Fidler[3] treated the transient state of a binary mixture theoretically by solving the differential equations of the separation. The transient state was also studied by Mikkers *et al.*[4,5] and the

0021-9673/89/$03.50

criterion of the separation was discussed in detail. Using the equations derived, they compared the simulated resolution time with the observed values. The most important conclusion of these studies was that for an isotachophoretic separation the ratio of the effective mobilities of the samples must be different from unity in the transient mixed zone, not at the steady state. Therefore the pH of the leading electrolyte is decisive for separation.

According to the theoretical approach of Mikkers *et al.*[4] in which the moving boundary equation was applied to the initial interface between the sample injected and the mixed zone formed, the separability was affected also by the properties of the sample solution such as the pH (pH_S), the concentrations and the effective mobilities of the constituents. We call the model proposed in the simulation by Mikkers *et al.*[4,5] the SPR (sample property reflecting) model hereafter. As discussed in ref. 5, the agreement between the simulated and the observed resolution time was very good when the samples were weak acids. However, for a mixture of weak and strong acids, the simulated pH_S dependence of the resolution time was overestimated. The SPR model was not present on the separation diagram proposed by Brouwer and Postema[2]. However the formulation of the SPR model is very persuasive and the discrepancy of 50% found for formic and chloric acids ($pH_S = 2.4$) may not be a problem from the practical viewpoint[5]; it probably suggests that a fundamentally important problem still remains in the SPR model.

As described in a later section, the theoretical estimates of the boundary velocities and the resolution time depend considerably on whether the velocity of the initial boundary between the solution injected and the mixed zone formed in the separation process is zero or not, in other words, whether the initial boundary can be treated as an ideal concentration boundary.

In this study, first the validity of the separation diagram proposed by Brouwer and Postema[2] was examined using a zone scanning analyzer. Next the resolution time and the boundary velocities of binary mixtures were measured accurately and compared with the theoretical estimates on the basis of some different physical models concerning the initial boundary in the separation process.

THEORETICAL

Assuming a binary mixture of constituents A and B, the stack configuration supposed at the transient state is the leading zone (L), A, the mixed zone AB, B and the terminating zone (T).

Brouwer and Postema[2] discussed the separation process in isotachophoresis and suggested a separation diagram of a binary mixture in a separation tube as illustrated in Fig. 1. On the basis of this simple model, an important relationship between the sample concentration in the steady state zones and that of the mixed zone can be derived, which is closely related with the resolution time, t_{res}.

The distance, D, of the boundaries from the sample-injected position (the initial interface between the sample solution injected and the leading zone) was expressed as a linear function of time, t,

$$D_{L/A} = V_{IP}t \tag{1}$$

$$D_{A/AB} = V_{A/AB}t \qquad t \leqslant t_{res} \tag{2}$$

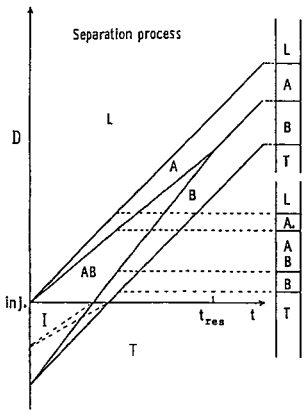

Fig. 1. Separation diagram for a binary mixture in a separation tube. D = Distance from injection port (inj); t = time; t_{res} = resolution time; I = zone of sample solution injected; L = leading zone; A, B = steady state zones; AB = mixed zone; T = terminating zone.

$$D_{A/B} = V_{IP}t - l_A \qquad t \geqslant t_{res} \tag{3}$$

$$D_{AB/B} = V_{AB/B}t - (l_A + l_B) \qquad t \leqslant t_{res} \tag{4}$$

$$D_{B/T} = V_{IP}t - (l_A + l_B) \tag{5}$$

where V_{IP} denotes the isotachophoretic velocity, $V_{A/AB}$ and $V_{AB/B}$ the velocity of the boundaries A/AB and AB/B and l_A and l_B are the zone lengths of components A and B at the steady state, which vary in proportion to the sample amount. We will call eqns. 1–5 the boundary functions hereafter. They express the solid lines in Fig. 1, where the zone length of the sample solution injected is equal to $l_A + l_B$. When the concentration is high keeping the sample amount constant, the separation process may follow the broken lines. The gradients of the broken lines depend on the sample concentration, however the separation diagram suggests that $V_{AB/B}$ and $V_{A/AB}$ are independent of the concentration of the sample solution. Therefore the behaviour of the zone boundaries in the transient state may be treated as illustrated by the solid lines in Fig. 1.

From the separation diagram, t_{res} can be expressed by the following equations:

$$t_{res} = l_A/(V_{IP} - V_{A/AB}) \tag{6}$$

or

$$t_{res} = l_B/(V_{AB/B} - V_{IP}) \tag{7}$$

As far as the separation diagram is valid, the values of t_{res} from eqns. 6 and 7 must coincide. A different expression of t_{res} can be obtained by eliminating V_{IP} from eqns. 6 and 7:

$$t_{res} = (l_A + l_B)/(V_{AB/B} - V_{A/AB}) \tag{8}$$

This equation can be derived also from the relationship $D_{A/AB} = D_{AB/B}$ at t_{res}. The velocity of the mixed zone boundaries can be derived from the moving boundary equation[6] as

$$V_{A/AB} = E_{AB}\bar{m}_{B,AB} \tag{9}$$

$$V_{AB/B} = E_{AB}\bar{m}_{A,AB} \tag{10}$$

where E_{AB} denotes the potential gradient of the mixed zone, $\bar{m}_{B,AB}$ and $\bar{m}_{A,AB}$ the effective mobilities of the constituents in the mixed zone.

The total amount of samples in the zone interposed by the L/A and B/T boundaries equals the amount injected, and is constant regardless of the separation process being at the transient state or at the steady state. Therefore the concentration of sample A in the mixed zone AB, $C^t_{A,AB}$, and that in the steady zone, $C^t_{A,S}$, can be correlated as:

$$(V_{IP} - V_{A/AB})tC^t_{A,S} + [V_{A/AB}t - V_{AB/B}t + (l_A + l_B)]C^t_{A,AB} = l_A C^t_{A,S} \tag{11}$$

The separation diagram suggested that eqn. 11 may be valid from $t = 0$ to $t = t_{res}$ irrespective of whether the zone length of the sample solution injected is equal to the sum $l_A + l_B$ or not. Then eqn. 11 can be reduced by inserting $t = 0$:

$$C^t_{A,AB} = l_A/(l_A + l_B)C^t_{A,S} \tag{12}$$

For component B, similarly:

$$C^t_{B,AB} = l_B/(l_A + l_B)C^t_{B,S} \tag{13}$$

Then the ratio of the concentrations is expressed as:

$$\frac{C^t_{B,AB}}{C^t_{A,AB}} = \frac{l_B C^t_{B,S}}{l_A C^t_{A,S}} \tag{14}$$

Eqn. 14 suggests that the ratio of the total concentrations of the sample constituents in the mixed zone is correlated with that of the sample amounts, and is completely independent of the properties of the initial sample solution. Hereafter we will refer to this transient model as the non-SPR model. As discussed in refs. 4 and 5, t_{res} depends strongly on the ratio $C^t_{B,AB}/C^t_{A,AB}$.

In the SPR model[4], on the other hand, the ratio was derived by applying the moving boundary equation[6] to the initial interface, namely, the boundary between the sample solution injected and the transient mixed zone. The moving boundary equation for component A can be written as

$$\frac{\bar{m}_{A,I}C^t_{A,I}E_I - \bar{m}_{A,AB}C^t_{A,AB}E_{AB}}{C^t_{A,I} - C^t_{A,AB}} = V_{I/AB} \tag{15}$$

where $\bar{m}_A$ denotes the effective mobility (the product of the mobility and the degree of

dissociation) of ion A, E the potential gradient, and the subscript I the zone of the sample solution injected. A similar equation can be written for component B:

$$\frac{\bar{m}_{B,I}C^t_{B,I}E_I - \bar{m}_{B,AB}C^t_{B,AB}E_{AB}}{C^t_{B,I} - C^t_{B,AB}} = V_{I/AB} \tag{16}$$

An assumption was made that the boundary is an ideal concentration boundary, namely the boundary velocity, $V_{I/AB}$, is null. Consequently, from eqns. 15 and 16, the following relationship was obtained:

$$\frac{C^t_{B,AB}}{C^t_{A,AB}} = \frac{\bar{m}_{A,AB}\bar{m}_{B,I}C^t_{B,I}}{\bar{m}_{B,AB}\bar{m}_{A,I}C^t_{A,I}} \tag{17}$$

The effective mobilities $\bar{m}_{A,I}$ and $\bar{m}_{B,I}$ in eqn. 17, hence $\bar{m}_{B,AB}$ and $\bar{m}_{A,AB}$ in eqns. 6–10, will depend on the pH of the sample solution, pH_S. Besides the concentration ratio, t_{res} depends on the relative mobility of the samples and buffer ions, the mobility of the leading ion, the dissociation constants, the degree of dissociation of samples in the mixed zone and those of the samples in the solution injected[4]. Therefore, even if the sample amount is constant, the SPR model demands that the resolution time depends on pH_S especially for the separation of a pair of weak and strong electrolytes.

The SPR formulation reported is applicable to a binary system, where the component ions are monovalent and the ionic strength of all zones is zero[4]. We extended the previous SPR model to treat multivalent ions by considering ionic strength as follows.

(1) The mobilities of the sample components A, B and the buffer ion Q were calculated on the basis of the dissociation constants and the pH of the mixed zone. For simplicity a monovalent buffer ion was assumed. At the first stage of iteration the pH of the mixed zone was assumed equal to the average of the pH values of the zones at the steady state.

(2) The potential gradient of the mixed zone, E_{AB}, was calculated from the following equation derived from the moving boundary equation for the boundary A/AB:

$$E_{AB} = \frac{\bar{m}_A E_A C^t_A}{\bar{m}_{A,AB}C^t_{A,AB} + \bar{m}_{B,AB}(C^t_A - C^t_{A,AB})} \tag{18}$$

(3) The total concentration of the buffer ion in the mixed zone, $C^t_{Q,AB}$, was calculated from the following equation derived from the moving boundary equation for the boundary A/AB:

$$C^t_{Q,AB} = \frac{\bar{m}_{Q,A}E_A + \bar{m}_{B,AB}E_{AB}}{(\bar{m}_{Q,AB} + \bar{m}_{B,AB})E_{AB}} \cdot C^t_{Q,A} \tag{19}$$

The partial concentration of the buffer ion at the pH was also calculated.

(4) From the electroneutrality relationship in the mixed zone, the concentrations of components A and B can be calculated as

$$C^{t}_{A,AB} = F_1/(F_2 + F_3F_4) \tag{20}$$

$$C^{t}_{B,AB} = C^{t}_{A,AB}F_4 \tag{21}$$

$$F_1 = -[C_H - C_{OH} + C^{t}_{Q,ABC}/(1 + k_Q/c_H)] \tag{22}$$

$$F_2 = \frac{\sum_{i=1}^{n_A} [z_{A,i}(\Pi k_{A,i})/C_H^i]}{1 + \sum_{i=1}^{n_A} (\Pi k_{A,i})/C_H^i} \tag{23}$$

$$F_3 = \frac{\sum_{i=1}^{n_B} [z_{B,i}(\Pi k_{B,i})/C_H^i]}{1 + \sum_{i=1}^{n_B} (\Pi k_{B,i})/C_H^i} \tag{24}$$

$$F_4 = \frac{\bar{m}_{B,I}C^{t}_{B,I}\bar{m}_{A,AB}}{\bar{m}_{A,I}C^{t}_{A,I}\bar{m}_{B,AB}} \tag{25}$$

where C_H and C_{OH} denote the concentrations of H^+ and OH^-, $C^{t}_{Q,ABC}$ the total concentration of buffer in the zone ABC, k_Q, k_A and k_B the acid dissociation constants, $z_{A,i}$ and $z_{B,i}$ the ionic charge of the ith constituent ion of component A and B, and n_A and n_B the numbers of the constituent ions. A monovalent cationic buffer was assumed in eqn. 22. The partial concentrations of the component ions at the pH were also calculated.

(5) The specific conductivity of the mixed zone, κ_{AB}, was calculated considering all ionic constituents in the mixed zone.

(6) The consistency of the current density was checked by the following RFQ function:

$$RFQ = (E_A\kappa_A/E_{AB}\kappa_{AB}) - 1 \tag{26}$$

Until RFQ was considered as zero (actually we used a threshold value of 10^{-5}), steps (1)–(6) were repeated by varying the pH of the mixed zone.

A computer program SIPSR was written in order to simulate the transient state according to the above procedure by modification of a program SIPS for the steady state analysis[7,8]. The above procedure was essentially the same as the previously proposed SPR model in principle. Actually the result obtained by SIPSR (see below) was very similar to that reported by Mikkers *et al*[5], when the SPR model was used. In SIPSR, however, the effect of the ionic strength on the mobility and dissociation constants was taken into account together with the contributions of H^+ and OH^- to the zone conductivity, all of which were neglected in refs. 4 and 5. By introducing these corrections, the algebraic expression of t_{res} cannot be given in a simple form. The value of t_{res} was obtained as a result of an iterative calculation. The non-SPR model using eqn. 14 instead of eqn. 17 for the ratio of the concentrations of the components in the

mixed zone can also be tested by SIPSR. As shown in this section, the dependences of pH_S on t_{res} in the non-SPR model and the SPR model will be different. The difference between the theoretical estimates obtained by these models will be discussed in a later section in comparison with the experimental results.

EXPERIMENTAL

The samples were 4,5-dihydroxy-3-(*p*-sulphophenylazo)-2,7-naphthalenedisulphonic acid (SPADNS), picric acid (PIC) and monochloroacetic acid (MCA). Except for MCA, these samples absorb visible and ultraviolet light. The sodium salt of SPADNS was obtained from Dojin in the most pure form. The other compounds were obtained from Tokyo Kasei (extra pure grade). Stock sample solutions (*ca.* 10 m*M*) were prepared by dissolving them in distilled water without further purification. As discussed later, the resolution time of PIC and MCA was measured by varying the pH of the mixture solution. The pH was adjusted to 2.5–3.7 by adding β-alanine. The pH measurements were carried out using a Horiba expanded pH meter, Model F7ss.

The leading electrolyte (hydrochloric acid) used was 5 and 10 m*M*. The pH was adjusted to 3.6 by adding β-alanine. The terminator was 5 and 10 m*M* caproic acid. Hydroxypropylcellulose (HPC, 0.2%) was added to the leading and terminating electrolytes to suppress electroendosmosis. The sample solution was injected into the terminating electrolyte near the boundary between the leading and the terminating electrolytes. The pH of the terminating electrolyte was also adjusted by β-alanine to ensure the pH of the sample solution at the initial stage of migration was equal to the prepared value. The separating tubes used were 0.51 mm I.D. and 1 mm O.D., and 0.54 mm I.D. and 1 mm O.D. All experiments were carried out at 25°C.

The data processing and the simulation were carried out by the use of NEC PC9801E and PC9801VX microcomputers. The figures were plotted by a Roland DG Model DXY-980.

TABLE I

PHYSICO-CHEMICAL CONSTANTS USED IN SIMULATION (25°C)

m_0 = Absolute mobility ($cm^2\ V^{-1}\ s^{-1}$) · 10^5; pK_a = thermodynamic acid dissociation constants, assumed value being used for Cl^-.

Ion	m_0	pK_a
Cl^-	79.08	−2
β-Alanine$^+$	36.7*	3.552
GABA$^+$	30**	4.03
Histidine$^+$	29.7	6.04
Formate$^-$	56.6	3.752
Glycolate$^-$	42.4	3.886
ClO_3^-	67.0	−2.7
Monochloroacetate$^-$	41.1*	2.865
Picrate$^-$	31.5	0.708

* The mobilities were obtained by our isotachophoretic method or conductivity measurement. The other mobilities and pK_a values are taken from ref. 9.

** γ-Aminobutyric acid, ref. 5.

RESULTS AND DISCUSSION

Under the electrolyte condition used, the samples were detected in the order of SPADNS, MCA and PIC. The simulated effective mobilities, $\bar{m}$, at the steady state were $47.7 \cdot 10^{-5}$, $35.1 \cdot 10^{-5}$ and $29.3 \cdot 10^{-5}$ $cm^2\ V^{-1}\ s^{-1}$, and the R_E values ($R_E = \bar{m}_L/\bar{m}_S = E_S/E_L$, where E is the potential gradient, and L and S the leading and sample ions, respectively) were 1.59, 2.16 and 2.59 respectively. Table I shows the m_0 and pK_a values of the samples and electrolyte constituents used in the simulations.

Separation diagram

First the boundary functions (eqns. 1–5) were determined for a 1:1 mixture of SPADNS(S) and MCA(M) to compare with the separation diagram (Fig. 1). These functions can be determined accurately by the least-squares method using the exact positions of the photocells and the times when the boundaries passed each cell. The sample concentration was varied in the range of 1.25–10 m*M*. A small amount of PIC was added to the mixture to distinguish the UV-transparent terminating zone. When the sample concentration was 2.5 m*M* and the concentration of the leading electrolyte was 10 m*M*, the zone length of the solution injected was almost equal to the sum of the zone lengths of the separated samples at the steady state. In this case, the separation processes expected were those illustrated in Fig. 1 by the solid lines.

Fig. 2. shows the transient isotachopherograms obtained for the 1.25 (A) and 10 m*M* (B) mixtures respectively. The sample amount was 60 nmol and pH_S = *ca.* 2.5. The time-based zone lengths at the steady state were 377.9 and 380 s respectively. The boundaries between the leading and the SPADNS zones were rearranged at the same abscissa position. The mixed zone observed was that of SPADNS and MCA. The small peak adjacent to the terminating zone was due to the absorption of PIC. The zone

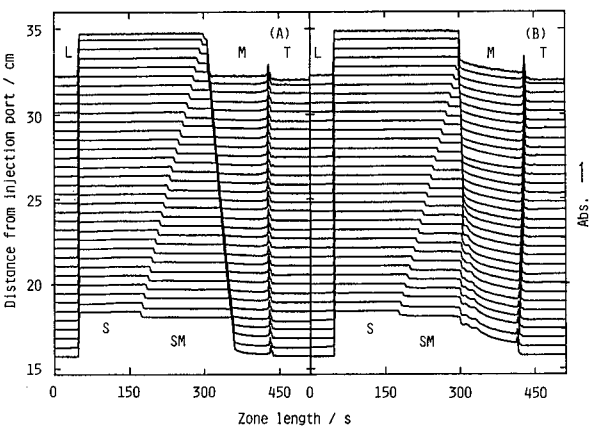

Fig. 2. Transient isotachopherogram of SPADNS and monochloroacetic acid observed by the use of the 32-channel UV-photometric detector. The sample concentration was 1.25 (A) and 10 m*M* (B). The sample amount was 60 nmol. The position of the baselines of the UV absorption shows the distance of the photocell from the sample injection port. The migration current was 98.4 μA. The leading electrolyte was 10 m*M* hydrochloric acid and the pH was adjusted to 3.6 (buffer β-alanine). The terminator was 10 m*M* caproic acid.

imposed by the peak and the mixed zone (SM) is that of MCA (M). The time-based zone lengths of the whole sample zones were almost constant during detection. In such cases, the correlation coefficients obtained in the linear least-squares fitting were better than 0.99999 for all boundary functions; the value 1 was obtained frequently. The observed pherograms for 2.5 and 5 m*M* samples were very similar to that for 1.25 m*M*.

When the 10 m*M* mixture was analyzed, as shown in Fig. 2B, loose boundaries were observed between the SM and M zones with high reproducibility. Such loose boundaries were never observed at the boundary S/SM. Besides the uniform mixed zone, it is apparent from the UV absorption that the MCA zone was contaminated with a considerable amount of SPADNS, although this amount decreased gradually with time. This phenomena was found also in the 5-m*M* case, but to a much smaller extent. In such cases the linearity of the boundaries L/S and S/SM was as good as that for the dilute samples, however that of the boundaries SM/M and M/T was slightly worse. From Fig. 2, the so-called mixed zone found in the 10-m*M* case diminished more rapidly than in that of the 1.25-m*M* case. However, a considerable amount of SPADNS still remained in the MCA zone after the mixed zone had diminished.

The cause of the loose boundaries in the 10 m*M* mixture (the different types of concentration boundaries which are not shown in Fig. 1) can be elucidated as follows: the sample solution injected mixed partially with the terminating electrolyte and the resulting solution was not homogeneous in concentration. The potential gradient in the initial solution decreases with increasing concentration, therefore a longer period will be necessary to reject, *e.g.*, terminating ions from the initial zone when the concentrated sample is analyzed. For the diluted mixtures, the inhomogeneities of the initial solution will diminish rapidly and the observed transient state can be regarded as an ideal pattern in the ideal binary system. Thus the transient state observed for the 10

TABLE II

DEPENDENCE OF SAMPLE CONCENTRATION ON THE OBSERVED RELATIVE BOUNDARY VELOCITY AND THE INTERCEPTS OF THE BOUNDARY FUNCTIONS FOR THE SPADNS–MONOCHLOROACETATE SYSTEM (1:1)

Time-based zone length is normalized to 300 s. Operational system: leading electrolyte 10 m*M* hydrochloric acid–*β*-alanine (pH 3.60); current = 98.4 *μ*A; diameter of the separation tube = 0.51 mm; sample amounts (S, M) each 20.0 nmol (S = SPADNS, M = monochloroacetic acid). V_R = relative velocity (boundary velocity/V_{IP}); D_0 = intercepts of the boundary function (mm).

	Concentration of samples (mM)			
	1.25	*2.5*	*5*	*10*
$V_{R,S/SM}$	0.798 ± 0.002	0.796 ± 0.003	0.798 ± 0.005	0.791 ± 0.004
$V_{R,SM/M}$	1.105 ± 0.003	1.088 ± 0.005	1.071 ± 0.007	1.046 ± 0.007
$V_{R,M/T}$	1.004 ± 0.003	1.006 ± 0.005	0.984 ± 0.005	0.977 ± 0.005
$D_{0,L/S}$*	0	0	0	0
$D_{0,S/SM}$	0.7 ± 0.3	1.1 ± 0.5	1.9 ± 0.9	− 0.3 ± 0.7
$D_{0,S/M}$	− 67.8 ± 1.5	−68.1 ± 2.4	−60.2 ± 2.2	−58.0 ± 2.3
$D_{0,SM/M}$	−101.3 ± 1.2	−96.5 ± 2.0	−86.4 ± 2.4	−76.4 ± 3.2
$D_{0,M/T}$	− 98.6 ± 1.2	−97.4 ± 1.5	−90.4 ± 1.9	−90.7 ± 1.9

* The position of injection port is the frame of reference.

mM solution in the present experiments cannot simply be compared with those for the 1.25, 2.5 and 5 mM solutions.

Table II summarizes the dependences of the sample concentration on the relative boundary velocity, V_R, and the intercepts of the boundary functions, D_0. The intercepts were normalized to the time-based zone length of 300 s, which corresponded to the absolute zone length of 97 mm in the separating tube (I.D. = 0.51 mm). $V_{R,SM/M}$ decreased with increasing sample concentration, while that of S/SM was kept almost constant. If the migration model in Fig. 1 is valid, the intercepts of the boundary functions of L/S and S/SM should be zero (eqns. 1 and 2). In the present work this was valid considering the probable error. The intercepts of the boundary functions of SM/M and M/T (eqns. 4 and 5) also must coincide with each other and in this case the value should be -97 mm. When the sample concentration was 1.25 and 2.5 mM, these conditions were satisfied approximately. At higher concentrations, however, the conditions were not satisfied.

The conclusion is that the migration model in Fig. 1 is valid to a first approximation. Although the observed discrepancy between the intercepts of the SM/M and M/T boundary functions suggested a limitation of the model, so far we cannot deny the non-SPR model absolutely because the discrepancy was small. Another important conclusion was that the use of eqn. 6 is adequate for the evaluation of t_{res}. However the use of eqns. 7 and 8 is not always adequate for practical samples, since the boundary functions of the AB/B and B/T zones are easily perturbed by the mixing with the terminator.

It may be interesting to compare how different are the estimations of the separation process obtained by the non-SPR and the SPR models. Therefore we simulated the boundary velocities and resolution times of some binary systems by use of the models and compared them with the observed values.

Dependence of sample properties on the separation process

As already mentioned, the only difference between the SPR model and the non-SPR model is the expression for the ratio of the constituent concentrations, $C^i_{B,AB}/C^i_{A,AB}$, which are given by eqns. 14 and 17. Eqn. 14 of the non-SPR model contains only the zone length and the sample concentration at the steady state. On the other hand, eqn. 17 contains the effective mobility and the concentrations of the constituents both in the initial solution and in the mixed zone AB.

When the pK_a values of the samples are equal, in the SPR model, $\bar{m}_{A,I}$ and $\bar{m}_{B,I}$ in eqn. 17 vary in a similar manner corresponding to the pH of the sample solution, pH_S. Therefore t_{res} will be hardly affected by the variation of pH_S. This estimation by the SPR model has been verified by the observation of t_{res}[5] for glycolic acid (pK_a = 3.83) and formic acid (pK_a = 3.752)[9]. The agreement was very good and the deviations were 2–10% in the range pH 2.5–4.3. This system was studied first.

Mikkers *et al.* introduced the concept of the separation number, S, which enables the criterion of separation irrespective of the instrumental condition except for the migration current, i

$$S = \frac{F}{i} \cdot \frac{\partial n_A}{\partial t} = \frac{F}{i} \cdot \frac{n_A}{t_{res}} \tag{27}$$

where F is the Faraday constant and n_A the sample amount of constituent A. Table III summarizes t_{res} and S simulated by the Mikkers SPR model (SPR-I), the present SPR model (SPR-II), the non-SPR model and the observed values[5]. Apparently the agreement is good. The slight difference observed between SPR-II and SPR-I is due to whether the ionic strength correction was considered or not. For such a binary system, it is apparent that the SPR and the non-SPR are both useful for the transient state analysis. The simulated S value in ref. 5 for this system was 0.100 and which is 20% smaller than the present result. From the good agreement in the formate–chlorate system shown below, the discrepancy was attributed to the difference between the absolute mobility of glycolate used. This mobility was not cited in ref. 5. The estimated mobility to give $S = 0.1$ was $45 \cdot 10^{-5}$ cm^2 V^{-1} s^{-1}.

Then, the S and t_{res} observed[5] for a pair of strong acid and weak acid (chloric acid, $pK_a < 1$; and formic acid, $pK_a = 3.752$) were compared with the simulated values (Table III). The significant dependence of pH_S on S and t_{res} was simulated by the SPR model (<70%); on the other hand, no pH_S dependence was simulated by the non-SPR model. The observed pH_S dependence was less than 25% in the pH range. It is apparent that the non-SPR model is not suitable to simulate the observed pH_S dependence, however the S and t_{res} simulated by the non-SPR model agreed well with those by the SPR model at relatively high pH_S. Thus the transient state estimated by the non-SPR model is essentially the same as that estimated by the SPR models at high pH_S. In other words, the validity of eqn. 14 derived from the separation diagram in Fig. 1 depends on the pH_S.

TABLE III

SIMULATED AND OBSERVED SEPARATION NUMBER AND RESOLUTION TIME FOR FORMATE–GLYCOLATE AND CHLORATE–FORMATE SYSTEMS (1:1)

Operational system: leading electrolyte 10 mM hydrochloric acid–γ-aminobutyric acid (GABA, pH 4.03); current = 80 μA; diameter of the separation tube = 0.45 mm; sample amount = 100 nmol. S = separation number, see text; t_{res} = resolution time.

pH of sample	*Simulated*						*Observed*	
	*SPR-I**		*SPR-II***		*Non-SPR***		S	t_{res}***
	S	t_{res}	S	t_{res}	S	t_{res}		
Formate–glycolate system								
2.5	0.119	1014	0.124	972	0.113	1065	0.098	1230
3.0	0.118	1025	0.123	980	0.113	1065	0.098§	1230
3.5	0.115	1050	0.120	1003	0.113	1065	0.097§	1240
4.0	0.111	1088	0.116	1037	0.113	1065	0.095§	1270
Chlorate–formate system								
2.4	0.276	437	0.270	447	0.154	782	0.179	674
3.0	0.244	493	0.236	512	0.154	782	0.170§	709
3.5	0.202	597	0.193	624	0.154	782	0.155§	778
4.0	0.165	732	0.160	754	0.154	782	0.142§	849

* Mikkers formulation was used (ionic strength = 0).
** Present formulation, ionic strength was considered.
*** Estimated from S.
§ From Fig. 3 in ref. 5.

The cause of the overestimation of the pH_S dependence by the SPR model has been explained by the fact that the model made no allowance for the influence of a relatively high proton concentration at low pH_S and the functioning as a mobile counter constituents will decrease the efficiency of separation[5]. The elucidation may not be suitable in this case because the resolution times of the weak acid mixtures were observed under similar pH_S conditions. Moreover, in our SPR model (SPR-II), the influence of the proton was considered in the evaluation of the zone conductivity, however the simulated t_{res} values were essentially the same as those obtained with Mikkers SPR model (SPR-I) as shown in Table III.

Then the assumptions made in the SPR formulation were examined by simulation. The most important assumption was that the initial interface between the sample solution injected and the gradually formed mixed zone (I/AB) is treated as the ideal concentration boundary, namely the boundary is solvent-fixed. The other important assumption was that the pH of the sample solution injected was kept constant during analysis.

Mikkers *et al.*[4] suggested that it is not necessary to incorporate the hydrogen constituent into the moving boundary equation, quoting the literature[10–13]. When E_I in eqns. 15 and 16 is calculated from the zone conductivity of the injected solution for the evaluation of $V_{I/AB}$, therefore, two different ways were used. First the calculation was carried out as usual considering all ionic species in the injected solution: the partial contribution of H^+ to the conductivity was evaluated by $C_H\bar{m}_H F$ (C_H = concentration of H^+, $\bar{m}_H$ = mobility of H^+, F = Faraday constant). Next, the contribution of H^+ was evaluated by $C_H\bar{m}_Q F$ ($\bar{m}_Q$ = mobility of buffer). Table IV summarizes the

TABLE IV

SIMULATED VELOCITY OF THE BOUNDARY BETWEEN THE INJECTED SAMPLE ZONE AND THE MIXED ZONE FORMED FOR CHLORATE–FORMATE SYSTEM (1:1)

For the operational system see Table III. Simulated isotachophoretic velocity = 0.3732 mm/s. Cond. = simulated conductivity of the sample solution injected. E_I = Potential gradient of the sample solution injected.

	Contribution of H^+ to zone conductivity							
	*Strictly evaluated**				*Approximated**			
pH of sample	*Cond. ($mS\,cm^{-1}$)*	*E_I ($V\,cm^{-1}$)*	*Velocity ($mm\,s^{-1}$)*		*Cond. ($mS\,cm^{-1}$)*	*E_I ($V\,cm^{-1}$)*	*Velocity ($mm\,s^{-1}$)*	
			Chlorate	*Formate*			*Chlorate*	*Formate*
Sample concentration = 50 mM								
2.5	5.33	9.44	−0.0113	−0.0005	4.36	11.5	0.0042	0.0002
3.0	5.06	9.95	−0.0008	−0.0001	4.75	10.6	0.0038	0.0005
3.5	5.63	8.94	0.0022	0.0007	5.53	9.10	0.0033	0.0011
4.0	6.48	7.76	0.0026	0.0015	6.45	7.80	0.0028	0.0016
Sample concentration = 10 mM								
2.5	1.92	26.3	−1.3210	−0.0089	0.92	54.4	0.0879	0.0006
3.0	1.32	38.2	−0.2763	−0.0110	1.00	50.1	0.0442	0.0018
3.5	1.27	39.6	−0.0308	−0.0576	1.17	43.0	0.0236	0.0044
4.0	1.41	35.7	0.0058	0.0294	1.38	36.5	0.0157	0.0080

* For explanation, see text.

velocities of the boundary I/AB for the chlorate–formate system (50 and 10 mM) evaluated by eqns. 15 and 16, when the pH_S was varied in the range of 2.5–4. Apparently the volocities of the boundary I/AB were small enough when the sample concentration was 50 mM and E_I was evaluated by use of $C_H\bar{m}_QF$. However, unacceptably large values were simulated at low pH_S, when the exact E_I was used and the concentration of the mixture was 10 mM. Although the boundary velocities of the mixed zones and t_{res} are not affected by the concentration of the samples injected according to the present transient state models, the validity of the assumption used was lost for the dilute samples. Even if E_I was evaluated by use of $C_H\bar{m}_QF$, the simulated $V_{I/AB}$ from the concentration of chloric acid became so large that it could no longer be disregarded compared to $V_{I/AB}$ from that of formic acid. A similar situation was simulated when the non-SPR model was used.

The above simulation may suggest that $V_{I/AB}$ was not strictly zero when the concentration of H^+ was considered. Far from $V_{I/AB} = 0$, a rapidly moving pH boundary may exist in the initial sample zone. Namely, the pH of the solution actually interfacing with the mixed zone formed may vary significantly from the pH_S at the initial stage of migration. If this estimation is valid, the overestimation of the increasing separability at low pH_S by the SPR model can be elucidated properly. Although we did not observe the initial stage of migration by the present apparatus, this phenomenon is very plausible.

On the basis of these simulations, we incorporated the initial pH change in the SPR model. The velocity of the buffer ions (Q) toward the terminating side in the initial solution can be written as

$$V_{Q,I} = E_I\bar{m}_{Q,I} \tag{28}$$

where E_I denotes the potential gradient of the solution injected and $\bar{m}_{Q,I}$ the effective mobility of the buffer ion. A zone (I*) of which the pH is different from pH_S is considered between the injected position and the boundary moving with velocity $V_{Q,I}$. The counter ion from the leading electrolyte migrates into this zone immediately after starting migration. Then, on the assumption that the velocity of the boundary between the zone I* and the mixed zone is zero and the same kind of buffer ions are contained in the sample and the leading electrolyte, the following equation for the concentration of the counter ions in the sample zone, $C^i_{Q,I}$*, may be valid from the continuity principle

$$C^i_{Q,I}{}^* = E_L\bar{m}_{Q,L}C^i_{Q,L}/E_I\bar{m}_{Q,I} + C^i_{Q,I} \tag{29}$$

where E_L denotes the potential gradient of the leading zone, $\bar{m}_{Q,L}$ the effective mobility of the buffer ions in the leading zone, $C^i_{Q,L}$ the total concentration and $C^i_{Q,I}$ the concentration of the buffer ion in the injected samples. Apparently, eqn. 29 suggests that the pH of the solution actually interfacing with the mixed zone will be higher in an anionic separation. Therefore the concentration ratio (eqn. 17) estimated from the formed zone I* will be different from that obtained by the use of pH_S. We call this model SPR-III hereafter.

Table V shows the pH_S dependence of the simulated t_{res} and S for chlorate–formate system. Fig. 3 also shows the pH_S dependence of the observed[5] and simulated S. Apparently the agreement is quite good, confirming the validity of the model

TABLE V

OBSERVED AND SIMULATED SEPARATION NUMBER AND RESOLUTION TIME FOR THE CHLORATE–FORMATE SYSTEM (1:1) BY CONSIDERING THE INITIAL pH CHANGE (SPR-III)

OS = Operational systems: for I, see Table III. II = buffer β-alanine, pH_L = 3.60; III = buffer histidine, pH_L = 6.02. Sample amount = 100 nmol. pH_S = pH of the sample solution injected. pH_S* = Simulated pH of the solution actually interfacing with the mixed zone. Sim. = Value simulated by SPR-III model. Dev. (%) = Percent deviation.

OS	pH_S	pH_S*	*S*			t_{res}		
			*Obs.**	*Sim.*	*Dev. (%)*	*Obs.**	*Sim.*	*Dev. (%)*
I	2.4	3.75	0.179	0.174	−2.8	674	692	2.7
I	3.0	3.84	0.170	0.169	−0.6	709	716	1.0
I	3.5	4.09	0.155	0.156	0.6	778	773	−0.6
I	4.0	4.43	0.142	0.145	2.1	849	830	−2.2
II	2.4	3.43	0.259	0.250	−3.5	466	482	3.4
III	2.4	4.14	0.075	0.070	−6.7	1608	1717	6.8

* Observed values from ref. 5.

SPR-III. The simulated values of $E_t\bar{m}_{Q,I}$ were $2.18 \cdot 10^{-2}$ and $1.05 \cdot 10^{-2}$ mm/s in the case of pH_S = 2.4 and 4.0 respectively (migration current = 80 μA, I.D. of the separation tube = 0.45 mm). The simulated isotachophoretic velocity was 0.373 mm/s. As shown, the simulated pH shift was large (1.7–0.4). The shift reduced considerably the pH_S effect estimated by SPR-II, where the sample pH was kept constant during the separation.

Table VI shows the simulated R_E values, effective mobilities and concentrations of the zone constituents of the chlorate–formate system at both the steady state and the transient state. A significant difference between the models used was found only for the estimates of the sample concentrations in the mixed zone.

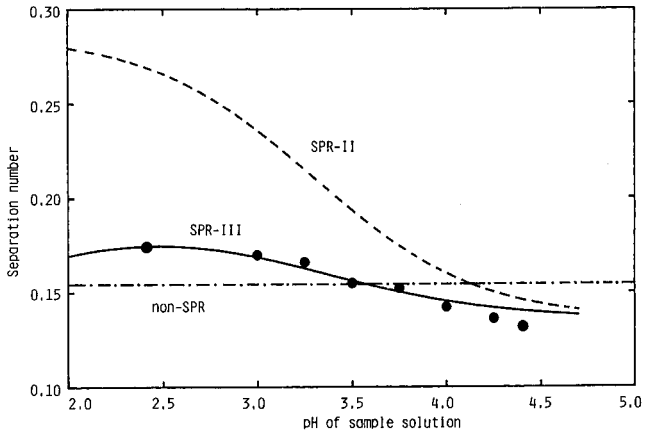

Fig. 3. The observed (●) and simulated separation number for the chlorate–formate system. The observed values were taken from ref. 5. For the operational system, see Table III. For the definitions of the transient state models, see text.

TABLE VI

SIMULATED R_E VALUES, EFFECTIVE MOBILITIES AND CONCENTRATIONS IN THE SEPARATION OF THE CHLORATE–FORMATE SYSTEM AT pH_L = 4.03 (25°C)

pH_S = pH of sample solution injected. R_E = Ratio of potential gradients, $E_{Sample}/E_{Leading}$. $\bar{m}_{CHL}$, $\bar{m}_{FOR}$ = Effective mobilities of chlorate (CHL) and formate (FOR) ions ($cm^2\ V^{-1}\ s^{-1}$) · 10^5. pH = pH of zones at the steady and transient states. C^t_{CHL}, C^t_{FOR} = Total concentrations (m*M*) of chlorate and formate. C^t_Q = Total concentration (m*M*) of buffer (β-Ala). $\bar{m}_Q$ = Effective mobility of buffer ($cm^2\ V^{-1}\ s^{-1}$) · 10^5. I = ionic strength · 10^3.

	pH_S	R_E	pH	$\bar{m}_{CHL}$	$\bar{m}_{FOR}$	C^t_{CHL}	C^t_{FOR}	$\bar{m}_Q$	C^t_Q	I
Steady state zone										
Chlorate		1.19	4.054	63.0	–	9.49	–	13.7	18.4	9.49
Formate		1.80	4.264	–	41.5	–	8.97	10.6	17.8	7.00
Transient mixed zone										
Non-SPR*	–	1.46	4.173	63.2	39.4	4.62	4.62	11.9	18.1	8.05
SPR-II	2.4	1.22	4.073	63.0	36.9	8.81	0.65	13.4	18.3	9.26
SPR-II	4.0	1.45	4.169	63.2	39.3	4.81	4.44	11.9	18.1	8.10
SPR-III	2.4	1.42	4.158	63.2	39.1	5.30	3.97	12.1	18.1	8.23
SPR-III	4.0	1.48	4.180	63.3	39.6	4.32	4.90	11.8	18.1	7.97

* For definitions of the transient state models, see text.

The applicability of the SPR models and the non-SPR model was examined for the different pair of a weak and a strong electrolyte, monochloroacetic acid (MCA: pK_a = 2.865, m_0 = 41.1 · 10^{-5} $cm^2\ V^{-1}\ s^{-1}$) and picric acid (PIC: 0.708, 31.5 · 10^{-5}). The pH_S dependence of both the velocity of the mixed zone boundaries and t_{res} was observed by the use of the multichannel UV detection system. Plots of the effective mobility *vs.* pH_S for these samples cross at pH *ca.* 3.4 and such a pair was called the reversed pair[4]. The pH_S was varied in the range of 2.5–3.7. The pH range is

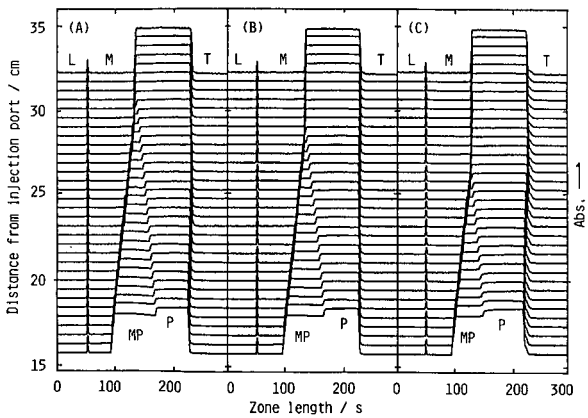

Fig. 4. Transient isotachopherogram of monochloroacetic acid (MCA) and picric acid (PIC) obtained by the use of the 32-channel UV-photometric detector. The pH of the sample solution was 2.5 (A), 3.0 (B) and 3.6 (C). The sample amount was 17.5 nmol (MCA) and 16.3 nmol (PIC). The migration current was 49.2 μA. The leading electrolyte was 5 m*M* hydrochloric acid and the pH was adjusted to 3.6 (buffer β-alanine). The terminator was 10 m*M* caproic acid. For pherograms, see Fig. 2.

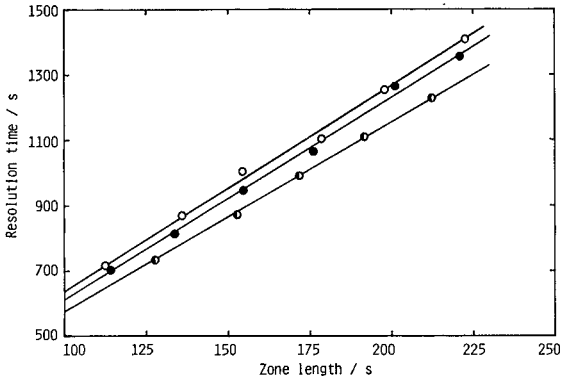

Fig. 5. The pH_S dependence of the resolution time *vs.* the whole time-based zone length in the monochloroacetic acid–picric acid system. For the operational system, see Fig. 4. pH_S = 2.5 (○), 3.0 (●) and 3.6 (◐).

sufficiently wide to study the present problem, since the degree of dissociation of MCA varies from 0.32 to 0.86 and $\bar{m}_{MCA,I}$ ($\bar{m}_{A,I}$ in eqn. 17) varies from $12 \cdot 10^{-5}$ to $33 \cdot 10^{-5}$ $cm^2\ V^{-1}\ s^{-1}$. The degree of dissociation of PIC and $\bar{m}_{PIC,I}$ ($\bar{m}_{B,I}$ in eqn. 17) is almost constant in this pH range and the values are *ca.* 1 and $29 \cdot 10^{-5}$ $cm^2\ V^{-1}\ s^{-1}$.

Fig. 4 shows the observed transient isotachopherogram of MCA (16 nmol) and PIC (16 nmol) at pH_S = 2.5, 3.0 and 3.6. A small amount of SPADNS was added to the mixture. The boundaries between the leading and SPADNS (small peaks in Fig. 4) zones were rearranged at the same abscissa position to demonstrate clearly the change in the individual zone length at the transient state. The observed overall time-based zone lengths were 154.4, 154.7 and 152.6 s respectively. These were the averaged values after the mixed zone had diminished. The t_{res} was given by eqn. 6. It may be evaluated by the following equation obtained by replacing the absolute zone length by the time-based zone length and the absolute velocity by the relative velocity ($V_R = V_{boundary}/V_{IP}$)

$$t_{res} = t_M/(1 - V_{R,M/MP}) \tag{6'}$$

where t_M is the time-based zone length of MCA. Eqns. 6 and 6′ are valid providing the intercepts of eqns. 1 and 2 are equal (zero). However, as already shown in Table II for the SPADNS–MCA system, a slight difference between the intercepts was observed in the MCA–PIC system, and this difference considerably affects the resolution time. Therefore we solved the following simultaneous boundary functions of M/MP and M/P:

$$D_{M/MP} = V_{M/MP}t + D_{0,M/MP} \tag{2'}$$

$$D_{M/P} = V_{IP}t + D_{0,M/P} \tag{3'}$$

When eqn. 3′ was not available because of a relatively large sample amount, the following equation for the boundary MP/P was used instead:

$$D_{MP/P} = V_{MP/P}t + D_{0,MP/P} \quad (4')$$

The boundary velocities and the intercepts in these equations were determined by the least-squares method. The resolution times in Fig. 4 were 1004, 946 and 871 s respectively and the experimental error was less than *ca.* ±20 s.

Fig. 5 shows t_{res} *vs.* the whole zone length at pH_S = 2.5, 3 and 3.6. The best-fitted linear functions were

$$\begin{aligned} t_{res} &= 6.33\ t_{zone} + 5.1 \quad pH_S = 2.5 \\ t_{res} &= 6.18\ t_{zone} - 4.7 \quad pH_S = 3.0 \\ t_{res} &= 5.81\ t_{zone} - 5.3 \quad pH_S = 3.6 \end{aligned} \quad (30)$$

where t_{zone} is the time-based zone length of the whole sample. Apparently t_{res} depends on pH_S, however the change was within *ca.* 10% in the pH range.

Table VII shows the simulated and the observed velocity of the mixed zone boundaries relative to the isotachophoretic velocity together with t_{res}. Apparently the values simulated by SPR-III agreed well with those observed. The discrepancy between the observed and the t_{res} simulated by the non-SPR model was always less than 20%. It should be noted that the non-SPR approach coincides with the SPR approach when pH_S is relatively high.

The relative velocity of the boundaries M/MP and MP/P may be expressed from eqns. 9 and 10 as:

$$V_{R,M/MP} = \bar{m}_{P,MP}E_{MP}/V_{IP} \quad (9')$$

$$V_{R,MP/P} = \bar{m}_{M,MP}E_{MP}/V_{IP} \quad (10')$$

TABLE VII

SIMULATED AND OBSERVED RELATIVE VELOCITY OF THE MIXED ZONE BOUNDARIES AND RESOLUTION TIME IN THE MONOCHLOROACETATE–PICRATE SYSTEM (1:1) AT pH_S = 2.5, 3.0 AND 3.6

Operational system: leading electrolyte 5 m*M* hydrochloric acid–β-alanine (pH 3.60); current = 49.2 μA; diameter of the separation tube = 0.51 mm; sample amounts, monochloroacetic acid (M) 20 nmol, picric acid (P) 19.87 nmol.

pH_S		*Simulated**			*Observed***
		Non-SPR	*SPR-II*	*SPR-III*	
2.5	$V_{R,M/MP}$	0.916	0.955	0.919	0.924 ± 0.003
	$V_{R,MP/P}$	1.099	1.148	1.104	1.087 ± 0.007
	t_{res}(s)	1054	1981	1102	1229 (1168)
3.0	$V_{R,M/MP}$	0.916	0.932	0.918	0.920 ± 0.002
	$V_{R,MP/P}$	1.099	1.120	1.103	1.083 ± 0.006
	t_{res}(s)	1054	1312	1089	1191 (1110)
3.6	$V_{R,M/MP}$	0.916	0.918	0.915	0.918 ± 0.001
	$V_{R,MP/P}$	1.099	1.102	1.098	1.067 ± 0.005
	t_{res}(s)	1054	1080	1041	1119 (1083)

* For definitions of the transient state models, see text.

** Probable error of velocity ratio was calculated from six experiments. The values in parentheses were calculated by eqn. 6'.

The effective mobility of picric acid, $\bar{m}_P$, is not affected by pH_S but that of monochloroacetic acid, $\bar{m}_M$, is affected. Therefore the observed decrease of $V_{R,M/MP}$ in Table VII suggested that E_{MP} decreased slightly with increasing pH_S.

Table VIII summarizes the simulated pH_S dependence on several parameters of the mixed zone, where E_{MP} was expressed as the ratio to the potential gradient of the leading zone ($R_{E,MP} = E_{MP}/E_L$). The slight decrease in $R_{E,MP}$ with increasing pH_S was simulated by the SPR models. According to this simulation, the pH of the mixed zone was almost independent of the change in pH_S. As mentioned before, therefore, the exact evaluation of the concentration ratio of the sample constituents, $C^t_{P,MP}/C^t_{M,MP}$, and E_{MP} are decisive for the simulation of the transient state.

Finally the dependence of the molar fraction on t_{res} and V_R was observed and compared with that simulated. Fig. 6 shows the pherograms observed for the MCA and PIC system upon varying the molar fraction of PIC from *ca.* 0.1 to 0.5 (the total amount was *ca.* 40 nmol and the pH of the solution was *ca.* 2.5). A small amount of SPADNS was added to the mixture. Apparently the mixed zones diminished at the same channels 31 and 32, suggesting that the resolution time was independent of the variation of the molar fraction of PIC. The boundary velocity of M/MP increased and that of MP/P decreased with increasing molar fraction of PIC. Consequently the mixed zones diminished at the same resolution time.

TABLE VIII

SIMULATED CONCENTRATION RATIO OF SAMPLES, R_E, pH OF ZONES AND EFFECTIVE MOBILITIES IN THE MIXED ZONE OF THE MONOCHLOROACETATE–PICRATE SYSTEM (1:1) AT pH_S = 2.5, 3.0 AND 3.6

For the operational system, see Table VII. Sample amounts: monochloroacetic acid (M), 20 nmol; picric acid (P), 18.68 nmol. $C^t_{P,MP}/C^t_{M,MP}$ = Ratio of the total concentrations of M and P in the mixed zone; $R_{E,MP}$ = ratio of potential gradient to that of the leading zone; pH_{MP} = pH of the mixed zone; $\bar{m}$ = effective mobility ($cm^2\ V^{-1}\ s^{-1}$).

	pH_S	*Simulated value**		
		Non-SPR	*SPR-II*	*SPR-III*
$C^t_{P,MP}/C^t_{M,MP}$	2.5	0.993	2.776	1.086
	3.0	–	1.490	1.062
	3.6	–	1.043	0.968
$R_{E,MP}$	2.5	2.360	2.460	2.369
	3.0	–	2.402	2.367
	3.6	–	2.365	2.357
pH_{MP}	2.5	3.830	3.835	3.830
	3.0	–	3.832	3.830
	3.6	–	3.830	3.830
$\bar{m}_{P,MP}$	2.5	29.44	29.46	29.44
	3.0	–	29.45	29.44
	3.6	–	29.44	29.44
$\bar{m}_{M,MP}$	2.5	35.35	35.39	35.35
	3.0	–	35.37	35.35
	3.6	–	35.35	35.34

* For definitions of the transient state models, see text.

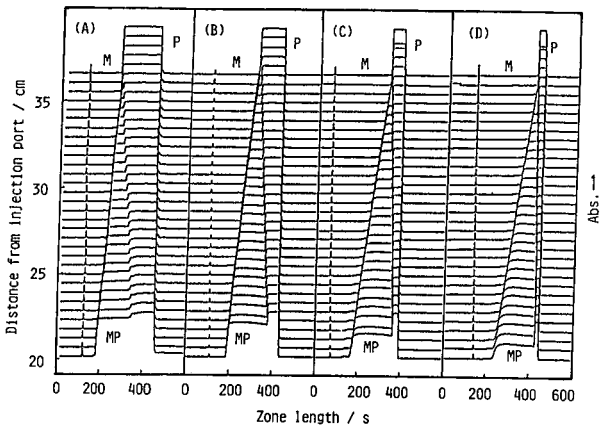

Fig. 6. Transient isotachopherogram of monochloroacetic acid (MCA) and picric acid (PIC) obtained by the use of the 32-channel UV-photometric detector. (A) 20.0 nmol MCA, 18.7 nmol PIC, (B) 26.7 nmol MCA, 12.4 nmol PIC; (C) 33.3 nmol MCA, 6.2 nmol PIC and (D) 36.4 nmol MCA, 3.4 nmol PIC. For the analytical conditions, see Fig. 4.

TABLE IX

OBSERVED AND SIMULATED RELATIVE VELOCITY AND RESOLUTION TIME FOR THE MONOCHLOROACETATE–PICRATE SYSTEM

For the operational system, see Table VII. I.D. of the separation tube = 0.54 mm. Sample amounts: monochloroacetic acid (M): picric acid (P) = 20.0:18.68 (1:1), 26.68:12.44 (2:1), 33.32:6.24 (5:1) and 36.36 nmol:3.40 nmol (10:1).

Molar fraction		*Simulated**				*Obs.***
		Non-SPR	*SPR-II**		*SPR-III**	*2.5*
			2.5		*2.5*	
			pH_S = 2.5	*4.0*		
1:1	$V_{R,M/MP}$	0.913	0.953	0.911	0.917	0.923
	$V_{R,MP/P}$	1.096	1.145	1.094	1.101	1.097
	t_{res}(s)	1015	1892	1003	1072	1155
2:1	$V_{R,M/MP}$	0.886	0.927	0.885	0.891	0.896
	$V_{R,MP/P}$	1.063	1.113	1.061	1.069	1.055
	t_{res}(s)	1040	1624	1027	1084	1144
5:1	$V_{R,M/MP}$	0.860	0.891	0.859	0.864	0.875
	$V_{R,MP/P}$	1.031	1.069	1.030	1.036	1.036
	t_{res}(s)	1057	1353	1050	1086	1121
10:1	$V_{R,M/MP}$	0.848	0.868	0.848	0.850	0.847
	$V_{R,MP/P}$	1.017	1.041	1.016	1.020	1.009
	t_{res}(s)	1065	1047	1061	1082	1101

* For definitions of the transient state models, see text.

** The probable error in V_R was 0.001–0.004.

TABLE X

SIMULATED R_E VALUES, EFFECTIVE MOBILITIES AND CONCENTRATIONS OF ZONE CONSTITUENTS IN THE STEADY STATE ZONE AND THE TRANSIENT MIXED ZONE OF THE MONOCHLOROACETATE–PICRATE SYSTEM AT pH_L = 3.6 (25°C)

For operational system, see Table VII. For sample amount, see Table IX. pH_S^* = pH of sample zone actually interfacing with the mixed zone. For definition of other symbols, see Table VI.

	pH_S^*	R_E	pH	$\bar{m}_{MCA}$	$\bar{m}_{PIC}$	C^t_{MCA}	C^t_{PIC}	$\bar{m}_Q$	C^t_Q	I
Steady state zone										
MCA		2.16	3.821	35.1	–	3.66	–	12.6	8.68	3.32
PIC		2.59	3.841	–	29.3	–	3.09	12.2	8.33	3.08
Transient mixed zone										
1:1	3.47	2.35	3.829	35.3	29.4	1.78	1.59	12.4	8.51	3.21
2:1	3.40	2.28	3.826	35.3	29.4	2.40	1.07	12.5	8.57	3.25
5:1	3.33	2.22	3.823	35.3	29.4	3.03	0.54	12.6	8.63	3.28
10:1	3.30	2.19	3.822	35.3	29.4	3.32	0.30	12.6	8.66	3.30

Table IX shows the dependence of the molar fraction on the observed and the simulated boundary velocities and t_{res}. The observed values were the averages from three experiments at 25°C. The agreement between the observed and the values simulated by the SPR-III model was again very good.

Table X summarizes the simulated R_E values, effective mobilities and concentrations of the zone constituents of the MCA and PIC system at both the steady state and the transient state. A significant difference between the models used was found only for the estimates of the sample concentrations and potential gradient of the mixed zone MP, E_{MP}.

Thus, the overestimation by the transient state models SPR-I and SPR-II at low pH_S may be explained properly only by the pH perturbation at the initial stage. From the present work, an important conclusion was deduced that the properties of the mixed zone are regulated not only by those of the sample solution injected itself but also by those of the leading zone. As discussed, the simulated pH shift was large and it reduced considerably the pH_S effect in the separation process. The shift of the pH boundary in the sample solution injected might be observed by the use of an appropriate pH indicator; it was not observed in the present work because of the structural restriction of the apparatus.

Although the observed small pH dependence on t_{res}, etc., cannot be simulated by the non-SPR model, it seems that the approximation by thus model is not far from reality. Especially from the practical viewpoint, the applicability of the non-SPR model to the transient state may be highly rated, because the discrepancy between the observed and the simulated t_{res} was always small, not only for a pair of a strong acid and a weak acid but also for a pair of weak acids.

We have investigated a convenient model to estimate the resolution time of samples on the basis of the zone lengths, concentrations, etc., at the steady state, which can be simulated exactly. The usefulness of the non-SPR model will be reported in a subsequent paper dealing with two- and three-component systems.

ACKNOWLEDGEMENTS

T.H. thanks the Ministry of Education, Science, and Culture of Japan for support of the part of this work under a Grant-in-Aid for Scientific Research (No. 61540423). We are also grateful for the helpful suggestions made by Dr. F. M. Everaerts (Eindhoven University of Technology, The Netherlands).

REFERENCES

1 T. Hirokawa, K. Nakahara and Y. Kiso, *J. Chromatogr.*, 463 (1989) 39–49.
2 G. Brouwer and G. A. Postema, *J. Electrochem. Soc.*, 117 (1970) 874.
3 J. Vacik and V. Fidler, in F. M. Everaerts (Editor), *Analytical Isotachophoresis*, Elsevier, Amsterdam, 1981, pp. 19–24.
4 F. E. P. Mikkers, F. M. Everaerts and J. A. F. Peek, *J. Chromatogr.*, 168 (1979) 293.
5 F. E. P. Mikkers, F. M. Everaerts and J. A. F. Peek, *J. Chromatogr.*, 168 (1979) 317.
6 R. A. Alberty, *J. Am. Chem. Soc.*, 72 (1950) 2361.
7 T. Hirokawa and Y. Kiso, *Shimadzu Kagaku Kikai News*, 25 (1984) 24.
8 T. Hirokawa and Y. Kiso, *J. Chromatogr.*, 242 (1983) 227.
9 R. A. Robinson and R. H. Stokes, *Electrolyte solutions*, Butterworths, London, 1959.
10 T. M. Jovin, *Biochemistry*, 12 (1973) 871.
11 T. M. Jovin, *Biochemistry*, 12 (1973) 879.
12 T. M. Jovin, *Biochemistry*, 12 (1973) 890.
13 H. Svenson, *Acta Chem. Scand.*, 2 (1948) 841.

Journal of Chromatography, 463 (1989) 73–80
Elsevier Science Publishers B.V., Amsterdam — Printed in The Netherlands

CHROM. 20 996

SOME FACTORS IN SOLUTE PARTITIONING BETWEEN WATER AND MICELLES OR POLYMERIC MICELLE ANALOGUES

DENNIS G. TABOR* and A. L. UNDERWOOD*
Department of Chemistry, Emory University, Atlanta, GA 30322 (U.S.A.)
(First received June 27th, 1988; revised manuscript received September 19th, 1988)

SUMMARY

Micelle–water partition coefficients of *p*-nitroaniline and *p*-nitrophenol have been determined for several alkyltrimethylammonium salts including a polymer of undecenyltrimethylammonium bromide. Solubilization depends upon the "concentration" of micellized alkyl carbon atoms regardless of micelle size. Counterion effects are an important aspect of the process. Micelle-like polymers may be useful in theoretical studies by eliminating some of the interactive variables which complicate pseudophase liquid chromatography with ordinary micelles.

INTRODUCTION

Recent reviews describe a growing interest in liquid chromatography (LC) with micellar mobile phases, sometimes termed "pseudophase LC"[1–3]. It is understandable that most studies in this relatively new area have been based upon two surfactants which are readily available in high purity (sodium dodecyl sulfate and hexadecyltrimethylammonium bromide), but optimization cannot be guaranteed unless surfactants with other head groups, chain lengths, and counterions are also evaluated. Micelle–water partition coefficients (K_{MW} values) are important for interpreting solute retention behavior in terms of the three-phase model[4,5]; these values are likewise important in other contexts, *e.g.*, theoretical treatments of micellar catalysis[6]. Armstrong and Stine[7] have described a simple, efficient, and inexpensive method for obtaining K_{MW} values by thin-layer chromatography (TLC): the plot of $R_F/(1 - R_F)$ *vs.* mobile phase micellized surfactant concentration is linear and the ratio of slope to intercept is shown to be $(K_{MW} - 1)\bar{v}$, where $\bar{v}$ is the partial specific volume of the surfactant calculated from density measurements. Results obtained by this method have disclosed several interesting aspects of micellar solubilization with the solutes *p*-nitroaniline and *p*-nitrophenol: solubility essentially depends upon the "concentration" of micellized alkyl carbon atoms regardless of micelle size; a micelle-like polymer or "polysoap" accepts solutes in the same manner as do micelles; solubility is lowered by an organic counterion (benzoate) which is highly promotional in regard to

* Present address: Lee Wan & Associates, Atlanta, GA 30316, U.S.A.

0021-9673/89/$03.50

micelle formation, and becomes lower still at surfactant concentrations above the sphere-to-rod transition.

EXPERIMENTAL

Materials

10-Undecenyltrimethylammonium bromide (UTAB) was prepared by routine alkylation of ethanolic trimethylamine with 10-undecenyl bromide and recrystallized from ethanol–diethyl ether. The critical micelle concentration (CMC) of this material in water was 0.053 *M* and the aggregation number was 31 as determined by light scattering. Polyundecenyltrimethylammonium bromide (PUTAB) was prepared by irradiation of aqueous 0.5 *M* UTAB solutions in sealed ampoules with 25 Mrad delivered in 100 h in a ^{60}Co γ source. The chemical shift of the head group methyl protons changed sufficiently upon polymerization to allow the process to be monitored by ^{1}H NMR spectroscopy; after 100 h, the level of unreacted monomer remained nearly constant at about 30% of the starting material. The pooled solutions were lyophilized and the solid residue was dissolved in ethanol and precipitated with diethyl ether. The latter process was repeated three times. Monomer residue was $<2\%$. (With a comparable compromise between purity and yield, the polymer can also be cleaned up by gel filtration on a Sephadex G-25 column or by dialysis with a cellophane membrane.) The polymerization number by light scattering was 32 and by the luminescence quenching method employed by Turro and Yekta[8] and others, 38. In other words, the polymer molecule is about the same size as the original, unirradiated micelle. This material is a cationic counterpart of the polymerized sodium undecenoate prepared in the same way and characterized as micelle-like by Sprague *et al.*[9].

Decyltrimethylammonium bromide ($D_{10}TAB$) and the tetradecyl salt (TTAB) were prepared and purified in a conventional manner[10]. Eastman dodecyltrimethylammonium bromide ($D_{12}TAB$) was recrystallized from ethanol–diethyl ether. Baker reagent hexadecyltrimethylammonium bromide (HTAB) was used as received. Bromides were converted to chloride (HTAC) or benzoate (HTABz) salts by ion exchange on Bio-Rad AG1-X8 columns; a bromide ion-selective electrode was used to confirm the adequacy of the exchange process. The solutes *p*-nitroaniline and *p*-nitrophenol were Aldrich materials. TLC plates, 5 × 20 cm, were cut from the Macherey-Nagel Polyamid-6 UV_{254} product distributed by Brinkmann.

Methods

Chromatography was performed at ambient temperature of 22 ± 0.5°C. Samples were pipetted onto the plates 2 cm from the bottoms, and the solvent was allowed to migrate about 15 cm. R_F values were determined visually from the diminished luminescence of the stationary phase fluorophore at the solute spots. Partial molar volumes were obtained by a standard method as described, for example, by Güvelli *et al.*[11]. Light scattering measurements were performed as described earlier[10].

With pure water as the mobile phase, the values of $R_F/(1 - R_F)$ for *p*-nitroaniline and *p*-nitrophenol are 0.07 and 0.05, respectively. As surfactant is added, the values at first hold at these levels and then break upward, suggesting that CMC values are obtainable from the abrupt slope changes. The study of Armstrong

and Stine[7] suggests that, for cationic surfactants, this behavior is not an artifact resulting from mobile phase concentration changes as the solvent wets the plate. Furthermore, CMC values obtained in this manner are close to literature values where the latter are available; for example, the recommended value in a critical compilation[12] for $D_{12}TAB$ in water is $1.59 \cdot 10^{-2}$ *M*, while the value from our plots is $1.7 \cdot 10^{-2}$ *M*. Because the intercept is very sensitive to CMC, and K_{MW} to the intercept, CMC values from the TLC data were preferred to those from other sources, which may vary considerably with the method of measurement[12], for calculating micellized surfactant concentrations. Slopes were obtained from a standard program for linear regression of $R_F/(1 - R_F)$ on micellized surfactant concentration.

RESULTS

Fig. 1 shows typical data sets obtained with the solute *p*-nitroaniline and several mobile phase surfactants, including the polymer, with bromide counterions. To avoid clutter, actual data points are shown for only one of the lines. Each point represents the average of eight individual R_F measurements on four separate plates. The correlation coefficients were as follows: $D_{10}TAB$, 0.99; PUTAB, 0.99; UTAB, 0.91; $D_{12}TAB$, 0.99; TTAB, 0.98 and HTAB, 0.97. The limited concentration range of the HTAB data reflects the low solubility of this material[13]; solutions near the upper end of the curve were probably, in fact, supersaturated.

The lines shown in Fig. 2 were generated by multiplying micellized surfactant concentrations by the numbers of carbon atoms in the alkyl chains (*e.g.*, by 16 in the case of HTAB). The "spread" in the slopes is clearly decreased by this operation, although not all of the confidence intervals of the slopes at a probability level of 0.95 overlap. Statistically, at this probability level, one cannot quite say that the slopes are identical, but they are very nearly so; of the six lines, two different sets of five meet the test.

Lines similar to those in Figs. 1 and 2 are obtained with the solute *p*-nitrophenol,

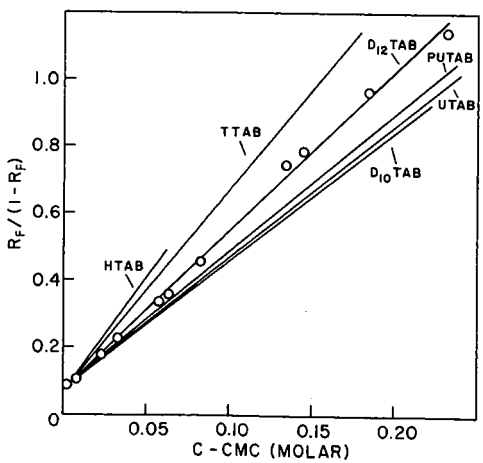

Fig. 1. Armstrong plots for *p*-nitroaniline, bromide counterions. To avoid clutter, data points are shown for $D_{12}TAB$ only.

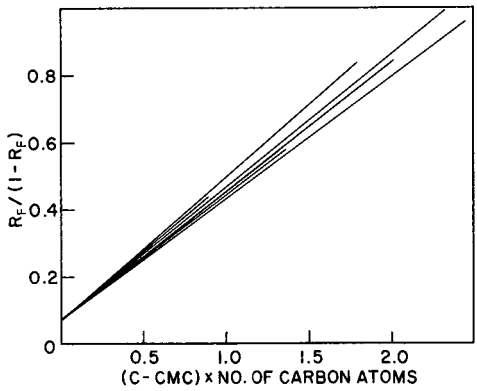

Fig. 2. Armstrong plots for *p*-nitroaniline, bromide counterions, normalized for the number of carbon atoms in the surfactant alkyl chain. In order from largest to smallest slope: TTAB, HTAB, D_{12}TAB, D_{10}TAB, PUTAB, UTAB.

although, of course, the slopes are numerically different. Fig. 3 shows an interesting effect of the benzoate counterion which is discussed below in relation to the superimposed light scattering curve obtained with solutions of HTABz. Data and calculated partition coefficients are given in Table I, and the latter are displayed in Fig. 4.

DISCUSSION

For the four cases common to both studies, our K_{MW} values agree reasonably with those of Armstrong and Stine[7] except for *p*-nitrophenol in HTAC, where ours is unaccountably 48% larger. It is seen in Table I and Fig. 4 that the K_{MW} values for both solutes are the same with D_{10}TAB as with UTAB, perhaps reflecting the fact that the terminal unsaturation of the latter is expected to have about the same effect upon micellar properties as removal of one methylene unit from a saturated alkyl chain[14].

Armstrong's review[2] provides an excellent summary of the manner in which the interpretation of solute retention behaviour is complicated by the complexity of micellar LC systems. Some of the problems relate to the inevitable presence of unmicellized surfactant ions in solutions of ordinary micelles, including head group interactions with ionic solutes and modification of the stationary phase by monomer accumulation. Others arise in the use of mobile phase modifiers such as methanol, which introduce additional confusion by their generally unknown effects upon micellar properties. We suggest that polymeric micelle analogues may help chromatographers sort out some of these effects. Solutions of PUTAB give a linear light scattering curve which rises from the origin. There is no CMC, nor monomer to form ion pairs or to coat a surface, yet the polymer points in Fig. 4 lie in the same domain as those for micelles. It should also be noted that "pure" counterion effects can be studied using such polymers, without the intrusion of the changes in CMC and aggregation number which often attend the substitution of one counterion for another with ordinary micelles. One expects, for example, that cationic micelles with bromide counterions will be larger than their chloride counterparts[15], but the size here remains

TABLE I

DATA SUMMARY AND CALCULATED PARTITION COEFFICIENTS

*Surfactant**	*Partial molar volume*	*Slope*** *(Fig. 1)*	*Slope**** *(Fig. 2)*	*Intercept*	K_{MW}[§]	K^*_{MW}[§§]
p-Nitroaniline solute						
D_{10}TAB	0.2607	3.865	0.387	0.070	213	22
UTAB	0.2699	4.007	0.364	0.070	213	20
PUTAB	0.2491	4.138	0.376	0.070	238	23
D_{12}TAB	0.2950	4.760	0.397	0.070	232	20
TTAB	0.3271	6.025	0.430	0.070	264	20
HTAB	0.3555	6.787	0.424	0.070	274	18
D_{10}TAC	0.2496	3.395	0.340	0.070	195	20
PUTAC	0.2351	3.569	0,324	0.070	218	21
D_{12}TAC	0.2877	4.649	0.387	0.070	232	20
HTAC	0.3479	6.559	0.410	0.070	269	18
TTABz	0.3855	3.362	0.240	0.070	126	10
HTABz	0.4182	3.537[§§§]	0.221[§§§]	0.070	122[§§§]	9[§§§]
p-Nitrophenol solute						
D_{10}TAB	0.2607	3.871	0.387	0.050	298	31
UTAB	0.2699	4.006	0.364	0.050	298	28
PUTAB	0.2491	4.681	0.426	0.050	377	35
D_{12}TAB	0.2950	5.619	0.468	0.050	383	33
TTAB	0.3271	7.546	0.539	0.050	462	34
HTAB	0.3555	9.039	0.565	0.050	510	33
D_{10}TAC	0.2496	4.221	0.422	0.050	339	35
PUTAC	0.2351	4.786	0.435	0.050	408	38
D_{12}TAC	0.2877	6.844	0.570	0.050	477	41
HTAC	0.3479	10.716	0.670	0.050	617	40
TTABz	0.3855	5.851	0.418	0.050	305	23
HTABz	0.4182	3.806[§§§]	0.238[§§§]	0.050	183[§§§]	12[§§§]

* For abbreviations, see section on Materials. Counterions are: B, Br^-; C, Cl^-; Bz, benzoate ($C_6H_5CO_2^-$).

** Concentration is molarity of micellized surfactant, *i.e.*, (M_{surf} − CMC), as plotted in Fig. 1.

*** Concentration is "molarity" of surfactant alkyl chain CH_3– and $-CH_2-$ groups, *i.e.*, (M_{surf} − CMC) × number of C atoms in alkyl chain, as plotted in Fig. 2.

§ K_{MW} is the usual dimensionless micelle–water partition coefficient as defined by Armstrong and Nome[4] and others.

§§ K^*_{MW} values are obtained using slopes as seen in Fig. 2 rather than those of Fig. 1. See Discussion.

§§§ Calculated from data for surfactant concentrations below the sphere-to-rod transition. See Fig. 3 and Discussion.

the same because the chloride was prepared from the bromide after polymerization. Further, the polymer will not be disrupted by solvents such as methanol and acetonitrile.

A striking counterion effect is seen in the decreased K_{MW} values for both solutes attending the substitution of benzoate for chloride or bromide. Hydrophobic counterion substituents promote micelle formation in a fairly predictable manner[16],

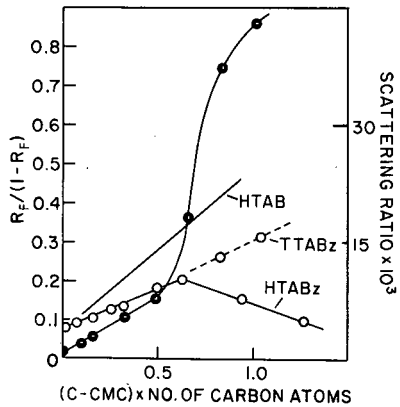

Fig. 3. Effect of benzoate counterions with *p*-nitroaniline. The HTAB curve from Fig. 2 is shown for comparison; solid circles show ratios of scattered radiant power (90°) to incident power for light scattering on aqueous HTABz solutions.

acting somewhat as solubilizates. In terms of the Menger micelle model[17–19], they readily infiltrate the porous, open, highly disordered surface region, perhaps displacing water and creating a higher degree of organization than would simple inorganic counterions. The Hartley micelle[20], despite its more clearly differentiated interior and surface regions, is considered sufficiently fluid to accept hydrophobic insertions whose removal from bulk water is highly favorable. In either case, it is reasonable that a counterion which possesses qualities of an organic solubilizate may induce changes in micellar organization that diminish hospitality toward additional guest molecules.

The light scattering curve in Fig. 3 shows, near about 0.6 on the abscissa, a steepening associated with micellar growth. The simultaneous appearance of

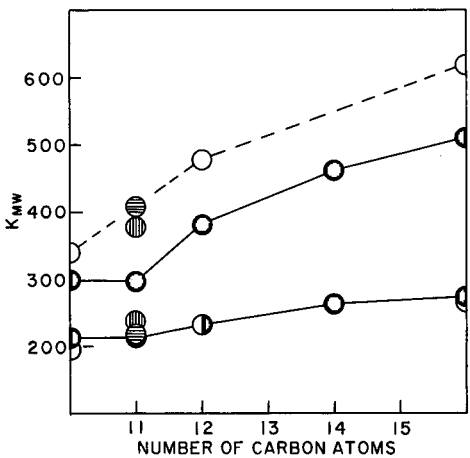

Fig. 4. Pictorial summary of data from Table I. Open circles, Cl^- counterions; solid circles, Br^- counterions; vertically hatched circles, PUTAB; horizontally hatched circles, PUTAC; lower solid line, *p*-nitroaniline solute; upper solid and dotted lines, *p*-nitrophenol solute.

dissymmetry (based upon measurements at scattering angles of 45 and 135°) suggests that the larger aggregates are rod-like. In other words, a sphere-to-rod transition, not seen with the other surfactants in this study at the concentrations employed, occurs in this region. (Some writers have designated the transition a "second CMC", but IUPAC has attempted to discourage this usage.) The corresponding transition for HTAB occurs at much higher concentrations[21]. It is plausible that closer packing in rod-like micelles may diminish solute intrusion, perhaps even to the degree that surfactant increments above the sphere-to-rod transition scarcely increase a solute's mobile phase solubility. This alone does not explain, however, the negative slope seen in Fig. 3 for *p*-nitroaniline in HTABz, since presumably spherical micelles, on thermodynamic grounds, coexist with rods in this region. (*p*-Nitrophenol exhibits a similar slope change in the same HTABz concentration region.) The magnitudes of other terms are such that negative slopes correspond to physically meaningless negative K_{MW} values.

The mobile phases were unbuffered (to avoid the introduction of extraneous counterions), and questions were raised during manuscript review regarding possible pH effects upon the charge status of the solutes as discussed by Arunyanart and Cline-Love[22]. However, protonation of *p*-nitroaniline ($pK_b \approx 13$) would require solutions far more acidic than ours, particularly in the face of the pK shifts known to result from incorporation in micelles[23]. Further, although benzoate solutions are more alkaline than those with Br^- or Cl^-, increasing ionization of *p*-nitrophenol (pK_a = 7.15) would presumably increase its mobility as it became itself an effective counterion. Nor is it clear how the abrupt divergence of the TTABz and HTABz plots near the sphere-to-rod transition (Fig. 3), seen with both solutes, could relate to poor pH control. Thus the negative slopes at higher HTABz concentrations remain difficult to explain and attest to the complexity of micellar LC.

The K^*_{MW} values in Table I were calculated using slopes based upon the abscissa units shown in Fig. 2. Although we do not wish to exaggerate their obviously limited usefulness, in principle, taken with $\bar{v}$ values and carbon chain lengths, they could be used to calculate equivalent concentrations in substituting one surfactant for another. The striking feature, however, is how nearly independent of surfactant chain length are the K^*_{MW} values. It has been known for many years that, *ceteris paribus*, micellar aggregation numbers increase with chain length; for example, in one study the "molecular weights" of the micelles in water were 10 200 for D_{10}TAB, 15 500 for D_{12}TAB, and 25 300 for TTAB[24]. Yet, carbon atom for micellized carbon atom, the larger micelles are no more effective solubilizers than are smaller ones.

Chain length and counterion effects seen in Table I and Fig. 4 are far from insignificant, and are complicated by their dependence upon the nature of the solute. With *p*-nitroaniline, for example, K_{MW} increases by only 29% when HTAB replaces D_{10}TAB, whereas with *p*-nitrophenol there is a 71% increase. The ratio of K_{MW} values for the two solutes ($K_{MW_{PNP}}/K_{MW_{PNA}}$) ranges from 1.4 with D_{10}TAB to 2.3 with HTAC. With HTA^+, replacing Br^- with Cl^- has virtually no effect upon $K_{MW_{PNA}}$ but increases the value for *p*-nitrophenol by over 20%. Thus even a study limited to two solutes and three counterions leads one to suppose that many reported pseudophase LC separations are probably not optimized.

ACKNOWLEDGEMENTS

The authors thank Dr. John Noakes for his help in our use of the ^{60}Co γ source at the Center for Applied Isotope Studies, University of Georgia, Athens, GA, U.S.A. We are also grateful to Prof. C. G. Trowbridge for helpful discussions and computing assistance.

REFERENCES

1 L. J. Cline-Love, J. G. Habarta and J. G. Dorsey, *Anal. Chem.*, 56 (1984) 1132A.
2 D. W. Armstrong, *Sep. Purif. Methods*, 14 (1985) 213.
3 E. Pelizzetti and E. Pramouro, *Anal. Chim. Acta*, 169 (1985) 1.
4 D. W. Armstrong and F. Nome, *Anal. Chem.*, 53 (1981) 1662.
5 M. Arunyanart and L. J. Cline-Love, *Anal. Chem.*, 56 (1984) 1557.
6 C. A. Bunton, L. S. Romsted and G. Savelli, *J. Am. Chem. Soc.*, 101 (1979) 1253.
7 D. W. Armstrong and G. Y. Stine, *J. Am. Chem. Soc.*, 105 (1983) 2962.
8 N. J. Turro and A. Yekta, *J. Am. Chem. Soc.*, 100 (1978) 5951.
9 E. D. Sprague, D. C. Duecker and C. E. Larrabee, *J. Am. Chem. Soc.*, 103 (1981) 6797.
10 E. W. Anacker and A. L. Underwood, *J. Phys. Chem.*, 85 (1981) 2463.
11 D. E. Güvelli, J. B. Kayes and S. S. Davis, *J. Colloid Interface Sci.*, 82 (1981) 307.
12 P. Mukerjee and K. J. Mysels, *Critical Micelle Concentrations of Aqueous Surfactant Systems*, NSRDS-NBS 36, U.S. Dept. of Commerce, Washington, DC, 1971.
13 F.-P. Tsao and A. L. Underwood, *Anal. Chim. Acta*, 136 (1982) 129.
14 B. Durairaj and F. D. Blum, *J. Colloid Interface Sci.*, 106 (1985) 561.
15 A. L. Understood and E. W. Anacker, *J. Colloid Interface Sci.*, 117 (1987) 242.
16 A. L. Underwood and E. W. Anacker, *J. Phys. Chem.*, 88 (1984) 2390.
17 F. M. Menger, *Acc. Chem. Res.*, 12 (1979) 111.
18 F. M. Menger and D. W. Doll, *J. Am. Chem. Soc.*, 106 (1984) 1109.
19 F. M. Menger, in K. L. Mittal and B. Lindman (Editors), *Surfactants in Solution*, Vol. 1, Plenum, New York, NY, 1984, p. 347.
20 G. S. Hartley, *Aqueous Solutions of Paraffin-Chain Salts: A Study in Micelle Formation*, Hermann, Paris, 1936, Fig. 11A and accompanying discussion.
21 J. Ulmius and H. Wennerström, *J. Magn. Reson.*, 28 (1977) 309.
22 M. Arunyanart and L. J. Cline-Love, *Anal. Chem.*, 57 (1985) 2837.
23 A. L. Underwood, *Anal. Chim. Acta*, 140 (1982) 89.
24 P. Debye, *J. Phys. Chem.*, 53 (1949) 1.

Journal of Chromatography, 463 (1989) 81–93
Elsevier Science Publishers B.V., Amsterdam — Printed in The Netherlands

CHROM. 21 017

USE OF GAS CHROMATOGRAPHY IN THE STUDY OF THE OXIDATIVE DECOMPOSITION OF SPENT ORGANIC SOLVENTS FROM REPROCESSING PLANTS

LUIGI NARDI

ENEA, Centro Ricerche Energia Casaccia, Dipartimento Ciclo del Combustibile, Divisione ME.P.I.S., S.P. Anguillarese 301, 00060 S.M. di Galeria, Rome (Italy)

(First received May 20th, 1988; revised manuscript received September 19th, 1988)

SUMMARY

A new approach to quantify the oxidizing efficiency of hydrogen peroxide with respect to a complex organic mixture simulating a radioactive organic waste is described, involving capillary gas chromatographic analysis of the reaction mixture with *n*-dodecane as an internal standard.

INTRODUCTION

The solvent extraction systems used in nuclear fuel reprocessing plants for the treatment of irradiated fuels make extensive use of organic extractants[1], and some of the extractants are invariably discarged and treated as secondary radioactive waste. The major problem associated with the management of these wastes is the suitable reduction of their volume, in which all the radioactivity is retained, with a view to less expensive and safer disposal. To date, the methods proposed for the volume reduction of organic radioactive wastes can be divided into dry processes, such as incineration and thermal decomposition, and wet processes, such as acid digestion and related procedures[2].

Recently many papers[3–11] have appeared on wet oxidation methods, describing the use of concentrated aqueous hydrogen peroxide in the presence of a catalyst, especially copper and iron salts, in the oxidation of tributyl phosphate and various kinds of organic substances and diluents used in irradiated nuclear fuel processing.

The processes using hydrogen peroxide–catalyst systems are very convenient for the following main reasons: the process is simple, easy and safe, being managed at atmospheric pressure, at relatively low temperature and under water, and giving rise essentially to water and carbon dioxide; and the off-gases produced are essentially free from radioactivity and also from any dangerous gas (such as NO_x or SO_x).

Currently available papers on the wet oxidation with hydrogen peroxide of organic solvents used as extractants in nuclear fuel reprocessing plants report only that the final products are essentially carbon dioxide and water[3] and prove the effectiveness of the treatment by presenting a non-specific (*i.e.*, cumulative) curve of the residual organic content *versus* the oxidant amount or the parameters of oxidation.

0021-9673/89/$03.50

The oxidizing efficiency of hydrogen peroxide towards organic substrates has been occasionally evaluated by total organic carbon (TOC) analysis[4]. However, methods based on TOC analysis are not suitable unless the compounds are completely oxidized to carbon dioxide.

Despite the straightforward nature and the selectivity of chromatographic methods, they are not generally used, probably because of the problems associated with the quantification of the results. In fact, it is not generally too difficult to follow the composition of the organic phase in an organic–aqueous medium (where chemical reactions are proceeding), but the absolute amount of organic phase cannot be exactly determined unless time-consuming procedures are used.

This paper describes the use of capillary gas chromatography (GC) to investigate wet oxidation by 36% (m/v) hydrogen peroxide of a particular simulated (*i.e.*, not radioactive) organic mixture, with a view to volume reduction and safe disposal, and the optimization of the reaction conditions for maximum conversion of the starting organic to inorganic materials.

EXPERIMENTAL

Chemicals

Solvesso 100, a complex mixture composed principally of C_9 (84.5%), C_8 (10.2%) and C_{10} (3%) alkylaromatic hydrocarbons, was supplied by Esso Chemicals (Milan, Italy).

Technical-grade tri-*n*-octylamine containing at least five long-chain tertiary aliphatic amines (TAAs) was supplied by Chemical Procurement (New York, U.S.A.). Mesitylene (1,3,5-trimethylbenzene), tributyl phosphate (TBP) and *n*-dodecane of analytical-reagent-grade were obtained commercially. *n*-Hexane (HPLC grade) and tetrachloroethylene were purchased from E. Merck (Darmstadt, F.R.G.). N,N-Dibutyloctanamide (DBOA) (97%) was obtained from Prochimica (Pavia, Italy), and used without further purification. Hydrogen peroxide (36%) was purchased from Carbo Erba (Milan, Italy). The solid catalysts copper(I) oxide, copper(II) oxide and iron(II) sulphate were also obtained from Carlo Erba.

The reference simulated organic mixture had the following composition: DBOA 30.3, mesitylene 29.5, Solvesso 100 21.2, TBP 4.8, TAAs 3.7 and *n*-dodecane 17.9 volumes.

Apparatus

A Perkin-Elmer Model 8510 gas chromatograph was used, in a version equipped with three detectors (flame ionization, thermal conductivity and nitrogen–phosphorus) and three injectors [a programmed temperature vapourizer (PTV) capillary column injector and two packed column injectors], built-in data handling with re-integration and connected with a Perkin-Elmer GP-100 printer–plotter.

All GC analyses were performed on a Perkin-Elmer BP1 (0.25 μm) column (12 m $\times$ 0.22 mm I.D.).

For gas chromatography–mass spectrometry (GC–MS), electron impact mass spectral data were obtained with a Hewlett-Packard quadrupole HP 5970B/5890A instrument with an HP-1 (0.33 μm) capillary column (12 m $\times$ 0.22 mm I.D.).

For capillary GC analyses the oven temperature was held at 45°C for 17 min, then programmed at 8°C/min to 300°C and held (3 min).

The PTV injector temperature was set at 300°C 0.01 min after the start of the run and at 0.3 min it was switched off. The septum purge flow-rate was 2 ml/min. The carrier gas was helium at a pressure of 10 p.s.i. and a linear velocity of 30 cm/s. The detector temperature was 330°C, the flame ionization detector attenuation range was $4 \cdot 10^{-11}$ a.u.f.s. and the time constant was 45 ms. The injection volume was 1 μl. Organic samples were diluted 1:11 with hexane (57–60°C from light petroleum). The PTV splitting ratio was 1:100.

Quantitative analyses

In all GC analyses the internal standard method was used with *n*-dodecane as the internal standard (I.S.) and retention times relative to *n*-dodecane being used for identification. Peak-area measurements were used for quantitation.

Wet oxidation

A 250-ml three-necked, round-bottomed flask was equipped with an efficient tap-water reflux condenser with a non-return valve at the top (reaction gases were permitted only to escape). Solid catalyst in an amount ranging from $9 \cdot 10^{-5}$ to $1.44 \cdot 10^{-3}$ mol (ref. 4) was added, followed by 6 ml of the organic mixture.

The reactor was heated at reflux temperature with vigorous magnetic stirring, then 36% hydrogen peroxide was added continuously at a fixed flow-rate, ranging from about 2 to 30 ml/h, with a good-quality peristaltic pump equipped with silicone-rubber tubing. Magnetic stirring was stopped at intervals and samples (a few drops) were removed periodically with the aid of a small I.D. PTFE tube and a syringe, and stored in 1-ml PTFE-faced screw-cap vials.

At the end of the wet oxidation run all the collected samples were diluted with hexane and analysed by capillary GC.

RESULTS AND DISCUSSION

Preliminary runs showed that both copper oxides and iron(II) sulphate are suitable catalysts for the wet oxidation of the reference organic mixture by 36% hydrogen peroxide. However, copper(II) oxide[3] and copper(I) oxide gave irreproducible results whereas iron(II) sulphate did not show effect and was therefore selected as the catalyst for the subsequent study.

Hydrogen peroxide–iron(II) is a well established oxidizing system (Fenton's reagent)[12–14] which acts by means of the production in solution of hydroxyl radicals. It is also well known that secondary reactions lead to hydroperoxy radicals[15], which are much less reactive and promote the unwanted decomposition of hydrogen peroxide to oxygen and water[16]. Hence in wet oxidation processes using metal salt catalysts there is an unwanted but unavoidable production of oxygen. An initial rapid addition of iron(II) to the reaction medium causes a temporary excess, which has been reported to be beneficial in reducing the production of oxygen[16]. Therefore, iron(II) sulphate was introduced at the beginning of the wet oxidation reaction, and the results confirmed the efficiency of this procedure.

Fig. 1 shows the gas chromatogram of a fresh, simulated organic mixture obtained with the oven temperature programmed from 45 to 300°C. All peaks eluting between 3 and 25 min are due to Solvesso 100 components, peaks 1–9 being selected for

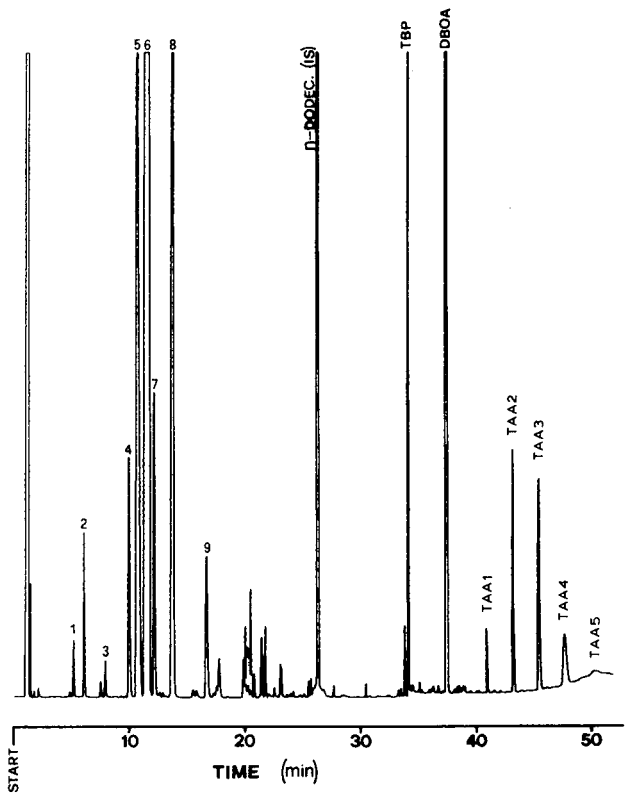

Fig. 1. Gas chromatogram of fresh simulated organic waste diluted 1:11 with hexane. Temperature programmed from 45°C (17 min) to 300°C at 8°C/min. Helium carrier gas, 10 p.s.i. PTV injection of 1 μl with a 1:100 splitting ratio. Linear velocity, 30 cm/s. Flame ionization detector, $4 \cdot 10^{-11}$ a.u.f.s. Peaks 1–9 relate to Solvesso 100 components; peak 6 is a composite, with mesitylene as the major constituent. Components TAA1–5 were all present in the technical-grade trioctylamine sample.

quantitative evaluation of wet oxidation. Peak 6 corresponds also to mesitylene (see second footnote to Table I). Peaks with retention times below 2 min are due to the hexane used to dilute the original samples.

Fig. 2 shows the gas chromatogram of a wet oxidized organic mixture after reaction with 22 volumes of 36% hydrogen peroxide per volume of fresh organic mixture. In this instance $2.4 \cdot 10^{-4}$ mol of iron(II) sulphate per millilitre of fresh organic mixture were used. A dramatic change in composition can be seen: all aromatic hydrocarbons were almost eliminated and many very small peaks with retention times ranging from about 27 to about 46 min were observed. Here *n*-dodecane was more concentrated, because other lipophilic substances disappeared.

These minor peaks appeared gradually after the beginning of the contact with hydrogen peroxide. They are byproducts formed in the oxidative decay of the organic matter. Their height was always very low, indicating that once a low concentration of such intermediates had been established, true conversion to carbon dioxide occurred, a situation resembling a stationary state (*i.e.*, a chemical sequence with the concentrations of the oxidized byproducts remaining almost constant), the net result of which is the conversion of organic substances to carbon dioxide and water.

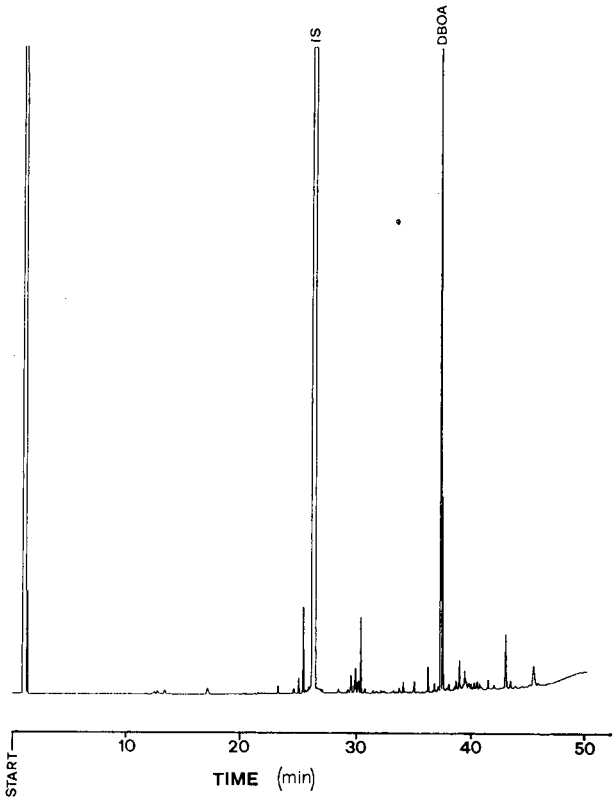

Fig. 2. Organic mixture after addition of 22 volumes of 36% hydrogen peroxide per volume of initial organic mixture [$2.4 \cdot 10^{-4}$ mol of iron(II) sulphate]. Conditions as in Fig. 1.

It should be noted that the oxygen-to-carbon dioxide ratio in the gas phase can be used as an indication of the efficiency of wet oxidation. The variation of this ratio with time can be followed by GC analysis of the off-gases using a system of parallel 2 m × 1/8 in. I.D. packed columns of molecular sieve 5A and Chromosorb 101, both 100–120 mesh, each connected to one side of a thermal conductivity detector[17].

Figs. 3 and 4 illustrate the influence of the amount of catalyst on the oxidative behaviour of all the components of interest in the simulated organic mixture, and Table I reports the GC–MS identification data for the fractions of interest of Solvesso 100 and for the TAAs (for a recent review on the use of GC and GC–MS in the identification of alkylbenzenes, see ref. 18). For clarity, experimental points are reported only for component 1.

As Figs. 3 and 4 show, all aromatic hydrocarbons behave in a very similar manner. A study of the precision of the method described under Experimental gave average relative standard deviations (R.S.D.) below 5% ($n = 3$).

At a constant amount of hydrogen peroxide, the oxidation rate invariably increased with increasing amount of catalyst (from curves a to f). When large amounts of catalyst were used, as in runs e and f, the kinetics showed only minor differences, indicating that larger amounts are impractical.

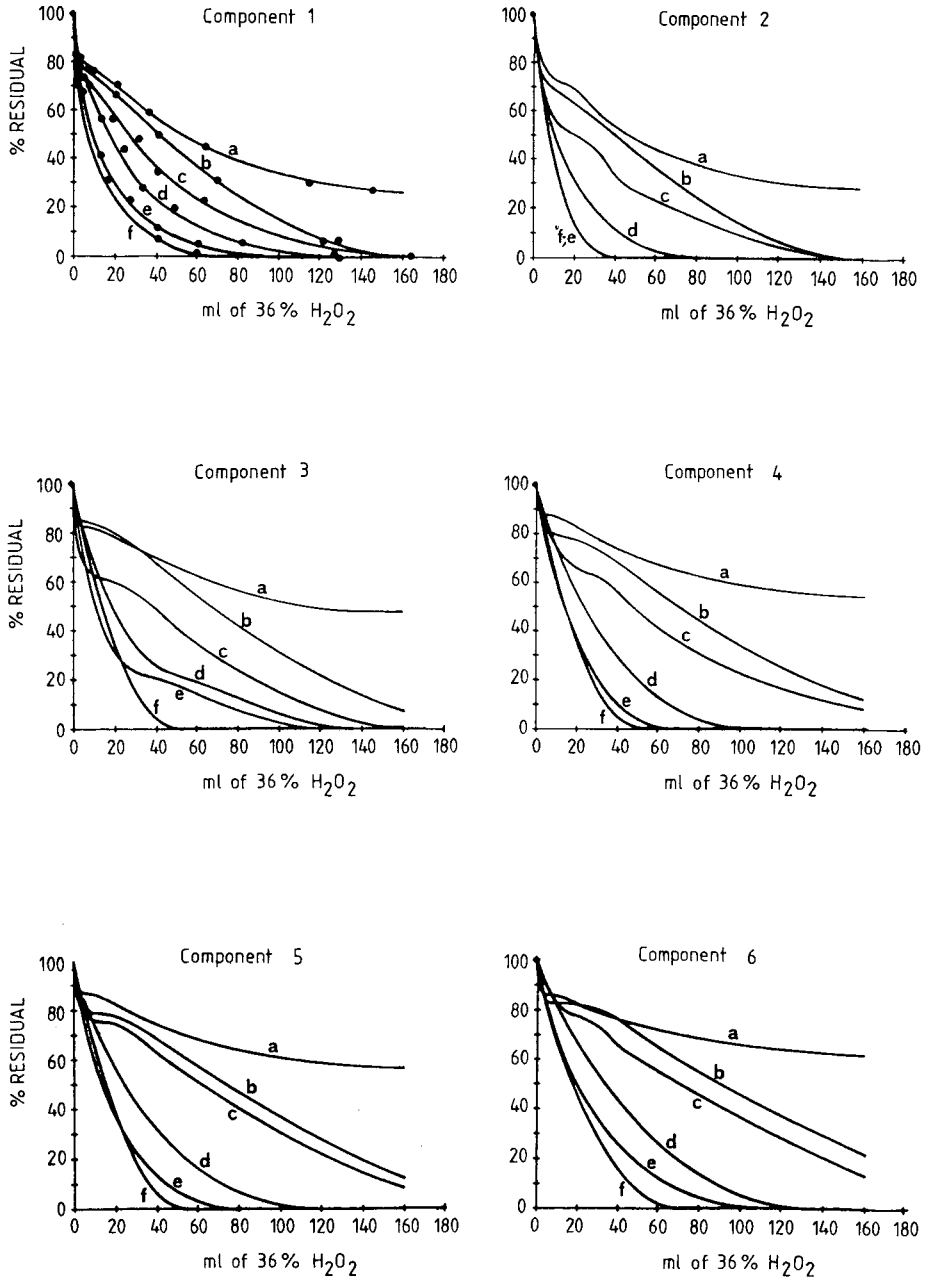

Fig. 3. Residual percentages of components 1–6 (listed in Table I) *versus* volume of 36% hydrogen peroxide. Curves a–f relate to runs in wich different amounts of iron(II) catalyst were used: (a) $8.99 \cdot 10^{-5}$ mol; (b) = 2(a); (c) = 4(a); (d) = 8(a); (e) = 12(a); (f) = 16(a).

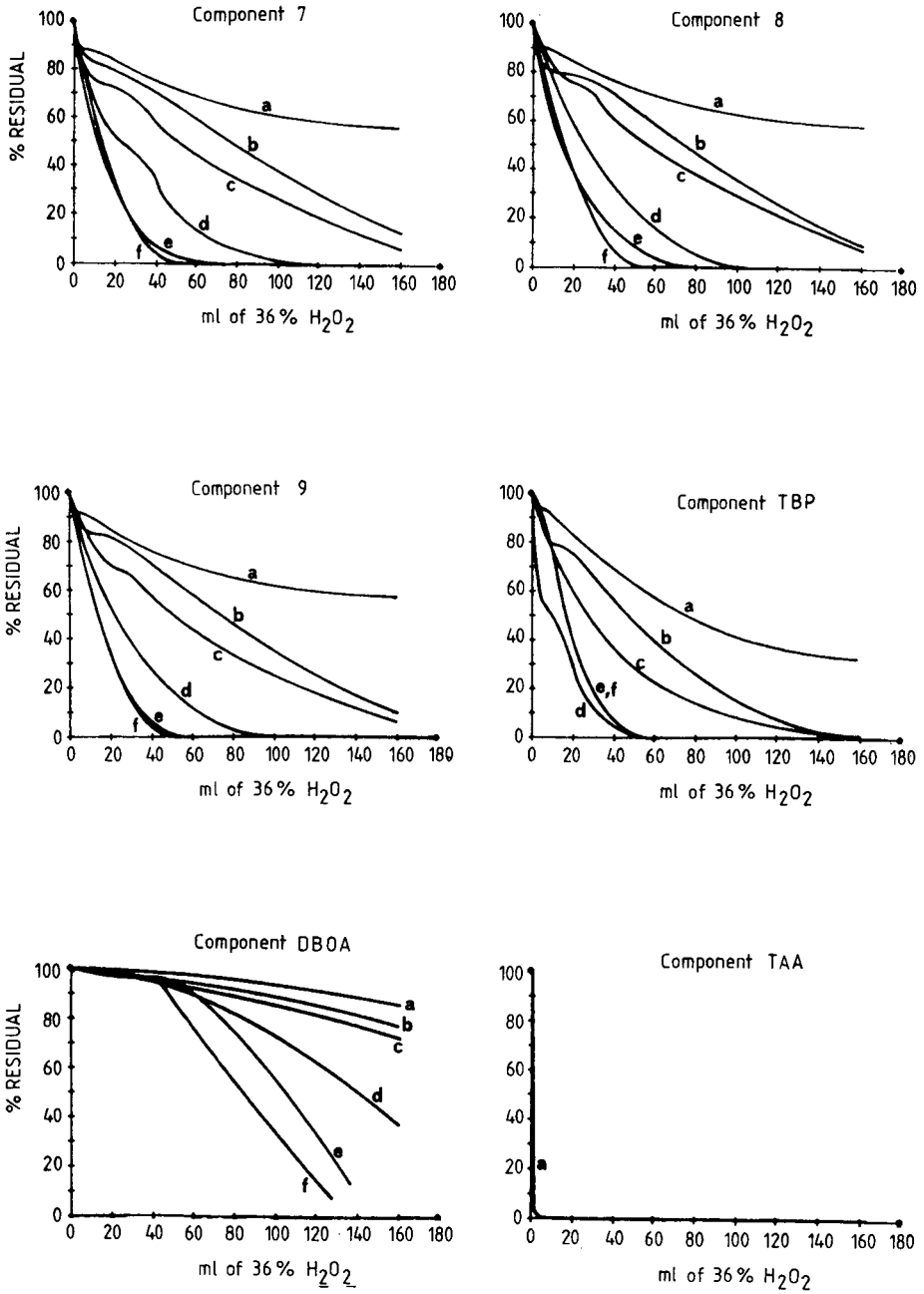

Fig. 4. Residual percentages of components 7, 8 and 9 (Table I), TBP, DBOA and TAAs. Conditions as in Fig. 3. All TAAs reacted very rapidly with concentrated hydrogen peroxide and their concentrations decreased to trace levels until the beginning of the wet oxidation runs. When the differences among runs a–f are not substantial, only run a is shown.

TABLE I
GC–MS IDENTIFICATION DATA FOR THE NUMBERED PEAKS IN FIG. 1

Peak No.	*MS-correlation*	*Correlation factor**
1	1,4-Dimethylbenzene	9813
	1,3-Dimethylbenzene	9795
	1,2-Dimethylbenzene	9737
2	1,2-Dimethylbenzene	9808
	Ethylbenzene	9806
	1,4-Dimethylbenzene	9747
3	1-Ethyl-3-methylbenzene	9739
	1-Ethyl-2-methylbenzene	9685
4	Propylbenzene	9918
5	1-Ethyl-3-methylbenzene	9905
	1-Ethyl-2-methylbenzene	9902
	1-Ethyl-4-methylbenzene	9901
6**	1,3,5-Trimethylbenzene	9842
	1,2,4-Trimethylbenzene	9864
7	1-Ethyl-3-methylbenzene	9904
	1-Ethyl-4-methylbenzene	9899
	1-Ethyl-2-methylbenzene	9871
8	1,2,4-Trimethylbenzene	9853
	1-Ethyl-3-methylbenzene	9834
9	1-Ethyl-3-methylbenzene	9868
	1-Ethyl-4-methylbenzene	9938
TAA1	Triheptylamine	8696
TAA2	Trioctylamine	9971
TAA3	Unknown	
TAA4	Unknown	
TAA5	Not seen with the GC–MS system	

* A correlation factor of 10000 means a formally exact MS identification based on the NBS Standard Library.

** This is a composite peak in which mesitylene predominates.

It is evident that the reaction rate is highest at the beginning of wet oxidation and is almost independent of the amount of iron(II) salt used. This is confirmed by the fact that, when iron(II) sulphate and organic compounds are mixed, the concentration of iron(II) remains almost constant for a certain time after the start-up of the hydrogen peroxide feed, until the aqueous phase becomes undersaturated with iron(II) owing to the water that is added with the hydrogen peroxide. After a certain time, depending on the initial amount of iron(II) salt and the flow-rate of the peristaltic pump, dilution of the iron(II) really starts, occurring with slower oxidizing kinetics.

The shoulders on the curves in Figs. 3 and 4 may be due to the complexity of the reaction mixture. Oxidized byproducts, formed as intermediates, are more soluble than hydrophobic precursors in the aqueous phase and are probably more easily attacked by concentrated hydrogen peroxide. In the initial stage of wet oxidation, the concentration of these byproducts increases and a substantial proportion of reactive oxidizing radicals is captured by them. When the concentration of intermediates reaches a maximum, the overall rate of wet oxidation is at a minimum, and subsequently the curves show a normal exponential decay due to hydrogen peroxide and catalyst dilution.

The same happens with TBP, whose decay curves closely resemble those of the aromatic components. TBP decomposes to carbon dioxide, inorganic phosphate and phosphoric acid, whereas DBOA is decomposed especially in the final stage of the oxidation run, presumably owing to the gradual decrease in pH that occurs when hydrogen peroxide oxidation takes place. Hence it appears that DBOA is more sensitive to acid hydrolysis than hydrogen peroxide oxidation. Wet combustion of hydrolytic byproducts of DBOA probably proceeds faster, owing to an increased solubility in the aqueous medium of octanoic acid and dibutylamine; these are not observed by GC.

All the TAAs show a very high reactivity with concentrated hydrogen peroxide and no amine peaks are detected by GC even when only a small volume of 36% hydrogen peroxide is added to the reaction vessel. Indeed, it has been known for a long time that tertiary amines react with peracids or concentrated hydrogen peroxide to give N-oxides, which are easily decomposed to alkenes by gently heating (Cope elimination of tertiary amine N-oxides[19,20]).

Fig. 5 shows the effectiveness of wet oxidation with 36% hydrogen peroxide with respect to some of the most significant organic components of the simulated waste as a function of the volumetric flow-rate of addition. The delivery rate ranged from (a) 30 ml/h to (d) about 2 ml/h; the slower the pumping flow-rate of the peroxide, the more efficient is the oxidation.

Particular mention should be made of the behaviour of *n*-dodecane, whose inertness towards 36% hydrogen peroxide, in the presence of different metallic catalysts and even under reflux conditions, is considered to be remarkable. This result contrasts with the postulated oxidation of *n*-dodecane to carbon dioxide[3].

Detailed experiments on this *n*-alkane (Table II) showed that its amount, evaluated by the external standard method, decreased linearly only by *ca.* 10% after 1 week under wet oxidation conditions. This result suggests that there were exclusively diffusive leaks of *n*-dodecane to the exterior, mainly with the off-gases, and that no appreciable reactions took place with concentrated hydrogen peroxide. The inertness of *n*-dodecane towards concentrated hydrogen peroxide is due to its negligible solubility in water and its molecular structure, which is uniformly hydrophobic and lacking in reactive sites.

Evidence that alkanes are resistant to 36% hydrogen peroxide was also obtained wet oxidizing a mixture composed of kerosene, tetrachloroethylene and *n*-dodecane as internal standard. The GC temperature programme (100°C for 3 min then increased to 200°C at 25°C/min) was applied in order to obtain as far as possible a non-resolved system for the kerosene fraction. Cumulative peak areas and a single response factor were applied to the kerosene peaks. Figs. 6 and 7 show that as the composition of kerosene remained almost unchanged, both qualitatively and quantitatively, the kerosene was not attacked by hydrogen peroxide whereas tetrachloroethylene was easily decomposed. The linear trend (Fig. 7) is distinctive for a non-wet-oxidisable system.

The inertness of *n*-dodecane towards hydrogen peroxide allowed its use as an internal standard and solved the otherwise extremely difficult problem of quantitative GC analyses in non-homogeneous wet oxidation systems.

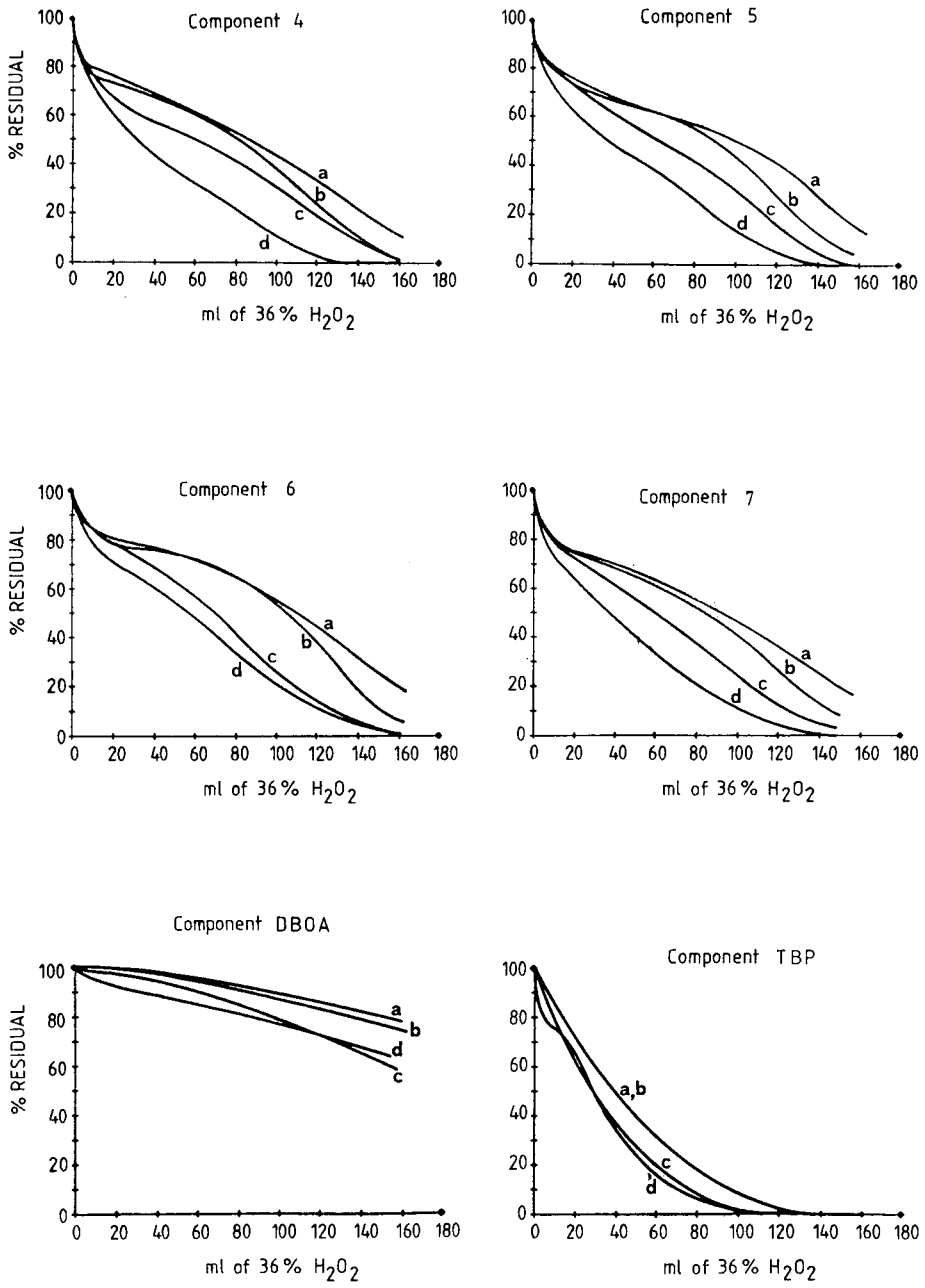

Fig. 5. Influence of the volumetric flow-rate of addition of concentrated hydrogen peroxide: (a) 1.96 ml/h; (b) = 3(a); (c) = 10(a); (d) = 15(a). Conditons as in Fig. 1.

TABLE II

CONDITIONS AND RESULTS OF WET OXIDATION RUNS CARRIED OUT TO VERIFY THE INERTNESS OF *n*-DODECANE TOWARDS HYDROGEN PEROXIDE

Organic mixture	*Organic to 36% H_2O_2 ratio (v/v)*	*Catalyst**		*Reaction time (h)*	*Residual (%)***	
		Components	*Amount (mg)*		*TBP*	*n-Dodecane*
TBP–*n*-dodecane (30:70, v/v)	1:20	CuO–Cu_2O (50:50)	90	96	0	94***
n-Dodecane	1:30	$FeSO_4 \cdot 7H_2O$	40	168		91
TBP–*n*-dodecane (30:70, v/v)	1:20	None§		144	40	97
	1:20	Pt–C (1:99, w/w)	90	72	100	93
	1:20	Pt–C (2:98)	45	72	87	98
	1:30	$FeCl_3$	200	72	2	93

* 5 ml of organic mixture reacted.

** Values obtained using the external standard calibration method. R.S.D. = 5 to 7 ($n=3$).

*** Average of two values (R.S.D. > 10).

§ Finely emulsified system by the use of 0.5 ml of a concentrated soap builder solution.

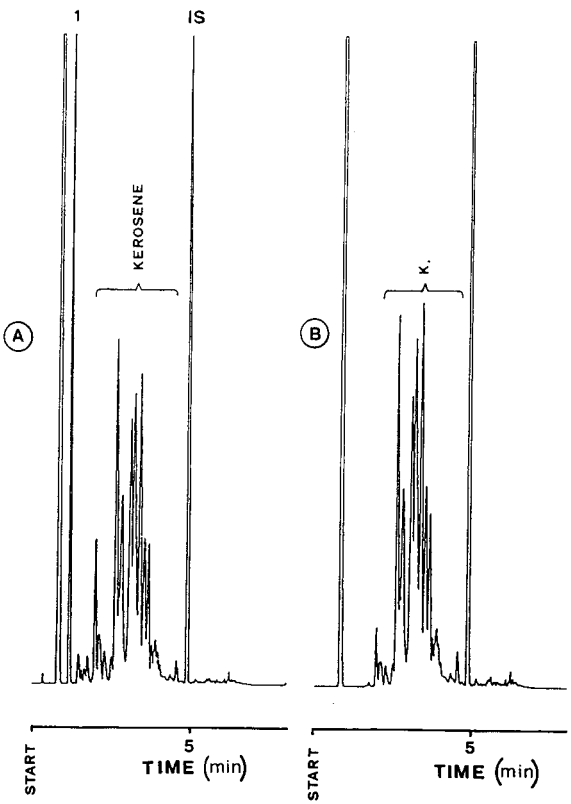

Fig. 6. Wet oxidation run to study the oxidizability of kerosene components and tetrachloroethylene (peak 1). Chromatogram A refers to a fresh mixture composed of hexane (solvent) and tetrachloroethylene–kerosene–dodecane (2:3.2:1) (point A in Fig. 7); B shows the composition of the mixture after addition of 33.3 volumes of a solution of 36% hydrogen peroxide–96% sulphuric acid, (99:1, v/v) (point B in Fig. 7). One volume of organic mixture reacted.

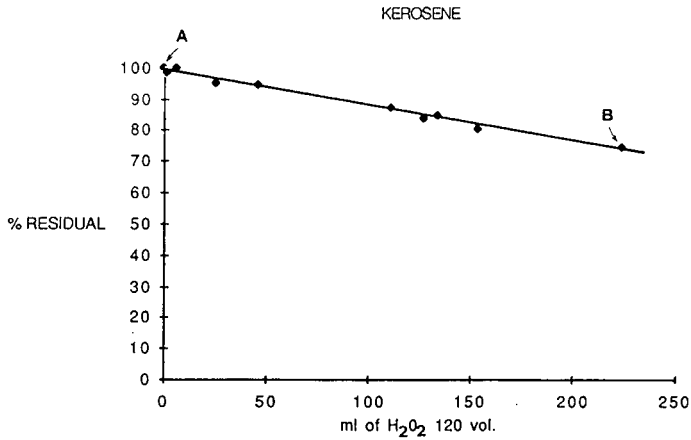

Fig. 7. Plot of the amount of residual kerosene *versus* the volume of hydrogen peroxide–concentrated sulphuric acid (99:1, v/v). The abscissa represents undiluted (36%) hydrogen peroxide.

CONCLUSION

The concentrated hydrogen peroxide–iron(II) salt system is suitable for the wet oxidation (*i.e.*, wet combustion to carbon dioxide and water) of a simulated organic mixture that reproduces a real radioactive waste coming from an Italian pilot-scale nuclear fuel reprocessing plant.

A quantitative approach has shown that a substantial volume reduction of the waste, composed of alkylaromatic hydrocarbons, TBP, DBOA, long-chain tertiary aliphatic amines and *n*-dodecane, can be achieved, probably with no problems of off-gas radioactivity.

Aromatic hydrocarbons and the alkyl groups of tributyl phosphate and tertiary aliphatic amines are totally and easily decomposed to carbon dioxide and water. Long-chain N,N-dialkylamides such as DBOA show a higher resistance to the oxidative decomposition, but they can also be degraded by wet oxidation in acidic media.

In contrast, *n*-dodecane is not decomposed or attacked by 36% hydrogen peroxide under the conditions used, even in very finely emulsified biphasic systems. At the end of the treatment *n*-dodecane constitutes a very pure alkane phase that can be recovered and reused for other nuclear purposes.

The efficiency of hydrogen peroxide in the wet oxidation depends on the amount of iron(II) sulphate used as the catalyst and also on the rate of addition of hydrogen peroxide to the reactor. Further optimization of these process parameters and a study of the effects of pH and UV light [36% hydrogen peroxide–96% sulphuric acid (99:2, v/v) appears to be very effective] on the wet oxidation process are now in progress. The main objective is the reduction of the excess of hydrogen peroxide needed for quantitative decomposition, with a view to the application of the wet oxidation process to other hazardous non-radioactive organic wastes.

n-Dodecane and homologous compounds can act as suitable internal standards for quantitative capillary GC applied to wet oxidation experiments.

ACKNOWLEDGEMENT

The author thanks Prof. G. Ortar, University of Rome, for his suggestions and criticisms.

REFERENCES

1 T. Braun and G. Ghersini (Editors), *Extraction Chromatography (Journal of Chromatography Library*, Vol. 2), Elsevier, Amsterdam, 1975.
2 *Alternatives for Managing Wastes From Reactors and Post-Fission Operations in the LWR Fuel Cycle*, U.S. Energy Research and Development Administration Springfield VA, ERDA-76-43.
3 T. Ichihashi, A. Hasegawa, K. Unoki, H. Matsuura and T. Mitsuzuka, in *Proceedings of International Conference on Nuclear Fuel Reprocessing and Waste Management, RECOD 87, Paris, France, August 23–27, 1987*, Vol. 2, Société Française d'Energie Nucléaire, Paris.
4 A. Yamanaka, M. Toshikuni and K.Suzuki, *U.S. Pat.*, 4 624 792, 1986; *C.A.*, 106 (1987) 109796x.
5 G. Kemmler, E. Schlich, *Nucl Technol.*, 59 (1982) 321.
6 T. Morioka, T. Ishikawa, H. Hoshikawa and T. Toyokichi, *Jpn., Pat.*, 61 283 899, 1985; *CA.*, 106 (1985) 164324s.
7 D. Tignmouth Shore, *Br. Pat.*, 2 070 580, 1980; *C.A.*, 96 (1980) 129173v.
8 T. Morioka, T. Ishikawa and H. Hoshikawa, *Jpn. Pat.*, 61 189 500, 1985; *C.A.*, 106 (1985) 127740d.
9 K. Unoki, T. Ichihashi, A. Hasegawa and T. Sato, *Jpn. Pat.*, 61 165 691, 1985; *C.A.*, 105 (1985) 234335b.
10 Nippon Atomic industry Group Co., Ltd.; Toshiba Corp., *Jpn. Pat.*, 60 061 697, 1983; *C.A.*, 103 (1984) 44670t.
11 Nippon Genshiryoku Jigyo; Toshiba KK, *Jpn. Pat.*, 61 269 096, 1986; *C.A.*, 106 (1987) 127749p.
12 H. J. H. Fenton, *Proc. Chem. Soc.*, 9 (1893) 113.
13 H. J. H. Fenton, *J. Chem. Soc.*, 65 (1894) 899.
14 C. Walling, *Acc. Chem. Res.*, 8 (1975) 125.
15 F. Minisci, *Chim. Ind. (Milan)*, 65 (1983) 487.
16 I. M. Kolthoff, E. B. Sandell, E. J. Meehan and S. Bruckenstein, *Quantitative Chemical Analysis*, Piccin/Macmillan, Padova, 1974, p. 808.
17 B. Thompson, *Fundamentals of Gas Analysis by Gas Chromatography*, Varian, Palo Alto, CA, 1977, p. 36.
18 E. Matisová, *J. Chromatogr.*, 438 (1988) 131.
19 A. C. Cope and E. R. Trumbull, *Org. React.*, 11 (1960) 317.
20 C. H. DePuy and R. W. King, *Chem. Rev.*, 60 (1960) 431.

Journal of Chromatography, 463 (1989) 95–106
Elsevier Science Publishers B.V., Amsterdam — Printed in The Netherlands

CHROM. 21 031

THERMOSPRAY HIGH-PERFORMANCE LIQUID CHROMATOGRAPHIC–MASS SPECTROMETRIC CHARACTERIZATION OF BIOLOGICAL MACROMOLECULES

I. ANALYSIS OF ACID HYDROLYSATE OF PEPTIDES

TENG-MAN CHEN* and JOHN E. COUTANT
Merrell Dow Research Institute, Analytical Chemistry Department, 2110 E. Galbraith Road, P.O. Box 156300, Cincinnati, OH 45215-6300 (U.S.A.)
(First received July 6th, 1988; revised manuscript received October 5th, 1988)

SUMMARY

A method for the routine analysis of phenylthiocarbamyl (PTC) amino acids by thermospray high-performance liquid chromatography–mass spectrometry (TSP LC–MS) is described. Data were acquired on a small dedicated TSP LC–MS system in which the temperature of the vaporizer and ion source block were optimized. PTC-amino acids exhibited unique TSP mass spectra containing sufficient fragment ions to determine structural data. Therefore, using this method the amino acids contained in the acid hydrolysates of unique and modified peptides were able to be positively identified. Additionally, the amino acid composition of peptides as determined by TSP LC–MS in the selected ion monitoring mode corresponded well with the theoretical value. The detection limits for the PTC-amino acids were at the low picomole level.

INTRODUCTION

Within the last few years the use of high-performance liquid chromatography (HPLC) for the analysis of derivatized amino acids obtained from the acid hydrolysis of proteins and peptides has overtaken classical technique used for amino acid analysis as the accepted method of choice. Several reagents including phenyl isothiocyanate (PITC), dansyl chloride, dabsyl chloride, *o*-phthalaldehyde, ninhydrin and fluorescamine have been used[1]. One of the more popular methods involving the use of PITC to form phenylthiocarbamyl (PTC) amino acid derivatives was first demonstrated by Koop *et al.*[2] and later commercialized by Waters Assoc. as the Pico-Tag™ system[3]. The advantages of this method include reaction with primary and secondary amino acids, producing quantitatively stable derivatives, and relatively easy and fast derivatization. A disadvantage is the dependence on retention time data for the qualitative identification of amino acids. The PTC-amino acids all have the same chromophore and, although this is an advantage for quantitation by UV methods, it

0021-9673/89/$03.50

makes identification very difficult. This is also a problem with other derivatization methods because the chromophore is usually contained in the derivatizing reagent and differences in the UV spectra obtained with a diode-array detector are slight.

On-line liquid chromatography–mass spectrometry (LC–MS) has been increasingly used in the past few years. Many of the early studies dealt with the analysis of both underivatized and derivatized amino acids[4–6]. The recent refinements in thermospray (TSP) ion source design, the availability of inexpensive, dedicated mass spectrometer systems and the development of HPLC systems designed for LC–MS have made the routine application of TSP LC–MS to quantitative and qualitative amino acid analysis practical[7]. This paper describes a TSP LC–MS procedure for the analysis of the acid hydrolysate of peptides using currently available commercial equipment. PITC was used for derivatizing the acid hydrolysates prior to TSP LC–MS analysis.

EXPERIMENTAL

Materials

Individual amino acid standards, an amino acid standard mixture (2.5 μmol/ml in 0.1 *M* hydrochloric acid) and angiotensin I were purchased from Sigma (St. Louis, MO, U.S.A.). PTH-amino acids, PITC reagent and 6 *M* hydrochloric acid of protein sequencing grade were obtained from Pierce (Rockford, IL, U.S.A.). N-Methylamino acids were obtained from Peptides International (Louisville, KY, U.S.A.). Rat atrial natriuretic peptides (rANP) were prepared at the Merrell Dow Research Institute. Acetonitrile was an HPLC-grade product from Burdick & Jackson Labs. (Muskegon, MI, U.S.A.). Water was purified with a Barnstead NANOpure/ORGANICpure system. All other chemicals used were of analytical-reagent grade.

TSP LC–MS

The TSP LC–MS apparatus consisted of a Hewlett-Packard (Palo Alto, CA, U.S.A.) 5970 mass-selective detector mounted in a Vestec (Houston, TX, U.S.A.) 101 TSP interface consisting of both the TSP ion source and associated vacuum systems. Data were acquired and the instrument controlled by a Hewlett-Packard 59970 ChemStation.

The HPLC system consisted of a 600-MS multi-solvent delivery system (Waters Assoc., Milford, MA, U.S.A) that was designed with a hydraulic system to optimize flow stability and included a high-pressure switching valve to change from direct loop injection to separations using a column. Manual injections were done using a Waters Assoc., UK6 injector. A Waters Assoc. 490-MS programmable multi-wavelength detector with a high-pressure flow cell was installed in series between the column and the TSP vaporizer, allowing UV data to be obtained at the same time as the LC–MS data. In addition, a Waters Assoc. 590 programmable pump was used to add buffers via a post-column device to enhance response in the thermospray process. Chromatography was performed at 35°C using a Waters Assoc. Nova-Pak C_{18} column (15 cm × 3.9 mm I.D.), preceded by an Alltech C_{18} guard column (2 cm × 2 mm I.D.), with gradient elution using acetonitrile–0.05 *M* ammonium acetate at a flow-rate of 1 ml/min. The detailed mobile phase composition and the gradient elution used for the separation of PTC-amino acid standard mixture are described in Table I. The column

TABLE I
LINEAR GRADIENT FOR THE SEPARATION OF PTC-AMINO ACID STANDARDS

Time (min)	*Mobile phase A**	*Mobile phase B***
0	100	0
2	100	0
12	70	30
17	70	30
31	20	80
32	0	100
50	0	100

* 0.05 *M* Ammonium acetate in water.
** 0.05 *M* Ammonium acetate in water–acetonitrile (50:50).

effluent was mixed, through the use of a mixing tee located between multi-wavelength detector and TSP interface, with 0.5 *M* ammonium acetate at a flow-rate of 0.2 ml/min. The amount of sample injected was 10 μl (0.5 nmol).

The optimum temperature for the thermospray vaporizer was determined to be 162°C for the initial gradient conditions (100% mobile phase A). The vaporizer temperature was then gradually adjusted, through a pre-set automatic gradient compensation controller, to 154°C when the gradient elution reached 100% mobile phase B. The ion source block temperature (desolvation chamber) was maintained constantly at 280°C.

Acid hydrolysis of peptides

Acid hydrolysis was performed using the procedure described in the operator's manual of Waters Pico-Tag workstation. Culture tubes (6 × 50 mm) made of Pyrex (Corning, NY, U.S.A.) were used as sample containers, pre-cleaned with 6 *M* hydrochloric acid and heated at 120°C. Peptide samples (25 nmol) were hydrolyzed *in vacuo* for 24 h at 110°C in 6 *M* hydrochloric acid containing 1% phenol. All drying steps were carried out in a Speed Vac concentrator (Savant Instruments, Farmingdale, NY, U.S.A.) without heat.

PITC derivatization

Derivatization was performed essentially as described by Bidlingmeyer *et al.*[3]. The dried amino acid standards and acid hydrolysate of peptide were dissolved in 10 μl of coupling buffer (absolute ethanol–water–triethylamine, 2:2:1). The solutions were dried and then derivatized with 20 μl of fresh coupling reagent (absolute ethanol–water–triethylamine–PITC, 7:1:1:1). After reaction for 30 min at room temperature, the derivatized samples were dried and dissolved in 500 μl of mobile phase A for immediate TSP LC–MS analysis.

RESULTS AND DISCUSSION

Although several LC methods have been developed for the separation of PTC-amino acids[8–10], the buffers used in the mobile phase were either non-volatile or varied in concentration while performing the gradient elution, thus making them

unsuitable for TSP LC–MS work. In this study, ammonium acetate was selected as a mobile phase buffer as it is volatile and can also be used as a reagent to induce TSP ionization. The concentration of the buffer was maintained constant throughout the gradient elution, which is essential for obtaining a stable baseline. A post-column device was used to adjust the concentration of ammonium acetate, independent of that needed for separation, to be about 0.1 *M*. This has been reported to be the optimum region to perform TSP ionization[11].

Fig. 1 shows a total ion chromatogram of PTC-amino acid standards obtained by TSP LC–MS. As noted by others[8–10], derivatization of amino acids with PITC produced reagent-related byproducts such as the peaks R shown. The other byproducts (not shown in Fig. 1) were eluted between 35 and 45 min. In fact, byproduct R eluting at 23.2 min was not observed with UV detection and could be easily eliminated by drying the sample in the Speed Vac for about 20 min. Byproduct R eluted at 25.7 min was detected by both total ion and UV detection and exhibited an $[M + H]^+$ ion at *m/z* 181.

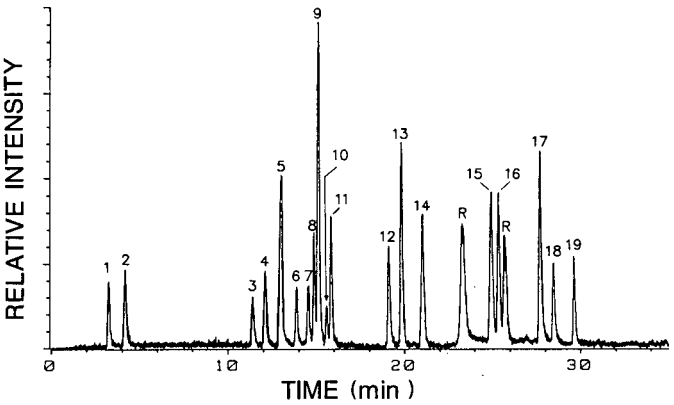

Fig. 1. Total ion chromatogram (*m/z* 125–500) of PTC-amino acids obtained by TSP LC–MS. For identification of peaks 1–19, see Tables II and III. Peak R = reagent-related byproduct. For chromatographic conditions, see Table I.

The TSP mass spectral data for the PTC-amino acids are given in Tables II and III. Note that Lys and Orn formed a bis-derivative with PITC and therefore yielded more fragment ions than the other PTC-amino acids. Owing to intense background ions present in the low mass range, the mass spectra acquired were restricted to be above *m/z* 125. Two fragment ions, which are not listed in Table II, were also found to be significant in the TSP mass spectra of some PTC-amino acids. One was the protonated phenylthiourea ion (*m/z* 153) and the other was the $[M + H - PITC]^+$ ion.

The data in Tables II and III indicate that each PTC-amino acid exhibited a unique base peak and characteristic fragment ions that reveal structural information. Accordingly, the amino acids obtained from acid hydrolysis of peptides can be positively identified. Except those of Asp, Glu, Gly, Lys, Orn, Pro, Ser and Thr, the base peaks of the PTC-amino acid studied all correspond to the $[M + H - H_2O]^+$ ions.

The base peaks of Asp and Glu (acidic amino acids) correspond to the $[M + H - H_2O - HCOOH]^+$ ions; Ser and Thr (hydroxyamino acids) correspond to the $[M + H - 2H_2O]^+$ ions; Lys and Orn (basic amino acids) correspond to the $[M + H - PITC - H_2O]^+$ ions; and Gly and Pro correspond to the $[M + H - H_2S]^+$ and $[M + H - H_2O - C_6H_4]^+$ ions, respectively. Because of the thermal instability of PTC-amino acids, the $[M + H]^+$ ions were found to be fairly weak or completely absent in the spectra. It was also noted that the abundance of the fragment ions in the TSP mass spectra was sensitive to the temperatures of the vaporizer and the ion source block. Therefore reproducible temperature control at these two positions is very critical in order to obtain a reproducible TSP mass spectrum.

N-Methylamino acids had also been examined in order to apply TSP LC–MS to the analysis of the acid hydrolysate of modified peptides. N-Methylated peptides are normally used to improve the biological potencies and to increase the resistance to enzymatic digests. However, the N-methylamino acids obtained from the acid hydrolysis of N-methylated peptides can not be confirmed using conventional PTC-amino acid analysis because of their unusually long retention times and the probable interference by the reagent-related byproducts. However, these modified amino acids can be unambiguously assigned by the TSP LC–MS method.

Unlike primary amino acids, the PITC-derivatized N-methylamino acids exhibited only the $[M + H]^+$ ion in their TSP mass spectra as listed in Table IV. This characteristic had also been observed in the TSP mass spectra of PTH-amino acids (Table V). A comparison of the TSP mass spectra of PITC-derivatized Ile and N-methyl-Ile ([N-Me]Ile) is given in Fig. 2. If N-methyl-Ile and PITC had formed a PTC derivative, it would have exhibited a fragmentation scheme similar to that of PTC-Ile except for the formation of the $[M + H - H_2S]^+$ ion. Instead, it yields only an ion at m/z 263 that corresponds to the $[M + H]^+$ ion of PTH-N-methyl-Ile, suggesting that N-methylamino acids and PITC formed a PTH derivative under the reaction conditions described. This suggestion is also supported by their relatively long retention times (capacity factor, k') compared with those of PTC- and PTH-amino acids. In theory, PTC-amino acids need an acid to initiate the cyclization and form the PTH-amino acid analogs[12]. It could be possible that N-methylamino acids are much more sensitive to trace amounts of residual acid.

Fig. 3 shows the application of TSP LC–MS to the analysis of an acid hydrolysate of an N-methylated rANP which is currently under study as an antihypertensive agent. The sample was chromatographed using the same gradient elution as described for the separation of PTC-amino acid standards. The peak identities were confirmed according to their TSP mass spectra.

Fig. 4 shows the application of TSP LC–MS to the confirmation of a modified dipeptide, ArgΨ[CH_2NH]Ile, obtained from the acid hydrolysis of a modified rANP. The sample was chromatographed using gradient elution with a higher concentration of acetonitrile in the mobile phase. Two peaks (a and b) were found to exhibit identical TSP mass spectra that correspond to the bis-PTC derivative of ArgΨ[CH_2NH]Ile. As L-amino acids were used to prepare the peptide, the formation of the diastereoisomers is probably due to the racemization occurring at the Arg moiety caused by the synthetic route used to prepare that peptide.

TSP LC–MS had also been evaluated for determining the amino acid composition of peptides. The base peaks of PTC-amino acids were used for selected-

TABLE II
TSP MASS SPECTRAL DATA FOR PTC-AMINO ACIDS

No.	*PTC-amino acid*	*Mol.wt.*	*k'*	*m/z (relative intensity, %)*		
				$[M + H]^+$	$[M + H - H_2O]^+$	$[M + H - H_2S]^+$
1	Asp	268	1.6	–	251 (11)	–
2	Glu	282	2.1	–	265 (25)	–
3	Ser	240	5.7	–	223 (10)	–
4	Gly	210	6.1	211 (10)	193 (62)	177 (100)
5	Asn	267	6.5	268 (8)	250 (100)	234 (3)
6	Gln	281	7.0	282 (18)	264 (100)	248 (10)
7	His	290	7.3	–	273 (100)	257 (22)
8	Thr	254	7.4	255 (11)	237 (39)	–
9	Ala	224	7.6	225 (9)	207 (100)	191 (18)
10	Arg*	309	7.8	–	292 (100)	276 (45)
11	Pro	250	8.0	–	233 (37)	–
12	Tyr	316	9.5	317 (7)	299 (100)	283 (8)
13	Val	252	9.9	253 (7)	235 (100)	219 (20)
14	Met	284	10.5	285 (5)	267 (100)	251 (29)
15	Ile	266	12.4	267 (14)	249 (100)	233 (23)
16	Leu	266	12.8	267 (13)	249 (100)	233 (26)
17	Phe	300	13.8	301 (13)	283 (100)	267 (52)

* Fragment ions at *m/z* 293, 275 and 231 were also observed.

TABLE III
TSP MASS SPECTRAL DATA FOR $(PTC)_2$-ORN AND $(PTC)_2$-LYS

*Fragment ion**	*m/z (relative intensity, %)*	
	(18) Orn (k' = 14.3)	*(19) Lys (k' = 14.8)*
$[M + H - H_2O]^+$	385 (21)	399 (23)
$[M + H - H_2O - H_2S]^+$	351 (17)	365 (18)
$[M + H - H_2O - C_6H_5NH_2]^+$	292 (51)	306 (45)
$[M + H - H_2O - PITC]^+$	250 (100)	264 (100)
$[M + H - H_2S - PITC]^+$	234 (15)	248 (60)
$[M + H - H_2O - C_6H_4 - PITC]^+$	174 (20)	188 (36)
$[M + H - 2PITC]^+$	133 (55)	147 (65)

* The fragment ions of relative intensity $\geqslant 15\%$ are included.

TABLE IV
TSP MASS SPECTRAL DATA FOR PITC-DERIVATIZED N-METHYLAMINO ACIDS

N-methylamino acid	*k'*	*m/z (relative intensity, %)*
Ala	16.7	221 (100)
Ile	21.3	263 (100)
Leu	21.8	263 (100)
Phe	21.0	297 (100)

$[M + H - 2H_2O]^+$	$[M + H - H_2O - HCOOH]^+$	$[M + H - H_2O - C_6H_4]^+$
–	205 (100)	–
–	219 (100)	–
205 (100)	–	–
–	–	–
–	–	–
–	–	–
–	–	–
219 (100)	–	–
–	–	–
–	–	–
–		157 (100)
–	–	–
–	–	159 (16)
–	–	191 (6)
	–	173 (15)
–	–	173 (16)
–	–	207 (10)

* Fragment ions at *m/z* 293, 275 and 231 were also observed.

TABLE V
TSP MASS SPECTRAL DATA FOR PTH-AMINO ACIDS

PTH-amino acid	*Molecular weight*	*k'*	*m/z (relative intensity, %)*
Ala	206	12.7	207 (100)
Ile	248	18.2	249 (100)
Leu	248	18.5	249 (100)
Phe	282	18.1	283 (100)

TABLE VI
RESPONSE FACTORS FOR PTC-AMINO ACIDS WITH SIM DETECTION

PTC-amino acid	*m/z*	*Response factor*	*PTC-amino acid*	*m/z*	*Response factor*
Asp	205	1.5	Pro	157	1.5
Glu	219	1.8	Tyr	299	1.9
Ser	205	1.7	Val	235	4.6
Gly	177	0.8	Met	267	2.6
Gln (I.S.)*	264	1.0	Ile	249	4.4
His	273	0.5	Leu	249	4.4
Thr	219	1.5	Phe	283	3.4
Ala	207	1.7	Lys	264	1.1
Arg	292	0.3			

* Internal standard.

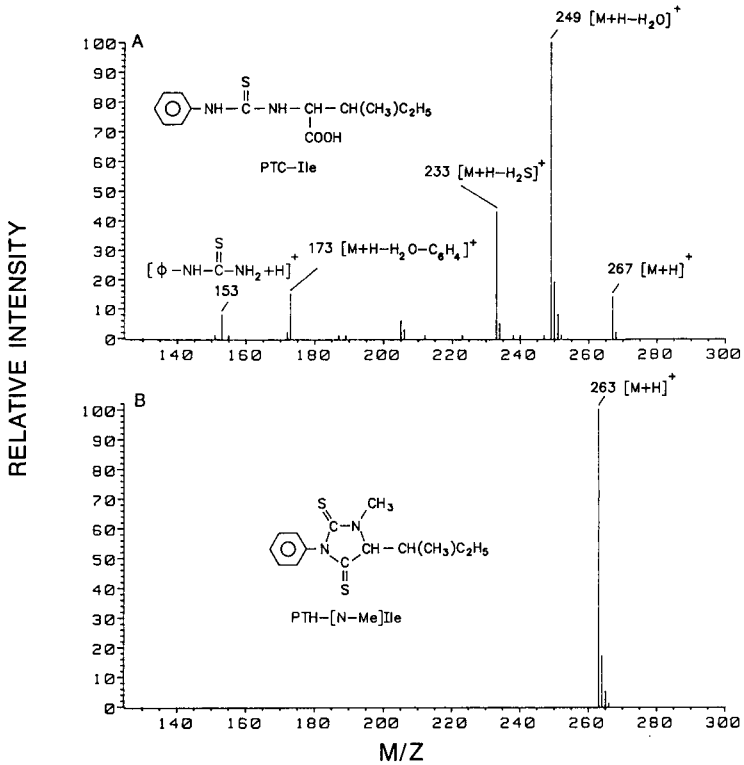

Fig. 2. TSP mass spectra of PITC-derivatized Ile (A) and N-methyl-Ile (B).

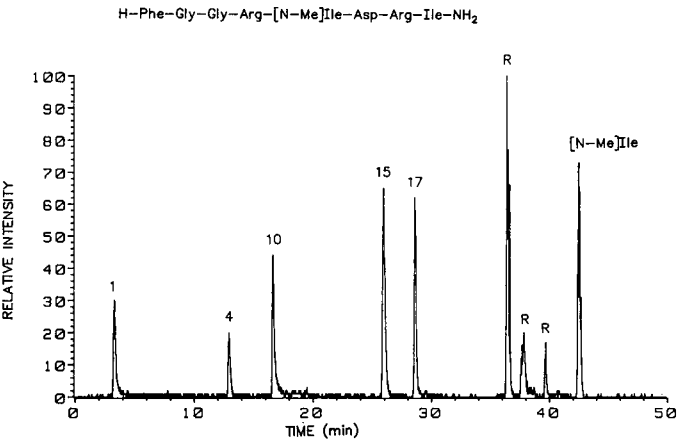

Fig. 3. Total ion chromatogram (*m/z* 125–500) of an acid hydrolysate of an N-methylated rANP. Peaks: 1 = Asp; 4 = Gly; 10 = Arg; 15 = Ile; 17 = Phe; R = reagent-related byproduct. For chromatographic conditions, see Table I.

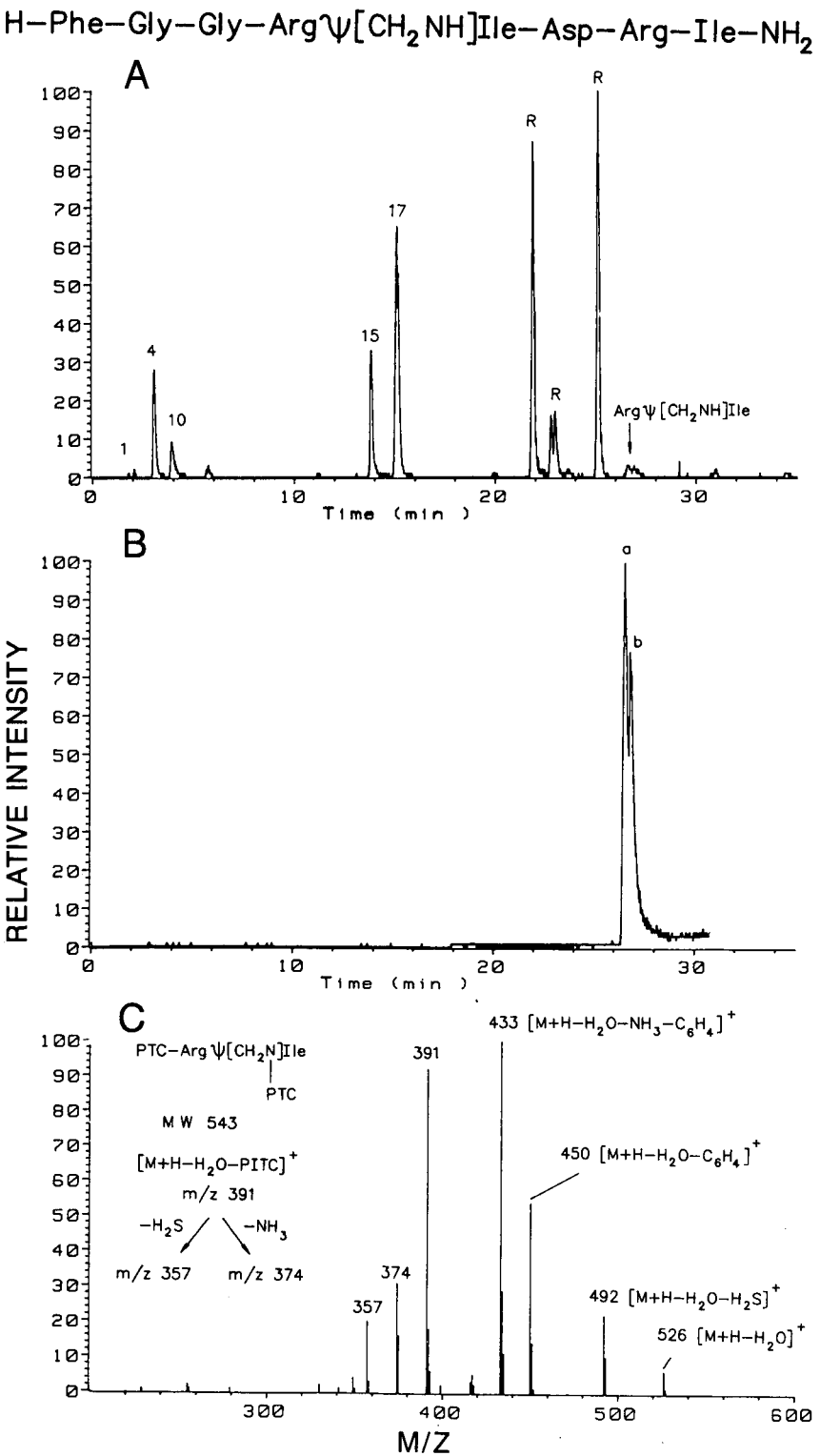

Fig. 4. Identification of ArgΨ(CH_2NH)Ile obtained from the acid hydrolysis of a modified rANP. (A) Total ion chromatogram (m/z 125–600); (B) selected ion chromatogram (m/z = 433); (C) TSP mass spectrum of the bis-PTC derivative of ArgΨ[CH_2NH]Ile. Mobile phase A = 0.05 *M* ammonium acetate in water–acetonitrile (90:10); mobile phase B = 0.05 *M* ammonium acetate in water-acetonitrile (25:75); linear gradient from 100% A to 100% B in 30 min at a flow-rate of 1 ml/min. Peaks: 1 = Asp; 4 = Gly; 10 = Arg; 15 = Ile; 17 = Phe; R = reagent-related byproduct. MW = Molecular weight.

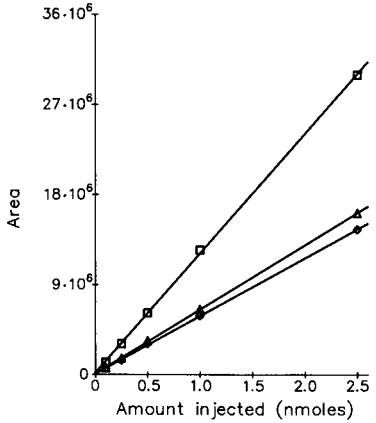

Fig. 5. Linearity of response. △ = Asp; ◇ = Gly; □ = Leu.

ion monitoring (SIM) detection. The peak areas were calibrated using Gln as an internal standard, which was added to the sample prior to PITC derivatization (Table VI).

The precision of the system was evaluated using five consecutive injections of Asp, Gly and Leu standards (0.5 nmol). The average relative standard deviation of the peak areas was 4.3%. Using the same standards the responses of the peak areas were found to be linear in the range of 0.1 to 2.5 nmol, as illustrated in Fig 5. The correlation

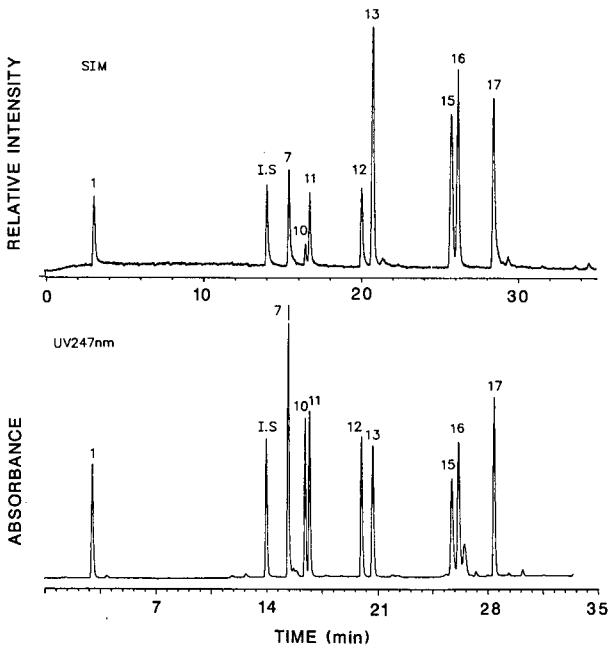

Fig. 6. Chromatograms of an acid hydrolysate of angiotensin I. Peaks: 1 = Asp; 7 = His; 10 = Arg; 11 = Pro; 12 = Tyr; 13 = Val; 15 = Ile; 16 = Leu; 17 = Phe; I.S. (internal standard) = Gln. For chromatographic conditions, see Table I.

TABLE VII
AMINO ACID COMPOSITION OF ANGIOTENSIN I

Amino acid	*Theoretical value*	*SIM value*	*UV (247 nm) value*
Arg	1	1.0	0.7
Asp	1	0.8	0.8
His	2	2.3	1.6
Ile	1	0.7	0.9
Leu	1	0.9	1.0
Phe	1	1.0	1.0
Pro	1	0.7	0.8
Tyr	1	0.7	0.7
Val	1	0.9	0.8

coefficients for these data exceeded 0.9998. The detection limits (signal-to-noise ratio = 2) for PTC-amino acids were found to be about 15 pmol except that for Arg (about 115 pmol).

An example of the determination of amino acids by TSP LC–MS applied to angiotensin I is shown in Fig. 6. The chromatogram obtained with UV detection is also given for comparison. The resulting amino acid compositions determined with SIM and UV detection correspond well with the theoretical values, as shown in Table VII.

CONCLUSIONS

TSP LC–MS is a sensitive and specific technique that can be used for the positive identification of acid hydrolysates of peptides. Therefore, it facilitates the procedure for confirming the structures of both natural and modified peptides whose structures normally can not be confirmed using conventional techniques for amino acid analysis. The quantitative result determined by TSP LC–MS with SIM detection is comparable to that obtained with UV detection. The results of this study reinforce the utility of having a detection system that can be sensitive, specific and quantitative and provide high-quality structural data.

ACKNOWLEDGEMENTS

The authors are indebted to Mr. C. F. Hassman and Dr. J. M. Berman for synthesizing the rat atrial natriuretic peptides.

REFERENCES

1 H. Engelhardt, *Chromatogr. Forum*, 1, No. 3 (1986) 39.
2 D. R. Koop, E. T. Morgan, G. E. Tarr and M. J. Coon, *J. Biol. Chem.*, 257 (1982) 8472.
3 B. A. Bidlingmeyer, S. A. Cohen and T. L. Tarvin, *J. Chromatogr.*, 336 (1984) 93.
4 D. Pilosof, H.-Y. Kim, M. L. Vestal and D. F. Dyckes, *Biomed. Mass Spectrom.*, 11 (1984) 403.
5 K. Matsumoto and S. Tsuge, *Shitsuryo Bunseki*, 34, No. 4 (1986) 243.
6 A. E. Ashcroft, J. R. Chapman and J. S. Cottrell, *J. Chromatogr.*, 394 (1987) 15.
7 E. G. Cassis, T. A. Dourdeville and M. P. Balogh, paper presented at the *Pittsburgh Conference and Exposition, New Orleans, LA, February 22–26, 1988.*

8 R. L. Heinrikson and S. C. Meredith, *Anal. Biochem.*, 136 (1984) 67.
9 S. A. Cohen, B. A. Bidlingmeyer and T. L. Tarvin, *Nature (London)*, 320 (1984) 769.
10 R. F. Ebert, *Anal. Biochem.*, 154 (1986) 431.
11 R. D. Voyksner and C. A. Haney, *Anal. Chem.*, 57 (1985) 991.
12 P. Edman and A. Henschen, *Mol. Biol. Biochem. Biophys.*, 8 (1975) 232.

Journal of Chromatography, 463 (1989) 107–118
Elsevier Science Publishers B.V., Amsterdam — Printed in The Netherlands

CHROM. 21 006

SELECTIVE, STABILITY-INDICATING ASSAY OF THE MAJOR IPECACUANHA ALKALOIDS, EMETINE AND CEPHAELINE, IN PHARMACEUTICAL PREPARATIONS BY HIGH-PERFORMANCE LIQUID CHROMATOGRAPHY USING SPECTROFLUORIMETRIC DETECTION

D. A. ELVIDGE*, G. W. JOHNSON and J. R. HARRISON
Analytical Development, The Boots Company, PLC, R4 Pennyfoot Street, Nottingham (U.K.)
(Received August 22nd, 1988)

SUMMARY

A selective high-performance liquid chromatographic procedure has been developed for the determination of the major Ipecacuanha alkaloids, emetine and cephaeline, in a number of linctus and pastille preparations. The reversed-phase chromatographic procedure uses an octadecyl-bonded column with a mobile phase of aqueous methanol containing an ion-pairing reagent. A spectrofluorimetric detector is used for increased sensitivity and selectivity. Sample preparation is simple, involving either straight dilution for linctus formulations or simple dissolution for pastilles. The procedure has been shown to be stability-indicating. Validation studies, to show that the method is precise, accurate and rectilinear, have been carried out on four linctus formulations and two pastille formulations. The method has been used to determine both emetine and cephaeline at levels as low as 5 μg/g in formulations.

INTRODUCTION

Various methods have been published for the determination of emetine and cephaeline in Ipecacuanha and formulations containing extracts of Ipecacuanha. The official British Pharmacopoeial method for assaying Ipecacuanha, liquid extract of Ipecacuanha and Ipecacuanha tincture involves extraction and titration of the total alkaloids. The method is not selective and is not stability-indicating. The United States Pharmacopoeial assay, based on a method developed by Smith *et al.*[1], requires a determination of the total diethyl ether-soluble alkaloids by extraction and titration, and a separate determination of the cephaeline and emetine by a complex and tedious liquid–liquid partition chromatographic isolation of the individual alkaloids, followed by a spectrophotometric determination. The method is reported to remove minor alkaloids such as emetamine and psychotrine.

More selective procedures, using high-performance liquid chromatography (HPLC) with spectrophotometric detection, have been published by various workers[2–5]. These methods have generally been applied to Ipecacuanha root or liquid extracts in which the alkaloid content is relatively high, between 0.1 and 2%. These

0021-9673/89/$03.50

methods are not sufficiently selective or sensitive when applied to multicomponent formulations containing very low levels of the alkaloids.

In order to improve the limit of determination other workers have used conductance detectors[6], whilst methods involving pre-column derivatisation[7] and post-column derivatisation[8,9] to produce fluorescent compounds have also been described. Crouch *et al.*[10], has recently determined the two alkaloids in biological materials by HPLC using a spectrofluorimetric detector to measure their natural fluorescence.

The current paper describes a selective procedure, using HPLC and a spectrofluorimetric detector, for the rapid, accurate and reproducible determination of emetine and cephaeline at very low levels in a range of pharmaceutical formulations.

EXPERIMENTAL

Chromatographic equipment

A high-performance liquid chromatograph comprising a Waters Assoc. Model 6000A reciprocating pump, a WISP automatic sampler, a Perkin-Elmer LS 4 fluorescence spectrophotometer and an LCI 100 computing integrator was used for routine sample examination.

Chromatographic column

A Waters Assoc. μBondapak C_{18} column, 15 cm × 3.9 mm I.D., was contained in a column oven set at 35°C.

Chromatographic conditions

The pump was set to deliver the mobile phase at 2 ml/min. The fluorescence detector was set with an excitation wavelength of 276 nm, an emission wavelength of 304 nm, a fixed scale value of 0.4 and a response of 4.

Reagents and solutions

Emetine dihydrochloride was supplied by Sigma (Poole, U.K.) and assessed to contain 72% emetine base. Cephealine dihydrobromide was supplied by Sandoz (Basle, Switzerland) and assessed to contain 68% cephaeline base. The other Ipecacuanha related alkaloids were kindly donated by Wellcome Research Lab. (Beckenham, U.K.). All reagents were either HPLC grade or analytical grade and supplied by FSA (Fisons) (Loughborough, U.K.).

The mobile phase was prepared by dissolving 1.0 g of 1-heptanesulphonic acid sodium salt in water; 400 ml of methanol and 1 ml of orthophosphoric acid were added and the solution diluted to 1 l with water. Before use the mobile phase was filtered through a Whatman GF/F filter contained in a Hartley funnel.

Preparation of standard solutions

The required standard solutions were prepared in the following manner.

Internal standard solution: 0.1 g of ethyl 4-hydroxybenzoate was dissolved in 50 ml of acetonitrile and the solution diluted to 500 ml with mobile phase.

Solution of emetine and cephaeline (solution A): 0.01 g of each of emetine dihydrochloride and cephaeline dihydrobromide of known purities were accurately

TABLE I

PREPARATION OF STANDARD SOLUTIONS OF EMETINE AND CEPHAELINE CONTAINING INTERNAL STANDARD

Formulation	*Theoretical Ipecacuanha content (%)**	*Preparation of standard solution*		
		Emetine/cephaeline solution (A) (ml)	*Internal standard (ml)*	*Mobile phase (ml)*
Linctus A and B	0.125	5	10	85
Linctus C	0.3	10	20	70
Linctus D	0.5	20	20	60
Pastilles A and B	0.4	25	50	125

* Expressed as percentage of Ipecacuanha Liquid Extract B.P.

weighed into a 500-ml graduated flask and dissolved in and diluted to volume with mobile phase.

Standard solution of emetine and cephaeline: different strengths of standard solutions were required, depending on the level of Ipecacuanha present in the sample. The standard solutions for the different formulations were prepared as shown in Table I.

Preparation of sample solutions

Sample preparation was dependent on the type of sample being examined *i.e.* liquid or solid, and on the level of Ipecacuanha present. Liquid samples were diluted with mobile phase. Pastilles were dissolved in the mobile phase either with or without gentle heating. The sample solution for the different formulations were prepared as shown in Table II.

Assay procedure

The instrumentation was assembled as previously indicated and the chromatographic column was conditioned by means of a series of injections of the appropriate standard solution of emetine and cephaeline containing internal standard. Before use, and in order to evaluate the chromatographic system, a number of system suitability tests were performed. A standard solution of emetine and cephaeline containing internal standard was injected and the resolution (R) between the cephaeline and internal standard peaks was calculated using the following equation:

TABLE II

PREPARATION OF SAMPLE SOLUTIONS

Formulation	*Sample taken*	*Internal standard (ml)*	*Mobile phase (ml)*
Linctus A and B	10 g	10	80
Linctus C and D	10 g	20	70
Pastilles A and B	10 pastilles	50	150

$$R = \frac{1.18\ (t_2 - t_1)}{W_1 + W_2}$$

where t_1 and t_2 are the retention distances of the peaks and W_1 and W_2 are the widths of the peaks at their half-heights. Typical values for R were in the range 4–6.

At the same time the number of theoretical plates per column (n) was calculated from the cephaeline peak using the following equation:

$$n = 5.54\left(\frac{t}{W}\right)^2$$

where t is the retention distance of the peak, and W = width of peak at its half height. Typical values for n were in the range 1000–2000.

The precision of the chromatographic system was also determined using the percentage relative standard deviation of the ratio of the areas of the cephaeline peak to the area of the internal standard peak and calculated from the result of six successive injections. Typically the percentage relative standard deviation was in the range 0.5–2.

Sample solutions were injected in duplicate with the appropriate standard solution of emetine and cephaeline containing internal standard chromatographed before, after and interspersed with the samples. Volumes of 10 μl were found to be suitable for all samples except Linctus A and B when a volume of 25 μl was used.

Calculations

The areas of emetine, cephaeline and internal standard peaks were measured in the standard and sample chromatograms by integration. Typical retention times of cephaeline and emetine were 1.8 and 3.0 measured relative to the internal standard which was eluted from the column in about 5 min. For each chromatogram the following ratios were calculated:

$$\frac{\text{area of cephaeline peak}}{\text{area of internal standard peak}} \quad (1)$$

$$\frac{\text{area of emetine peak}}{\text{area of internal standard peak}} \quad (2)$$

The mean ratios for cephaeline and emetine in the standard (S_1 and S_2, respectively) and the mean ratios for cephaeline and emetine in the sample (E_1 and E_2, respectively) were calculated.

For the liquid samples the content of cephaeline and emetine was calculated from the following equations:

$$\text{Cephaeline } (\mu\text{g/g}) = \frac{E_1}{S_1} \cdot \frac{W_1}{500} \cdot \frac{\text{Volume of solution A taken (ml)}}{\text{Weight of sample taken (g)}} \cdot P \cdot 10\,000$$

$$\text{Emetine } (\mu\text{g/g}) = \frac{E_2}{S_2} \cdot \frac{W_2}{500} \cdot \frac{\text{Volume of solution A taken (ml)}}{\text{Weight of sample taken (g)}} \cdot F \cdot 10\,000$$

For pastilles the content of cephaeline and emetine was calculated from the following equations:

$$\text{Cephaeline (mg per pastille)} = \frac{E_1}{S_1} \cdot \frac{W_1}{500} \cdot \frac{\text{Volume of solution A taken (ml)}}{\text{Number of pastilles taken}} \cdot \frac{P}{100}$$

$$\text{Emetine (mg per pastille)} = \frac{E_2}{S_2} \cdot \frac{W_2}{500} \cdot \frac{\text{Volume of solution A taken (ml)}}{\text{Number of pastilles taken}} \cdot \frac{F}{100}$$

where W_1 is the weight of cephaeline dihydrobromide (g) taken to prepare solution A, W_2 is the weight of emetine dihydrochloride (g) taken to prepare solution A, P is the percentage of cephaeline in the cephaeline dihydrobromide, F is the percentage of emetine in the emetine dihydrochloride.

METHOD EVALUATION

Selectivity

The use of a spectrofluorimetric detector with variable adjustment of both excitation and emission wavelengths increased the selectivity and the sensitivity of the method. The excitation and emission wavelengths, although not exactly at the maximum values for emetine and cephaeline, were chosen to give a good response for both alkaloids and to allow simultaneous determination of other components present in some of the formulations.

Emetine and cephaeline were separated from each other and from other Ipecacuanha-related alkaloids using the recommended chromatographic conditions. The retention times of the alkaloids, relative to the internal standard are given in Table III.

In order to assess the possibility of interference to emetine and cephaeline from coeluting related alkaloids, diode-array scans were performed on the two alkaloids after chromatographic separation. Because low levels of alkaloids in the formulations precluded accurate spectrophotometeric measurements a sample of Ipecacuanha

TABLE III

RELATIVE RETENTION TIMES OF IPECACUANHA-RELATED ALKALOIDS

Alkaloid	*Relative retention time*
Ethyl 4-hydroxybenzoate (internal standard)	1.0
Cephaeline	1.8
O-methylpsychotrine*	2.1
Didehydroemetine	2.2
Emetamine*	2.7
Tetradehydroemetine*	2.8
Emetine	3.0

* Not detected by fluorimetric detection at recommended wavelengths, retention times measured using a UV detector at 214 nm.

liquid extract was used. The diode-array scans obtained were found to be superimposable with those of a standard solution containing emetine and cephaeline.

The absence of interference in the method (a) from other components of the formulations, (b) from the internal standard and (c) to the internal standard was demonstrated by applying the method (a) to the formulation bases containing no Ipecacuanha liquid extract, (b) to a solution of the internal standard and (c) to samples of the complete formulations without the addition of internal standard, respectively.

Rectilinearity of response

For the chromatographic procedure the relationship between the response, in terms of the ratio of the area of the emetine and cephaeline peaks to that of the internal standard peak, and the amount of each alkaloid chromatographed, was determined. Solutions containing the same concentration of internal standard but different concentrations of emetine and cephaeline were chromatographed. The rectilinearity of concentration–response relationship for emetine and cephaeline is given in Table IV.

Recovery experiments

The accuracy of the method was assessed by applying the method to the appropriate formulation base incorporating accurately weighed amounts of emetine and cephaeline. Recovery experiments were carried out for each formulation and the results obtained are given in Table V.

Precision

The precision of the method was determined by replicate assay of samples with ten complete determinations being performed in each case. The precision results obtained on all the formulations are given in Tables VI and VII.

Stress storage

In order to assess the HPLC procedure as being stability-indicating it was necessary to check the retention times and responses of known degradation products. Schuijt *et al.*[11] had previously shown that on refluxing emetine in water until about

TABLE IV

RECTILINEARITY OF CONCENTRATION–RESPONSE RELATIONSHIP

The estimated regression equations for each analyte are as follows: (1) peak area ratio = 50.8 · (μg of emetine) − 0.03, (2) peak area ratio = 37.6 · (μg of cephaeline) + 0.02. The correlation coefficient for both analytes was 0.999.

Emetine		*Cephaeline*	
μg injected	*Peak area ratio*	*μg injected*	*Peak area ratio*
0.0071	0.319	0.0104	0.413
0.0107	0.525	0.0156	0.599
0.0143	0.704	0.0207	0.801
0.0179	0.876	0.0259	0.992
0.0214	1.063	0.0311	1.180
0.0250	1.235	0.0363	1.389

TABLE V
RECOVERY OF EMETINE AND CEPHAELINE FROM THE FORMULATIONS

Formulation	*Formulation base taken (g)*	*Emetine*			*Cephaeline*		
		Added (mg)	*Found (mg)*	*Recovery (%)*	*Added (mg)*	*Found (mg)*	*Recovery (%)*
Linctus A	10	0.0713	0.0708	99	0.0756	0.0761	101
Linctus B	10	0.0720	0.0723	100	0.184	0.183	99
Linctus C	10	0.178	0.180	101	0.319	0.317	99
Linctus D	10	0.236	0.238	101	0.613	0.615	100
Pastilles A	20	0.500	0.493	99	0.600	0.614	102

TABLE VI
PRECISION DATA FOR CEPHAELINE ASSAY PROCEDURE

Determination	*Linctus A (μg/g)*	*Linctus B (μg/g)*	*Linctus C (μg/g)*	*Linctus D (μg/g)*	*Pastille A (mg/pastille)*	*Pastille B (mg/pastille)*
1	11.6	11.6	27.9	60.4	0.0101	0.098
2	11.5	11.3	28.3	61.0	0.096	0.097
3	11.5	11.3	27.6	59.2	0.098	0.095
4	11.5	11.4	27.2	59.2	0.099	0.096
5	11.6	11.3	27.8	58.7	0.101	0.098
6	11.5	11.3	28.0	58.5	0.102	0.097
7	11.5	11.4	28.2	59.4	0.098	0.099
8	11.6	11.3	28.2	59.5	0.097	0.100
9	11.5	11.5	28.2	59.0	0.097	0.098
10	11.4	11.0	28.4	57.8	0.097	0.098
Mean	11.5	11.3	28.0	59.3	0.099	0.098
Relative standard deviation (%)	0.5	1.4	1.3	1.5	2.1	1.5

TABLE VII
PRECISION DATA FOR EMETINE ASSAY PROCEDURE

Determination	*Linctus A (μg/g)*	*Linctus B (μg/g)*	*Linctus C (μg/g)*	*Linctus D (μg/g)*	*Pastille A (mg/pastille)*	*Pastille B (mg/pastille)*
1	6.6	6.7	15.8	23.1	0.062	0.057
2	6.4	7.2	15.7	23.1	0.060	0.057
3	6.4	6.9	15.5	21.6	0.060	0.055
4	6.4	7.0	15.2	23.3	0.061	0.054
5	6.5	7.0	15.5	21.8	0.063	0.056
6	6.5	6.9	15.6	22.4	0.065	0.055
7	6.5	6.9	15.7	22.6	0.061	0.056
8	6.7	7.0	15.8	23.0	0.061	0.057
9	6.6	6.9	15.8	22.9	0.061	0.057
10	6.5	7.1	16.1	22.8	0.060	0.056
Mean	6.5	7.0	15.7	22.7	0.061	0.056
Relative standard deviation (%)	1.5	1.9	1.5	2.5	2.6	1.9

15% decomposition of the emetine had occurred the major degradation products were O-methylpsychotrine and didehydroemetine, with small amounts of emetamine and tetradehydroemetine also being produced. The same degradation products were also identified in aqueous solutions of emetine irradiated with UV light at 254 nm, although in this case the degradation was more complex with many additional degradation products also being formed. The recommended HPLC procedure has been shown to be stability-indicating for emetine since it is well separated from its two major degradation products, O-methylpsychotrine and didehydroemetine. The two minor degradation products, emetamine and tetrahydroemetine have no significant fluorescence at the excitation and emission wavelengths recommended and hence do not interfere with the assay. Since cephaeline is very similar to emetine it might be expected to degrade in a similar manner.

In order to show that the assay procedure was stability-indicating for both alkaloids, stress-storage tests were carried out on emetine dihydrochloride, cephaeline dihydrobromide and Ipecacuanha liquid extract solutions in water, 0.1 *M* hydrochloric acid and 0.1 *M* sodium hydroxide solutions. The solutions were heated at 70°C in clear glass vials and sealed with PTFE-lined septa. After two weeks the samples were examined by the recommended HPLC procedure. Emetine and cephaeline were found to degrade readily in aqueous solution, particularly in presence of alkali, as indicated by loss of the analyte when measured by the assay procedure. However, no significant level of degradation products were detected by HPLC. Result of the stress-storage tests are given in Table VIII.

Ruggedness

The ruggedness of the chromatographic system was determined by evaluating alterations to several key parameters. The results of the experiments were used to establish variaton limits for each of the parameters investigated. The parameters investigated included concentration of ion-pair reagent, orthophosphoric acid and methanol in the mobile phase, and column temperature. The following parameter variations could be made for the chromatography to be acceptable to adequately assay samples for emetine and cephaeline.

Concentrations of the mobile phase components were varied as follows; ion-pair

TABLE VIII

RESULTS OF STRESS-STORAGE TESTS ON EMETINE DIHYDROCHLORIDE, CEPHAELINE DIHYDROBROMIDE AND IPECACUANHA LIQUID EXTRACT

Stress-storage test	*Emetine dihydrochloride remaining (%)*	*Cephaeline dihydrobromide remaining (%)*	*Ipecacuanha liquid extract*	
			Cephaeline (%, w/w)*	*Emetine* (%, w/w)*
Two weeks in water in daylight cabinet	96	88	0.70	0.36
Two weeks in water at 70°C	99	62	0.85	0.46
Two weeks in 0.1 *M* hydrochloric acid at 70°C	100	95	1.02	0.50
Two weeks in 0.1 *M* sodium hydroxide at 70°C	11	–**	–**	0.05

* Initial values were: cephaeline, 1.06% (w/w) and emetine, 0.50% (w/w).

** None detected.

reagent: 0.09–0.11%, orthophosphoric acid: 0.05–0.2% and methanol: 36–42%. Within these limits changes of mobile phase composition had little significant effect on the relative separations of the alkaloids and internal standard. Although an increase in column temperature gave a predictable decrease in retention times, temperatures between 30 and 40°C gave satisfactory separations and a column temperature of 35°C was chosen. The use of a controlled temperature improved the precision of the analysis and was essential for automated analysis over a long period of time.

RESULTS AND DISCUSSION

The analytical procedure presented represents a selective, precise, accurate, linear and stability-indicating method for the simultaneous determination of the two major Ipecacuanha alkaloids, emetine and cephaeline, in linctus and pastille formulations.

Selectivity was demonstrated by showing that emetine and cephaeline peaks were free of interference from other Ipecacuanha-related alkaloids and from other components of the formulation bases.

The precision of the method was evaluated for each of the alkaloids in all of the formulations. Relative standard deviations for individual sample preparations were in the range 0.5–2.1% for cephaeline assays and 1.5–2.6% for emetine assays.

The recovery of emetine and cephaeline added to each formulation base was determined. Recoveries of between 99 and 102% were obtained for both alkaloids from all formulations.

The procedure was shown to give a rectilinear response for amounts of emetine injected in the range 0.007–0.025 μg and for cephaeline injected in the range 0.01–0.036 μg.

By showing that known degradation products give no interference with emetine and cephaeline and by examination of stress-stored samples of the alkaloids the procedure has been shown to be stability-indicating.

Although the procedure was developed specifically for the stability-indicating determination of emetine and cephaeline in linctus and pastille formulations it has been used to determine the emetine and cephaeline content of Ipecacuanha liquid extract samples obtained from a number of suppliers. The results obtained are given in Table IX.

TABLE IX

EMETINE AND CEPHAELINE CONTENT OF IPECACUANHA LIQUID EXTRACT SAMPLES

Ipecacuanha liquid extract Sample No.	*Emetine (%, w/w)*	*Cephaeline (%, w/w)*
1	0.57	1.27
2	0.55	1.35
3	0.39	0.98
4	0.50	1.04
5	0.50	1.06
6	0.54	0.80
7	0.55	0.88

Several formulations have been examined for emetine and cephaeline content by the recommended procedure. Each sample was assayed ten times and the results obtained are presented in Tables VI and VII (precision data). Chromatograms of typical linctus and pastille extracts containing internal standard are presented in Figs. 1 and 2, respectively.

Samples of Linctus A after storage for up to six months have been examined for emetine and cephaeline content by the recommended procedure. The results obtained are given in Table X. No significant degradation of the two alkaloids was observed.

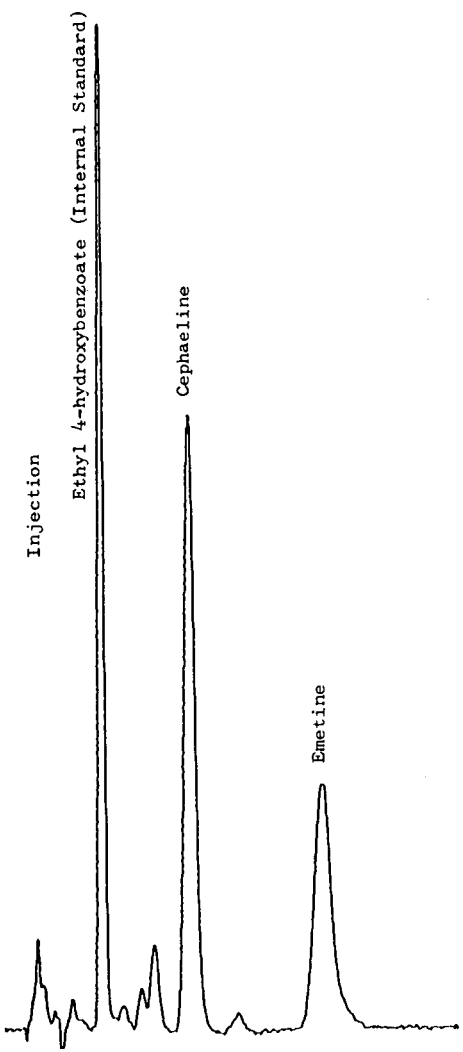

Fig. 1. Chromatogram of linctus solution containing I.S.

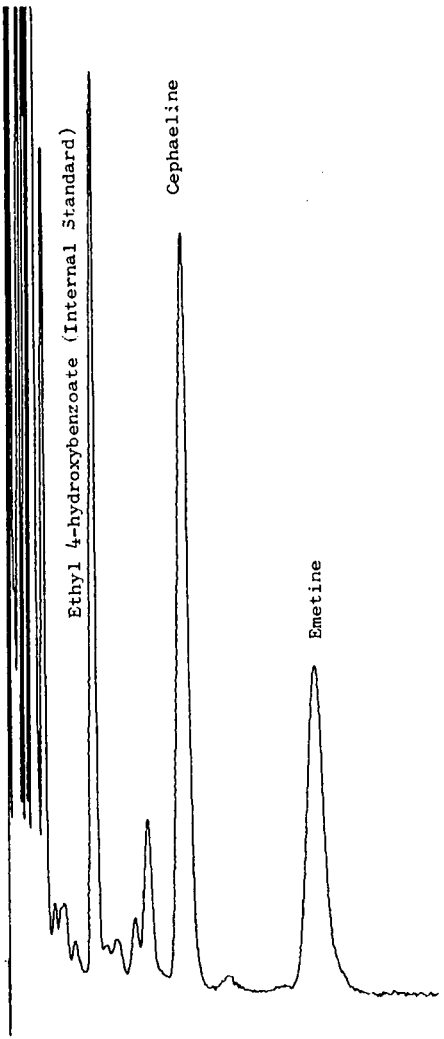

Fig. 2. Chromatogram of pastille extract containing I.S.

TABLE X
EMETINE AND CEPHAELINE CONTENT OF STORED SAMPLES OF LINCTUS A

Linctus A (sample 1)	*Emetine (μg/g)*	*Cephaeline (μg/g)*
Initial	6.6	11.4
One month in daylight cabinet	6.4	11.4
One month at 50°C	6.5	11.2
Three months at 0–5°C	6.4	11.5
Three months at 30°C	6.4	11.4
Three months at 40°C	6.7	11.3
Six months at 22°C	6.5	11.7
Six months at 30°C	6.6	11.8
Six months at 40°C	6.5	11.7

CONCLUSION

The method represents a rugged stability-indicating analytical procedure for the determination of the major Ipecacuanha alkaloids, emetine and cephaeline, in pharmaceutical dosage forms. Selectivity and sensitivity are achieved by the use of a spectrofluorimetric detector. The sample preparation is simple and the analysis time short. The method is amenable to the analysis of a large number of samples and gives precise and accurate results.

REFERENCES

1 E. Smith, M. F.Sharkey and J. Levine, *J. Assoc. Off. Anal. Chem.*, 54 (1971) 609.
2 R. Verpoorte and A. B. Svendsen, *J. Chromatogr.*, 100 (1974) 227.
3 N. P. Sahu and S. B. Mahato, *J. Chromatogr.*, 238 (1982) 525.
4 K. F. Ilett, R. Tjokrosetio and R. W. Unsworthy, *Aust. J. Hosp. Pharm.*, 13 (1983) 121.
5 L. J. Kraus, J. Carstens and R. Richter, *Dtsch Apoth.-Ztg.*, 125 (1985) 863.
6 Y. Hashimoto, M. Moriyask, E. Kato, M. Endo, N. Miyamoto and H. Uchida, *Mikrochimica Acta II*, (1978) 159.
7 R. W. Frei, W. Santi and M. Thomas, *J. Chromatogr.*, 116 (1976) 365.
8 J. C. Gfeller, G. Frey, J. M. Huen and J. P. Thevenin, *J. Chromatogr.*, 172 (1979) 141.
9 S. J. Bannister, J. Stevens, D. Musson and L. A. Sternson, *J. Chromatogr.*, 176 (1979) 381.
10 D. J. Crouch, D. M. Moran, B. S. Finkle and M. A. Peat, *J. Anal. Toxicol.*, 8 (1984) 63.
11 C. Schuijt, G. M. J. Beijersbergen van Henegouwen and K. W. Gerritsma, *Pharm WeekBl. Sci. Ed.*, 1 (1979) 10.

Journal of Chromatography, 463 (1989) 119–125
Elsevier Science Publishers B.V., Amsterdam — Printed in The Netherlands

CHROM. 20 981

MAILLARD-REAKTION VON RINDERSERUMALBUMIN MIT GLUCOSE HOCHLEISTUNG-FLÜSSIGKEITSCHROMATOGRAPHISCHER NACHWEIS DES 2-FORMYL-5-(HYDROXYMETHYL)PYRROL-1-NORLEUCINS NACH ALKALISCHER HYDROLYSE

MANFRED SENGL, FRANZ LEDL und THEODOR SEVERIN*
Institut für Pharmazie und Lebensmittelchemie der Universität München, Sophienstrasse 10, 8000 München 2 (F.R.G.)
(Eingegangen am 11. Mai 1988; geänderte Fassung eingegangen am 11. August 1988)

SUMMARY

Maillard reaction of bovine serum albumin with glucose. Determination of 2-formyl-5-(hydroxymethyl)pyrrole-1-norleucine by high-performance liquid chromatography after alkaline hydrolysis

Reactions between glucose and bovine serum albumin proceed predominantly at the side chain amino groups of lysine residues. Among other products, protein-bound 2-formyl-5-(hydroxymethyl)pyrrole-1-norleucine is formed. After alkaline hydrolysis and fractionation of the protein hydrolysate on RP-18 material this substance can be separated by high-performance liquid chromatography. The identity of the norleucine derivative with a synthesized compound can be determined with fast atom bombardment-mass spectrometry spectral data. A colour reaction with thiobarbituric acid is also suitable for detection.

EINLEITUNG

Erhitzt man reduzierende Zucker mit Aminosäuren oder Proteinen, so tritt rasch Bräunung ein und es entstehen eine grosse Anzahl verschiedenartiger Produkte (Maillard-Reaktion)[1]. Derartige Umsetzungen sind vor allem in erhitzten oder länger gelagerten Lebensmitteln von Bedeutung (Bräunung, Bildung von Röstaromen). Auch unter physiologischen Bedingungen reagieren Zucker, wenn auch langsamer, mit Proteinen. Bei einer Reihe von Eiweiss-Verbindungen wie Hämoglobin[2], Albumin[3], Kollagen[4], Augenlinsenprotein[5] und Erythrozytenmembranprotein[6] wurden nichtenzymatische Glycosylierungsreaktionen nachgewiesen. Derartige Vorgänge treten verstärkt bei Diabetikern auf[7]. Man diskutiert auch, ob Alterungsvorgänge mit Protein–Zucker-Reaktionen verbunden sind.

Aminosäuren addieren sich leicht an Glucose zu Glycosylaminen, die in einer Amadori-Umlagerung in die entsprechenden N-substituierten 1-Desoxy-1-aminofructosen übergehen. Durch Folgereaktionen kommt es zur Bildung zahlreicher Heterocyclen.

0021-9673/89/$03.50

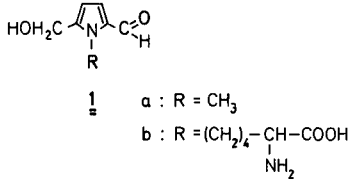

Fig. 1. N-substituierte 2-Formyl-5-(hydroxymethyl)pyrrole.

Sowohl in der Lebensmittelchemie wie auch in der medizinischen Chemie sucht man Methoden zum Nachweis der Maillard-Reaktion. Für das Anfangsstadium sind Amadori-Verbindungen charakteristisch; sie sagen jedoch wenig über den Umfang von Folgereaktionen aus.

Erhitzt man Glucose oder Fructose mit Methylamin in neutraler oder schwach saurer, wässriger Lösung, so ist aus dem Produktgemisch 2-Formyl-5-(hydroxymethyl)-1-methylpyrrol (**1a** in Fig. 1) in verhältnismässig grosser Menge isolierbar[8]. Analoge Verbindungen wurden mit anderen primären Aminen oder Aminosäuren erhalten[9–11]. Von besonderem Interesse ist das Norleucin-Derivat **1b**, da bei Umsetzungen von Zuckern mit Proteinen bevorzugt die Aminogruppe der Lysinseitenketten angegriffen wird. Diese Verbindung wurde aus einer Glucose–Lysin-Reaktionsmischung isoliert[12] und auf unabhängigem Wege synthetisiert[13]. Es wurde berichtet, dass **1b** mutagene[14] und enzymhemmende Eigenschaften[15] besitzt.

Aufgrund dieser Ergebnisse konnte man davon ausgehen, dass auch im proteingebundenen Lysin die ε-Aminogruppe bei der Umsetzung mit Glucose teilweise zum Formyl-hydroxymethylpyrrol reagiert. Wir haben analytische Verfahren zum Nachweis von **1b** in Proteinen ausgearbeitet. Es zeigte sich, dass das Pyrroll-Derivat **1b** nach alkalischer Spaltung des Proteins hochdruckflüssigchromatographisch (HPLC) nachweisbar ist. Auch eine Farbreaktion mit Thiobarbitursäure brachte gute Ergebnisse.

EXPERIMENTELLES

Geräte

Das HPLC-System bestand aus einer L-6000 Pumpe, einem L-4000 UV-Detektor (gemessen wurde bei 296 nm) und einem D-2000 Integrator (alle Merck-Hitachi) sowie einem 7125 Loop Injektor (Rheodyne). Die folgenden Säulen und mobilen Phasen wurden verwendet: (1), LiChrosorb RP-18 (Merck, 10 μm, 250 × 10 mm I.D.), 0,1 *M* Triethylammoniumformiat–Methanol (9:1, v/v), 2 ml/min; (2), LiChrosorb RP-18 (Bischoff, 10 μm, 250 × 8 mm I.D.), Wasser–Acetonitril (9:1, v/v), 2 ml/min; (3), LiChrosorb RP-18 (Bischoff, 5 μm, 250 × 4,6 mm I.D.), Eluent wie (1), 1 ml/min.

Für die Niederdruckchromatographie wurde eine 6000-A Pumpe (Waters) und eine LiChroprep RP-18 Säule [Merck, 40–63 μm, 0,1 *M* Triethylammoniumformiat–Methanol (8:2, v/v), 4 ml/min] kombiniert und ein 2112 Redirac Fraktionssammler (LKB, 450 Tropfen je Fraktion) angeschlossen, Zur Aminosäuretrennung stand ein 4400 Gerät (LKB) zur Verfügung, die Säule (295 × 4 mm I.D.) war mit Ultro Pac-8 gefüllt. Temperaturen: T_1 = 45°C, T_2 = 56°C, T_3 = 73°C; Eluenten: 0,1 mol Natri-

um-Citrat puffer, pH_1 = 3,20, pH_2 = 4,25 und pH_3 = 6,45 (+ 1,0 mol Natriumchlorid). Detektion erfolgte nach Anfärben mit Ninhydrin bei 440 und 570 nm.

Dünnschichtchromatographische (DC) Trennungen wurden mit Kieselgel 60 F_{254} (Merck, 0,2 und 0,5 mm) durchgeführt. Für die Säulenchromatographie wurde Kieselgel 60 F_{254} (Merck, 40–63 μm) verwendet.

Die colorimetrische Bestimmung erfolgte mit einem PMQ II Spektralphotometer (Zeiss). Das FAB-MS wurde mit einem HSQ 30 Massenspektrometer (Stossgas Argon, 8 kV, 400 A) mit Datensystem SS 300 (Finnigan/MAT) aufgenommen.

Zur Messung von NMR-Spektren stand ein Varian 60-A Instrument und ein Jeol GSX 400 Gerät zur Verfügung (Tetramethylsilan als innerer Standard).

Herstellung des Pyrrolaldehyds **1b**

Eine Menge von 3,4 g N^{α}-Acetyllysin[16–18] (18 m*M*) wurde mit 0,9 g Glucose-Monohydrat (4,5 m*M*) in 60 ml Ethanol unter Zugabe von 20 Tropfen Eisessig gemischt und die Suspension 24 h unter Rückfluss gerührt. Anschliessend wurde filtriert und der Rückstand wieder in 60 ml Ethanol suspendiert und nach Zugabe von 15 Tropfen Eisessig und 0,8 g Glucose-Monohydrat wie oben umgesetzt. Dieses Verfahren wurde insgesamt 4 Mal durchgeführt. Die gesammelten, konzentrierten Filtrate wurden über eine Kieselgelsäule [beginnend mit dem Gemisch Ethylacetat–Methanol (2:1, v/v) und mit steigender Menge Methanol) fraktioniert. In einer mit Ester–Methanol (2:3, v/v) eluierten Fraktion liess sich die Hauptmenge an acetyliertem **1b** nachweisen. [DC-Kontrolle mit Ester–Methanol (2:3, v/v) ein UV-detektierbarer Fleck mit R_F = 0,5 wurde nach Besprühen mit einer Dinitrophenylhydrazin-Lösung rostbraun.] Die Ausbeute an acetyliertem Rohprodukt betrug *ca.* 300 mg. ^{1}H-NMR ($C^2H_3O^2H$, 60 MHz): δ 1,7 (m, 6H), 2,0 (s, 3H), 4,3 (m, 3H), 4,7 (s, 2H), 6,3 (d, 1H), 7,0 (d, 1H), 9,45 (s, 1H).

Die Abspaltung der Acetylgruppe erfolgte nach zwei Methoden: (A) 150 mg Rohprodukt wurden mit 4 ml 2,5 *M* Bariumhydroxyd-Suspension 40 h unter Rückfluss erhitzt, ungelöstes Bariumhydroxyd abfiltriert, mit 1 *M* Schwefelsäure neutralisiert und ausgefallenes Bariumsulfat abfiltriert. Der Rückstand des Filtrats wurde schichtchromatographisch (0,5 mm) mit 4:1:1 Acetonitril–Ethanol–Wasser (4:1:1, v/v) getrennt (R_F = 0,2, Ninhydrinreaktion) und mit heissem Methanol aus der Zone eluiert (Ausbeute *ca.* 10 mg). (B) 150 mg Rohprodukt wurden in 7 ml Phosphatpuffer (pH = 8,0) aufgenommen und mit 100 mg Acylase (aus Aspergillus species, Sigma) 36 h bei 37°C inkubiert. Die Reinigung von **1b** erfolgte über HPLC (Säule 2, Retentionszeit t_R = 11,0 min).

1b: ^{1}H-NMR (^2H_2O, 400 MHz): δ 1,3 (m, 2H), 1,65 (m, 2H), 1,75 (m, 2H), 3,6 (t, 1H), 4,15 (t, 2H), 4,6 (s, 2H), 6,25 (d, 1H), 7,0 (d, 1H), 9,2 (s, 1H). MS (FAB): 255 (84%, M + 1), 237 (56), 175 (100), 148 (74), 84 (88).

Derivat **1b** (6 mg) wurde in 1 l Wasser gelöst. Davon wurde 1 ml entnommen, mit 2 ml Thiobarbitursäure (0.025 *M* in 1 *M* Phosphorsäure gelöst) und Wasser im Messkolben auf 10 ml aufgefüllt, 30 min auf 75°C erhitzt und nach dem Abkühlen sofort bei 456 nm gegen eine Blindprobe gemessen; $E - E_o$ = 0,12.

Von der Stammlösung (6 mg/l) wurde 1 ml entnommen, konzentriert und in wenig Citrat puffer (pH 2,2) aufgenommen. Nach Injektion von 100 μl in den Aminosäureanalysator wurde ein Peak nach 41,2 min erhalten.

Aus der Stammlösung wurde 1 ml abpipettiert und mit dem Eluenten der Säule 3 auf 10 ml aufgefüllt. Die HPLC-Analyse (Säule 3) ergab einen Peak nach 18,26 min.

Umsetzung von Rinderserumalbumin mit Glucose und Bestimmung des Pyrrolaldehyds **1b**

Wässrige Lösungen (25 ml) von 1,82 g Rinderserumalbumin (Serva) und 2,5 g Glucose (Merck) wurden 4 Wochen bei pH 5 (Citratpuffer) auf 37°C bzw. 3 Wochen bei pH 7 (Phosphatpuffer) auf 50°C erwärmt. Die Proteinlösungen wurden anschliessend 72 h gegegen destilliertes Wasser dialysiert, das Wasser unter reduziertem Druck weitgehend entfernt und der verbliebene Rückstand bei 0,1 Torr getrocknet. Eine Menge von 200 mg des so erhaltenen Proteins wurden in 45 ml 5 *M* Natronlauge 16 h bei 121°C im evakuierten Autoklaven erhitzt, die Lösung mit Salzsäure neutralisiert, filtriert und konzentriert. Das Konzentrat wurde mit 0,1 *M* Triethylammoniumformiat–Methanol (8:2, v/v) auf 60 ml verdünnt und jeweils 5 ml über die Niederdrucksäule fraktioniert. Derivat **1b** konnte in den Fraktionen 16, 17 und 18 nachgewiesen werden [DC-Kontrolle, Acetonitril–Ethanol–Wasser (4:1:1, v/v), UV-Detektion und Ninhydrinreaktion, R_F = 0,2]. Der Rückstand aus den vereinigten Fraktionen wurde an Säule 1 des HPLC-Systems aufgetrennt (t_R = 26,5 min, t_R Tryptophan = 24,9 min) und die bei 26,5 min eluierte Verbindung gesammelt (mehrmalige Injektion, aufgetrennt wurde das Hydrolysat von *ca.* 200 mg Protein).

Zur Absicherung der Identität und der Konzentration wurden folgende Bestimmungen durchgeführt (dazu wurde jeweils 1/5 der gesammelten Substanz eingesetzt).

(1) Bei der Farbreaktion mit Thiobarbitursäure (siehe Herstellung des Pyrrolaldehyds **1b**) wurde eine Extinktionsdifferenz von 0,15 gemessen, entsprechend einer Menge von 7,5 μg **1b** in 40 mg Protein (3 Wochen auf 50°C erhitzt). Daraus ergibt sich bei einem Gehalt von 10% Lysin im Rinderserumalbumin, dass *ca.* eine von tausend Lysinseitenketten reagiert hat. Bei der auf 37°C erhitzten Probe liess sich keine auswertbare Extinktionsdifferenz ermitteln.

(2) Die Probe (*ca.* 40 mg, 3 Wochen auf 50°C erhitzt) wurde in 10 ml des Eluenten der Säule 3 gelöst. Die HPLC-Bestimmung (Säule 3) von **1b** ergab einen Peak nach 18,26 min aus dessen Grösse sich ein Gehalt von *ca.* 7 μg **1b** abschätzen liess (Vergleich mit der Stammlösung, siehe Bestimmung des Pyrrolaldehyds **1b**). Die auf 37°C erhitzte Probe wurde in 1 ml des Eluenten gelöst. Die HPLC-Analyse ergab einen Gehalt von *ca.* 0.9 μg **1b** in 40 mg Protein.

(3) Das FAB-MS-Spektrum zeigte die für Verbindung **1b** charakteristischen Massenfragmente (gemessen wurde mit der MS–MS-Technik).

ERGEBNISSE UND DISKUSSION

2-Formyl-5-(hydroxymethyl)pyrrol-1-norleucin (**1b**) ist durch Umsetzung von Glucose mit Lysin nur in schlechter Ausbeute erhältlich und schwer zu reinigen. Miller und Olsson[13] konnten diese Verbindung aus 2,5-Diformylpyrrol und 6-Brom-2-acetylamino-capronsäure in einer Reihe von Reaktionsschritten darstellen. Wir haben N^{α}-Acetyllysin mit Glucose erhitzt und aus der Reaktionsmischung das N^{α}-Acetyl-Derivat von **1b** isoliert, aus dem die Acetylgruppe enzymatisch leicht abspaltbar ist.

Beim Nachweis von **1b** in Proteinen kann man die übliche Säurehydrolyse nicht vornehmen, da unter diesen Bedingungen der Pyrrolring zerstört wird. Bei alkalischer Spaltung der Peptidbindungen bleibt jedoch der Pyrrolkern weitgehend unverändert.

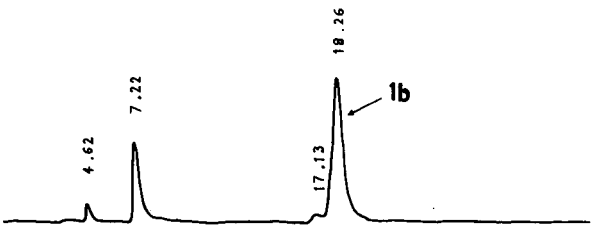

Fig. 2. HPLC-Bestimmung von vorgereinigtem **1b** mit einer 5-μm RP-18-Säule (UV-Detektion bei 296 nm). Retentionszeit in min.

Die zunächst versuchte gaschromatographische-Bestimmung der Aminosäure **1b** brachte kein positives Ergebnis. Eine saure Veresterung ist aus den genannten Gründen nicht möglich. Silylierung von **1b** führte unter den von uns angewandten Bedingungen nicht zu einem gaschromatographisch erfassbaren Derivat[19].

Mit HPLC lässt sich das Norleucin-Pyrrol **1b** im Gemisch mit den übrigen Aminosäuren gut bestimmen. Bei einer Vorreinigung über eine Niederdruck-RP-18-Säule erhält man **1b** in einer Fraktion gemeinsam mit Tryptophan. Auf einer semipräparativen RP-18-Säule mit Ammoniumformiat puffer lassen sich **1b** und Tryptophan gut trennen. Die Bestimmung von **1b** erfolgt schliesslich auf einer analytischen Säule unter ähnlichen Bedingungen (Fig. 2). Bei einer Trennung der Aminosäuren auf einer Ionenaustauschersäule unter den üblichen standardisierten Bedingungen (Anfärbung mit Ninhydrin) erscheint **1b** an der gleichen Stelle wie Phenylalanin. Fraktioniert man jedoch vorher wie oben beschrieben auf einer RP-18-Säule, so ist Phenylalanin abgetrennt und man kann anschliessend die Bestimmung auch auf einem Ionenaustauscher vornehmen (Fig. 3). Schliesslich lässt sich **1b** nach einer HPLC-Vorfraktionierung auch durch eine Farbreaktion mit Thiobarbitursäure nachweisen. Dabei erfolgt eine Kondensation an der Formylgruppe des Pyrrolringes. Die Reaktion ist daher nur spezifisch, solange andere Carbonylgruppen nicht vorliegen.

Um die Bildung von **1b** im Protein nachzuweisen, haben wir Rinderserumalbumin mit Glucose bei 50°C sowie 37°C 3 bzw. 4 Wochen reagieren lassen, also die Maillard-Reaktion bei relativ niedrigen Temperaturen durchgeführt. Nach der Dialyse wurde die höhermolekulare Fraktion alkalisch hydrolisiert. Die chromatogra-

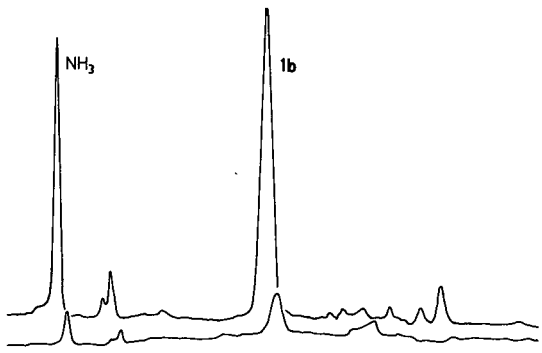

Fig. 3. Aminosäureanalyse von **1b** unter Standartbedingungen. Obere Linie: 570 nm, unter Linie: 440 nm.

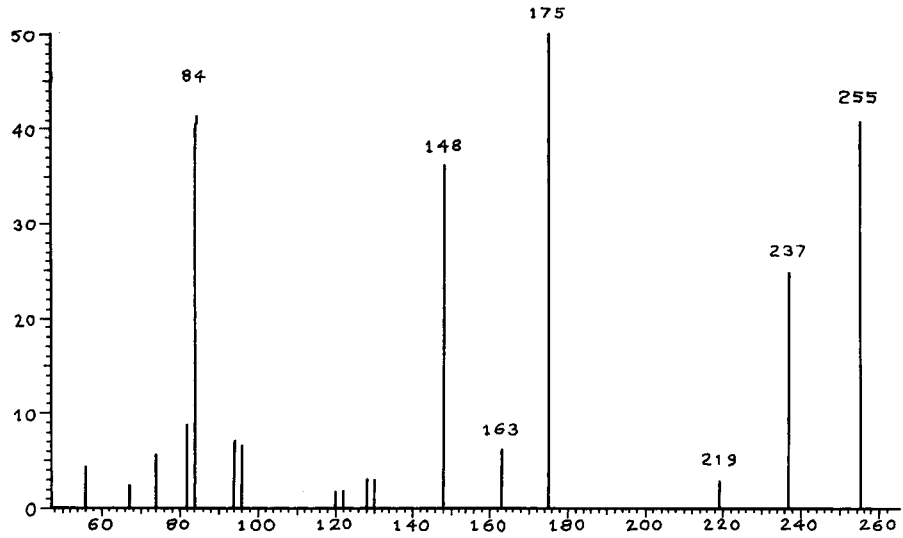

Fig. 4. FAB-MS von **1b**.

phische Trennung der Hydrolyseprodukte erfolgte in der Reihenfolge RP-Niederdrucksäule, semipräparative RP-Säule und analytische RP-Säule. Die Identität der abgetrennten Verbindung mit den Pyrrolaldehyd **1b** wurde mit der FAB-MS–MS-Methode überprüft (Fig. 4). Das dabei erhaltene Spektrum war identisch mit dem der synthetisierten Verbindung **1b**.

Durch Vergleich der Peakhöhen bekannter Konzentrationen an synthetisiertem **1b** mit der des isolierten Produkts (analytische Säule) liess sich die Menge des aus der Protein–Glucose-Reaktion gebildeten Pyrrolaldehyds **1b** abschätzen. Dabei wurde davon ausgegangen, dass der Lysinanteil im Rinderserumalbumin *ca.* 10% beträgt. Für das auf 37°C erhitzte Rinderserumalbumin ergab sich demnach, dass mehr als eine von zehntausend ε-Aminogruppen reagierten. Bei der höher erhitzten Probe war es *ca.* eine von tausend Seitenketten des Lysins.

ZUSAMMENFASSUNG

Die Reaktion von Rinderserumalbumin mit Glucose findet überwiegend mit den Aminogruppen der Lysinseitenketten statt. Neben anderen Produkten bildet sich proteingebundenes 2-Formyl-5-(hydroxymethyl)pyrrol-1-norleucin. Nach alkalischer Spaltung und Auftrennung des Proteinhydrolysats an RP-18-Material kann diese Substanz isoliert werden. Die Identität des Norleucinderivats mit einer synthetisierten Verbindung lässt sich mit dem FAB-MS-Spektrum überprüfen. Zusätzlich kann die Farbreaktion mit Thiobarbitursäure zum Nachweis herangezogen werden.

LITERATUR

1 H. Paulsen und K. Pflughaupt, in W. Pigman und D. Horton (Herausgeber), *The Carbohydrates, Chemistry and Biochemistry*, Academic Press, New York, 1980, S. 881.

2 R. J. Koenig, S. H. Blobstein und A. Cerami, *J. Biol. Chem.*, 252 (1977) 2992.
3 J. F. Day, S. R. Thorpe und J. W. Baynes, *J. Biol. Chem.*, 254 (1979) 595.
4 S. P. Robins und A. J. Bailey, *Biochem. Biophys. Res. Commun.*,48 (1972) 76.
5 V. J. Stevens, C. A. Rouzer, V. M. Monnier und A. Cerami, *Proc. Natl. Acad. Sci. U.S.A.*, 75 (1978) 2918.
6 J. A. Miller, E. Gravallese und H. F. Bunn, *J. Clin. Invest.*, 65 (1980) 896.
7 B. W. Vogt, E. D. Schleicher und O. H. Wieland, *Diabetes*, 31 (1982) 1132.
8 G. R. Jurch und J. H. Tatum, *Carbohydr. Res.*, 15 (1970) 233.
9 K. Olsson, P. A. Pernemalm und O. Theander, *Acta Chem. Scand. B*, 32 (1978) 249.
10 F. Hayase und H. Kato, *Agric. Biol. Chem.*, 49 (1985) 467.
11 F. G. Njoroge, M. S. Lawrence und V. M. Monnier, *Carbohydr. Res.*, 167 (1987) 211.
12 T. Nakayama, F. Hayase und H. Kato, *Agric. Biol. Chem.*, 44 (1980) 1201.
13 R. Miller und K. Olsson, *Acta Chem. Scand. B*, 39 (1985) 717.
14 H. Omura, N. Jahan, K. Shinohara und H. Murakami, *Am. Chem. Soc. Symp. Ser.*, 215 (1984) 537.
15 R. E. Öste, R. Miller, H. Sjöström und O. Noren, *J. Agric. Food Chem.*, 35 (1987) 938.
16 A. Neuberger und F. Sanger, *Biochem. J.*, 37 (1943) 515.
17 H. Zahn, H. Huber, W. Ditscher, D. Wegerle und J. Meienhofer, *Chem. Ber.*, 89 (1956) 407.
18 P. M. Hardy, A. C. Nicholls und H. N. Rydon, *J. Chem. Soc., Perkin Trans.*, 1 (1976) 958.
19 H. Frank, in W. Fresenius, H. Günzler, W. Huber und G. Tölg (Herausgeber), *Analytiker-Taschenbuch, Band 4*, Springer, Berlin, Heidelberg, New York, 1st ed., 1984, p. 337.

Journal of Chromatography, 463 (1989) 127–132
Elsevier Science Publishers B.V., Amsterdam — Printed in The Netherlands

CHROM. 21 023

DETERMINATION OF STYRENE AND 2-VINYLPYRIDINE MONOMERS IN POLY(2-VINYLPYRIDINE–STYRENE)

L. A. COOK, J. L. HENSLEY, E. G. MILLER and G. W. TINDALL*
Tennessee Eastman Company, Kingsport, TN 37664 (U.S.A.)
(First received July 5th, 1988; revised manuscript received September 25th, 1988)

SUMMARY

Residual monomers such as styrene can be determined in polymers at microgram per kilogram concentrations by headspace techniques. However, such techniques often do not have adequate sensitivity for the determination of monomers less volatile than styrene. A method is described for the determination of trace concentrations of monomers that are less volatile than styrene and also monomers that are traditionally determined in polymers by headspace techniques. The method involves dissolution of the polymer, removal of the polymer by molecular ultrafiltration and determination of the monomer in the filtrate by gas chromatography–mass spectrometry. Concentrations of styrene and 2-vinylpyridine of less than 200 μg/kg were successfully determined in a copolymer used for the post-ruminal delivery of nutritional supplements and drugs.

INTRODUCTION

Eastman Chemicals has developed a post-ruminal delivery system for nutritional supplements and drugs based on a copolymer of styrene and 2-vinylpyridine[1–3]. Because vinyl monomers can be toxic to animals, an established manufacturing practice is to maintain the amount of residual monomer in polymers used for food applications well below levels that are considered harmful. The manufacturing specification for poly(2-vinylpyridine–styrene) requires that each monomer must not exceed a concentration of 200 μg/kg in the final polymer. Hence, a method is required for the determination of less than 200 μg/kg concentration of styrene and 2-vinylpyridine in this copolymer.

There have been several approaches to the determination of monomers in polymers[4]. The simplest approach is to dissolve the polymer in an appropriate solvent and analyze the solution by gas chromatography. This approach is not normally useful for determining low concentrations of monomers because the large amount of polymer deposited in the chromatographic system with repeated injections degrades the chromatographic separation and causes loss of sensitivity. With the present copolymer and some other vinyl polymers, the polymer that is deposited in the injection system can decompose to monomers which interfere with the analysis. For the determination

of styrene in polystyrene, a non-solvent such as methanol has been added to precipitate much of the polymer prior to analysis[5,6]. This approach has the potential disadvantage of further diluting the sample and raising the detection limit for monomers and also there is the possibility that the monomer can adsorb on the precipitated polymer. Styrene and other volatile monomers are commonly determined by headspace techniques[7–9]. This approach eliminates the disadvantages of the direct injection techniques. Detection limits of 1 mg/kg of polymer have been reported for styrene using flame ionization detection[7]. For monomers less volatile than styrene (b.p. 145°C) the detection limits increase rapidly with decreasing volatility. No methods for the determination of 2-vinylpyridine have been published.

This paper describes a method for the determination of trace amounts of monomers that have a boiling point too high to be determined with adequate detection limits by headspace techniques. This method is also applicable to the determination of volatile monomers such as styrene. The method consists in dissolving the polymer sample, removing the polymer by molecular ultrafiltration and determining the monomer in the filtrate by gas chromatography–mass spectrometry (GC–MS) using selected ion monitoring (SIM). The utility of this approach for residual monomer analysis is demonstrated by the successful development of a method for the determination of 2-vinylpyridine and styrene at the 200 μg/kg level in poly(2-vinylpyridine–styrene).

EXPERIMENTAL

Materials and equipment

Standards of styrene (99+% purity) and 2-vinylpyridine (97% purity) were obtained from Aldrich (Milwaukee, WI, U.S.A.). Acetone and methanol, obtained from Burdick and Jackson Labs. (Muskegon, MI, U.S.A.), were used without further treatment.

Polymer solutions were filtered with a Millipore (Bedford, MA, U.S.A.) molecular filtration apparatus equipped with a 62-mm Diaflo YM2 ultrafiltration membrane (Amicon, Danvers, MA, U.S.A.) with a molecular-weight cut-off of 1000. Air at a pressure of 380 kPa was used to force solutions through the membrane. The membranes were inspected visually for defects prior to use. Acceptable membranes were conditioned according to the manufacturer's instructions.

The analytical system consisted of a Hewlett-Packard (Avondale, PA, U.S.A.) Model 5890A gas chromatograph equipped with a Model 7673A autosampler and a Model 5970B mass-selective detector. Data were collected, integrated and reported with a Hewlett-Packard Model 59970C ChemStation, which also controlled the analytical instrumentation. The separation was performed on a 30 m × 0.25 mm I.D. fused-silica capillary column coated with a 0.25-μm film of DB-17 (J&W Scientific, Folsom, CA, U.S.A.). Ultra-high-purity helium (Matheson, Secaucus, NJ, U.S.A.) was used as the carrier gas at a head pressure of 70 kPa. Sample introduction was made with the Model 7673A autosampler into a split–splitless capillary inlet operated in the splitless mode. The glass insert in the splitless injector was routinely cleaned and resilylated. Silylation was performed using a 10% solution of dimethyldichlorosilane (Pierce, Rockford, IL, U.S.A.) in toluene (Burdick and Jackson), followed by immersion in methanol and toluene. The insert was then dried before installation. The

TABLE I
INSTRUMENT CONDITIONS

Parameter	*Condition*	*Parameter*	*Condition*
Initial temperature	30°C	Injector temperature	250°C
Initial time	0.6 min	Transfer line	275°C
Programming rate	30°C/min	Splitless injection period	0.6 min
Oven temperature 1	85°C	Open split interface to MSD	Set to vent 1 ml/min
Hold Time	4.0 min	Electron multiplier	700 relative
Programming rate	30°C/min	Mode	Set to selected ion monitoring (SIM)
Oven temperature 2	200°C	Resolution	Set to low for greater sensitivity
Hold time	2.0 min	SIM mass	104.00
Equilibration time	0.5 min	Dwell time	400 ms
		SIM mass	105.00
		Dwell time	400 ms

volume of injection was 5 μl. Other operating conditions are summarized in Table I. Styrene was monitored at *m/z* 104 and 2-vinylpyridine at *m/z* 105. In some samples other ions may occasionally yield better signal-to-noise ratios. These ions are summarized with their relative abundance in Table II.

Calibration

A stock solution containing 10 mg/l of each monomer was prepared in acetone–methanol (85:15, w/w). Standards of 10, 20 and 30 μg/l were prepared from this stock solution by dilution with acetone–methanol (85:15, w/w). The 10 mg/l stock solution was prepared weekly; the 10, 20 and 30 μg/l standards were prepared daily. The neat monomers were kept at −15°C and the stock solutions at 5°C during storage.

Before samples were analysed, the analytical system was calibrated by running each standard three times and averaging the area count obtained. The data were fitted to a linear calibration graph. Examples of the calibration graphs are shown in Fig. 1. A calibration standard was analysed after every ten samples and at the end of each set of samples to check for drift in the mass spectrometer response.

Sample preparation

Polymer solutions of various concentrations and polymer powders were analysed. For all sample types a polymer solution of known concentration in the range

TABLE II
APPROXIMATE RELATIVE ABUNDANCES OF MASS FRAGMENTS

Monomer	*Ion (m/z)*	*Percent of most abundant fragment*
Styrene	104	100
	103	45
	78	32
2-Vinylpyridine	105	100
	79	93
	104	55

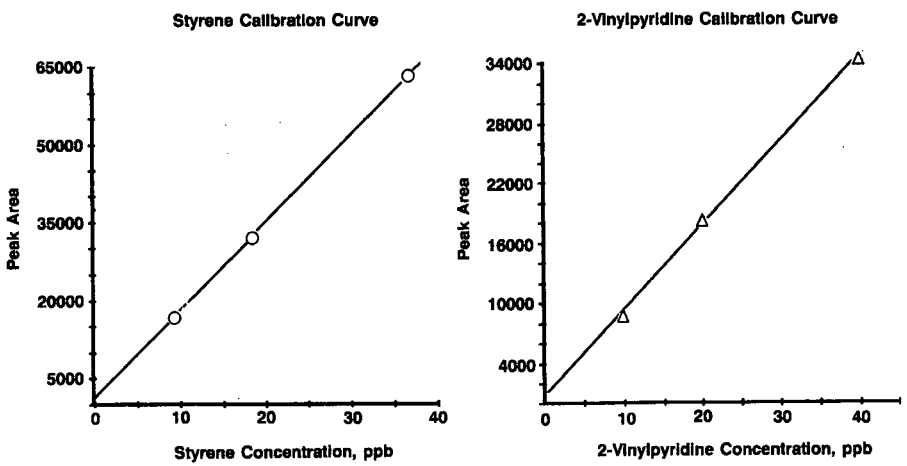

Fig. 1. Calibration graphs for the determination of styrene and 2-vinylpyridine in filtrates by SIM GC–MS. ppb = μg/l.

of 5 ± 0.5% was prepared in acetone–methanol (85:15, w/w). The filtration cell and membrane were washed by filtering 10 ml of methanol through the membrane. A 2-ml volume of the 5% polymer solution was added to the cell. The first 0.5 ml of filtrate was discarded, after which 0.5 ml of filtrate was collected in a sample vial for analysis. The vial was fitted against the filtration apparatus to avoid losses by evaporation.

RESULTS AND DISCUSSION

A method was required to ensure that polymer used to prepare rumen-protected formulations contained less than 200 μg/kg of each residual monomer. Polymer solutions more concentrated than 5% were too viscous to analyze. As the solution analyzed contains approximately 5% of polymer, the method must provide a reliable analysis of each monomer at the 10 μg/l level in the polymer solution. Preliminary work showed that the methods traditionally used for the determination of residual monomers in polymers did not provide adequate detection limits for 2-vinylpyridine. Direct injection of 5% polymer solutions was inadequate. If the polymer was precipitated prior to injection, some of the 2-vinylpyridine was absorbed by the precipitate. 2-Vinylpyridine (b.p. approximately 159°C) was not volatile enough to provide adequate detection limits by headspace techniques.

The method described provided acceptable detection limits, precision and recovery for both 2-vinylpyridine and styrene. The calibration is linear for both monomers up to a concentration of 2000 μg/l. Typical limits of detection, defined as three times the estimated standard deviation when the concentration approaches zero[10], are 1 μg/l for styrene and 2 μg/l for 2-vinylpyridine in the filtered polymer solution or 20 and 40 μg/kg, respectively, for the polymer. On several occasions the capability of the method was determined. A single polymer sample, a spiked polymer sample or a standard was analyzed 5–10 times during the course of a day by one person. At the 10 μg/l level the relative standard deviation was 5–10% for styrene and

8–13% for 2-vinylpyridine. This precision was essentially the same for monomer concentrations up to 40 μg/l. Recoveries ranged from 74 to 100% for both monomers at spiking levels of 10–40 μg/l in 5% polymer solutions.

Several steps are necessary to maximize the sensitivity and minimize interferences. As the levels of monomer detected are in the low micrograms per liter range, scrupulous care must be taken to avoid contamination of standards and solvents. Polystyrene is a ubiquitous material about the laboratory, and it typically contains significant concentrations of styrene monomer. It is essential to avoid any contact of samples with polystyrene. Bottles of solvents were analyzed before use to ensure the absence of interfering compounds. Trace levels of styrene were found in some batches of methanol and acetone. It was necessary to condition the column by repeated cycling through the temperature program to minimize the background associated with column bleeding. A non-linear response for 2-vinylpyridine indicates active sites in the system. Cleaning the injector or changing the column cured this problem. When detection limits could not be met, maintenance of the mass spectrometer source was performed, or a new column was installed.

A chromatogram for a typical sample is shown in Fig. 2. The main criteria for the choice of ions to monitor are their abundance and freedom from interferences. The molecular ions of styrene and 2-vinylpyridine are preferred. The other ions listed in Table II are of adequate intensity for this analysis, and on occasion they have been used when there were interferences. Interferences are detected by comparing the ratio of intensities given in Table II with those of the sample. Most often, the interference is an obvious broad peak in the single ion chromatogram.

For this type of analysis, three or more ions are usually monitored for each component. However, the number of ions monitored can depend on the objectives of the analysis and the kind of errors that are acceptable. For regulatory work the presence of an unacceptable concentration of some component must be confirmed with certainty. Hence, the regulatory agencies typically require three or more unique ions to be monitored in a GC–MS analysis. In production, the objective of the analysis is to ensure that the concentration of impurities in the product does not exceed the specification. The "risk" in only using one ion for analysis is that the product can be rejected if there is a positive interference for that ion. The improved sensitivity and convenience of using one ion for analysis outweighs the risk of a false positive result for this work. On the rare occasions where a positive interference was suspected the sample was analyzed again using the ions given in Table II. An analysis based on using three ions from Table II is suitable for regulatory analysis, but more effort is required to maintain adequate detection limits.

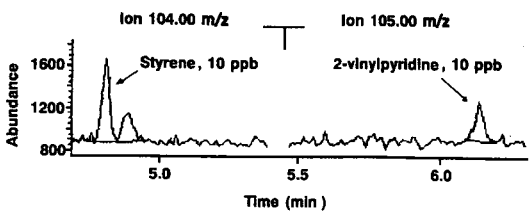

Fig. 2. Typical single-ion chromatogram obtained by SIM GC–MS analysis of the filtrate from molecular filtration of poly(2-vinylpyridine–styrene). ppb = μg/l.

The effectiveness of the filter in removing the polymer was investigated. The absorbance of the filtrate was measured at 263 nm, a wavelength suitable for measuring the aromatic components of the polymer. The absorbance measurement was calibrated against a solution of polymer of known concentration. A typical filtrate from a 5% polymer solution contained less than 20 mg/l of polymer. The effectiveness of this filtration enabled dozens of samples to be injected before the performance of the chromatographic separation was degraded.

The splitless injection mode can be the worst method for the analysis of thermally labile material owing to the high temperature needed to vaporize many samples and the relatively long residence time of the sample in the hot inlet. An investigation was made to determine if the small amount of polymer that passed through the filter could decompose in the inlet to form monomer that would interfere with the analysis. When a filtrate sample was analyzed at injection temperatures of 150, 250 and 350°C, a corresponding increase in the area of the monomer peaks was observed. However, when a 50 μg/l standard was analyzed at these injection temperatures, the area counts for styrene and 2-vinylpyridine increased in the same proportion as the area counts for the filtrate sample. This result supports the hypothesis that the observed increase in area counts is the result of physical transport processes in the injector. The increased variability of the areas at 150°C also supports this hypothesis. From these data, it is concluded that the recommended inlet temperature of 250°C did not cause detectable polymer decomposition.

CONCLUSIONS

Ultrafiltration of the polymer solution proved to be a convenient and effective means of separating monomers from the bulk of the polymer sample. We believe that this technique will prove to be generally applicable to the preparation of samples for the determination of residual monomers in polymers. The precision and accuracy of the method developed for 2-vinylpyridine and styrene meet the need for a method for monitoring polymer production.

REFERENCES

1 J. A. Rogers, U. Krishnamoorthy and C. A. Sniffen, *J. Dairy Sci.*, 70 (1987) 789.
2 A. M. Papas, J. L. Vicini, J. H. Clark and S. Peirce-Sandner, *J. Nutr.*, 114 (1984) 2221.
3 A. M. Papas, C. J. Siffen and T. V. Muscato, *J. Dairy Sci.*, 67 (1983) 545.
4 B. V. Ioffe and A. G. Vitenberg, *Head-Space Analysis and Related Methods in Gas Chromatography*, Wiley-Interscience, New York, 1982.
5 W. Pfab and D. Noffz, *Fresenius' Z. Anal. Chem.*, 195 (1963) 37.
6 T. R. Crompton, L. W. Meyers and D. Blair, *Br. Plast.*, 38 (1965) 740.
7 R. J. Steichen, *Anal. Chem.*, 48 (1976) 1398.
8 G. A. Eiceman and M. Carpen, *Anal. Lett.*, 15 (1982) 1169.
9 S. L. Varner and C. V. Breder, *J. Assoc. Off. Anal. Chem.*, 64 (1981) 647.
10 J. K. Taylor, *ChemTech*, (1986) 756.

Journal of Chromatography, 463 (1989) 133–138
Elsevier Science Publishers B.V., Amsterdam — Printed in The Netherlands

CHROM. 21 013

DETECTION AND MEASUREMENT OF THE ALKALOID PERAMINE IN ENDOPHYTE-INFECTED GRASSES

B. A. TAPPER* and D. D. ROWAN

Biotechnology Division, Department of Scientific and Industrial Research, Private Bag, Palmerston North (New Zealand)

and

G. C. M. LATCH

Plant Diseases Division, Department of Scientific and Industrial Research, Private Bag, Palmerston North (New Zealand)

(Received September 20th, 1988)

SUMMARY

Two methods are described for the detection and measurement of peramine, an alkaloid from endophyte-infected grasses with insect feeding deterrent activity. Both procedures involve ion-exchange work up of extracts followed by either thin-layer chromatography with detection by Ehrlich's reagent or quantitation by reversed-phase high-performance liquid chromatography with UV detection at 280 nm.

INTRODUCTION

Perennial ryegrass (*Lolium perenne*) infected with the endophytic fungus *Acremonium lolii* has field resistance to infestation by the Argentine stem weevil (*Listronotus bonariensis*)[1,2]. A major factor in this resistance is the production of a chemical deterrent to feeding of adult weevils. The chemical basis of the feeding deterrence has been examined by solvent extraction and fractionation procedures in conjunction with a bioassay test for activity[3]. The predominant activity was attributed to a single compound, peramine[4], the structure of which is shown in Fig. 1. Recent studies[5] have demonstrated the presence of peramine in some other endophyte-grass combinations.

Endophyte-infected perennial ryegrass also contains the neurotoxin lolitrem B and related compounds which may cause the "ryegrass staggers" disorder in grazing animals[6].

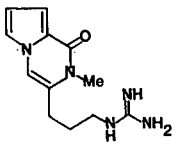

Fig. 1. Structure of peramine. Me = methyl.

0021-9673/89/$03.50

A method for measuring peramine in small samples of ryegrass herbage was required for studies on variation in peramine content of a range of endophyte-grass combinations. A target for accuracy of ± 10% was considered sufficient provided the method was relatively simple and convenient. The peramine isolation method of Rowan and Gaynor[3] involved solvent partitioning, followed by high-performance liquid chromatography (HPLC) using sodium *n*-heptanesulfonate as a reversed-phase modifier in a gradient elution system. This was considered to be unsuitable for routine analytical measurements.

We report herein on convenient methods for the detection and measurement of peramine, based on knowledge of its chemical structure and properties. Ion-exchange methods of purification were chosen because of the relatively strong basic character of the guanidino group of the peramine molecule. A two-phase extraction process permits a parallel determination of lolitrem B by minor modifications of the method of Gallagher *et al.*[7].

EXPERIMENTAL

Plant material

For method development plants of perennial ryegrass either infected with, or free from, *A. lolii* were grown in pots containing composted bark in a greenhouse (12–24°C) and harvested when 20–30 cm tall. Herbage was cut from plants at the crown and in some cases was divided into top and basal portions with a further cut 8–10 cm from the crown. Herbage from Italian ryegrass (*L. multiflorum*), free from endophyte and peramine, was used in tests measuring the recovery through extraction and work up of added peramine. All herbage samples were freeze dried, fine ground in a coffee mill and stored at 4°C.

Standard peramine

Crystalline peramine sulphate and peramine bromide were obtained from ryegrass seed[8] and solutions in 20% (v/v) aq. propan-2-ol were calibrated based on an extinction coefficient for peramine at 290 nm of 8300 l mol^{-1} cm^{-1}.

Extraction of plant material

Weighed samples, typically 100 mg, of dry ground herbage were extracted in two stages into a two-phase solvent system. The first stage of the extraction was with 3 ml of methanol–chloroform (1:1, v/v) for 30 min at about 18°C in polyethylene-capped glass vials with mixing by continuous gentle inversion. For the second stage 3 ml of hexane and 3 ml of water were added for a further 30 min of mixing before centrifugation to separate the two phases and sediment the plant residues. The two solvent phases were each of about 4.5 ml in volume.

TLC detection of peramine

A 3-ml volume of the aqueous lower phase extract was aspirated through small tandem ion-exchange columns of (i) 0.5 ml bed of BioRad AG2 × 8 (200–400 mesh) (hydroxide form) approximately 9 × 8 mm, followed by (ii) an Analytichem Bond Elut CBA column, 100 mg absorbent, in the free acid form. The columns were washed with 3 ml of 80% (v/v) methanol, separated, and the peramine eluted from the Bond

Elut CBA with 0.5 ml of 80% aq. methanol containing 5% (v/v) formic acid. The eluted sample was concentrated to dryness under a stream of nitrogen and redissolved in 50 or 100 μl of 80% aq. methanol.

Small volumes (5–20 μl) of the concentrated extracts were spotted on to Merck silica gel 60 aluminum-foil-supported layers and chromatograms developed with a solvent of chloroform–methanol–acetic acid–water (20:10:1:1) until the solvent front advanced 6–10 cm. The chromatograms were dried before dipping very briefly in an Ehrlich's reagent consisting of nine parts of 1% (w/v) *p*-dimethylaminobenzaldehyde dissolved in acetone and one part of aqueous 6 *M* hydrochloric acid mixed immediately before use. Peramine, with an R_F of 0.43, developed as a purple-blue spot on standing or with gentle warming for a few minutes. Alternative spray versions of Ehrlich's reagent were also used successfully.

HPLC measurement of peramine

A 1-ml portion of the lower aqueous phase of the extract was passed through a single Analytichem Bond Elut CBA column, 100 mg absorbent, in the ammonium ion form. The sample was washed through with 1 ml of water and the bound peramine eluted with 0.5 ml of 5% (v/v) aqueous formic acid. Gentle centrifugation was used at each step. The net weight of the solution and an estimate of its density was used to calculate the eluted volume of peramine containing solution.

The efficiency of the extraction of peramine from herbage and of the subsequent work up by ion exchange was tested by adding peramine standard to dry herbage samples, removing the solvent under vacuum, and then extracting the sample for 30 min for each stage.

Peramine was measured by reversed-phase HPLC using a Waters Assoc. Liquid Chromatograph fitted with a Waters Radial-Pak Resolve C_{18} column, 5 μm particle size, 100 × 8 mm. Detection was with a fixed-wavelength UV detector at 280 nm, close to a peak of peramine UV absorption. The isocratic mobile phase was 33% aq. acetonitrile containing guanidinium formate and excess formic acid to give a solution of approximately pH 3.7. This buffer was prepared by dissolving guanidinium carbonate (1.44 g/l) in water, adding reagent grade (98–100%) formic acid (1.6 ml/l), chromatography grade acetonitrile (330 ml/l), and making up to volume before degassing. The flow-rate was 1 ml/min.

The quantity of peramine in 50-μl injection samples was estimated by comparisons of peak heights with those from standard solutions of peramine bromide. Peramine eluted at about 7 min after injection and was often followed by some other unidentified UV absorbing substances. Each HPLC analysis could be completed in approximately 12 min.

The efficiency of extraction of peramine from herbage and subsequent work up by ion exchange was tested by adding small standard amounts of peramine to dry herbage samples and then extracting with the two-phase solvent system.

RESULTS AND DISCUSSION

Thin-layer chromatographic detection of peramine

The tandem ion-exchange step offered convenient purification and concentration of peramine from extracts into a solution with relatively low salt content. The

procedure for detecting peramine by thin-layer chromatography (TLC) is a refinement of the methods used by Rowan and Gaynor[3]. The addition of small amounts of water and acetic acid to the TLC solvent improved reproducibility of the peramine R_F at 0.43, while the tandem ion-exchange work up was effective in removing other compounds in the extracts which react with Ehrlich's reagent. The detection limit was approximately 10 ng of peramine per spot. The intensity of colour reaction may be used to indicate a broadly high or low concentration of peramine in the samples.

Measurement of peramine

The two-phase extraction of peramine from freeze dried herbage samples was adopted after preliminary tests indicated that, as a single cycle of extraction, it was more efficient and convenient than extraction with single phases of aqueous ethanol, aqueous methanol, or chloroform–methanol followed by separate partitioning steps. When using 3 ml of chloroform–methanol (1:1, v/v) and subsequently adding 3 ml each of hexane and water the final extract partitioned into very nearly equal volumes of lipophilic top phase and aqueous bottom phase. By repartitioning portions of the top phase it was shown that negligible amounts of peramine were in the top phase of the extracts. Two notable advantages were (i) the simple removal of lipids and pigments from the peramine extract and (ii) the use of the lipophilic top phase for measurement of lolitrem B by a modification of the method of Gallagher *et al.*[6].

A single step extraction under mild conditions cannot be expected to be complete, therefore reproducible extraction efficiency must be sought and quantified by standard addition methods.

Variation of extraction times (Table I) for each of the two stages of the extraction demonstrated that doubling the times from the standard 30 min did not significantly enhance extraction while a shorter 10-min first stage was less efficient. The two 30-min extraction periods were adopted as convenient and near optimum times.

The overall recovery measured by standard additions was 79% with standard deviation of 2–4%. The degree of extraction of the added peramine was shown to be similar to that of naturally occurring peramine by reextracting the plant residue for 30 min with 50% aq. ethanol and showing that the residual peramine was extracted in proportion regardless of whether or not peramine had been added. The range of

TABLE I

EFFECT OF VARIATION OF EXTRACTION TIMES RELATIVE TO THE STANDARD PROCEDURE OF 30 min FOR EACH STAGE OF EXTRACTION

1st stage of extraction (min)	*2nd stage of extraction (min)*	*Relative extraction efficiency (%)*	*S.D. (%)*
10	30	93.7	1.3*
30	30	100	1.8*
60	30	101.1	2.6*
30	10	98.0	1.6*
30	60	98.8	2.3**

* $n = 4$.
** $n = 3$.

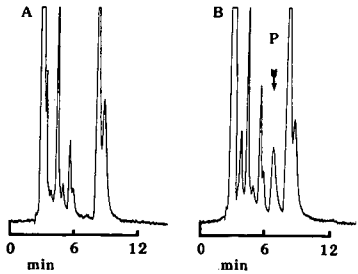

Fig. 2. Typical chromatograms of extracts from ryegrass. (A) endophyte-free herbage, (B) endophyte-containing herbage with peramine, P.

response of the overall extraction and HPLC analysis was demonstrated with standard additions up to the equivalent of 75 ppm of peramine as the free base in dry plant material. The response was shown to be linear by regression analysis through the origin with a standard error of 4.7%. There was no indication of lack of linearity at concentrations higher than the equivalent of 75 ppm. The lower limit for routine detection was approximately 1 ppm.

The isocratic HPLC solvent of 33% (v/v) aq. acetonitrile, 8 m*M* guanidinium formate with excess formic acid was adopted after trials with solvents containing methanol, propan-2-ol and various other salts at various concentrations. Guanidinium salts reduced the tailing of the peramine peak in comparison with sodium, ammonium, or trimethylammonium acetates. Acetonitrile was preferred for the longer retention of peramine on the column relative to other compounds from the extracts with UV absorption. Typical elution patterns are shown in Fig. 2. In as far as no peak was observed at the normal peramine elution time for samples from endophyte-free grasses there was no interference in the HPLC assay. The typical time for each peramine measurement of 12 min compares favorably with the 27 min elution time for peramine in the gradient system of Rowan and Gaynor[3].

Peramine measurements have been made on a range of grasses. No peramine was detected in endophyte-free plants and up to 47 mg peramine/kg dry weight of whole plant herbage was found in plants of perennial ryegrass infected with *A. lolii*. Where plants were divided into top and basal portions the latter contained relatively higher concentrations of peramine (Table II). The age of plants and growth condi-

TABLE II

TYPICAL RESULTS OF PERAMINE MEASUREMENT OF ENDOPHYTE-INFECTED *L. Perenne* HERBAGE

Cultivar (clone)	*Part of plant*	*Peramine (ppm)*
Grasslands Nui (1)	Basal	25
Grasslands Nui (1)	Upper	16
Grasslands Nui (3)	Basal	15
Romanian selection	Basal	9
Romanian selection	Upper	5
Regal (5)	Basal	19
Regal (7)	Basal	32

tions affected peramine concentration. These biological factors and their effect on peramine production will be reported elsewhere. The natural variation from a variety of biological and environmental factors was considerably greater than the variation in results attributable to the analysis method.

REFERENCES

1 R. A. Prestidge, R. P. Pottinger and G. M. Barker, *Proc. NZ Weed Pest Control Conf.*, 35 (1982) 119.
2 D. L. Gaynor and D. D. Rowan, *Proc. NZ Grass. Assoc.*, 47 (1986) 115.
3 D. D. Rowan and D. L. Gaynor, *J. Chem. Ecol.*, 12 (1986) 647.
4 D. D. Rowan, M. B. Hunt and D. L. Gaynor, *J. Chem. Soc., Chem. Commun.*, (1986) 935.
5 M. R. Siegel and D. D. Rowan, unpublished results.
6 R. T. Gallagher, E. P. White and P. H. Mortimer, *NZ Vet. J.*, 29 (1981) 189.
7 R. T. Gallagher, A. D. Hawkes and J. M. Stewart, *J. Chromatogr.*, 321 (1985) 217.
8 D. D. Rowan and B. A. Tapper, *J. Nat. Prod.*, in press.

Journal of Chromatography, 463 (1989) 139–145
Elsevier Science Publishers B.V., Amsterdam — Printed in The Netherlands

CHROM. 21 007

QUANTITATIVE THIN-LAYER CHROMATOGRAPHY BY LASER PYROLYSIS AND FLAME IONIZATION OR ELECTRON-CAPTURE DETECTION

JIANZHONG ZHU and EDWARD S. YEUNG*
Ames Laboratory, U.S. Department of Energy, and Department of Chemistry, Iowa State University, Ames, IA 50011 (U.S.A.)
(First received June 30th, 1988; revised manuscript received September 22nd, 1988)

SUMMARY

A new quantitation method, laser pyrolysis, is demonstrated for thin-layer chromatography (TLC). No spray reagent or "color" developing process is necessary for detecting any organic compound. A complete analysis including sample introduction, separation and detection takes less than 20 min. Two amino acids, serine and phenylalanine, and two pesticides, *p,p*-DDT and methoxychlor were used as the test samples. The sensitivity and linearity compare favorably to conventional densitometry. The detection limit for phenylalanine with flame ionization detection was 100 ng and for methoxychlor with electron-capture detection was 20 ng. This technique combines the advantages of the separation power of TLC and the broad spectrum of detection methods of gas chromatography.

INTRODUCTION

Thin-layer chromatography (TLC) is a simple, rapid and versatile separation technique. Features of two-dimensional separation and multiple sample handling have also contributed to its widespread application. TLC readily provides qualitative results. For quantitative determinations, densitometry, fluorimetry, fluorescence quenching, visual comparison, spot area measurement, and radioactive methods are representative of the methods currently available[1].

Laser-based fluorimetry is the most sensitive technique. Detection limits are often in the 1–10 pg range[2]. Fluorescence detection is however limited to those compounds which fluoresce or can be conveniently derivatized to become fluorescent. Densitometry is the most common quantitation method in TLC. Detection limits with commercial scanners and high-performance plates are typically at the nanogram levels for compounds that absorb visible or UV light strongly. With the recent development of a laser photo-acoustic densitometer[3,4], detection limits of 7.5 pg for α-ionone and 170 pg for orange G have been reported. All the quantitative techniques except radioactive methods are highly dependent on the optical properties (absorbance or fluorescence) of the analytes. Sensitivity varying over several orders of magnitude is observed.

0021-9673/89/$03.50

Many interesting applications of TLC are for "colorless" or very weakly absorbing compounds, *e.g.*, hydrocarbons, lipids, pesticides, carbohydrates, amino acids, proteins and glycols. Normally a "color" developing or spraying process is needed. "Color" developing processes are often undesirable. Heating and even UV radiation are usually involved to promote the reaction. For example, one determination of amino acids with densitometry was described as follows: spray with ninhydrin reagent at a distance of 30 cm from the plate; heat it in an oven for 15 min at 60°C; and place it in a dark cupboard for 4 h before scanning[5]. Two spray reagents and two heating procedures were proposed recently for amino acids analysis with a limit of detection of 0.5–1.0 μg[6]. Quantitative results rely on the choice of spray reagent, spraying skill, heating temperature and heating time. Reproducibility is therefore poor. Even after spraying, optical detection on an opaque and intensely light scattering TLC plate is a difficult task. The Kubelka-Munk correction is often needed for nonlinear effects, although implementation is not difficult with the help of personal computers.

In this paper we describe a new quantitative TLC method: laser pyrolysis scanning (LPS). This technique is simple, rapid, highly instrumental, and has little dependence on the optical properties of the analytes. There is no need for spray reagents and "color" developing, and is applicable to all organic compounds. Briefly, a TLC plate after separation of the analytes is irradiated with an infrared laser to produce a high-temperature spot. The analyte is thus pyrolyzed and swept into a flame ionization detector or an electron-capture detector by a carrier gas.

EXPERIMENTAL

Apparatus

The schematic arrangement of laser pyrolysis scanning with a flame ionization detection (LPS–FID) system is shown in Fig. 1a. A CO_2 cw laser (Molectron Model C250, Sunnyvale, CA, U.S.A.) was used and the laser beam was focused to 2.5 mm on the TLC plate with a 1.0-m concave mirror. Either a flame ionization detector or an electron-capture detector [both were dismounted from a Model 550 gas chromatograph (Tracor, Austin, TX, U.S.A.)] was directly connected to one end of the cell. The carrier gas used was hydrogen–helium (1:2) for FID and argon–methane (9:1) for electron-capture detection (ECD), and the flow-rate was 80–100 ml/min. The signal was collected by an integrator (CI 3000).

Fig. 1b shows the details of the pyrolysis cell. The cell was made of copper and has a 70-mm long, 12-mm wide, and 7-mm high chamber to accommodate a 50 mm × 12 mm TLC plate. The open end of the cell can be closed with an O-ring seal. A potassium chloride window (50 mm in diameter) was attached to the cell with epoxy (Eccobond, Waltham, MA, U.S.A.).

Chemicals

The test compounds were phenylalanine, serine, *p,p*-DDT, and methoxychlor. These were obtained from Aldrich and used as received. The amino acids were dissolved in water (pH = 4 with nitric acid) and the pesticides were dissolved in methanol–hexane (95:5). All solvents used were high-performance liquid chromatographic (HPLC) grade. Samples at various concentrations were prepared by dilution with the solvent used.

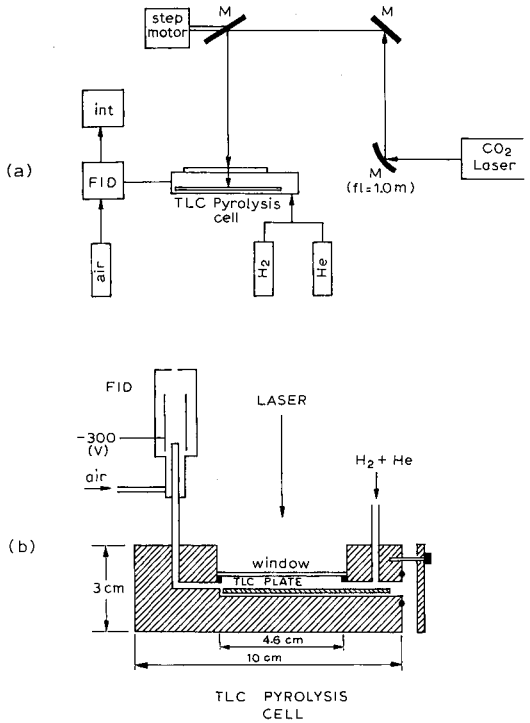

Fig. 1. (a) Schematic diagram of quantitative TLC with laser pyrolysis scanning and flame ionization detection. (b) Details of the laser pyrolysis cell. M = mirror, int = integrator.

TLC separation

Two kinds of silica gel glass-backed plates were used, one with calcium sulphate binder (Alltech, Deerfield, IL, U.S.A., Adsorbsil HPTLC) and the other without binder (Alltech, Adsorbsil-plus, soft layer). Plates were cut to the desired sizes with a glass cutter. The soft layer plate was cleaned with methanol and the plate with binder was treated with concentrated nitric acid overnight, washed with pH 10 buffer and then with deionized water, dried under a 200-W infrared lamp and passed quickly over a flame. Plates were stored in a beaker filled with nitrogen.

Mixtures of the test compounds were applied as 0.2-μl spots with a 10-μl Hamilton microsyringe. Plates were developed in a 30-ml beaker covered with aluminium foil, and dried under an infrared lamp in a nitrogen-filled beaker for about 3 min to evaporate the solvents. The plate was scanned as soon as possible. Both flame ionization and electron-capture detectors were stable within 2 min after the TLC plate was introduced.

Scanning

The laser beam was controlled by a rotating mirror driven by an EPC-012 stepping motor (Hurst, Princeton, IN, U.S.A.). A 46-mm length of the TLC plate was scanned with a speed of 20 mm/min in a direction opposite to the carrier gas-flow. The laser power varied from 1.0 to 5.6 W.

RESULTS

Flame ionization detection

Fig. 2 shows the thin-layer chromatogram of LPS–FID for two amino acids, serine and phenylalanine, both *ca.* 1.0 μg. They were separated on the TLC plate with binder, with water as developing solvent. R_F values were 0.85 for serine and 0.7 for phenylalanine. The response factors were in close agreement with the carbon content of the amino acids, which was expected for FID. The laser power used was 3.5 W.

The dependence of the FID signal on laser power has been examined and is shown in Fig. 3. Higher laser power gives more efficient pyrolysis and shows large FID signals. However, the background is also increased. For the best signal-to-noise ratio, 3.5 W was used. The limit of detection (LOD) is 100 ng for phenylalanine and 500 ng for serine. Linear calibration curves were obtained from the detection limits to 16 μg.

Electron-capture detection

The mixture of the organochlorine pesticides, *p,p*-DDT and methoxychlor, was separated on the TLC plate without binder. The developing solvent was hexane–methanol (99:1). R_F values were 0.6 for *p,p*-DDT and 0.1 for methoxychlor. Fig. 4 shows the thin-layer chromatogram of the pesticides with LPS–ECD. The laser power used was 2.5 W. The dependence on laser power is shown in Fig. 5. For laser powers above 2 W, the samples were almost completely pyrolyzed due to their low thermal stability. The LODs are 20 ng for methoxychlor and 50 ng for *p,p*-DDT. The response for methoxychlor was linear from 50 ng to 2.5 μg and that for *p,p*-DDT was linear from 200 ng to 2.5 μg. As one approaches the LOD, the signal was found to become non-linear and decrease rapidly.

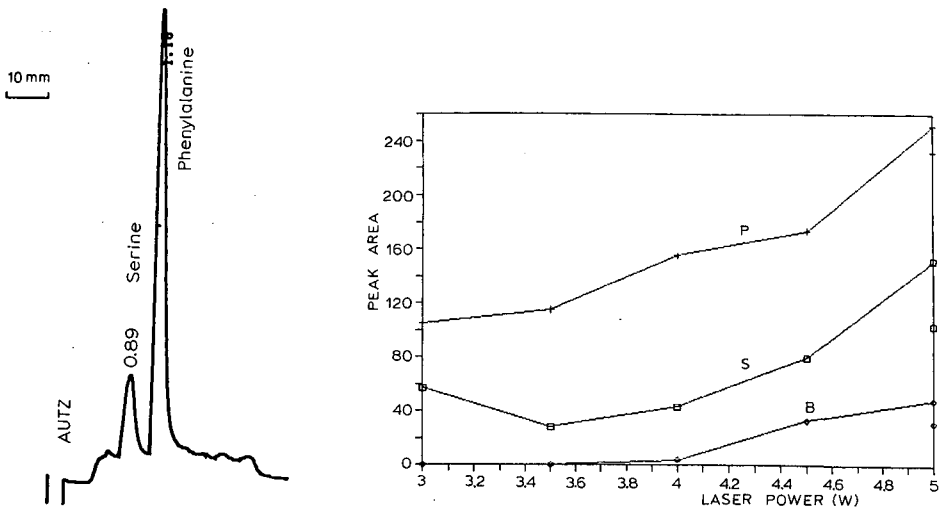

Fig. 2. Thin-layer chromatogram of two amino acids with LPS–FID. The sample contains 0.96 μg serine and 1.02 μg phenylalanine. Laser power, 3.5 W; AUTZ = auto-zero to denote start of scan.

Fig. 3. Laser power dependence of LPS–FID. S = serine, 0.96 μg; P = phenylalanine, 1.02 μg; B = background taken from the largest noise peak.

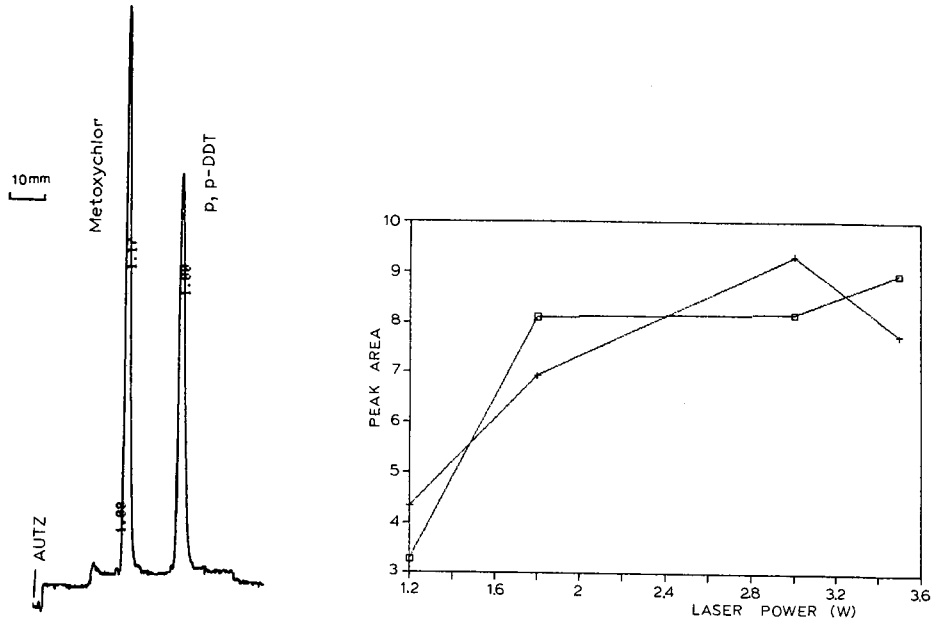

Fig. 4. Thin-layer chromatogram of two pesticides with LPS–ECD. The sample contains 220 ng *p,p*-DDT and 270 ng methoxychlor. Laser power: 2.5 W.

Fig. 5. Laser power dependence of LPS–ECD. (□) *p,p*-DDT, 440 ng; (+) methoxychlor, 530 ng.

DISCUSSION

The sensitivity and the linearity obtained are not very impressive compared to fluorescence[2] or photothermal methods[4]. However, they are comparable to, or even better than those obtained with conventional densitometers. In densitometry, the detection limit of amino acids was 0.1–0.5 μg with ninhydrin spray reagent and a commercial densitometer at 490 nm[5,7]. Proline and hydroxproline are not detectable by that method because of the lack of reactivity. Independent determination was recommended using another spray reagent and scanning at 620 nm. With LPS–FID, all amino acids separated will be detected in one scan. This is because the laser light is absorbed by the TLC plate. Heating is guaranteed regardless of the analytes involved. Most importantly, no spray reagents are needed for LPS–FID.

The calibration curve for amino acids in densitometry is obtained by plotting the peak area *vs.* the square root of the amount and is linear up to 5 μg only. With LPS–FID, peak area is linearly related to the amount of amino acids and the linearity was improved by a factor of three.

The organochlorine pesticides can be detected at the 0.1-μg level with silver nitrate followed by UV photochemical reaction and a fiber-optics densitometer[8]. The linear plot obtained was only over one order of magnitude. With LPS–ECD, both sensitivity and linearity are improved.

Further improvement of this technique relies on having a clean TLC plate, since the signal levels obtained are quite large. Contamination is believed to be the major

source of the background. This includes impurities incorporated during the manufacturing process, exposure in the laboratory atmosphere, and impurities in the developing solvent. The background decreased 62 times after the cleaning procedure for the TLC plates with binder. The plates without binder had a much lower background and thus required only a simple cleaning process. Okumura and co-workers[9,10] have discussed FID background in different types of silica gel quartz rods and found that sintered thin layers have low background. They burned the rod on a flame, which can be moved to scan, and collected ions on the top of the flame. Sintered TLC plates have also been made[11] and have been shown to possess good separation power.

Optimization of the experimental conditions is very important. This includes carrier gas flow-rate, laser scan rate, laser power and pyrolysis cell body temperature. These have not been fully explored in this work. Fast carrier gas flow will provide better resolution, but the sensitivity will decrease due to dilution. Higher laser power is better regardless of the background, for efficient pyrolysis and rapid vaporization. But, here it is limited to below 5 W, beyond which the glass-backed TLC plate may break. The scan rate is limited by the vaporization rate. The volume of the pyrolysis chamber must be kept to a minimum. Temperature control of the pyrolysis cell may be necessary since the analytes may evaporate before pyrolysis and deposit on the cell wall.

Low nanogram detection for LPS–FID and picogram detection for LPS–ECD are certainly possible. In gas chromatography (GC), FID is capable of detecting 10^{-11} g/s of methane with 10^8 linear range[12], and ECD is capable of detecting as little as 10^{-14} g/s of sulfur hexafluoride with 10^4 linear range. So, it may be possible to eventually improve on the LOD here. Most compounds can be easily pyrolyzed using laser powers of 5 W. The laser power (3.5 W) used in our experiments may produce a 600–700°C spot (estimated by the brightness of the spot).

Direct identification in TLC is an even more difficult task than quantitation. TLC–LPS should allow one to identify the separated compounds from the gas-phase fragments. For example, by connecting to a gas chromatograph, it is ready for pyrolysis–GC fingerprint identification. It should also be possible for mass spectrometry (MS), GC–MS and GC–Fourier transform IR analysis. For complex mixtures, the additional TLC step provides one more dimension for separation.

The LPS technique is presently limited to silica gel and alumina plates. Reversed-phase plates, cellulose plates and those plates with organic binder are not suitable for FID because of the high organic contents. Also, low boiling point solvents must be used for easy solvent evaporation in LPS–FID to minimize the background. Broad use of TLC–LPS will depend on new types of TLC plates with low background for FID or ECD.

In summary, we have presented a novel quantitation method for TLC based on LPS. No spray reagent is necessary. The analysis time was reduced from several to 20 min. The test samples were chosen for demonstration of the technique. The same principle should apply to all other organic compounds because pyrolysis is a universal mechanism for transferring species to flame ionization or electron-capture detectors.

ACKNOWLEDGEMENTS

The Ames Laboratory is operated by Iowa State University for the U.S. De-

partment of Energy. This work was supported by the Director of Energy Research, Office of Basic Energy Sciences, Division of Chemical Sciences.

REFERENCES

1 J. G. Kirchner, *Thin-layer Chromatography*, Wiley, New York, 1978.
2 M. E. Coddens, H. T. Butler, S. A. Schuette and C. F. Poole, *LC Mag.*, 1 (1983) 282.
3 H. Kawazumi and E. S. Yeung, *Appl. Spectrosc.*, 42 (1988) 1228.
4 I. I. Chen and M. D. Morris, *Anal. Chem.*, 56 (1984) 19.
5 J. C. Touchstone and J. Sherma, *Densitometer in Thin-layer Chromatography*, Wiley, New York, 1979.
6 S. Laskar and B. Basak, *J. Chromatogr.*, 436 (1988) 341.
7 B. Fried and J. Sherma, *Thin-layer Chromatography*, Marcel Dekker, New York, 2nd ed., 1986.
8 J. Sherma and K. Bloomer, *J. Chromatogr.*, 135 (1977) 235.
9 T. Okumura and T. Kadono, *Bunseki Kagaku (Jap. Anal.)*, 22 (1973) 980.
10 T. Okumura, T. Kadono and A. Iso'o, *J. Chromatogr.*, 108 (1975) 329.
11 T. Okumura, T. Kadono and M. Nakatani, *J. Chromatogr.*, 74 (1972) 73.
12 R. L. Grob, *Modern Practice of Gas Chromatography*, Wiley, New York, 2nd ed., 1985.

Journal of Chromatography, 463 (1989) 147–152
Elsevier Science Publishers B.V., Amsterdam — Printed in The Netherlands

CHROM. 21 045

DETERMINATION OF SELENIUM IN DRUGS BY OXYGEN FLASK COMBUSTION AND ION CHROMATOGRAPHY

MITSUNORI MURAYAMA*, MASAO SUZUKI and SHOJI TAKITANI
Faculty of Pharmaceutical Sciences, Science University of Tokyo, 12, Ichigaya-funagawara-machi, Shinjuku-ku, Tokyo 162 (Japan)
(First received July 29th, 1988; revised manuscript received October 11th, 1988)

SUMMARY

A method is described for the determination of trace selenium (impurities in medicinal organic compounds) by ion chromatography (IC) after oxygen flask combustion. All selenium compounds formed by oxygen flask combustion are converted to selenate ion by heating with nitric acid and potassium permanganate. The selenate ion is then determined by IC, using a simple recycle system to eliminate interfering ions. The detection limit of selenium is 0.4 nmol in 50 mg of sample. The recoveries of selenium added to seven drugs are *ca.* 95–103% with relative standard deviations of 1–6%.

INTRODUCTION

A sensitive, accurate and rapid method for the determination of trace selenium is required because of its environmental and physiological importance. In the pharmaceutical sciences, the analysis of drugs for selenium is provided in the JP XI[1] and USP XXI[2].

The determination of selenium in organic matter generally involves decomposition of the sample by wet digestion with an oxygen-containing acid[3,4] (*e.g.*, nitric acid and/or perchloric acid) and determination of selenite ion [Se(IV)] by fluorimetry with 2,3-diaminonaphthalene[3,4] or hydride generation atomic absorption spectrometry[3] (HG-AAS).

Recently, we reported a more rapid and accurate method for the determination of selenium in bulk prednisolone[5]. The method is based on oxygen flask combustion of samples, oxidation of the resulting selenium species to selenate ion [Se(VI)] by heating with hydrogen peroxide and potassium permanganate and determination of the Se(VI) by ion chromatography (IC). However, this method was not applicable to the determination of selenium in sulphur-containing drugs because of the large amounts of sulphate formed by oxygen flask combustion and oxidation with hydrogen peroxide.

In this work, all selenium species formed by oxygen flask combustion were oxidized to Se(VI) by heating with nitric acid and potassium permanganate and the

0021-9673/89/$03.50

resulting Se(VI) was determined by recycle IC to eliminate interfering ions. Recycle IC was used by Hoover and Yager[6,7] to determine Se(IV), Se(VI) and arsenate in water. We have constructed a simpler recycle IC system that is easier to operate.

EXPERIMENTAL

Reagents

Deionized water (Millipore RO-Q system) was used throughout. Stock solutions of Se(IV) and Se(VI) (1.0 mg/ml as selenium) were prepared by dissolving 331.69 mg of sodium selenite pentahydrate (Merck, analytical-reagent grade) and 238.83 mg of sodium selenate (Nakarai Chemicals, extra pure grade), respectively, in 100 ml of water. A stock solution of elemental selenium [Se(0)] (*ca.* 50 mg/ml in carbon disulphide) was prepared as reported previously[5]. The chemicals tested were acetazolamide (Sigma), chlorothiazide (Sigma), *p,p'*-diaminodiphenyl sulphone (dapsone; Tokyo Kasei Kogyo), dichlorophenamide (Sigma), hydroflumethiazide (Sigma), 2-mercapto-1-methylimidazole (methimazole; Nakarai Chemicals, extra pure grade) and prednisolone (Nakarai Chemicals, analytical-reagent grade). Other reagents used were of analytical-reagent grade.

Recycle IC conditions

Fig. 1 illustrates the recycle ion chromatograph system (Dionex 2010i) equipped with a sample loop (50 μl), an HPIC-TAC-1 concentration column, an HPIC-AG4 guard column (50 × 4 mm), an HPIC-AS4 separation column (250 × 4 mm), an AFS-1 packed hollow-fibre suppressor and a conductivity detector.

A sample solution was injected into the sample loop and a fraction of eluate containing Se(VI) was collected on a concentrator (C_1) by switching a valve (V_3). Switching times were defined in advance according to the retention time of Se(VI) (standard solutions for the calibration graph). This column and connection were washed with 2 ml of water through the injection port (I_2) using a disposable syringe. The collected Se(VI) was reinjected into the separation column by switching a valve (V_2).

The eluent selected was 4 m*M* sodium carbonate–4 m*M* sodium hydrogencarbonate and the flow-rate was 1.5 ml/min. The scavenger for the suppressor was 50 m*M* dodecylbenzenesulphonic acid (DBS) (Tokyo Kasei Kogyo) at a flow-rate of 2.0 ml/min.

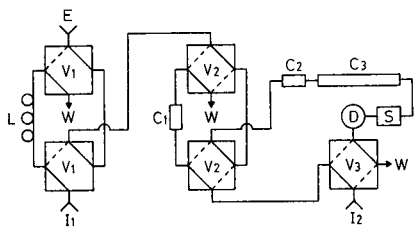

Fig. 1. Schematic diagram of recycle ion chromatography system. (C_1) Concentration column; (C_2) guard column; (C_3) separation column; (D) conductivity detector; (E) eluent in; (I_1, I_2) injection ports; (L) sample loop; (S) suppressor; (V_1–V_3) air-operated valves; (W) waste.

Preparation of samples

Each sample (50 mg) was weighed on a filter-paper (Toyo Roshi, No. 51A) and decomposed by the oxygen flask combustion method[1]. The oxygen flask used was a glass-stoppered 500-ml hard glass flask with a platinum basket and the absorbing liquid was 10 ml of 0.7% nitric acid. The flask was rinsed with 10 ml of water and the washings were combined with the contents of flask. The solution was boiled and concentrated to about 1 ml. To the solution were added dropwise 20 m*M* potassium permanganate until a purple colour remained. One more drop of 20 m*M* potassium permanganate was added to the mixture and the mixture was evaporated to dryness on a hot-plate (140°C). To the residue were added 10 ml of water. The mixture was filtered through a 0.45-μm membrane filter (Nihon Millipore Kogyo, SJHV 013 NS) and subjected to IC. Concentrations of selenium in the samples were calculated from a calibration graph of peak height *versus* concentration.

RESULTS AND DISCUSSION

Recycle IC conditions

The recycle system of Hoover and Yager[6,7] was equipped with a suppressor column but we employed a continuously usable fibre suppressor. Generally, sulphuric acid is used as a scavenger for the fibre suppressor[8–10], but some of the sulphate ions leaked from the membrane of the fibre suppressor, were collected on the concentrator and gave a large system peak of sulphate ion on reinjection (Fig. 2A). The use of DBS as a scavenger was recommended by Hanaoka *et al.*[11]. Although it also gave system peaks due to sulphite and sulphate ions (Fig. 2B and C), neither of these ions interfered seriously with the determination of Se(VI). Therefore, DBS was selected as a scavenger.

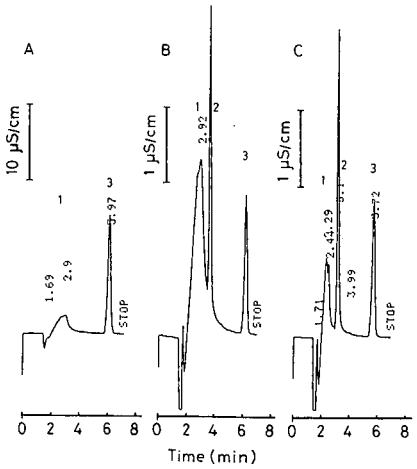

Fig. 2. System peaks in recycle ion chromatography. Scavenger: (A) 12.5 m*M* sulphuric acid; (B) 50 m*M* DBS; (C) DBS and the concentrator was washed with 2 ml of water before reinjection. The flow-rate of the scavengers was 2.0 ml/min and the recycle volume was 1.5 ml (1 min). Peaks: 1 = carbonate; 2 = sulphite; 3 = sulphate.

TABLE I

PERMISSIBLE CONCENTRATIONS OF FOREIGN IONS IN THE DETERMINATION OF SELENATE BY ION CHROMATOGRAPHY

Method	*Permissible concentration* (mM)*			
	Chloride	*Phosphate*	*Nitrate*	*Sulphate*
Conventional IC	25	10	2.4	0.4
Recycle IC	200	100	50	10

* Concentration causing the peak height for 2 μM selenate to be in error by more than 5%.

Carbonate ion in the eluent was also collected on the concentrator and gave a broad tailing system peak (Fig. 2A and B). As in the method of Hoover and Yager[6], carbonate ion was removed by washing the concentrator with 2 ml of water (Fig. 2C) after collection.

The same eluent as mentioned in the previous paper[5], 4 mM sodium carbonate–4 mM sodium hydrogencarbonate, was also used in this study because it gave the highest sensitivity and reproducible elution for the determination of Se(VI) on an HPIC-AS4 column.

The peak height of Se(VI) determined by recycle IC was 95% of that determined by conventional IC throughout the determination range. The determination range of Se(VI) by recycle IC was 42 nM–26 μM with relative standard deviations (R.S.D.) of 1.42% (1 μM, n = 10) and 0.61% (10 μM, n = 10). The proposed method permitted the coexistence of other anions at concentrations 10–25 times higher than in conventional IC, as shown in Table I. Fig. 3 shows typical chromatograms of Se(VI) in the presence of sulphate ion before and after recycling.

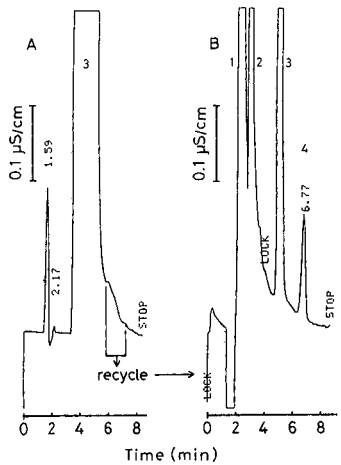

Fig. 3. Effect of recycle ion chromatography. Chromatograms (A) before and (B) after recycling. Sample: 380 nM Se(VI) in 10 mM sulphate. Peaks: 1 = carbonate; 2 = sulphite; 3 = sulphate; 4 = selenate.

Oxidation conditions for Se(0) and Se(IV)

'Selenium was converted to Se(0), Se(IV) and Se(VI) (in the ratio 5:75:20) by oxygen flask combustion as described previously[5]. Since Se(VI) was determined most sensitively and was well separated from other ions by IC[5], oxidation conditions for Se(0) and Se(IV) were examined.

All drugs to which the JP XI[1] and USP XXI[2] methods for the determination of selenium are applicable contain sulphur, except prednisolone. The sulphur was converted into sulphite and sulphate ions (in the ratio 80:20) by oxygen flask combustion. In our previous work[5], all of the sulphite was oxidized to sulphate by heating with hydrogen peroxide, and the sulphate ion obtained interfered with the determination of Se(VI) by IC. Therefore, we used nitric acid, which is generally used to oxidize Se(0)[1,2]. The sulphite was volatilized as sulphur dioxide by heating with nitric acid, and the recoveries of sulphur as sulphate were 15–25%. Further, nitrate ion was removed to a tolerable level for IC by heating to dryness.

However, when Se(0) was heated to dryness with nitric acid, Se(0) was oxidized to Se(IV) (recovery 40%) and Se(VI) (recovery 30%), and losses of 30% were observed. The losses are probably caused by volatilization of selenium dioxide formed from Se(IV). Therefore, Se(IV) was oxidized to Se(VI) by heating with potassium permanganate before the sample solution had been completely dried. Se(0) was oxidized to Se(VI) by heating with 0.1 ml of 70% nitric acid and 50 μl of 20 mM potassium permanganate solution (Fig. 4). The heating temperature was 140°C, because the recoveries of Se(VI) on heating at 100–140°C were nearly 100% whereas heating above 160°C reduced the recovery. The recovery of selenium was 99.4% with an R.S.D. of 0.86% [n = 8, 127-nmol sample of Se(0) (12.7 μM)].

Determination of selenium in drugs

When the above method was applied to analysis of drugs for selenium after oxygen flask combustion, reducing agents (not only sulphite but also halide and nitrite) were formed from many drug molecules. These reducing agents immediately consumed permanganate before the oxidation of Se(IV) had been completed. Therefore, the absorbing liquid obtained by oxygen flask combustion was boiled and concentrated to about 1 ml to volatilize the reducing agents. Then 20 mM potassium permanganate solution was added dropwise until the purple colour of permanganate remained, and one more drop was added. The times required for evaporation after

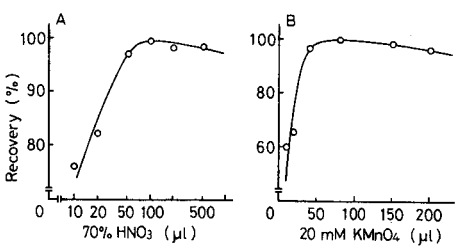

Fig. 4. Effect of reagent volume on the oxidation of Se(0) (127 nmol in 10 ml). (A) 50 μl of 20 mM potassium permanganate added; (B) 100 μl of 70% nitric acid added. The resulting Se(VI) was determined by conventional IC.

TABLE II

RECOVERY OF SELENIUM IN DRUGS BY ION CHROMATOGRAPHY

Sample (50 mg)	*Se(0) (nmol)*		*Recovery (%)*	*R.S.D. (%)*	*n*
	Added	*Found*			
Acetazolamide	0.0	0.0	–	0	4
	19.0	18.21	95.8	3.80	4
Chlorothiazide	0.0	0.0	–	0	4
	19.0	18.26	96.1	4.33	4
Dapsone	0.0	0.69	–	15.3	4
	19.0	19.86	100.9	2.70	4
Dichlorophenamide	0.0	0.0	–	0	4
	19.0	18.96	99.8	1.68	4
Hydroflumethiazide	0.0	0.0	–	0	4
	19.0	18.33	96.5	0.61	4
Methimazole	0.0	1.23	–	12.8	4
	6.33	7.54	99.8	4.61	8
	37.97	40.27	102.8	1.91	8
Prednisolone	0.0	0.0	–	0	4
	6.33	6.35	100.4	3.04	8
	37.97	36.04	94.9	5.69	5

addition of potassium permanganate were about 5 min, while the oxidation of Se(IV) was completed within 1–2 min.

Table II shows the recovery of selenium added to several drugs. Except for prednisolone, which could be analysed by the conventional IC, these drugs were analysed by recycle IC. The recoveries were in the range 95–103% with an R.S.D. of 1–6% in each instance.

The overall procedure was completed within 1.5 h. As oxygen flask combustion prevents the loss of analyte and is more rapid than wet digestion, and recycle IC permits the coexistence of many more substances than in fluorimetry and HG-AAS, this method is useful for the determination of trace amounts of selenium in organic compounds.

REFERENCES

1 *The Pharmacopoeia of Japan*, Ministry of Health and Welfare, 11th ed., 1986.
2 *US Pharmacopeia XXI–National Formulary XVI*, US Pharmacopeial Convention, Rockville, MD, 1985.
3 Analytical Methods Committee, *Analyst (London)*, 104 (1979) 778.
4 *Official Method of Analysis of the Association of Official Analytical Chemists*, AOAC, Arlington, VA, 14th ed., 1984, Sections 3.101, 25.001 and 25.154.
5 M. Murayama, M. Suzuki and S. Takitani, *Anal Sci.*, 4 (1988) 389.
6 T. B. Hoover and G. D. Yager, *Anal. Chem.*, 56 (1984) 221.
7 T. B. Hoover and G. D. Yager, *J. Chromatogr. Sci.*, 22 (1984) 435.
8 T. S. Stevens and J. C. Davis, *Anal. Chem.*, 53 (1981) 1488.
9 T. S. Stevens, G. L. Jewett and R. A. Bredeweg, *Anal. Chem.*, 54 (1982) 1206.
10 S. A. Bouyoucos, *J. Chromatogr.*, 242 (1982) 170.
11 Y. Hanaoka, T. Murayama, S. Muramoto, T. Matsuura and A. Nanba, *J. Chromatogr.*, 239 (1982) 537.

Journal of Chromatography, 463 (1989) 153–158
Elsevier Science Publishers B.V., Amsterdam — Printed in The Netherlands

CHROM. 21 057

Note

Non-steady pressure profiles in chromatographic columns

B. DEVALLEZ* and J. GUION
Laboratoire de Chimie Physique, Université de Nice, Parc Valrose, 06034 Nice (France)
and
G. COGNET
ENSEM, 2 Rue de la Citadelle, 54000 Nancy (France)
(First received June 15th, 1988; revised manuscript received October 18th, 1988)

The pressure change produced from steady-state flow at a tubular reactor inlet alters the pressure profile and makes it dependent on time, t. This perturbation travels down the reactor, and at time t_L arrives at the outlet. This time t_L is the so-called "response time". A pressure-programmed gas chromatographic column is a good example of this type of tubular reactor.

The treatment of non-steady flow is much more difficult. Non-steady profiles have been obtained as a numerical solution for a non-linear partial differential equation. Special cases, which correspond to sudden pressure jumps at the inlet[1] or to continuous pressure programming[2], have been solved.

Response time has been measured in different cases: (a) discontinuous inlet-pressure changes in packed columns[1] or capillary columns[3] and (b) pressure programming in packed columns[4].

This paper describes a method for calculating non-steady pressure profiles in chromatographic columns. The pressure profiles are calculated in accordance with the response time for the case of a continuous pressure variation.

EXPERIMENTAL AND RESULTS

The pressure profile at any given time t is assumed to be the section of the graph of the function $p(x,t)$ which is represented by a sum of the form:

$$p(x,t) = p_0(x,t) + p_1(x,t) + \ldots + p_n(x,t) \quad (1)$$

where x is the distance between a point in the column and the inlet section of the column; $p_0(x,t)$ represents the stationary profile at any time t with an inlet pressure which may vary according to

$$p_e = p_{e0} + h(t) \quad (2)$$

The expression of the function $h(t)$ reflects the type of pressure variation imposed.

The additional terms $p_i(x,t)$ allow the description of the exact pressure profile

0021-9673/89/$03.50

observed. Thus, it is possible to consider a "quasi-unchanged" pressure distribution. This distribution is always described by the basic equation

$$\frac{\kappa}{2\eta} \cdot \frac{\partial^2 p^2}{\partial x^2} = \frac{\partial p}{\partial t} \tag{3}$$

where κ is the column permeability and η the carrier gas viscosity.

Let us introduce the following set of reduced variables, each of which is dimensionless:

$$\begin{aligned} p^* &= p/p_s \quad \text{(reduced pressure)} \\ x^* &= x/L \quad \text{(reduced distance)} \\ t^* &= t/\tau \quad \text{(reduced time)} \end{aligned} \tag{4}$$

where p_s is defined as the outlet pressure. The reference time τ is defined as

$$\tau = 2\eta L^2/\kappa p_s \tag{5}$$

where L is the column length. When these reduced variables are used, the mathematical analysis is simplified and eqn. 1 is transformed to

$$\frac{\partial^2 p^2}{\partial x^2} = \frac{\partial p}{\partial t} \tag{6}$$

if the asterisk is removed. The term $p_0(x,t)$ corresponding to steady-state flow, at time t, is the solution of the equation

$$\frac{\partial^2 p_0^2(x,t)}{\partial x^2} = 0 \tag{7}$$

After two integrations we obtain the quadratic form

$$p_0^2 = A - Bx \tag{8}$$

where

$$A = p_0^2(0,t) = p_e^2$$

and

$$B = p_e^2 - p_0^2(1,t) = p_e^2 - 1$$

so that eqn. 8 may be written as

$$p_0(x) = | p_e^2 - (p_e^2 - 1)x|^{\frac{1}{2}} \tag{9}$$

which represents the classical James–Martin expression[5]. The shape of the function $p_0(x)$ is given in Fig. 1 and a net decompression appears near the column outlet.

Determination of p_1

Only p_1 will be calculated. We substitute the sum $p_0 + p_1$ for the variable p in eqn. (6). After linearization, the following equations, with dimensionless parameters, are obtained:

$$\frac{\partial^2 p^2}{\partial x^2} \approx \frac{\partial^2 (p_0^2 + 2p_0p_1)}{\partial x^2} = \frac{\partial p_0}{\partial t} = \frac{2p_e p_e' - 2p_e p_e' x}{2|p_e^2 - (p_e^2 - 1)x|^{\frac{1}{2}}} \tag{10}$$

where p_e' is the derivative of the function p_e with respect to reduced time. A first integration with respect to x gives

$$\frac{\partial (p_0^2 + 2p_0p_1)}{\partial x} = \alpha + \frac{2p_e p_e'}{(p_e^2 - 1)^2} \cdot p_0 + \frac{p_e p_e'}{p_e^2 - 1} \int p_0 \mathrm{d}x \tag{11}$$

where α is a constant. A second integration gives

$$p_0^2 + 2p_0p_1 = \alpha x + \beta + \frac{4}{3} \cdot \frac{p_e p_e'}{(p_e^2 - 1)^3} \left(\frac{p_0^5}{5} - p_0^3 \right) \tag{12}$$

where β is a constant.

For $x = 0$, we have $p_0 = p_e$ and $p_1 = 0$, hence β may be calculated as the initial conditions:

$$\beta = p_e^2 - \frac{4}{3} \cdot \frac{p_e p_e'}{(p_e^2 - 1)^3} \left(\frac{p_e^5}{5} - p_e^3 \right) \tag{13}$$

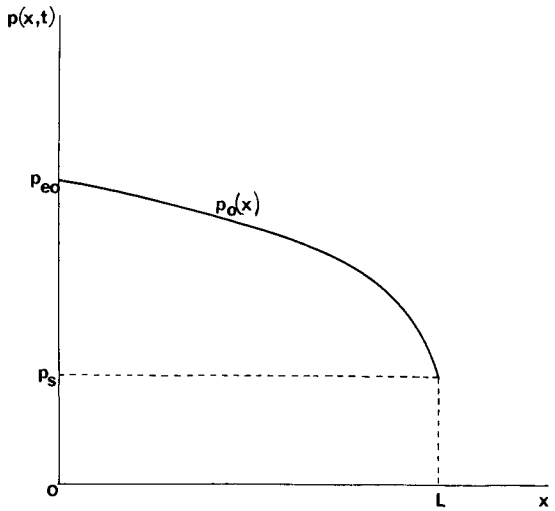

Fig. 1. Plot of $p(x,t)$ *versus* x.

TABLE I

EFFECTS OF THE REFERENCE TIME τ AND THE PROGRAMMING RATE b ON THE TERM p_1

τ	κ/η*	p_e	b**	x*	p_0	p_1
4	1	2	10^{-3}	0.5	1.58	$-1.94 \cdot 10^{-4}$
40	10^{-1}	–	–	–	–	$-1.94 \cdot 10^{-3}$
400	10^{-2}	–	–	–	–	$-1.94 \cdot 10^{-2}$
4	1	2	10^{-3}	0.25	1.80	$-1.42 \cdot 10^{-4}$
–	–	1.2	–	–	1.15	$-2.00 \cdot 10^{-4}$
4	1	2	10^{-3}	0.5	1.58	$-1.94 \cdot 10^{-4}$
–	–	–	10^{-2}	–	–	$-1.94 \cdot 10^{-3}$
–	–	–	10^{-1}	–	–	$-1.94 \cdot 10^{-2}$
40	10^{-1}	2	10^{-3}	0.25	1.80	$-1.42 \cdot 10^{-3}$
–	–	–	–	0.50	1.58	$-1.94 \cdot 10^{-3}$
–	–	–	–	0.75	1.32	$-1.50 \cdot 10^{-3}$

* Values are expressed in s atm m^{-2} for a column of length $L = 2$ m and outlet pressure $p_s = 1$ atm.
** Values are expressed in atm s^{-1}.

For $x = 1$, $p_0 = 1$ and $p_1 = 0$, we obtain

$$\beta = 1 - p_e^2 + \frac{4}{3} \cdot \frac{p_e p_e'}{(p_e^2 - 1)^3}\left(\frac{4}{5} + \frac{p_e^5}{5} - p_e^3\right) \tag{14}$$

and finally

$$p_1 = \frac{2p_e p_e'}{3p_0(p_e^2 - 1)^3}\left[\frac{4x}{5} + (x - 1)\left(\frac{p_e^5}{5} - p_e^3\right) + \left(\frac{p_0^5}{5} - p_0^3\right)\right] \tag{15}$$

p_1 is a linear function of the space variable x and is dependent on the type of programming of the inlet pressure.

TABLE II

VALIDITY OF THE APPROXIMATION $p^2 \approx p_0^2 + 2p_0p_1$: MAXIMUM VALUES OF b FOR DIFFERENT VALUES OF τ

Column length $L = 2$ m and outlet pressure $p_s = 1$ atm.

τ	κ/η*	*Maximum* b**
400	0.01	$5 \cdot 10^{-3}$
40	0.1	$5 \cdot 10^{-2}$
4	1	$5 \cdot 10^{-1}$

* Values are expressed in s atm m^{-2} for a column of length $L = 2$ m and outlet pressure $p_s = 1$ atm.
** Values are expressed in atm s^{-1}.

TABLE III

COMPARISON OF p (atm) OBTAINED BY THE PRESENT METHOD (A) AND A NUMERICAL METHOD (B)[2]

*Conditions**	*Method*	*x**										
		0	*0.1*	*0.2*	*0.3*	*0.4*	*0.5*	*0.6*	*0.7*	*0.8*	*0.9*	*1*
I	A	4.50_0	4.26_4	4.02_0	3.76_4	3.49_5	3.20_8	2.89_7	2.55_3	2.16_0	1.68_1	1.00_0
	B	4.50_0	4.26_5	4.02_1	3.76_6	3.49_7	3.21_0	2.90_0	2.55_6	2.16_3	1.68_4	1.00_0
II	A	2.25_0	2.24_8	2.14_3	2.03_4	1.91_9	1.79_7	1.66_7	1.52_7	1.37_4	1.20_1	1.00_0
	B	2.25_0	2.24_9	2.14_4	2.03_4	1.91_9	1.79_8	1.66_8	1.52_8	1.37_4	1.20_2	1.00_0

* Conditions: I, $p(0,0) = 3.5$, $\tau = 8$, $t = 0.25\tau$, $b = 5 \cdot 10^{-1}$ atm s^{-1}; II, $p(0,0) = 2.15$, $\tau = 8$, $t = 0.25\tau$, $b = 5 \cdot 10^{-2}$ atm s^{-1}.

Application to linear flow programming

Linear programming was chosen to test the present method; the function $h(t)$ is written as

$$h(t) = bt$$

Two parameters have an important effect on the term p_1 (see Table I); the reference time, $\tau = 2\eta L^2/\kappa p_s$, and the programming rate, b. The validity of the approximation $p^2 \approx p_0^2 + 2p_0p_1$ is limited by the values of b. Table II shows the maximum values of b for different values κ/η, with an error for 0.3% in the pressure p, the inlet pressure being 2 atm.

From Table III, it is possible to compare the present method (method A) with a numerical method (method B) used in previous work[3]. Method B gives a polynomial development of the pressure profile. There is good agreement between the two methods.

CONCLUSION

A continuous change in flow causes a departure from a steady state. The assumption that the time-varying pressure profile along the column is the same as that existing in constant-pressure operation for a given inlet pressure value is not satisfactory[6], so we have added a perturbation term to the classical pressure profile of James and Martin[5] to obtain the actual profile. A flow variation at the column inlet give rise to a perturbation that reaches the column outlet at a time t_L, which is usually small. The present method is rigorously applicable to pressure distributions after this time. In the theory, a second-order term is neglected owing to its smallness when the programming rate is not too high; when the permeability of a column decreases, the maximum programming rate likewise decreases. The results are in good agreement with those obtained by numerical methods.

REFERENCES

1 P. D. Schettler and J. C. Giddings, *Anal. Chem.*, 37 (1965) 835.
2 B. Devallez, J. Larrat and J. M. Vergnaud, *C.R. Acad. Sci.*, 277 (1973) 411.
3 L. Jacob and G. Guiochon, *Bull. Soc. Chim. Fr.*, 12 (1971) 4632.
4 B. Devallez, G. Cognet and J.-M. Vergnaud, *J. Chromatogr.*, 109 (1975) 1.
5 A. T. James and A. J. P. Martin, *Biochem. J.*, 50 (1952) 679.
6 J. D. Kelley and J. P. Walker, *Anal. Chem.*, 41 (1969) 1340.

Journal of Chromatography, 463 (1989) 159–164
Elsevier Science Publishers B.V., Amsterdam — Printed in The Netherlands

CHROM. 21 044

Note

Precalculation of gas chromatographic retention indices of linear 1-halogenoalkanes

N. DIMOV
Chemical Pharmaceutical Institute, 1156 Sofia (Bulgaria)
and
R. MILINA*
Petrochemical Research Institute, 8104 Burgas (Bulgaria)
(First received March 21st, 1988; revised manuscript received October 10th, 1988)

The precalculation of retention indices of alkyl halides in gas chromatography (GC) was performed by Kováts[1] and continues to be of interest[2–15]. Some authors used the experimentally found contributions of halogen atoms to the index values[1–3]. Morishita *et al.*[4] proposed an additive approach for precalculation of the retention index, I, of 1-halogenoalkanes. The maximum discrepancy between the experimental and calculated I value is 2 index units (i.u.).

Linear correlations with solute properties, such as the number of carbon atoms, n[5–7], boiling point[7–11], Van der Waals volume[9], etc., have been proposed. Sabljic[12], using the experimental data of Morishita *et al.*[4], proposed a topological approach. The correlation coefficient obtained is high (0.999), but the discrepancies between $I_{exp.}$ and $I_{calc.}$ are from 1 to 8 i.u.

When applied to a particular series of alkyl halides, *e.g.*, chlorides, bromides or iodides, some of the approaches proposed are sufficiently exact. However, none is able to predict the retention when different 1-halogenoalkanes are present in the sample.

The present paper proposes an equation for exact precalculation of the retention indices of various linear 1-halogenoalkanes. Isomers are not included, in order to obtain precise results. Once correctly identified, the 1-halogenoalkanes may serve for an easier identification of the isomers. The identification currently necessitates only a limited set of standards. This saves expense and time, especially if a GC–mass spectrometric (MS) system is involved in the investigation. Besides, the calculative identification is sufficient in many cases.

To assess the accuracy of the calculative identification approach, data on the reproducibility of the experimental results are necessary. Unfortunately there are few data in the literature to allow a reliable statistical calculation of the reproducibility. On the basis of the experimentally established repeatability of $\pm$ 2 i.u., we accepted for the reproducibility the value of 4 i.u.

EXPERIMENTAL

The retention indices of 21 (C_2–C_9 straight chain) 1-halogenoalkanes were

0021-9673/89/$03.50

obtained on a gas chromatograph Sigma 3B (Perkin-Elmer) equipped with flame ionization detection (FID). The column was a fused-silica capillary 50 m × 0.32 mm I.D. coated with silicon oil OV-101. Samples were injected in split mode. The carrier gas was hydrogen with a flow-rate of 20 cm s^{-1} and splitting ratio was 1:100. The temperature of the column oven was programmed linearly from 40 to 280°C at 2° min^{-1}.

Data handling

The calculations were based on the recently proposed model for deriving predictive equations in chromatography[16]

$$I_{calc.} = b_0 + \Sigma b_i \cdot B_i + \Sigma b_j \cdot T_j \quad (1)$$

where B and T are respectively basic and tuning contributors to the retention index value and b_0, b_i and b_j are constants. The term B includes such solute properties, which correlate very highly with the retention index and after calculation of $I_{calc.}$ its value covers 100 ± 10–15% of the experimental index value, $I_{exp.}$. This term may be used also in any relationship, linear or non-linear, connecting the retention with any solute physicochemical properties. The second part of the model also includes solute properties, which however have insignificant correlation with the retention, but which possess an high discrimination power and are able to approximate the roughly calculated value of $I_{calc.}$ to the value of $I_{exp.}$.

The selection of suitable solute properties is performed in two steps. First, the best parameters B are chosen, by studying the linear regression between a series of solute features and $I_{exp.}$.

$$I_{exp.} = b_0 + b_1 \cdot B \quad (2)$$

The non-linear regression between I and n proposed recently by Golovnya[17,18] and which has been confirmed by others[19,20] was also examined for the term B. The second step requires a study of the discrepancies between $I_{calc.}$ and $I_{exp.}$ in connection with specific solute features and definition of the term T.

RESULTS AND DISCUSSION

The correlation coefficients, r, of eqn. 2, the variances, s^2, as well as the values of the intercorrelation coefficients, R, are summarized in Table I. The best correlation is obtained with the molecular refraction, R_m, but the maximum deviation, Δ_{max}, of 21 i.u. is too high. The investigation of the quadratic regressions did not give better results. For the boiling point, B_p, the correlation coefficient was 0.9991, but Δ_{max} remains high, 23 i.u.

These deviations mean that the correlations are without practical significance. Obviously it is necessary to search for suitable solute features for the tuning of the $I_{calc.}$ values. A careful study of the discrepancies between $I_{exp.}$ and $I_{calc.}$ revealed that they depend on the type of halogen when the correlation is made with n, R_m or the molecular volume, V_{mol}. The discrepancies for chlorides are −80 i.u., for bromides ±10 i.u. and for iodides +90 i.u. (see Table II). The intergroup (one type of halogen) discrepancies

TABLE I

CORRELATION COEFFICIENT, r, VARIANCE, s^2, MAXIMUM DEVIATION, Δ_{max}, IN i.u. AND THE INTERCORRELATION COEFFICIENT, R

No.	Parameter	r	s^2	Δ_{max}	R				
					R_m	B_p	V_{mol}	n	M_m
1	Molecular refraction, R_m	0.9989	11	21	1	0.99	0.98	0.95	0.81
2	Boiling point, B_p	0.9967	381	35		1	0.97	0.94	0.82
3	Molecular volume, V_{mol}	0.9779	2524	74			1	0.99	0.66
4	Number of carbon atoms, n	0.9537	5244	102				1	0.58
5	Molecular mass, M_m	0.8064	$2 \cdot 10^4$	264					1

change systematically when the molecular mass, M_m, is the parameter. Hence, it is reasonable to examine the combination of M_m and any of the other solute features studied.

The combination of n with M_m gives the best results

$$I_{calc.} = 155.0217 + 76.9862n + 1.8828M_m \quad (3)$$

TABLE II

COMPARISON OF $I_{exp.}$ WITH $I_{calc.}$ CALCULATED ACCORDING TO DIFFERENT EQUATIONS

No.	Compound	$I_{exp.}$	I_n	$I_{calc.}$		
				Eqn. 3	Eqn. 6	Eqn. 7
1	C_2H_5Cl	432 ± 1	517	430.5	431.2	431.4
2	C_3H_7Cl	534 ± 1	617	533.9	534.4	533.9
3	C_4H_9Cl	638 ± 1	718	637.2	637.8	637.5
4	$C_5H_{11}Cl$	742 ± 1	818	740.6	741.2	741.6
5	$C_6H_{13}Cl$	845 ± 1	919	844.0	844.6	845.4
6	$C_7H_{15}Cl$	949 ± 1	1019	947.4	947.9	948.6
7	$C_8H_{17}Cl$	1051 ± 2	1119	1050.8	1051.3	1051.1
8	$C_9H_{19}Cl$	1152 ± 2	1219	1154.2	1154.7	1153.1
9	C_2H_5Br	514 ± 1	517	514.1	513.0	513.2
10	C_3H_7Br	618 ± 1	617	617.6	616.4	615.9
11	C_4H_9Br	719 ± 1	718	720.9	719.8	719.3
12	$C_5H_{11}Br$	822 ± 1	818	824.3	823.1	823.9
13	$C_6H_{13}Br$	926 ± 1	919	927.7	926.5	927.3
14	$C_7H_{15}Br$	1030 ± 2	1019	1031.1	1029.9	1030.4
15	$C_8H_{17}Br$	1133 ± 2	1119	1134.5	1133.3	1133.0
16	C_2H_5I	602 ± 1	517	602.6	603.4	603.5
17	C_3H_7I	705 ± 1	617	706.1	706.8	706.1
18	C_4H_9I	809 ± 1	718	809.5	810.1	809.6
19	$C_6H_{13}I$	1018 ± 1	919	1016.2	1016.9	1017.5
20	$C_7H_{15}I$	1122 ± 2	1019	1119.6	1120.2	1120.7
21	$C_8H_{17}I$	1225 ± 2	1119	1223.0	1223.6	1223.3

with $r = 0.999980$, $s^2 = 2.4$, standard deviation (S.D.) = 1.56 and $\Delta_{max} = 2.4$ i.u. We consider that the rôle of M_m accounts for the type of halogen at equal number of carbon atoms, *i.e.*, it belongs to the term T of the model. This was confirmed when M_m was exchanged for the contribution of the halogen atoms, calculated according to

$$I_{calc.} = b_0 + b_1 n + b_2(Cl^-) + b_3(Br^-) + b_4(I^-) \quad (4)$$

where (X^-) has values of 1 or 0 depending on the presence or absence of the corresponding halogen atom. To decrease the number of parameters a relative contributor, Halo(X^-), is calculated.

$$\text{Halo}(Cl^-) = b_2/b_3 \text{ and Halo}(I^-) = b_4/b_3 \quad (5)$$

assuming Halo$(Br^-) = 1.00$.

Using the calculated Halo(X^-) values as the term T in eqn. 1, the following equation is obtained

$$I_{calc.} = 12.6327 + 103.3724n + 293.645\text{Halo}(X^-) \quad (6)$$

where Halo$(Cl^-) = 0.7209$ and Halo$(I^-) = 1.3077$. The correlation coefficient is 0.999986, $s^2 = 1.5$, S.D. = 1.26 and $\Delta_{max} = 2.4$ i.u.

The index values calculated by eqns. 3 and 6 are very similar (Table II) which confirms the hypothesis about the rôle of M_m.

The use of Golovnya's equation as for the term B of eqn. 1 leads to

$$I_{calc.} = 112.1545 + 98.3908n - 229.3558(\log n/n) - 0.9564\,[(n-2)^2 + 0.1]^{-1} + 293.3475\text{Halo}(X^-) \quad (7)$$

with the highest $r = 0.99999$ and the lowest $s^2 = 1.3$. The maximum error, $\Delta_{max} = 2.1$ i.u. (see Table II).

Comparison of the variances of eqns. 3 and 7 according to the Fisher criterion

$$F_{exp} = 1.84 \qquad F_{21,21} = 2.08 \text{ at } \alpha = 0.95$$

shows that both equations are statistically equal, but eqn. 7 with its Δ_{max} about 2 i.u. is adequate considering the experimental repeatability.

In terms of the number of parameters, eqn. 3 is considered more suitable because less pure compounds are necessary for the calculation of the equation constants. We shall show this with an example. Considering only four alkyl halides, namely ethyliodide, butyl chloride, butyl bromide and hexyl iodide, and a sample the chromatogram of which consists of 21 peaks. After chromatographing the standards under the same conditions as those for the sample, we obtain the retention indices. Using these values, the following regression equation is obtained:

$$I_{calc.} = 152.26 + 77.54346n + 1.88638M_m \quad (8)$$

Applying this equation to the experimental I values of the sample, it is possible to

TABLE III

COMPARISON OF $I_{exp.}$ WITH $I_{calc.}$ ACCORDING TO EQN. 8 AND VERIFICATION OF THE TENTATIVE IDENTIFICATION BY $I_{calc.}$ ACCORDING TO THE NEWLY OBTAINED CONSTANTS FOR EQN. 7

No.	*Peak* $I_{exp.}$	$I_{calc.}$, *eqn. 8*	*Expected compound*	$I_{calc.}$, *new eqn. 7*	*Identified compound*
1	432	429	–	431.1	C_2H_5Cl
2	514	512.9	C_2H_5Br	513.7	C_2H_5Br
3	534	533	C_3H_7Cl	535.8	C_3H_7Cl
4	602 (standard)	601.6	C_2H_5I	602.2	C_2H_5I
5	618	616.9	C_3H_7Br	616.5	C_3H_7Br
6	638 (standard)	637.0	C_4H_9Cl	638.8	C_4H_9Cl
7	705	705.6	C_3H_7I	705.8	C_3H_7I
8	719 (standard)	720.9	C_4H_9Br	719.5	C_4H_9Br
9	742	741.0	$C_5H_{11}Cl$	741.6	$C_5H_{11}Cl$
10	809	809.6	C_4H_9I	809.3	C_4H_9I
11	822	824.9	–	822.7	$C_5H_{11}Br$
12	845	845.0	$C_6H_{13}Cl$	844.3	$C_6H_{13}Cl$
13	926	928.9	–	926.1	$C_6H_{13}Br$
14	949	949.0	$C_7H_{15}Cl$	947.3	$C_7H_{15}Cl$
15	1018 (standard)	1017.5	$C_6H_{13}I$	1017.1	$C_6H_{13}I$
16	1030	1032.9	–	1029.7	$C_7H_{13}Br$
17	1051	1053.0	$C_8H_{17}Cl$	1050.5	$C_8H_{17}Cl$
18	1122	1121.6	$C_7H_{15}I$	1121.2	$C_7H_{15}I$
19	1133	1136.9	–	1133.5	$C_8H_{17}Br$
20	1152	1157.0	–	1153.9	$C_9H_{19}Cl$
21	1225	1225.5	$C_8H_{17}I$	1225.4	$C_8H_{17}I$

identify 14 compounds (about 66% of the peaks) with the same reliability as if standard substances had been used. The discrepancies are in the limits of repeatability of $\pm$ 2 i.u. (see Table III). Now using all 14 data (instead of only the 4), new constants of eqn. 7 are recalculated. The new $I_{calc.}$ values are given in Table III too. It is noteworthy that the tentative identification of the 14 peaks is confirmed and that all the remaining peaks are identified within the same limit of $\pm$ 2 i.u.

To check eqn. 3, we transferred the experimental data published for alkyl chlorides[4] and those published for alkyl bromides[21] into one regression matrix. The following equation is obtained

$$I_{calc.} = 151.23 + 57.6037n + 3.60467M_m \quad (9)$$

with $r = 0.999932$, S.D. = 1.97 and $\Delta_{max} = 2.7$ i.u. Evidently, when the experimental results are reliable, even though from different sources, they can be handled together.

Eqn. 3 allows one to overcome the lack of all necessary pure standard compounds. Only a limited number of halides, irrespective of the halogen, satisfies the calculation demand. The reliability of the calculative identification is comparable with those obtained with standard substances.

REFERENCES

1 E. sz. Kováts, *Helv. Chim. Acta*, 41 (1958) 1915.
2 G. Niendrop and C. de Ligny, *J. Chromatogr.*, 154 (1978) 133.
3 O. Buchman, G.-Y. Cao and C. T. Peng, *J. Chromatogr.*, 312 (1984) 75.
4 F. Morishita, Y. Terashima, M. Ichise and T. Kojima, *J. Chromatogr. Sci.*, 21 (1983) 209.
5 N. Zakirov, *Zh. Anal. Khim.*, 35 (1980) 725.
6 G. Castello and G. D'Amato, *J. Chromatogr.*, 324 (1985) 363.
7 J. E. Premecz and M. E. Ford, *J. Chromatogr.*, 388 (1987) 23.
8 H. Lamparczyk, *Chromatographia*, 17 (1983) 664.
9 T. S. Calixto and A. Garsia-Raso, *Int. J. Environ. Anal. Chem.*, 17 (1984) 279.
10 J. Bermejo and M. Guillen, *J. High Resolut. Chromatogr. Chromatogr. Commun.*, 7 (1984) 191.
11 P. Buryan and J. Macák, *J. Chromatogr.*, 237 (1982) 381.
12 A. Sabljić, *J. Chromatogr.*, 314 (1984) 1.
13 G. Castello and T. C. Gerbino, *J. Chromatogr.*, 366 (1986) 59.
14 R. Kalishan, *CRC*, 16 (1986) 323.
15 G. Castello and T. Gerbino, *J. Chromatogr.*, 437 (1988) 33.
16 N. Dimov, *Anal. Chim. Acta*, 201 (1987) 217.
17 R. Golovnya and O. Grigoryeva, *Zh. Anal. Khim.*, 40 (1985) 316.
18 R. Golovnya, *J. Chromatogr.*, 364 (1986) 193.
19 O. Grigoryeva, R. Golovnya, T. Misharina and A. F. Aerov, *J. Chromatogr.*, 364 (1986) 63.
20 L. Soják, J. Ruman and J. Janák, *J. Chromatogr.*, 391 (1987) 79.
21 C. Landault and G. Guiochon, *J. Chromatogr.*, 13 (1964) 327.

Journal of Chromatography, 463 (1989) 165–170
Elsevier Science Publishers B.V., Amsterdam — Printed in The Netherlands

CHROM. 21 094

Note

Size-exclusion chromatography of cationic polyelectrolytes on Superose gel

MARK A. STREGE and PAUL L. DUBIN*

Department of Chemistry, Indiana University–Purdue University at Indianapolis, Indianapolis, IN 46227 (U.S.A.)

(First received July 22nd, 1988; revised manuscript received November 9th, 1988)

The surfaces of stationary phases used in aqueous size-exclusion chromatography (SEC) often contain polar functional groups which may interact with the macromolecules being chromatographed, leading to elution volumes different from those expected on the basis of size alone. Electrostatic adsorption and exclusion effects are prominent in aqueous chromatography because ionic groups are present in most aqueous SEC packings[1]. Hydrophobic interactions of amphiphilic substances with gel matrices can also occur, and these have been investigated by several workers[2–4].

Because most stationary phases for aqueous SEC bear a negative charge[1], substrate–macromolecule interactions have been especially problematic for polycations, often leading to irreversible adsorption. Such polyelectrolytes are valuable industrial chemicals in areas which involve flocculation, such as water clarification, sewage sludge dewatering and paper processing. Since the molecular weight distribution of polymers plays a central role in these applications, the availability of high-efficiency SEC columns for polycations has major consequences for these technologies.

Several groups have investigated derivatized silica-based packings for SEC of polycations. Talley and Bowman[5] grafted porous silica beads with reagents bearing quaternary ammonium groups and successfully chromatographed poly(2-vinylpyridine) in acidic media. A similar type of packing was investigated by Domard and Rinaudo[6] who observed universal calibration in 0.2 *M* ammonium acetate, indicating that this ionic strength was sufficient to eliminate electrostatic exclusion. A silica-based stationary phase, Fractosil (E. Merck, Darmstadt F.R.G.), was derivatized with dimethylaminoethanol (DMAE) by Stickler and Eisenbeiss[7]. Low-pH conditions provided by 0.1 *M* nitric acid in the eluent were utilized to protonate residual aminosilane groups and to keep any unsilanized hydroxyl groups in the uncharged state. A solvent ionic strength of 0.1 *M* was sufficient to suppress strong coulombic repulsive effects. However, the common calibration standards, dextran and poly(ethyleneoxide) (PEO), were found to adsorb onto the packing, thus requiring calibration using samples of the analyte itself. In addition, these three packings are still sensitive to ionic effects, and, at any rate, are not commercially available.

It is apparent that the use of quaternarized silica-based packings for SEC of polycations has limitations. The intense charge density of cationic bonded phases can exclude cationic polymers from the pores, and the high ionic strengths needed to

0021-9673/89/$03.50

suppress these effects may limit polyion solubility. Also, non-derivatized silanol groups present on the packing appear to be active, as evidenced by the adsorption of non-ionic hydrogen-bond acceptor polymers such as PEO.

Limited studies suggest that the goal of efficient and non-adsorptive SEC of polycations may be better met with organic hydrophilic gels than with derivatized silica. The problems of ionic exclusion and interactions with underivatized silanol groups are not encountered with semi-rigid neutral polymeric gels. Thus, characterization of cationic polymers has been accomplished with the hydrophilic cross-linked polyether PW gel packings[8,9]. Universal calibration studies revealed that ionic effects could be controlled using mobile phases of moderate ionic strength, such as 0.2 *M* sodium chloride[10]. However, even modest reduction in ionic strength led to retention of polycations because of the presence of residual carboxylic acid groups on the packing[11]. It is also important to note that PW gel displays strong hydrophobic interactions with amphilic solutes[12].

Superose (Pharmacia) is a cross-linked, agarose-based medium, recently developed for high-performance gel filtration of biomolecules. While small concentrations of sulfate and carboxylic groups are inherent in agarose, chromatographic studies with proteins and nucleic acids revealed that 0.15 *M* sodium chloride in the mobile phase suppresses ionic interactions between the charged macromolecules and anionic sites on the packing[13].

The current report describes the chromatography of cationic polymers on a commercially available Superose gel column used extensively in high-speed SEC of biomolecules. An aqueous mobile phase of low pH and moderate ionic strength was employed to reduce the adsorption of the solute molecules.

EXPERIMENTAL

Four types of synthetic cationic polymers were studied. Poly(dimethyldiallylammonium chloride) (PDMDAAC) was obtained from Calgon (Pittsburgh, PA, U.S.A.), with nominal molecular weigths of $1 \cdot 10^4$, $3 \cdot 10^4$, $5 \cdot 10^4$, $2 \cdot 10^5$ and $1.5 \cdot 10^6$. Poly(methacrylamidopropyltrimethylammonium chloride) (PMAPTAC) samples, donated by Clairol Research Laboratory (Stamford, CT, U.S.A.), had nominal average molecular weights of $5 \cdot 10^4$, $8.7 \cdot 10^4$, $2 \cdot 10^5$ and $4.3 \cdot 10^5$. Samples of poly(ethyleneimine) (PEI) with average molecular weights of $7 \cdot 10^3$ and $5 \cdot 10^4$ were from Polysciences (Warrington, PA, U.S.A.).

Exclusion chromatography was carried out on an apparatus comprised of a Minipump (Milton Roy), a Model 7012 injector (Rheodyne) equipped with a 100-μl loop, and an R401 differential refractometer (Waters). A Superose-6 column (30 cm × 1 cm O.D.) (Pharmacia) was eluted at 0.52 ml/min.. Column efficiency, determined with ^2H_2O, was at least 12 000 plates per meter.

The selection of mobile phase was based on previous studies utilizing a variable size simplex method[14]. Two variables, the mobile phase pH and ionic strength, were altered simultaneously until separations of proteins exhibited near-ideal behavior. The optimum solvent conditions of pH 5.5 and an ionic strength of 0.38 phosphate buffer were thus determined for SEC of proteins on Superose gel[15]. In this work, 0.4 *M* of sodium chloride–sodium acetate (9:1), (pH 5.5) was employed as the mobile phase. Sodium chloride and sodium acetate were substituted for phosphate because

polycations may precipitate during long-term storage in phosphate buffer, a phenomenon not observed with sodium acetate.

Polymers were dissolved in the mobile phase and filtered (0.20 μm Millipore). The concentration of polymer injected onto the column was approximately 0.3% (w/w), corresponding to a refractive index detector attenuation of 8 ×.

RESULTS AND DISCUSSION

The results of this investigation provide evidence for the non-adsorptive SEC of polycations using Superose gel packing. The chromatograms of PDMDAAC samples are shown in Fig. 1. While it is evident that the polymers are highly polydisperse, the distorted elution profiles characteristic of adsorbed polymers are not observed in these chromatograms. The peak at the high-molecular-weight end, for the two highest-molecular-weight samples, corresponds to the exclusion volume of the column, while the small peak near the low-molecular-weight end of the chromatograms arises from the presence of monomer. The high resolution of these chromatograms is also inconsistent with adsorption.

Adsorptive effects result in elution volumes greater than expected from size exclusion alone. Thus, adsorption vitiates the chromatographic preparation of molecular-weight fractions. Eleven 1-ml fractions were collected during the elution of the $3 \cdot 10^4$ mol.wt. PDMDAAC sample, and four of these fractions were reinjected, with the results shown in Fig. 2. These reinjected samples were found to possess elution volumes identical to the fractionation volumes, which is consistent with separation by molecular weight.

The absence of adsorption effects may be substantiated by demonstrating universal calibration for polymers with widely varying composition and charge state, because uniform dependence of elution volume on $J \equiv [\eta]M$ (where $[\eta]$ = intrinsic

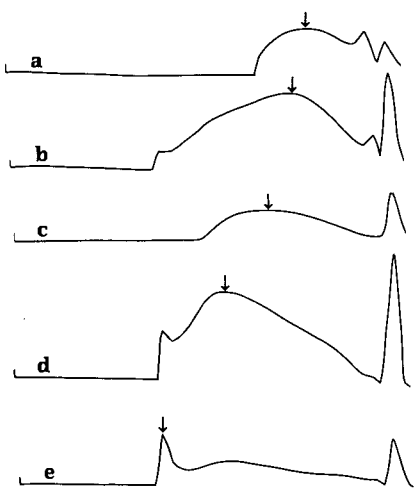

Fig. 1. Chromatograms of PDMDAAC with nominal molecular weight values: (a) $1 \cdot 10^4$; (b) $3 \cdot 10^4$; (c) $5 \cdot 10^4$; (d) $2 \cdot 10^5$; (e) $1.5 \cdot 10^6$. Peak at low-molecular-weight end is salt imbalance peak. Peak elution volumes are indicated by arrows.

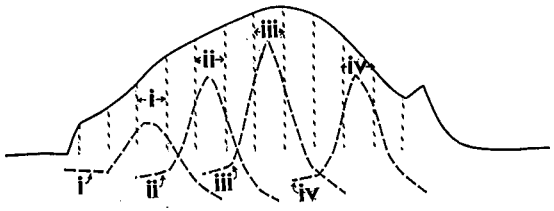

Fig. 2. Fractionation of PDMDAAC with a molecular weight of $3 \cdot 10^4$.

viscosity and M = molecular weight) only occurs if peak migration depends on molecular dimensions alone. For the highly polydisperse polycations of this investigation, universal calibration demands significant data manipulation[16]. Plotting J as a function of peak elution volume in the usual manner neglects differences between the molecular weight of the component eluting at the chromatographic peak (M_p) and the two moments of the distribution that correspond, respectively, to the measured values of $[\eta]$ and M. Thus, the difficulty of assigning a value of J to the species eluting at the chromatographic peak reduces the usefulness of peak elution volumes. Without undertaking the imposing treatment required for universal calibration, we still find evidence for the absence of adsorption effects from comparisons of peak retention volumes and reported molecular weight values.

Calibration plots of molecular weight *vs.* peak elution volume (V_e) are displayed in Fig. 3. Molecular weight values corresponding to the chromatographic peaks of the PDMDAAC samples were obtained by SEC–low-angle laser-light scattering as $2.5 \cdot 10^4$, $2.9 \cdot 10^5$ and $4.3 \cdot 10^5$ for nominal molecular weight values of $1.0 \cdot$

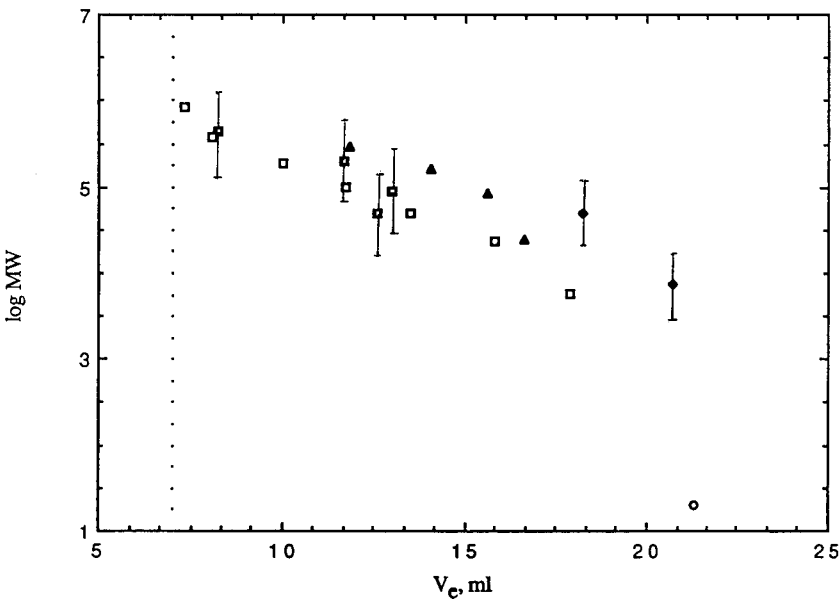

Fig. 3. Dependence of peak elution volume on nominal molecular weight (MW): □ = pullulan; ▲ = PDMDDAC; ■ = PMAPTAC; ◆ = PEI; ○ = ^2H_2O. Dotted line is the column exclusion volume from the elution of blue dextran.

10^4, $2.0 \cdot 10^5$ and $1.5 \cdot 10^6$, respectively[17]. The M_p values of the $3.0 \cdot 10^4$ and $5.0 \cdot 10^5$ samples were interpolated from their elution volumes as $8.5 \cdot 10^4$ and $1.6 \cdot 10^5$. For all other samples, the vertical bars represent the expected maximum difference between the nominal molecular weight and M_p.

In addition to the discrepancy between nominal molecular weight and M_p, the calibration curves for the different polymers would be expected to diverge because of differences in hydrodynamic volumes, *i.e.* J at constant M. Utilizing the relationship of $J = KM^{1+a}$, and literature values for the Mark–Houwink constants in the equation $[\eta] = KM^a$, for pullulan ($K = 1.79 \cdot 10^{-4}$dl/g, $a = 0.67$)[18] and for PDMDAAC ($K = 5.0 \cdot 10^{-5}$dl/g, $a = 0.72$)[19] in 0.4 M ionic strength solvents, the size differences between the two molecular species at various molecular weight values may be calculated. This analysis shows that, as constant J, $M_{PDMDAAC} \cong 2 \cdot M_{Pullulan}$, in close agreement with the typical separation of the data points for these two polymers in Fig. 3. Deviations among the calibration curves in excess of the amount expected would suggest adsorption. Instead, Fig. 3 reveals that divergence of the data for PDMDAAC, PMAPTAC and pullulan are within the range expected from considerations of size differences.

The large elution volumes associated with PEI may be due to the structure of the polycation: the extensive branching of PEI results in a greater degree of compactness. Less anomolous behavior of PEI in a methanol–water mobile phase would support these speculations.

CONCLUSION

Superose gel columns may be used for SEC analysis of polycations. Under appropriate ionic strength conditions, elution curves reveal no adsorptive effects for strongly cationic polymers.

REFERENCES

1 P. L. Dubin, in P. L. Dubin (Editor), *Aqueous Size Exclusion Chromatography*, Elsevier, Amsterdam, 1988, Ch. 3.
2 K. Ujimoto and H. Kurihara, *J. Chromatogr.*, 208 (1981) 183.
3 R. P. Bywater and N. V. B. Marsden, in E. Heftmann (Editor), *Chromatography, Fundamentals and Applications of Chromatographic and Electrophoretic Methods*, Part A, Elsevier, Amsterdam, 1983, Ch. 8.
4 M. Janado, in P. L. Dubin (Editor), *Aqueous Size Exclusion Chromatography*, Elsevier, Amsterdam, 1988, Ch. 2.
5 C. P. Talley and L. M. Bowman, *Anal. Chem.*, 13 (1979) 2239–2242.
6 A. Domard and M. Rinaudo, *Polym. Commun.*, 25 (1984) 55–58.
7 M. Stickler and F. Eisenbeiss, *Eur. Polym. J.*, 20 (1984) 849–853.
8 L. Hashimoto and Y. Kato, *J. Chromatogr.*, 235 (1982) 539–543.
9 P. L. Dubin and I. J. Levy, *I&EC Prod. Res. Dev.*, 21 (1982) 59–63.
10 P. L. Dubin and I. J. Levy, *J. Chromatogr.*, 235 (1982) 377–387.
11 H. Sasaki, T. Matsuda, O. Ishikawa, T. Takamatsu, K. Tanaka, Y. Kato and T. Hashimoto, *Sci. Rep. Toyo Soda Manuf. Co., Ltd.*, 29 (1985).
12 P. L. Dubin, I. J. Levy and R. Oteri, *J. Chromatogr. Sci.*, 22 (1984) 432.
13 J. Andersson, M. Carlsson, L. Hagel, P.-Å. Pernemalm and J.-C. Janson, *J. Chromatogr.*, 326 (1985) 33–44.
14 C. L. Shavers, M. L. Parsons and S. N. Deming, *J. Chem. Educ.*, 56 (1979) 307.
15 J. M. Principi, *Thesis*, Purdue University, Indianapolis, IN, 1988.

16 P. L. Dubin, K. L. Wright and S. W. Koontz, *J. Polym. Sci., Polym. Chem. Ed.*, 15 (1977) 2047.
17 F. M. Lin, Calgon Corp., personal communication.
18 T. Kato, T. Tokuya and A. Takahashi, *J. Chromatogr.*, 256 (1983) 61–69.
19 S. Maxim, E. Dumitriu, S. Ioan and A. Carpov, *Eur.Polym. J.*, 13 (1977) 105–108.

Journal of Chromatography, 463 (1989) 171–176
Elsevier Science Publishers B.V., Amsterdam — Printed in The Netherlands

CHROM. 21 106

Note

Application of metal β-diketonate polymers as selective sorbents in complex mixture analysis and for sulfur-containing compounds

THOMAS J. WENZEL*, PHILIP J. BONASIA and THOMAS BREWITT
Department of Chemistry, Bates College, Lewiston, ME 04240 (U.S.A.)
(First received September 7th, 1988; revised manuscript received November 14th, 1988)

The number of volatile constituents in most environmental and biological samples precludes the ability to completely resolve all of the components using gas chromatography (GC). Computer methods are available for deconvoluting overlapping peaks in the chromatogram[1–3]. An alternative approach is to simplify the chromatogram through the use of one or more selective sorbents. Any material that can selectively retain certain compounds from a gaseous mixture, while allowing other compounds to pass through unretained, can serve as a selective sorbent for GC. It is desirable to utilize selective sorbents that exhibit adsorption that is reversible with temperature[4–8]. In this case, the sorbent need only be heated to remove adsorbed compounds.

In a previous report, metal β-diketonate polymers of Ni(II), Cu(II), Zn(II) and La(III) were evaluated as selective sorbents for GC[8]. The ligands used to prepare the metal complexes are bis-β-diketones of structure I. The orientation of the β-diketone

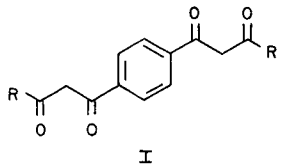

I

R	
$-C_6H_5$	H_2(ppb)
$-CH_3$	H_2(pbb)
$-CF_3$	H_2(ptb)
$-C_3F_7$	H_2(dihed)

units on the aromatic ring are such that polymeric materials result from the synthesis of metal complexes. The polymers are non-volatile and most are thermally stable. The metal ions in the polymers are coordinatively unsaturated and can form adduct complexes with suitable Lewis bases. The equilibrium constant for adduct formation depends on electronic and steric effects of the donor, the identity of the metal ion, the substituent group of the ligand, and temperature[8].

La(III) and Ni(II) exhibited the greatest retention of oxygen- and nitrogen-containing compounds, Zn(II) and Cu(II) the least. Polymers with the C_3F_7 substituent group, the most electron withdrawing of those studied, exhibited the greatest

* On leave, in 1989 at the Department of Chemistry, Paul Gross Laboratory, Duke University, Durham, NC 27706, U.S.A.

0021-9673/89/$03.50

retention of oxygen- and nitrogen-containing compounds. Polymers with the C_6H_5 substituent group exhibited the least retention. The following series of four sorbents was identified as that which offered the widest degree of selectivity with regard to retention of hard Lewis bases: Zn(ppb) > Cu(dihed) > La(pbb) > La(dihed).

In this report we demonstrate the application of this series of four sorbents in the analysis of complex mixtures. The sorbent series can be used to divide a mixture with one complex chromatogram into five simpler chromatograms. The use of Ag(I) and Ni(II) bis-β-diketonates as sorbents for sulfur-containing compounds is also described.

EXPERIMENTAL

Preparation of Ag_2(dihed)

The ligand H_2(dihed) was synthesized as previously described[4]. The complex with silver was prepared by a modification of a literature method[9]. To 1 g (0.0018 mol) of H_2(dihed) dissolved in 40 ml of methanol 0.9 ml of 4 *M* sodium hydroxide (0.0036 mol) was added. The solution was stirred vigorously and a solution of silver nitrate (0.61 g, 0.0036 mol) in 20 ml of distilled water was added. The resulting mixture was stirred for 30 min after which the brown solid was collected by suction filtration. The solid was dried for 24 h *in vacuo* over P_4O_{10}. The material decomposed over the range from 156 to 180°C. Anal. calc. for $Ag_2C_{18}H_6O_4F_{14}$: C, 28.15; H, 0.79. Found: C, 27.76; H, 0.99.

Preparation of pre-columns containing the metal polymers

Pre-columns containing the La(dihed), La(pbb), Cu(dihed), Ni(dihed), Ni(ppb) and Zn(ppb) polymers were prepared as previously described[8]. A pre-column containing Ag_2(dihed) was prepared using an analogous procedure. Gas Chrom Z 80–100 mesh (Applied Science) was first coated with a layer of 3% SE-30. A 3% loading of the Ag_2(dihed) was then applied. The metal complex was dissolved in methanol for the coating step. Since silver β-diketonates are slightly light sensitive, all glassware employed in the manipulations of the silver complex were covered with aluminum foil. The coated support was packed into a 25 cm × 2.2 mm I.D. pre-column (Valco). The sorbent was conditioned at 140°C under a flow of nitrogen gas for 30 min.

Apparatus and procedures

The valve system with sorbent pre-columns and gas chromatograph were as previously described[8]. Chromatograms were run on a 25-m cross-linked 5% phenyl methyl silicone fused-silica capillary column (Hewlett-Packard) at a flow-rate of 1 ml/min. Nitrogen was employed as the carrier gas. Procedures for employing and testing the sorbents were as previously described[8].

Samples of cigarette smoke were obtained by drawing smoke for a set period of time (usually 5 s) from the end of a cigarette through a trap containing Tenax GC. The volatile constituents of urine were obtained by placing 90 ml of urine in a three-necked flask fitted with helium inlet, thermometer and reflux condenser. The outlet of the reflux condenser was adapted to accommodate a sorbent containing Tenax GC. The sample was stirred and maintained at 67–70°C for 1 h. During this time the head space in the flask was continually swept with helium (30 ml/min).

RESULTS AND DISCUSSION

The utility of the sorbent series in the analysis of complex mixtures was demonstrated with cigarette smoke and urine. The results with cigarette smoke are shown in Fig. 1. Fig. 1a is the chromatogram of those compounds retained by Zn(ppb). The compounds unretained by the Zn(pbb) were then passed through a sorbent containing Cu(dihed). The chromatograms in Fig. 1b–d are of those compounds retained by the Cu(dihed), La(ppb) and La(dihed) sorbents respectively. The chromatogram in Fig. 1e is for those compounds unretained by the series of sorbents.

One trend in the series of chromatograms is that the compounds retained by each sorbent tend to cluster according to volatility. The majority of the compounds retained by Zn(ppb) are in the latter part of the chromatogram, and are therefore the less volatile Lewis bases in the sample. The peak shapes for early eluting compounds in this chromatogram exhibit tailing, which is indicative of highly polar compounds such as amines or alcohols. These two classes of compounds exhibit large association constants with metal β-diketonate complexes[8,10,11], and it is not surprising that they might be retained on the most selective sorbent of the series. A general progression

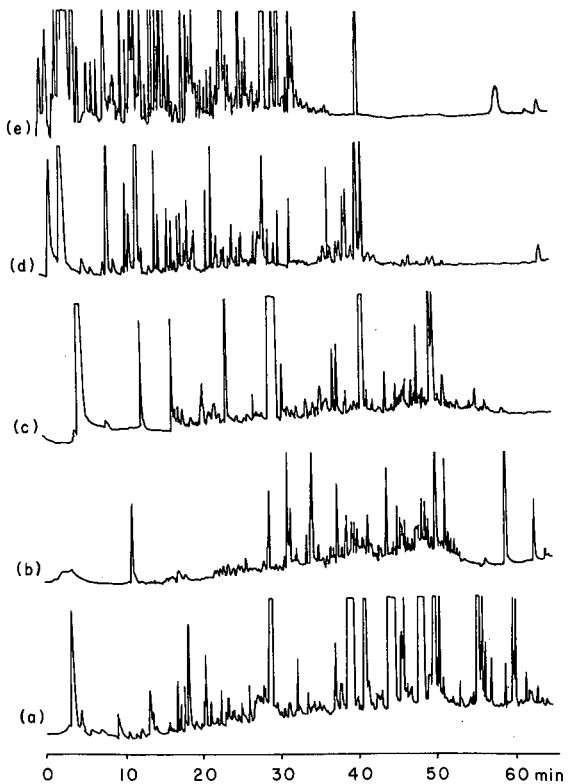

Fig. 1. Chromatograms of the volatile constituents of cigarette smoke (a) retained by Zn(ppb) at 100°C, (b) retained by Cu(dihed) at 100°C, (c) retained by La(pbb) at 100°C, (d) retained by La(dihed) at 100°C, and (e) unretained. Thermally focussed at −50°C for 5 min and then 3°C/min to 150°C. See Experimental section for column and sorbent description.

from less to more volatile constituents is observed for the chromatograms of the compounds retained by Cu(dihed), La(pbb) and La(dihed). The compounds unretained by the sorbent series elute in the earlier portion of the chromatogram and are therefore the more volatile components of the sample. The chromatograms obtained for cigarette smoke using the sorbent series were reproducible over a six-week period of analysis. Furthermore, the intensities of the peaks in the individual chromatograms were directly dependent upon the sampling time, and hence sample size.

The chromatograms obtained for the volatile constituents of urine are shown in Fig. 2. Although not as pronounced as with cigarette smoke, a general trend in the volatilities of the compounds retained by each sorbent is observed. The use of this four-sorbent series allows for the conversion of one complex chromatogram into five simpler chromatograms. Alternatively, the analysis of certain "target" compounds is facilitated. In the latter case, one need only analyze the sorbent, or sorbents, on which the target compounds are retained. All other fractions can be vented without analysis. Sorbents have been used for periods of several months with no observed change in performance.

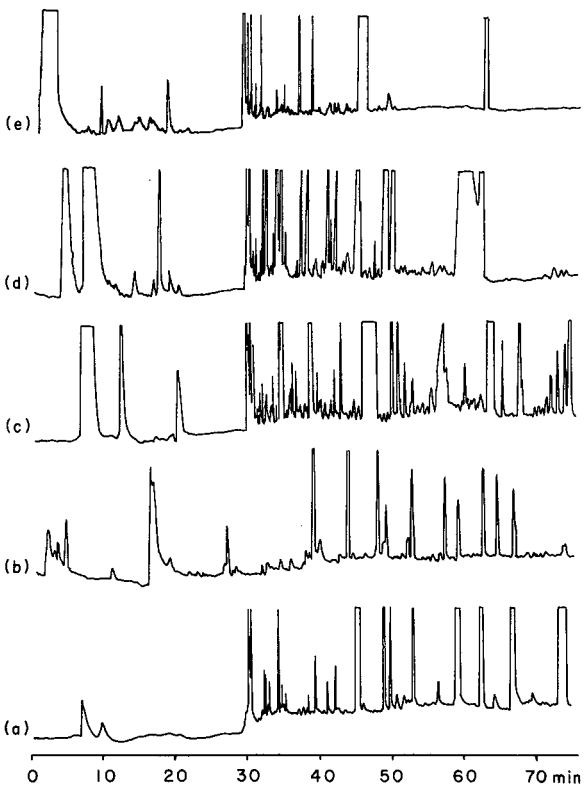

Fig. 2. Chromatograms of the volatile constituents of urine (a) retained by Zn(ppb) at 100°C, (b) retained by Cu(dihed) at 100°C, (c) retained by La(pbb) at 100°C, (d) retained by La(dihed) at 100°C, and (e) unretained. Thermally focussed at −50°C for five min and then 2°C/min to 100°C. See Experimental section for column and sorbent description.

Sorbent studies on sulfur-containing compounds:

The complexes Ag_2(dihed), Ni(dihed) and Ni(pbb) were tested for their ability to retain sulfur-containing compounds. Ag(I)[12] and nickel β-diketonates[13] are known to form adduct complexes with sulfur-containing compounds. Sulfur-containing compounds such as methanethiol can be selectively adsorbed on mercury salts such as mercuric acetate[14]. Removal of the thiol requires treatment with hydrochloric acid followed by extraction into an organic solvent. General sorbents such as Tenax GC and XAD resins have also been evaluated for their ability to retain sulfur-containing compounds[15]. Thiophene, tetrahydrothiophene, di-*n*-butyl sulfide and straight-chain thiols (C_5–C_8) were used as model substrates to test the sorbent properties of the metal β-diketonate polymers.

At 100°C, thiophene was not retained by any of the sorbents. This is not surprising since the conjugated ring system in thiophene is expected to reduce the basicity of the sulfur atom, much the same as is observed with furan and tetrahydrofuran[4,16]. All of the other compounds were completely retained by Ag_2(dihed) and Ni(dihed) at 100°C. The retention of these compounds by Ag_2(dihed), however, was irreversible at desorption temperatures of 130 and 140°C. This irreversible adsorption may well be the result of strong complexation between silver and sulfur-containing compounds[12]. A temperature of 140°C was judged as the upper limit for Ag_2(dihed) because of the decomposition that starts to occur at about 156°C. The retention of tetrahydrothiophene, di-*n*-butyl sulfide, and the straight chain thiols by Ni(dihed) was irreversible at desorption temperatures of 150°C. At 170°C, only tetrahydrothiophene was desorbed from Ni(dihed).

At 100°C, Ni(pbb) exhibited partial retention of tetrahydrothiophene (98%) and di-*n*-butyl sulfide (66%), and complete retention of the straight chain thiols. Tetrahydrothiophene, di-*n*-butyl sulfide and the C_5 thiol were succesfully desorbed at 150°C, whereas the C_6–C_8 thiols were not. The C_6–C_8 thiols were desorbed, however, at 170°C. The recovery of the sulfur-containing compounds from Ni(pbb) was assessed by comparing the integrated areas of the peaks in the chromatogram of the retained compounds to those obtained in the direct injection of the same sample. For each compound, the areas were essentially identical and complete recovery was indicated. Of the sorbents we tested, Ni(pbb), by virtue of its reversible adsorption, appears to be the best choice for sulfur-containing compounds.

ACKNOWLEDGEMENTS

We would like to thank the Petroleum Research Fund and the National Science Foundation (Two- and Four-Year College Science Instrumentation Program) for supporting this work.

REFERENCES

1 G. H. Rayborn, G. M. Wood, Jr., B. T. Upchurch and S. J. Howard, *Am. Lab. (Fairfield, Conn.)*, 18 (1986) 56.
2 S. C. Gates, M. J. Smisko, C. L. Ashendel, N. D. Young, J. F. Holland and C. C. Sweeley, *Anal. Chem.*, 50 (1978) 433.
3 R. G. Dromey, M. J. Stefik, T. C. Rindfleisch and A. M. Duffield, *Anal. Chem.*, 48 (1976) 1368.
4 J. E. Picker and R. E. Sievers, *J. Chromatogr.*, 203 (1981) 29.

5 J. E. Picker and R. E. Sievers, *J. Chromatogr.*, 217 (1981) 275.
6 E. G. Boeren, R. Beijersbergen van Henegouwen, I. Bos and T. H. Gerner, *J. Chromatogr.*, 349 (1985) 377.
7 E. J. Williams and R. E. Sievers, *Anal. Chem.*, 56 (1984) 2523.
8 T. J. Wenzel, L. W. Yarmaloff, L. Y. St. Cyr., L. J. O'Meara, M. Donatelli and R. W. Bauer, *J. Chromatogr.*, 396 (1987) 51.
9 T. J. Wenzel and R. E. Sievers, *Anal. Chem.*, 53 (1981) 393.
10 J. K. M. Sanders and D. H. Williams, *J. Am. Chem. Soc.*,93 (1971) 641.
11 R. T. Pflaum and L. E. Cook, *J. Chromatogr.*, 50 (1970) 120.
12 H. Sigel, K. H. Scheller, V. M. Rheinberger and B. E. Fischer, *J. Chem. Soc., Dalton Trans.*, (1980) 1022.
13 V. Schurig and W. Burkle, *J. Am. Chem. Soc.*, 104 (1982) 7573.
14 R. Knarr and S. M. Rappaport, *Anal. Chem.*, 52 (1980) 733.
15 A. Przyjazny, *J. Chromatogr.*, 333 (1985) 327.
16 R. E. Rondeau and R. E. Sievers, *Anal. Chem.*, 45 (1973) 2145.

Journal of Chromatography, 463 (1989) 177–182
Elsevier Science Publishers B.V., Amsterdam — Printed in The Netherlands

CHROM. 21 015

Note

A post-column immobilized leucine dehydrogenase reactor for determination of branched chain amino acids by high-performance liquid chromatography with fluorescence detection

NOBUTOSHI KIBA*, SACHIE HORI and MOTOHISA FURUSAWA
Department of Chemistry, Faculty of Engineering, Yamanashi University, Kofu 400 (Japan)
(First received July 4th, 1988; revised manuscript received September 27th, 1988)

Several cases of inborn errors of metabolism of branched chain amino acids (BCAAs) are known[1]. Usually, BCAAs are separated and quantitated by chromatographic procedures[2–8]. Post-column derivatization with ninhydrin, fluoresamine or *o*-phthalaldehyde is still the standard technique for amino acid analysis[9]. This paper describes a post-column reactor system for the high-performance liquid chromatographic (HPLC) determination of BCAA. The BCAAs from the separation column are mixed with a nicotinamide–adenine dinucleotide (NAD) solution and oxidized in a reactor containing immobilized leucine dehydrogenase (E.C. 1.4.1.9) (LDH). NAD is reduced to NADH according to the amount of BCAAs present in the solution. The NADH is monitored by fluorescence detection.

EXPERIMENTAL

Chemicals

Leucine dehydrogenase (38 U/mg of solid) was obtained from Toyobo (Osaka, Japan). Poly(vinyl alcohol) beads (9 μm, GS-520) were obtained from Asahi Kasei (Tokyo, Japan). NAD (grade II) was obtained from Boehringer Mannheim (Mannheim, F.R.G.). Capcell-C_{18} (10 μm) (Shiseido, Tokyo, Japan) and TSKgel SCX (5 μm) (Tosoh, Tokyo, Japan) were packed into stainless-steel columns of 250 mm × 4.6 mm and 300 mm × 7.8 mm, respectively, by the slurry-packing method. All other chemicals were of analytical grade.

For reversed-phase chromatography, the mobile phase was 25 m*M* sodium dihydrogenphosphate containing 0.5 m*M* Na_4EDTA. For ion-exchange chromatography, citrate buffer (pH 3.7) was used as the mobile phase and column temperature was kept at 60°C.

Immobilization of LDH

The method of epoxy activation and amination of the beads was similar to that of Matsumoto *et al.*[10]. The attached amine was measured by the Kjeldahl method[11] and amounted to 4.1 mequiv. per g of dry beads. The aminated beads were packed into a stainless-steel column (10 mm × 4 mm I.D.) by the dry-packing method. Glutaraldehyde solution (2.5%) in phosphate buffer (0.05 *M*, pH 7.0) was pumped

0021-9673/89/$03.50

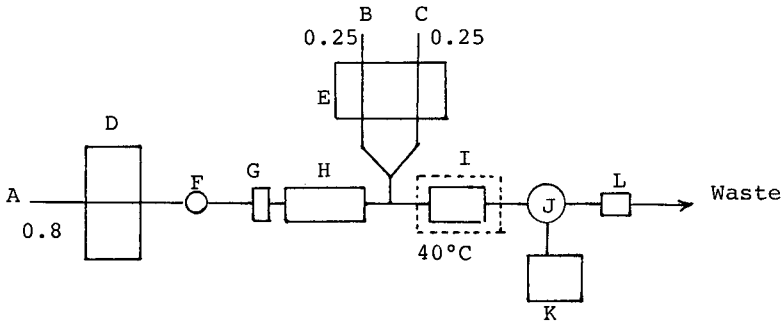

Fig. 1. An HPLC system for determination of valine, isoleucine and leucine with an immobilized leucine dehydrogenase reactor. A = Mobile phase (25 m*M* potassium dihydrogenphosphate + 0.5 m*M* Na_4EDTA); B = buffer (0.4 *M* glycine–potassium chloride/potassium hydroxide, pH 10.8 at 40°C); C = 35 m*M* NAD solution; D = HPLC pump; E = reagent pump; F = injector with 60-μl loop; G = precolumn (10 mm × 4.6 mm); H = analytical column (250 mm × 4.6 mm, Capcell-C_{18}); I = immobilized enzyme column reactor (10 mm × 4.0 mm); J = fluorescence spectrophotometer with a flow cell (18 μl); K = data processor; L = back pressure regulator. The column reactor was thermostatted at 40°C. The numbers given are flow-rates in ml/min.

through the column for 1 h at 0.1 ml/min and the column was washed with deaerated water for 20 min at 0.3 ml/min. The enzyme solution [5 mg in 10 ml of 0.05 *M* phosphate buffer (pH 7.0)] was circulated through the column at 0.1 ml/min for 3 h at room temperature. The enzyme solution was kept at about 4°C throughout the immobilization procedure.

HPLC system

The liquid chromatographic system is shown in Fig. 1. It consisted of a Bip 1 mobile phase pump (JASCO, Tokyo, Japan), a Rheodyne 7125 injector with 60-μl loop, a 1.0 cm × 4.6 mm I.D. stainless-steel precolumn, dry-packed with TSKgel ODS-120T (Tosoh), the separation column containing Capcell-C_{18} (250 mm × 4.6 mm), a double plunger KHU-W-52 reagent pump (Kyowa Seimitsu, Tokyo, Japan), the column reactor packed with the immobilized enzyme, a 650 fluorescence spectrophotometer (Hitachi, Tokyo, Japan) equipped with a flow cell (18 μl), a Chromatocorder II data processor (System Instruments, Tokyo, Japan) and a 02-0175 back pressure regulator (Chemco, Tokyo, Japan). The separation column and the column reactor were kept at ambient temperature and at 40°C, respectively.

The mobile phase, the NAD solution (35 m*M*) and the buffer 0.4 *M* glycine–potassium chloride/potassium hydroxide (pH 10.8 at 40°C) were pumped at 0.8, 0.25 and 0.25 ml/min, respectively, and mixed before the column reactor. Enzymatic reaction of Val, Ile and Leu proceeded in the reactor, and the NADH produced was monitored fluorimetrically at λ_{em} = 465 and λ_{ex} = 340 nm.

RESULTS AND DISCUSSION

Properties of immobilized LDH column reactor

The influence of pH on the reaction with Val, Ile and Leu was studied over the range between 10.0 and 11.5 using a glycine–potassium chloride/potassium hydroxide

(0.2 *M*) buffer. For this experiment, the guard and separation columns were omitted. Each standard (0.1 m*M*) was injected and mixed with NAD solution and buffer of various pH before the column reactor. As shown in Fig. 2, the optimum pH was about 10.8. Variation of the concentration of the buffer from 0.1 to 0.01 *M* did not affect the peak height. The peak height in the glycine buffer was about five times that in carbonate buffer at the same pH.

The peak height (at pH 10.8) increased with increasing temperature from 30 to 50°C, but at 55°C the enzyme was deactivated. For long-term usage, the reactor was thermostated at 40°C.

Since the Michaelis constants of the immobilized LDH for Leu and NAD were 1.3 and 0.50 m*M*, respectively, under the conditions of Leu < 0.1 m*M* and NAD > 5 m*M*, the kinetics of the reaction was first order and zero order, respectively. The concentration of NAD in the reactor was kept at 6 m*M*. The peak height for 0.01 m*M* Leu decreased linearly with increasing flow-rate from 0.5 to 1.5 ml/min.

D Isomers of BCAAs, Co^{2+} and Cu^{2+} inhibited the enzymatic reaction. Interference from the metal ions was avoided by addition of EDTA to the flow stream. The peak height of the L isomer (0.01 m*M*) was decreased by 10 and 50% in the presence of 0.01 and 0.02 m*M* of the D isomer, respectively.

As measured with 0.01 m*M* BCAAs and 6 m*M* NAD in glycine–potassium chloride/potassium hydroxide buffer (pH 10.8) at a flow-rate of 1.3 ml/min, the relative activities of the immobilized LDH for Leu, Ile and Val were 100, 82 and 72, respectively. On the other hand, in the free enzyme, the values were 100, 55 and 74,

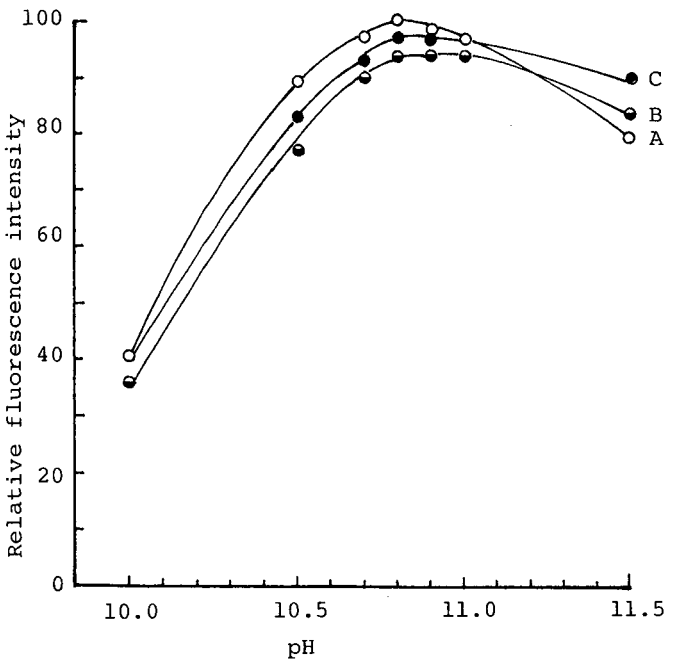

Fig. 2. Effect of pH on the activity of immobilized leucine dehydrogenase. A, L-leucine; B, L-valine; C, L-isoleucine.

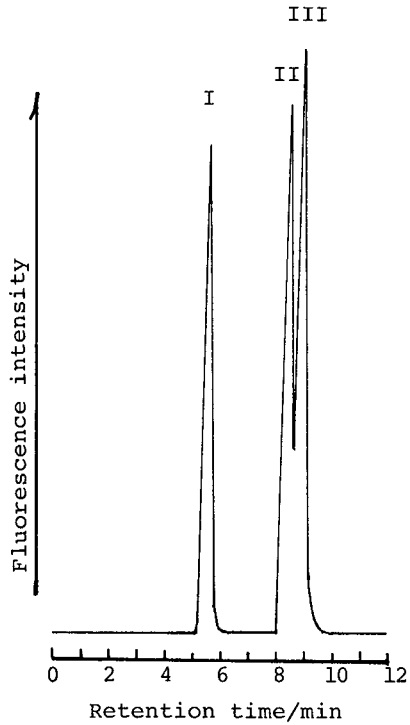

Fig. 3. Chromatogram of a standard solution (0.01 m*M* of each compound). Peaks: I = L-valine; II = L-isoleucine; III = L-leucine.

respectively. The free enzyme was examined by using an enzyme solution (7 U/ml) prepared by dissolving LDH in the NAD solution (6 m*M*) and a reaction tube (PTFE, 100 mm × 0.5 mm I.D.) instead of the reactor. Many examples of changed specificities of immobilized enzymes relative to free enzymes are known[12]. The change in specificity of LDH immobilized on the polymer beads may be attributed to steric interference caused by covalent attachment.

To confirm the long-term stability of the reactor, it was used for 6 h in a day and stored at 4°C in 0.1 *M* phosphate buffer containing 1 m*M* Na_4EDTA when not in use. The enzyme retained more than 60% of its original activity after 1 month.

TABLE I

SEPARATION PARAMETERS FOR BRANCHED CHAIN AMINO ACIDS

Amino acid	*Retention time (min)*	*Capacity factor*	*Resolution*	*Separation factor*
L-Valine	5.5	0.37		
			8.16	2.7
L-Isoleucine	8.3	1.0		
			0.71	1.2
L-Leucine	8.8	1.2		

TABLE II

RESULTS FOR FREE BRANCHED CHAIN AMINO ACIDS IN CONTROL SERA

Serum	*Amino acids found (μM)**					
	Proposed method			*o-Phthalaldehyde method*		
	Val	*Ile*	*Leu*	*Val*	*Ile*	*Leu*
Serum I**	233	76	124	235	79	130
Serum II***	220	61	119	221	66	121

* $n = 5$.
** Precinorm U, No. 155 657, Boehringer Mannheim.
*** Precinorm U, No. 155 171, Boehringer Mannheim.

Separation of BCAAs

A combination of separation of BCAAs by chromatography and the enzymatic reaction was attempted. In reversed-phase ion-pair chromatography, the immobilized LDH was unstable when allowed to stand in contact with ionic surfactants for a long time. In ion-exchange chromatography, the resolution of BCAAs was inferior to that in bonded phase chromatography. Separation of BCAAs was effected on a Capcell-C_{18} column with 25 m*M* sodium dihydrogenphosphate containing 0.5 m*M* Na_4EDTA as the mobile phase, as shown in Fig. 3. The separation parameters for the BCAAs are listed in Table I. The ratio of peak heights for the same concentration of Leu, Ile and Val was 100:90:83.

The peak heights were plotted against the concentrations of the amino acids. Four calibration graphs were prepared for Leu, Ile and Val, covering the ranges of 1–5, 5–10, 10–50 and 50–100 μ*M*. The detection limit was 0.5 μ*M*.

Application

The method was applied to the determination of free BCAAs in control serum. The serum (0.1 ml) was deproteinized by adding 0.8 ml of 1/6 *M* sulphuric acid and 0.1 ml of 10% sodium tungstate. The suspension was filtered through a column gurd filter (pore size 0.45 μm). An aliquot (60 μl) of the filtrate was injected into the column. The results obtained by the present method and by ion-exchange chromatography on the basis of post-column derivatization with *o*-phthalaldehyde–2-mercaptoethanol are shown in Table II.

In conclusion, this method proved to be simple for the determination of free branched chain amino acids, since only the separation of the three amino acids from each other is required for the assay. The method may easily be used routinely to determine BCAAs.

REFERENCES

1 M. L. Efron, *N. Engl. J. Med.*, 272 (1965) 1058.
2 S. A. Adibi, W. Fekl, U. Langenbeck and P. Schauder (Editors), *Branched Chain Amino and Keto Acids in Health and Disease*, Karger, Basel, 1984.
3 H. Terada, T. Hayashi, S. Kawai and T. Ohno, *J. Chromatogr.*, 130 (1977) 281.
4 B. C. Hemming and C. J. Gubler, *Anal. Biochem.*, 92 (1979) 31.

5 T. Hayashi, H. Tsuchiya and H. Naruse, *J. Chromatogr.*, 273 (1983) 245.
6 K. Kolke and M. Koike, *Anal. Biochem.*, 141 (1984) 481.
7 G. Livesey and E. T. E. Edwards, *J. Chromatogr.*, 337 (1985) 98.
8 G. A. Qureshi, *J. Chromatogr.*, 400 (1987) 91.
9 F. Lottspeich and A. Henschen, in A. Henschen, K.-P. Hupe, F. Lottspeich and W. Voelter (Editors), *High-Performance Liquid Chromatography in Biochemistry*, VCH, Weinheim, 1985, pp. 139–166.
10 I. Matsumoto, Y. Ito and N. Seno, *J. Chromatogr.*, 239 (1982) 747.
11 S. Williams (Editor), *Official Methods of Analysis of the Association of Official Analytical Chemists*, Association of Official Analytical Chemists, Arlington, VA, 1984, p. 16.
12 O. Zaborsky, *Immobilized Enzymes*, CRC Press, Cleveland, OH, 1974, pp. 56–57.

Journal of Chromatography, 463 (1989) 183–187
Elsevier Science Publishers B.V., Amsterdam — Printed in The Netherlands

CHROM. 21 058

Note

A post-column co-immobilized galactose oxidase/peroxidase reactor for fluorometric detection of saccharides in a liquid chromatographic system

NOBUTOSHI KIBA*, KAZUYOSHI SHITARA and MOTOHISA FURUSAWA
Department of Chemistry, Faculty of Engineering, Yamanashi University, Takeda 4-3-11, Kofu 400 (Japan)
(First received July 22nd, 1988; revised manuscript received October 18th, 1988)

Liquid chromatographic determination of trace amounts of saccharides typically needs derivatization to improve the detectability due to their low UV-absorptivities. Pre-column derivatization of saccharides, followed by reversed-phase chromatography is a sensitive method[1–4]. However, quantitation is one of the problems associated with the methods.

Post-column derivatization has been employed for the quantitative analysis of saccharides and a number of different fluorescent reagents have been examined for reducing saccharides[5–10]. However, very few fluorescent reagents are known for non-reducing saccharides[11,12].

Galactose oxidase (D-galactose:oxygen oxidoreductase, E.C. 1.1.3.9) (Gal-OD) catalyzes the oxidation of galactose by molecular oxygen. Oligosaccharides containing galactose such as raffinose and stachyose are oxidized much more rapidly than galactose itself. Gal-OD has been used as a reagent for the determination of galactose[13–16]. It has also been immobilized on glass beads and used as a reactor for the determination of galactose in flow injection analysis[17–19].

This paper describes the use of immobilized enzyme as a column reactor in a liquid chromatographic system for the specific detection of stachyose, raffinose, melibiose and galactose. Gal-OD and peroxidase (doner:hydrogen peroxide oxidoreductase, E.C. 1.11.1.7) (POD) were co-immobilized onto hydrophilic vinyl polymer beads. The saccharides were separated on a cation-exchange resin column with water as the mobile phase. In the column reactor, the saccharides were converted into hydrogen peroxide by Gal-OD, which reacts with *p*-hydroxyphenyl acetate in the presence of POD, and the fluorophore produced was detected. The fluorophore (6,6′-dihydroxy-3,3′-biphenyldiacetate) is formed in the following reaction sequence:

$$\text{D-Galactose} + O_2 \xrightarrow{\text{Gal-OD}} \text{D-galatohexodialdose} + H_2O_2$$
$$H_2O_2 + p\text{-hydroxyphenylacetate} \xrightarrow{\text{POD}} H_2O + \text{fluorophore}$$

This method is sensitive and highly specific for the detection of stachyose, raffinose, melibiose and galactose.

0021-9673/89/$03.50

EXPERIMENTAL

Reagents

D-galactose, D-melibiose, α-lactose, D-raffinose and stachyose tetrahydrate were obtained from Nakarai Tesque (Kyoto, Japan), galactose oxidase (from Dactylium sp., 28 U/mg of solid) and peroxidase (from horseradish, 266 U/mg) from Toyobo (Osaka, Japan). TSK gel Toyopearl HW-55S (20 − 40 μm, hydrophilic vinyl polymer beads) was obtained from Tosoh (Tokyo, Japan).

The purity of the *p*-hydroxyphenylacetic acid (HPA) had a large influence on the background signal. HPA was purified as follows. A 10-g amount was dissolved in 50 ml of aceton–benzene (10:3, v/v). The solution was passed through a column (10 cm × 1 cm I.D.) of activated alumina (*ca.* 200 mesh). The eluate was added dropwise to a mixture of *n*-hexane–benzene (5:5, v/v)(50 ml). The solution was left overnight at room temperature. The precipitated HPA was filtered off and dried under reduced pressure. The purified HPA (0.23 g) was dissolved in water (30 ml), adjusted to pH 7.5 with sodium hydroxide and then diluted in phosphate buffer (0.1 *M*, pH 7.5) to 100 ml. The solution was made up freshly every week. Stock solutions (0.1 *M*) of saccharides were prepared in water and allowed to mutarotate to anomeric equilibrium before use. All other chemicals were of analytical reagent grade.

Selection of support

Hydrophilic vinyl polymer beads (TSK gel Toyopearl HW-55S, 20 − 40 μm), polystyrene beads (Bio-Beads SX-8, 55 ± 20 μm) and glass beads (CPG-10, 500A, 55 ± 20 μm) were examined as supports for covalent attachment of the enzymes. Each support was aminoalkylated by several methods[20–22] and the amounts of amino group attached were measured by Kjeldahl method[23]: 0.6, 0.8 and 0.05 mequiv. per g of dry vinyl polymer beads, polystyrene beads and glass beads. The amounts grafted onto the glass beads were too little to co-immobilize the enzymes. The column reactor (50 mm × 4.6 mm I.D.) which was packed with the enzymes–polystyrene conjugates gave a pronounced peak tailing because of the adsorption of the fluorophore. The vinyl polymer beads gave a sharp peak and were chosen as the support.

Preparation of enzyme column reactor

The method of epoxy activation and amination of the vinyl polymer beads was similar to that of Matsumoto *et al.*[20]. The aminated polymer beads were packed into a stainless-steel column (50 mm × 4.6 mm I.D.) by the slurry-packing method. Glutaraldehyde solution (2.5%) in phosphate buffer (0.1 *M*, pH 7.0) was pumped through the column for 1 h at 0.3 ml/min and then the column was washed with deaerated water for 20 min at 0.5 ml/min. The Gal-OD solution (5 mg in 10 ml of phosphate buffer (0.05 *M*, pH 7.0) was circulated through the column for 1 h at 0.2 ml/min at room temperature and then, after addition of POD (5 mg) to the solution, the circulation was allowed to continue for 4 h. During the immobilization procedure the solution was kept at below 4°C.

System

The system is shown schematically in Fig.1. The apparatus consisted of a mobile phase pump, Hitachi 655A, an injector with an 100-μl loop, Rheodyne 7125, a

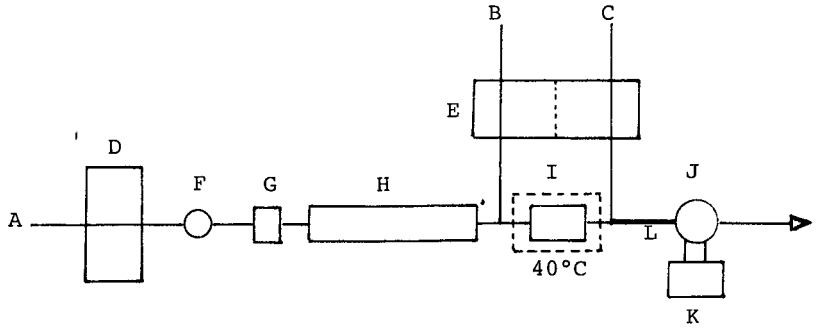

Fig. 1. A liquid chromatographic system for fluorometric detection of saccharides with an immobilized enzyme column reactor. A = Mobile phase (water, 0.5 ml/min); B = reagent solution (15 m*M* *p*-hydroxyphenylacetic acid, pH 7.5, 0.5 ml/min); C = buffer solution (0.3 *M* glycine-sodiumchloride/sodium hydroxide, pH 10.8, 0.25 ml/min); D = LC pump; E = reagent pump (double-plunger type); F = injector with 100-μl loop; G = guard column (50 mm × 6 mm); H = analytical column (60 cm × 7.8 mm); I = reactor (50 mm × 4.6 mm); J = fluorescence spectrophotometer; K = recorder; L = mixing tube (50 cm × 0.5 mm).

guard column of Shodex Ionpak KS800P (50 mm × 6 mm I.D.), a separation column (600 mm × 7.8 mm) of TSK gel SCX (5 μm), a reagent pump (double-plunger type), Kyowa Seimitsu KHU-W-52, a PTFE mixing coil (50 cm × 0.5 mm I.D.), a fluorescence spectrophotometer with a flow cell (18 μl), Hitachi 650-10s, and a strip-chart recorder, TOA FBR 251A.

The sample solution (100 μl) was injected onto the separation column with water as the mobile phase (0.5 ml/min). The temperature of the separation column was ambient. The HPA solution (15 m*M*) was added to the eluate at flow-rate of 0.5 ml/min. The mixture then passed into the column reactor, which was thermostatted at 40°C. Enzymatic reactions of saccharides and of hydrogen peroxide proceeded in the reactor, and the fluorophore produced was mixed with the buffer (0.3 *M* glycine–sodium chloride/sodium hydroxide, pH 10.8) (0.25 ml/min) in a mixing tube and was monitored at 410 and 330 nm.

RESULTS AND DISCUSSION

Experiments were conducted to optimize the reaction conditions, without the guard and separation columns. The influence of pH on the enzymatic reaction was studied over the range 6.0–8.0. A standard solution of stachyose (0.1 m*M*) was injected and mixed with HPA solution buffered with 0.1 *M* phosphate of various pH values before the reactor and then the stream emerging from the reactor was mixed with glycine–sodium chloride/sodium hydroxide buffer (pH 10.8). The optimum pH for the enzymatic reactions was about 7.5. The reactor was placed in a water-bath, the temperature was varied between 30 and 50°C and a standard solution of 0.1 m*M* stachyose was injected at each temperature. The reactor exhibited the highest activity at 40°C. The effect of the concentration of HPA was examined in the range of 1–10 m*M*. The peak height was constant above 6 m*M*. Michaelis constants of Gal-OD for galactose, melibiose, raffinose and stachyose are 0.3, 0.05, 0.03, and 0.02 *M* respectively[24]. Below the concentration of 0.1 m*M* saccharides the rate of the enzymatic

reaction (peak height) is directly proportional to the concentration. The peak height decreased linearly with increasing flow-rate from 0.8 to 1.5 ml/min. Lower flow-rates were preferable to higher ones for analytical sensitivity, but the peak broadening at lower flow-rates was undesirable. The fluorescence of the fluorophore emerging from the reactor was measured at pH from 9.0 to 12.0, with glycine–sodium chloride/sodium hydroxide buffer. The fluorescence was optimal at pH 10.8. Under the conditions of 7.5 m*M* HPA in phosphate buffer at pH 7.5 and 40°C the relative peak heights for stachyose, raffinose, melibiose, galactose and lactose were 240, 228, 88, 100 and 1, respectively. Under the same conditions, 100 μM stachyose was converted by Gal-OD into hydrogen peroxide in only 1.0% yield. By using this enzyme reactor, it was difficult to detect trace amounts of α-lactose. There were no peaks for D-glucose, D-mannose, D-fructose, D-tagatose, D-lyxose, D-ribose, D-xylose, maltose and sucrose.

Separation of mixtures of galactose, melibiose, raffinose and stachyose into their components was effected by anion-exchange chromatography on a column (TSK gel SAX, 5 μm, 300 mm × 6 mm I.D.) with 0.1 *M* borate pH 7.5 as the mobile phase at 70°C. However, the reproducibility of the chromatogram obtained was poor. A cation-exchange resin column (TSK gel SCX, 5 μm, 600 mm × 7.8 mm I.D.) was used in an attempt to separate the saccharides with water as the mobile phase at room temperature. A stable chromatogram was obtained, as shown in Fig.2. The separation of stachyose and raffinose was incomplete. The ratio of peak heights for stachyose, raffinose, melibiose and galactose was 445:336:182:100. In this liquid chromatographic system the band width of each peak was dominated by the separation

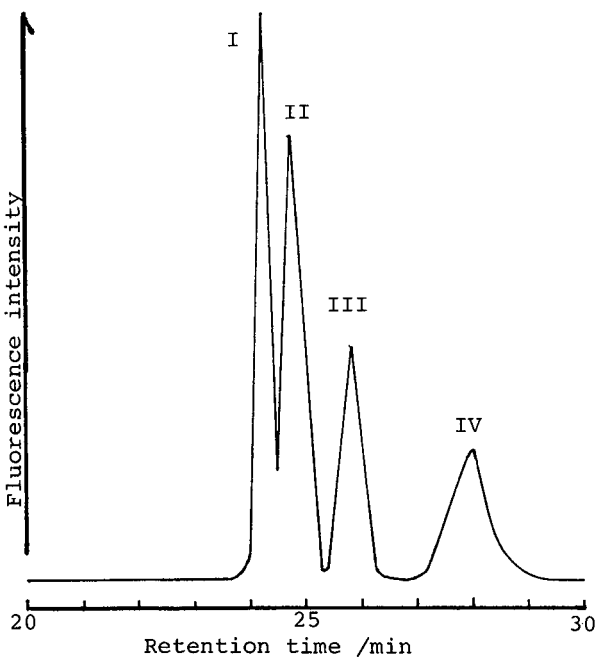

Fig. 2. Chromatogram of a standard solution: 0.01 m*M* each of stachyose (I), raffinose (II), melibiose (III) and galactose (IV).

column and the contribution of the post-column reaction system to the peak broadening was less than 40% in peak width. In the post-column reaction system, the peak broadening was due predominantly to the addition of HPA solution. Increasing the concentration of the HPA-solution and decreasing the flow-rate of the solution caused serious problems in reproducibility because of incomplete mixing of the solution with the mobile phase (water).

The peak height was plotted against the concentrations of the saccharides. The calibration graphs were linear from 100 to 5 μM for stachyose and raffinose and 100 to 10 μM for melibiose and galactose. The detection limits were 1.0, 1.0, 2.0 and 5.0 μM for stachyose, raffinose, melibiose and galactose, respectively.

The column reactor was used for 8 h in a day and stored at 4°C in 0.1 M phosphate buffer pH 7.0 when not in use. It retained more than 60% of its original activity after 6 weeks.

In conclusion, the co-immobilized Gal-OD/POD reactor is useful for the fluorometric detection of trace amounts of stachyose and raffinose. Stachyose and raffinose have been detected fluorometrically by anion-exchange chromatography using post-column derivatization with taurine-periodate[12]. The detection limits were 3 μM for each. This method is more sensitive (1 μM) and specific for the oligosaccharides.

REFERENCES

1 G. R. Her, S. Santikarn, V. N. Reinhold and J. C. Williams, *J. Carbohydr. Chem.*, 6 (1987) 129.
2 L. M. Dominguez and R. S. Dunn, *J. Chromatogr. Sci.*, 25 (1987) 468.
3 E. Mentasti, M. C. Gennaro, C. Sarzanini and V. Porta, *Ann. Chim. (Rome)*, 77 (1987) 579.
4 K. Muramoto, R. Goto and H. Kamiya, *Anal. Biochem.*, 162 (1987) 435.
5 J. H. M. Van den Berg, H. W. M. Horsels and R. S. Deelder, *J. Liq. Chromatogr.*, 7 (1984) 2351.
6 S. Honda, T. Konishi, S. Suzuki, M. Takahasi, K. Kakehi and S. Ganno, *Anal. Biochem.*, 134 (1983) 483.
7 M. Kai, K. Tamura, M. Yamaguchi and Y. Ohkura, *Anal. Sci.*, 1 (1985) 59.
8 T. D. Schlabach and J. Robinson, *J. Chromatogr.*, 282 (1983) 169.
9 H. Mikami and Y. Ishida, *Bunseki Kagaku*, 32 (1983) E207.
10 S. Honda, M. Takahashi, K. Kakehi and S. Ganno, *Anal. Biochem.*, 113 (1981) 130.
11 K. Mopper, *Anal. Chem.*, 52 (1980) 2018.
12 T. Kato and T. Kinoshita, *Bunseki Kagaku*, 35 (1986) 869.
13 J. M. Henderson and F. W. Wales, *Clin. Chem.*, 26 (1980) 282.
14 M. Hjelm, *Clin. Chim. Acta*, 15 (1976) 87.
15 F. S. Cheng and D. G. Christian, *Anal. Chim. Acta*, 104 (1979) 47.
16 M. Hjelm and C.-H. de Verdier, in J. Bergmeyer and M. Grassl (Editors), *Methods of Enzymatic Analysis*, Vol. 6, Verlag Chemie, Weinheim, 3rd ed., 1984, p. 281.
17 S. K. Dahodwala, M. K. Weibel and A. E. Humphrey, *Biotechnol. Bioeng.*, 18 (1976) 1679.
18 H. Lundback and B. Olsson, *Anal. Lett.*, 18 (1985) 871.
19 B. Olsson, H. Lundback and G. Johansson, *Anal. Chim. Acta*, 167 (1985) 123.
20 I. Matsumoto, Y. Ito and N. Seno, *J. Chromatogr.*, 239 (1982) 747.
21 N. Kiba, H. Maruyama and M. Furusawa, *J. Chromatogr.*, 456 (1988) 398.
22 H. H. Weetall, *Methods Enzym.*, 44 (1976) 134.
23 S. Williams (Editor), *Official Methods of Analysis*, Association of Official Analytical Chemists, Arlington, VA, 1984, p.16.
24 G. Avigad, D. Amaral, C. Asension and B. L. Horecker, *J. Biol. Chem.*, 237 (1962) 2736.

Journal of Chromatography, 463 (1989) 188–191
Elsevier Science Publishers B.V., Amsterdam — Printed in The Netherlands

CHROM. 21 025

Note

Analysis of benzalkonium chlorides by gas chromatography

SUKEJI SUZUKI*, YOSHIAKI NAKAMURA, MASAMI KANEKO, KEN'ICHIRO MORI and YOHYA WATANABE

Tokyo Metropolitan Research Laboratory of Public Health, 3-24-1, Hyakunincho, Shinjuku-ku, Tokyo 169 (Japan)

(First received June 4th, 1988; revised manuscript received October 4th, 1988)

Benzalkonium chlorides are widely used as an antimicrobial preservative in pharmaceutical preparations and sanitary products, and are a mixture of predominantly C_{12}, C_{14} and C_{16} alkylbenzyldimethylammonium chlorides.

Various analytical methods have been reported for the determination of benzalkonium chlorides by high-performance liquid chromatography (HPLC)[1–5] and gas chromatography (GC)[6–16]. HPLC analysis is available but difficult to use in combination with mass spectrometry in our laboratory. We wished to establish a GC method for the routine analysis of benzalkonium chlorides since their identification can be facilitated using GC–mass spectrometry (MS). These compounds are non-volatile and thus need to be converted into more volatile derivatives before GC[11–13]. The Hofmann degradation for ammonium compounds is one such conversion method[14–16]. Tanakano *et al.*[16] reported that a mixture of alkyldimethylamines, alkylbenzylmethylamines and α-olefins is obtained from benzalkonium chlorides by Hofmann degradation with sodium methoxide, but this approach requires too severe reaction conditions to decompose them.

In previous papers[17,18], we have reported that long-chain alkyltrimethyl- and dialkyldimethylammonium compounds can be analyzed by GC as the corresponding α-olefins and alkyldimethylamines which are formed by the Hofmann degradation with potassium *tert.*-butoxide under mild conditions. In the present work, a GC method for benzalkonium chlorides employing this degradation technique has been developed.

EXPERIMENTAL

Dodecylbenzyldimethylammonium chloride (I) was obtained from Kao Soap (Tokyo, Japan), tetradecylbenzyldimethylammonium chloride (II) and hexadecylbenzyldimethylammonium chloride (III) from Tokyo Kasei Kogio (Tokyo, Japan) and octadecylbenzyldimethylammonium chloride (IV) from Aldrich (Milwaukee, WI, U.S.A.). Standard solutions were prepared so as to contain 1 mg/ml of each compound in benzene–dimethyl sulphoxide (DMSO) (8:2). All other chemicals were of analytical grade.

0021-9673/89/$03.50

Degradation procedure

An aliquot of the standard solution containing 2–10 mg of compounds I–IV was pipetted into a 25-ml Pyrex glass test-tube with a ground glass stopper. The total volume was made up to 25 ml with benzene–DMSO (8:2). After the addition of 100 mg of potassium *tert.*-butoxide, the solution was vigorously shaken and allowed to stand for 10 min at room temperature. The reaction mixture was transferred to a 100-ml separating funnel. The test-tube was rinsed with two 5-ml portions of benzene. The rinsing solutions were added to the reaction mixture in a separating funnel and then shaken with 20 ml of 10% sodium chloride solution. The benzene layer was separated and transferred to a 100-ml round-bottom flask. After the solvent had been evaporated to dryness under reduced pressure, the residue was dissolved in 5 ml of acetone and 5 μl of this solution were injected into the gas chromatograph.

Gas chromatography

GC analysis was carried out with a Shimadzu Model GC-15A gas chromatograph equipped with an hydrogen flame ionization detector. Chromatography was performed on a glass column (2 m × 3 mm I.D.) packed with 5% SE-30 on Chromosorb W AW DMCS (80–100 mesh) under the following conditions: nitrogen flow-rate 40 ml/min; injection port and detector temperature 250°C; column temperature program from 140 to 230°C at 5°C/min.

RESULTS AND DISCUSSION

Benzalkonium chlorides shown in Fig. 1 were degraded with potassium *tert.*-butoxide by essentially the same manner as described in previous papers[7,8]. However, the formation of α-olefins and alkyldimethylamines as degradation products was found to vary with the reaction temperature. In searching for an optimum condition for alkyldimethylamine formation the effect of the reaction temperature for compounds I–IV was examined. As shown in Fig. 2, alkyldimethylamine formation was found to be accompanied by a decrease in that of α-olefin at temperatures lower than 40°C. These results indicate that the debenzylation of benzalkonium chlorides with potassium *tert.*-butoxide proceeds selectively at lower temperature to give akyldimethylamine, and on the other hand the β-elimination reaction at the nitrogen-bonded alkyl chain predominates at temperatures higher than 80°C to give

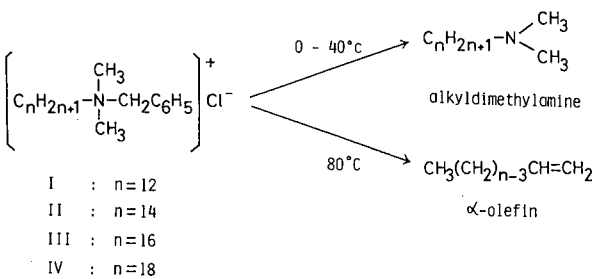

I : n=12
II : n=14
III : n=16
IV : n=18

Fig. 1. Degradation scheme of benzalkonium chlorides with potassium *tert.*-butoxide in benzene–DMSO (8:2).

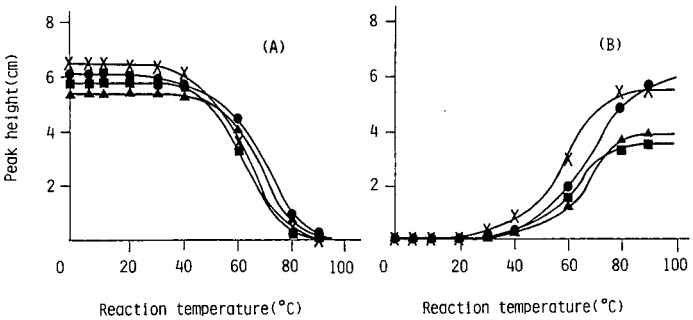

Fig. 2. Effects of reaction temperature on the formation of alkyldimethylamines (A) and α-olefins (B) from the four benzalkonium chlorides, compounds I (●), II (×), III (▲) and IV (■).

α-olefin (Fig. 1). Thus, room temperature was selected for the GC analysis of benzalkonium chlorides as their alkyldimethylamines. The reaction was rapid under mild conditions in comparison with debenzylation in the previously reported conversion methods[11–16] and was complete within 10 min at room temperature.

A typical gas chromatogram of compounds I–IV as their alkyldimethylamines on a 5% SE-30 column is shown in Fig. 3. Calibration graphs were constructed by plotting the peak heights of the alkyldimethylamines *versus* the concentrations of compounds I–IV. They showed good linearity over the concentration range 0.4–2 mg/ml. The minimum detectable amounts for compounds I–IV were found to be about 0.1 mg/ml.

For practical application *e.g.*, to a wet wiper containing benzalkonium chlorides, recovery tests were performed by adding 4 and 8 mg of compounds I–IV to an absorbent cotton (Table I). The cotton was extracted with ethanol under reflux for 60 min. The ethanol extract was filtered and evaporated to dryness. The analysis of

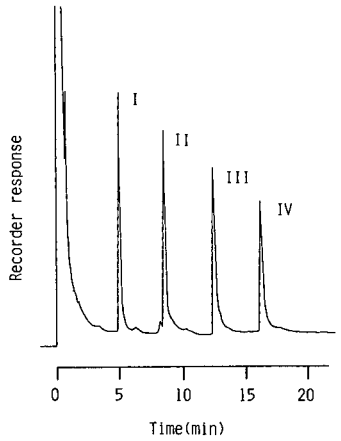

Fig. 3. Temperature-programmed gas chromatogram of the four benzalkonium chlorides as their alkyldimethylamines after degradation with potassium *tert.*-butoxide at room temperature, compounds I–IV: 6 mg.

TABLE I
RECOVERIES OF BENZALKONIUM CHLORIDES FROM ABSORBENT COTTON

*Compound**	*Amount added (mg)*	*Average recovery (n=3) (%)*	*C.V. (%)*
I	4	98.3	3.9
	8	103.4	1.9
II	4	104.2	1.4
	8	102.1	1.4
III	4	96.7	1.5
	8	92.4	3.3
IV	4	98.3	2.9
	8	96.3	4.5

* Benzalkonium chlorides (I–IV) were dissolved in 10 ml of water, added to 1.7 g of absorbent cotton (The Pharmacopoeia of Japan, 11th ed.) and autoclaved at 120°C for 30 min.

compounds I–IV was performed by the method described. As shown in Table I, the average recoveries in three experiments were 92.4–104.2% and a good reproducibility was obtained with coefficients of variation (C.V.) of 1.4–4.5%.

We have applied this method to the determination of benzalkonium chlorides in 36 samples of commercial wet wipers. These were found to contain 0.06–0.28% in 10 samples as a mixture of C_{12}, C_{14} and C_{16} alkylbenzyldimethylammonium chlorides.

These experiments have demonstrated that the method proposed can be applied to routine analysis of benzalkonium chlorides.

REFERENCES

1 R. C. Meyer, *J. Pharm. Sci.*, 69 (1980) 1148.
2 K. Nakamura, Y. Morikawa and I. Matsumoto, *J. Am. Oil Chem. Soc.*, 58 (1981)72.
3 K. Nakamura and Y. Morikawa, *J. Am. Oil Chem. Soc.*, 59 (1982) 64.
4 D. F. Marsh and L. T. Takahashi, *J. Pharm. Sci.*, 72 (1983) 521.
5 S. Sato and S. Tanaka, *Bunseki Kagaku*, 33 (1984) 338.
6 L. D. Metcalfe, *J. Am. Oil Chem Soc.*, 40 (1963) 25.
7 T. Uno, K. Miyajima and T. Nakagawa, *Bunseki Kagaku*, 15 (1966) 584.
8 H. Konig and W. Strobel, *Fresenius' Z. Anal. Chem.*, 314 (1983) 143.
9 Z. R. Cybulski, *J. Pharm. Sci.*, 73 (1984) 1700.
10 L.-K. Ng, M. Hupé and A. G. Harris, *J. Chromatogr.*, 351 (1986) 554.
11 H. P. Warrington, Jr., *Anal. Chem.*, 33 (1961) 1898.
12 S. L. Abidi, *J. Chromatogr.*, 200 (1980) 216.
13 S. Kawase and S. Ukai, *Eisei Kagaku*, 27 (1981) 296.
14 E. C. Jennings, Jr., and H. Mitchner, *J. Pharm. Sci.*, 56 (1967) 1590.
15 H. Mitchner and E. C. Jennings, Jr., *J. Pharm Sci.*, 56 (1967) 1595.
16 S. Takano, C. Takasaki, K. Kunihiro and M. Yamanaka, *J. Am. Oil Chem. Soc.*, 54 (1977) 139.
17 S. Suzuki, M. Sakai, K. Ikeda, K. Mori, T. Amemiya and Y. Watanabe, *J. Chromatogr.*, 362 (1986) 227.
18 S. Suzuki, K. Mori, T. Amemiya and Y. Watanabe, *J. Chromatogr.*, 387 (1987) 379.

Journal of Chromatography, 463 (1989) 192–200
Elsevier Science Publishers B.V., Amsterdam — Printed in The Netherlands

CHROM. 21 096

Note

Determination of volatile amines in air by on-line solid-phase derivatization and high-performance liquid chromatography with ultraviolet and fluorescence detection

CHUN XIN GAO and IRA S. KRULL*
Department of Chemistry, The Barnett Institute (341MU), Northeastern University, 360 Huntington Avenue, Boston, MA 02115 (U.S.A.)
and
THOMAS M. TRAINOR*
ERT, Inc., 33 Industrial Way, Wilmington, MA 01887 (U.S.A.)
(First received August 4th, 1988; revised manuscript received November 11th, 1988)

Aliphatic amines and polyamines are well known as odorous substances and as precursors of N-nitrosamines, which are carcinogenic substances in the atmosphere[1]. Gas chromatography (GC)[2,3] and particularly high-performance liquid chromatography (HPLC) have been used quite extensively for the determination of volatile amines in air, due to several advantages over other analytical methods, especially high specificity and sensitivity[4–6]. Chemical derivatization techniques have been the ideal choice when GC and HPLC have been used for the above purpose. Unfortunately, all those chemical derivatizations involved homogeneous reactions, which were tedious and time consuming[7,8]. We have synthesized, characterized and evaluated a polymeric activated ester–carbonate fluorenyl (FMOC) reagent for both off-line and on-line derivatizations in HPLC[9]. These prior results showed that this polymeric reagent was extremely reactive towards nucleophiles, such as amines, due to the labelling moiety (tag) being activated by electron-withdrawing groups on the polymeric backbone. In the present study, a reaction column containing the polymeric fluorenyl reagent was slurry packed, and placed just before the separation column (on-line, pre-column mode). Trace levels of aliphatic amines and a polyamine in environmental air samples were trapped with commercially available silica gel tubes. The amines were desorbed with an acidic aqueous–organic solution and neutralized with sodium hydroxide prior to HPLC injection. Recovered amine solutions were then directly injected into the on-line, pre-column derivatization, HPLC–UV/fluorescence detection system for quantitation.

EXPERIMENTAL

Chemicals, reagents and solvents

Chemicals used were obtained from a variety of commercial sources, including Aldrich (Milwaukee, WI, U.S.A.), Burdick & Jackson Labs. (Muskegon, MI,

* Present address: Bruker Instruments, Inc., Manning Park, Billerica, MA 01821, U.S.A.

0021-9673/89/$03.50

U.S.A.), J. T. Baker (Philipsburg, NJ, U.S.A.) Alfa Products, Morton Thiokol (Danvers, MA, U.S.A.), and Sigma (St. Louis, MO, U.S.A.). These chemicals were all of the highest purity available and were used without further purification. HPLC solvents were obtained from EM Science (Cherry Hill, NJ, U.S.A.), as their Omnisolv HPLC brand/grade. All HPLC solvents were used after filtration through a 0.45-μm solvent filter (GVWP; Millipore, Bedford, MA, U.S.A.) and degassed under vacuum with stirring.

Apparatus

The measurements were carried out on an apparatus consisting of a Waters (Milford, MA, U.S.A.) Model 6000A pump, a Rheodyne Model 7010 injection valve with 5- and 10-μl sample loops (Rainin, Emeryville, CA, U.S.A.), a Model SE 120 dual-pen recorder (Brown, Boveri & Co., Metrawatt/Goerz Division, Vienna, Austria), an EM Science LiChrospher C_{18} reversed-phase column, 250 mm × 4.6 mm I.D., 5 μm particle size, a Waters Model 480 variable-wavelength UV–VIS detector, a Hitachi (Naka Works, Mito City, Japan) Model F1000 fluorescence spectrophotometer, and a Hitachi Model D-2000 ChromatoIntegrator.

Air sample collection

Double-sealed glass tubes (110 mm × 10 mm O.D.) containing silica gel were obtained from SKC (Eighty-Four, PA, U.S.A.). The air in the work/sampling area was sampled at a flow-rate of 400 ml/min for 4 h using a DuPont (Wilmington, DE, U.S.A.) Alpha-1 air sampler pump.

Desorption and neutralization

All silica beads and glass wool in the sampling tube were transferred to a glass vial (10 ml volume), and the sampling tubes were washed with 5 ml 1 *N* sulfuric acid–acetonitrile (1:1) into the same vial. After sonication for 1 h, the resultant solution (0.5 ml) was removed and neutralized with 0.5 ml 1.00 *N* sodium hydroxide solution to pH 10.

On-line derivatizations

The stainless-steel reaction columns (27 mm × 2.0 mm I.D.) were made in this laboratory. Using a Rheodyne Model 7060 injector as a switching valve, the reaction column was connected to the loop position on the valve. The reaction column was placed into a constant-temperature water bath (60°C). The basic sample solution (10 μl) was injected and the switching valve was switched to the bypass position at the correct time (*ca.* 6 s). The analyte was held within the reaction column for a specific time period (5 min), and the valve was then switched back to flush the derivative from the reaction column into the separation/analytical column.

Quantitation of amines

Two different sample series were performed. Amines in the sample prepared from the single blind spike experiments were quantitated via external standards. Amines in air trapped from a fish inspection laboratory of the U.S. Food and Drug Administration (FDA) were quantitated via the standard addition method. Amines spiked were in the range of 0.2–1.0 ppm. Each sample was spiked with two different concentrations. Three injections were made for each sample with or without spiked,

known concentrations of amines. Three-point calibration plots were then constructed for the quantitation of amines in the individual air sample.

RESULTS AND DISCUSSION

The structure of the polymeric reagent indicated here is simplified, the exact structure of the reagent, specific synthetic methods, and reactions will be described elsewhere, as well as methods for the characterization and loading[9]. The general solid-phase reaction to form fluorenyl (FMOC) amine derivatives is shown in Fig. 1. Authentic standards for some of the amine/polyamine derivatives were previously prepared and characterized, so that known concentrations of each could be used here for accurate quantitations.

Acetonitrile consistently provided the highest percent derivatizations for all amine substrates[9]. Using this as the solvent, the optimized temperature and times were 60°C and 5 min, the percent derivatization for propylamine was 87% with a standard deviation (S.D.) 1.5, $n=3$, and 71% (S.D. = 1.0, $n=3$) for diethylamine. The efficiency of sampling and the desorption procedure were investigated by using direct spiking experiments. An acidic, aqueous elution solution (1 *N* sulfuric acid) was first used to desorb the trapped amines from sampling tubes containing silica gel. Recoveries for primary and secondary amines were 85–88% and 74–82%, respectively. Recoveries increased about 5% for primary amines and about 10% for secondary amines by mixing acetonitrile with the acidic, aqueous eluting solution (1:1). This may have been caused by the increased solubility of such amines with the organic modifier present. By a comparison of the levels of amines experimentally determined *vs.* the levels spiked, percent recoveries were calculated. Recoveries greater than 90% for all amines were realized, indicating the high efficiency for this overall sampling and desorption procedure.

To validate the method further before its application to real samples, a "single blind" study was performed. The sample desorption and neutralization steps were followed, as above, by the on-line real time derivatization–HPLC separation (Fig.2). The same sample solutions were analyzed using a conventional GC–flame ionization detection method performed by another analyst in a different laboratory. The results are compared in Table I. The relative standard deviations (R.S.D.) varied from 1.1% to 4.2%. The relative errors were from −1.2% to +2.8% after calculating the amount of amines found *vs.* spiked. The final accuracies, precision and reproducibilities were acceptable and comparable to most other air sample assays reported in the literature[2–8].

The minimum amounts of amines that could be both derivatized and detected

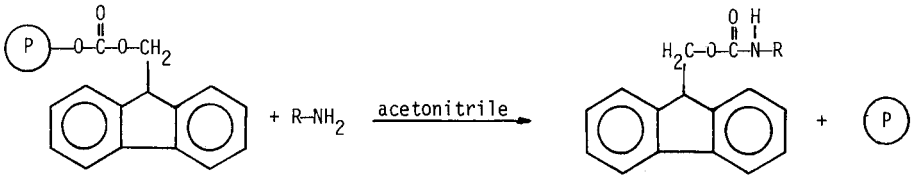

Fig. 1. Scheme of solid-phase derivatizations of typical amines using the polymeric FMOC reagent.

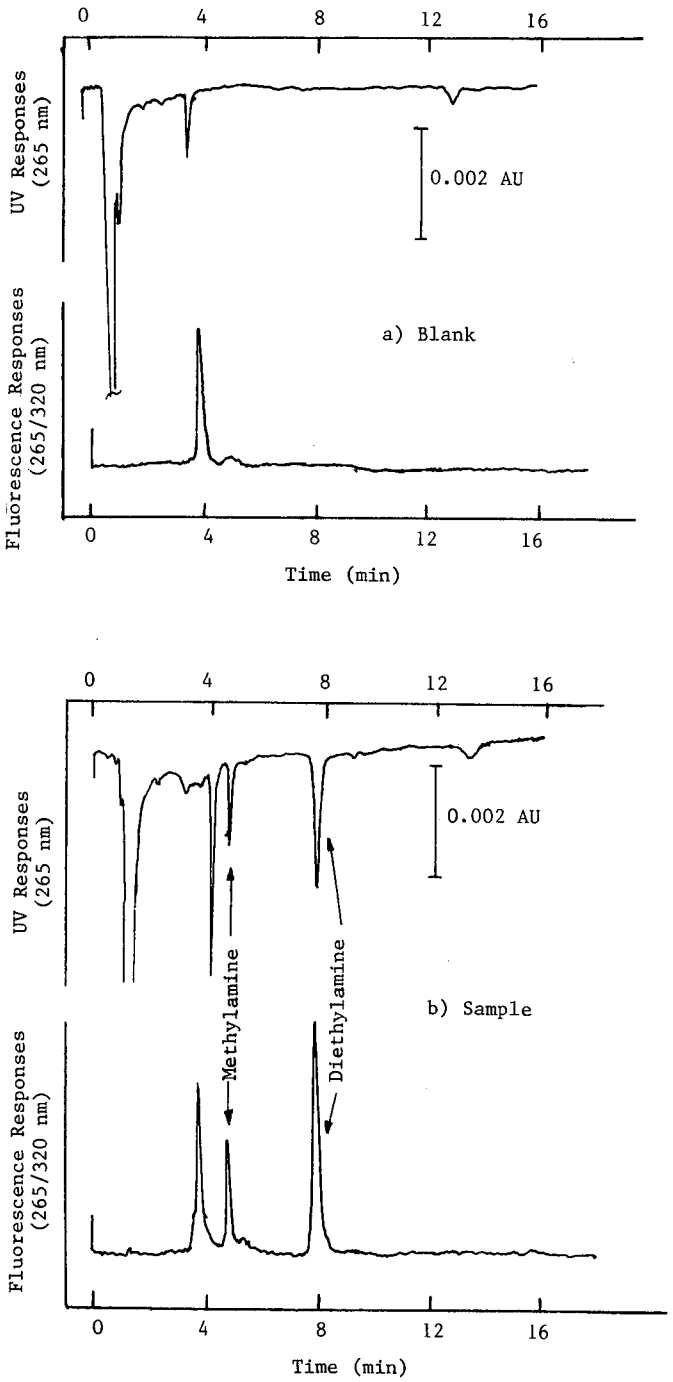

Fig. 2. Chromatogram of blind spiked experiment (a: blank; b: sample). Amines were spiked to silica adsorbent, acidicly eluted, neutralized, injected into on-line solid-phase derivatization–HPLC–UV/fluorescence detection system (10 μl), real time, room temperature, acetonitrile–water (60:40), 1.5 ml/min, LiChrospher C_{18}, 5 μm, 250 mm × 4.0 mm I.D., UV 265 nm, fluoresence 265/320 nm.

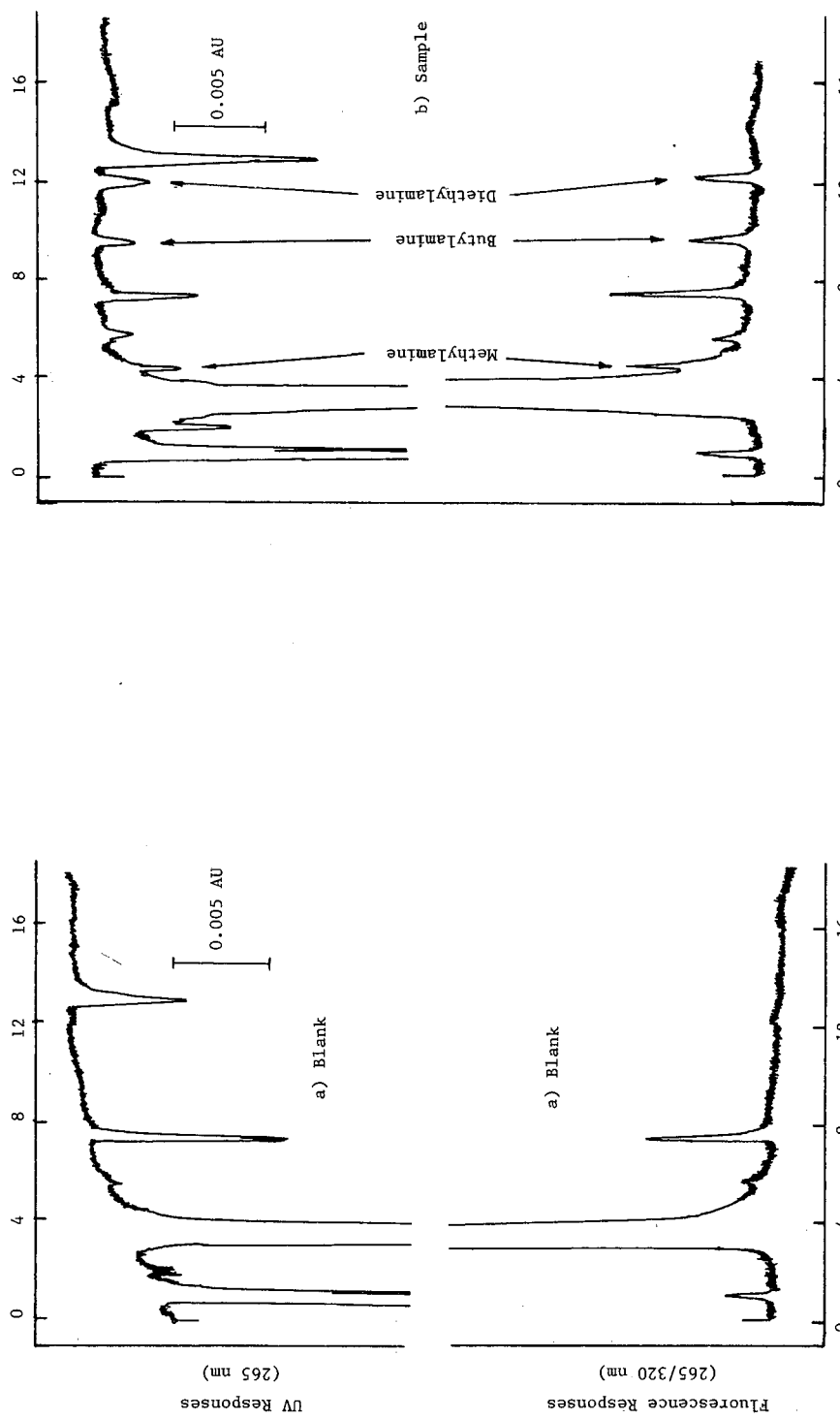

Fig. 3. On-line solid-phase derivatization–HPLC–UV/fluorescence detection for the minimum amounts of amines that could be both derivatized and chromatographically detected after air sampling procedure (a: blank; b: sample). Amines spiked to silica gel adsorbent, eluted, injected: 24 ppb for methylamine, 34 ppb for butylamine and 60 ppb for diethylamine. Specific reaction–HPLC–detection conditions: 60°C for 5 min. Other conditions as in Fig. 2.

TABLE I
SINGLE BLIND SPIKING EXPERIMENTS

See Fig. 2. Known levels of each amine, as a mixture, were spiked to the silica gel air sampling adsorbents and eluted, neutralized, and injected into the pre-column, on-line derivatization–HPLC–detection system. Comparison of levels spiked with levels experimentally determined. RE = Percent relative errors: (value found − true value)/true value × 100%.

Substrate	*Spiked (ppm)**	*Our method*			*GC–flame ionization detection****		
		*Found ± S.D. (n=3) (ppm)***	*R.S.D. (%)*	*R.E. (%)*	*Found ± S.D. (n=3) (ppm)*	*R.S.D. (%)*	*R.E. (%)*
Methylamine	14.7	15.1 ± 0.2	1.4	+2.0	14.2 ± 0.5	3.4	−3.4
Dimethylamine	31.4	32.3 ± 0.5	1.6	+2.8	32.1 ± 0.6	1.9	+2.2
Methylamine	44.1	43.2 ± 1.8	4.2	−2.0	45.4 ± 0.7	1.6	+2.7
Dimethylamine	94.4	93.3 ± 1.0	1.1	−1.2	96.2 ± 0.9	1.0	+5.1

* Sample spiked at Environmental Resource Technology, Inc.
** Amine concentration found with our method, corrected for percent recoveries.
*** NIOSH-accepted method performed at Environmental Resource Technology, Inc.

by UV/fluorescence after this sampling procedure were 24 ppb* (5.3 pmol) for methylamine, 34 ppb (5.7 pmol) for butylamine and 60 ppb (8.2 pmol) for diethylamine (Fig.3) with a signal-to-noise ratio of 3:1. Relatively higher concentrations of secondary amines were derivatized and detected due to the steric hindrance of such compounds, lowering their reactivity. The lowest concentrations of amines detected by the method were comparable with most GC and HPLC methods[2–8]. The linearities of the calibration plots were 3–4 orders of magnitude starting from the lowest concentrations of amines. The solvent front peak was the hydrolysis product of the polymeric reagent.

Amines in air were trapped from different sources, including: sewage area, fish processing company and a raw fish organoleptic (decomposition determination by odor) laboratory at the FDA. The air collections were performed according to the standard procedures issued by the National Institute for Occupational Safety and Health (NIOSH) and the Occupational Safety and Health Administration (OSHA)[10]. With the least sample preparation possible, the amine solution was directly injected into the on-line derivatization–HPLC system for quantitation. One single analysis, starting from injection, derivatization, separation, and detection of the aliphatic amines and polyamines was achieved within 30 min (Fig.4) for each sample.

Amine concentrations in a sewage area were less than the detectable levels of amines using this method. Amines at higher levels were found in the fish processing company and fish inspection/analysis laboratory, due to decomposition of the biological substances (Table II). Amine levels are known to correlate with the degree of biological decomposition. Higher levels of amines, especially of cadaverine, were found in the sample collected at the FDA fish inspection laboratory in the afternoon (P.M.) than those collected in the morning (A.M.) for the same collection time (4 h).

* Throughout this article, the American billion (10^9) is meant.

This was due to the higher degree of fish decomposition (higher temperature and less defrosting time) which occurred during the P.M. sampling period, releasing higher levels of amines. We should perhaps emphasize that the high levels of amines occurred when frozen fish was being thawed prior to organoleptic determinations. Such levels are not, we believe, routinely found within fish inspection laboratories, other than at times when all of the fish present has been thawed and is awaiting inspection.

The major limitations of the method were: (a) relatively poor derivatizations for sterically hindered compounds (secondary amines), and (b) gradual hydrolysis of the polymeric reagent when performing on-line fractions at higher temperatures for longer stop-flow times. The possible advantages in performing on-line solid-phase derivatizations in HPLC with this polymeric reagent were: (a) fast and efficient analysis, (b) sensitive for most amines in air samples, (c) accurate and precise analyses, (d) less sample work-up, (e) inexpensive, and (f) great potential for automation. It should be apparent that the application described here for volatile amines in air samples is but

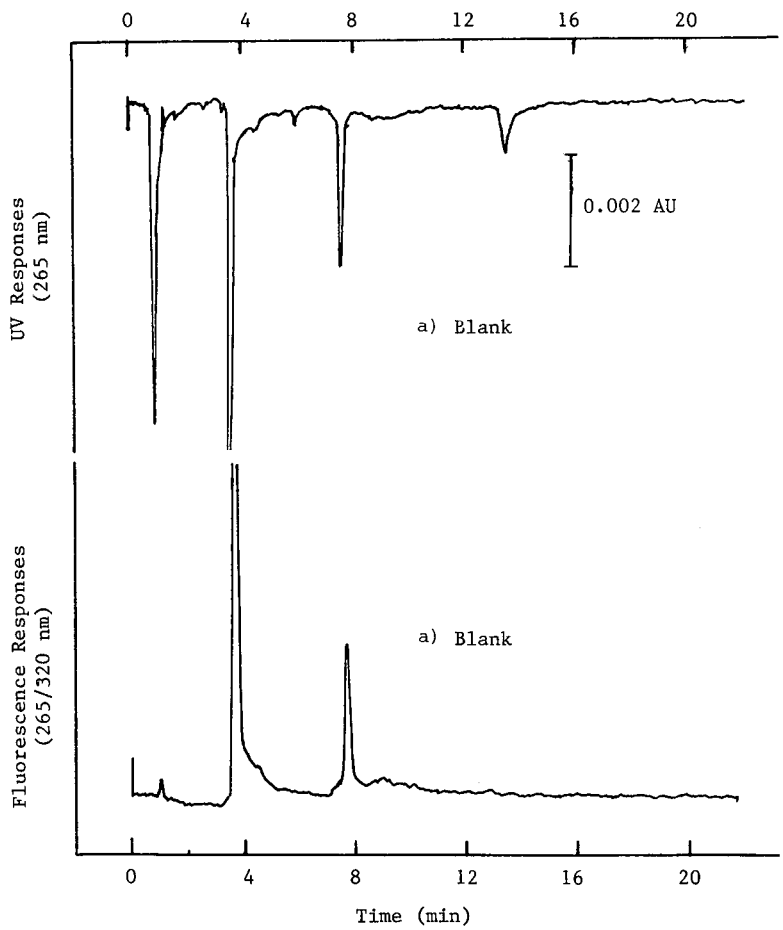

Fig. 4.

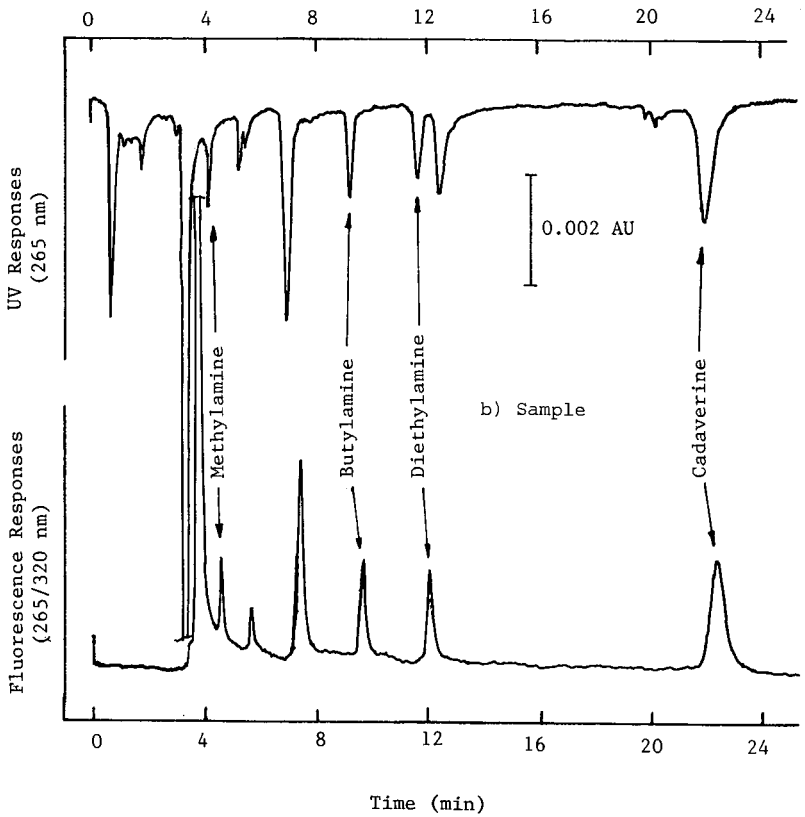

Fig. 4. HPLC–fluorescence detection of amines and polyamine determined in actual air sample taken from an FDA organoleptic laboratory (a: blank; b: sample). On-line derivatizations were at 50°C for 5 min, other conditions as in Fig. 2. See Table II for the results.

TABLE II

AMINE AND/OR POLYAMINE LEVELS IN ACTUAL AIR SAMPLES COLLECTED FROM AN FDA ORGANOLEPTIC LABORATORY

See Fig. 4.

Analyte	*Concentration*			
	Sample I (a.m.)		*Sample II (p.m.)*	
	ppm ± *S.D.* (*n*=3)	*mg/m*^{3} ± *S.D.* (*n*=3)	*ppm* ± *S.D.* (*n*=3)	*mg/m*^{3} ± *S.D.* (*n*=3)
Methylamine	0.36 ± 0.02	0.019 ± 0.001	0.50 ± 0.04	0.022 ± 0.002
Butylamine	0.40 ± 0.03	0.042 ± 0.003	0.96 ± 0.04	0.050 ± 0.005
Diethylamine	–*	–*	7.3 ± 0.30	0.380 ± 0.020
Cadaverine	0.56 ± 0.04	0.050 ± 0.002	2.2 ± 0.10	0.114 ± 0.005

* Less than the detectable levels of amines using this method.

one of many imaginable using an on-line, pre-column, solid-phase derivatization scheme in HPLC. Numerous other applications will prove possible and practical. The determination of total drug levels and/or enantiomer ratios of optically active drugs and bioorganics is one typical future application area[11].

ACKNOWLEDGEMENTS

This work was supported by the Analytical Research Department, Pfizer Central Research, Pfizer, Inc., Groton, CT, U.S.A., and by an NIH Biomedical Research Support Grant to Northeastern University, No. RR07143, Department of Health and Human Services (DHHS). A Spectronics Model 1201 scanning UV–VIS spectrophotometer was donated to Northeastern University by LDC/MRC. We would like to thank L. Dou, A. Bourque, J. Mazzeo and H. Stuting from Northeastern University. We also wish to thank L. Pounds, A. Pancaldo, D. Capen and D. Gouveia from ERT, Inc. for their technical assistance.

We acknowledge the assistance of A. Laterza (deceased), M. Lookabaugh, S. Krzysko, M. Finkelson and J. Fitzgerald from the Winchester Engineering & Analytical Center, FDA. I. S. K. is the current Science Advisor to this center.

This is contribution No. 370 from The Barnett Institute at Northeastern University, Boston, MA, U.S.A.

REFERENCES

1 P. Simon and C. Lemacon, *Anal. Chem.*, 59 (1987) 480–484.
2 K. Kuwata, E. Aklyama, Y. Yamazaki and H. Yamazaki, *Anal. Chem.*, 55 (1983) 2199–2201.
3 M. F. Boeniger, G. Choudhary and G. D. Foley, *Appl. Ind. Hyg.*, 2 (1987) 218–221.
4 J. N. Lepage and E. M. Rocha, *Anal. Chem*, 55 (1983) 1360–1364.
5 Y. Nishikawa and K. Kuwata, *Anal. Chem.*, 56 (1984) 1790–1793.
6 K. Andersson, C. Hallgren, J.-O. Levin and C. A. Nisson, *Am. Ind. Hyg. Assoc. J.*, 46 (1985) 225–229.
7 J. O. Levin, *Analyst (London)*, 113 (1988) 511–513.
8 K. Andersson, C. Hallgren, J.-O. Levin and C. A. Nilsson, *J. Chromatogr.*, 312 (1984) 482–488.
9 C. X. Gao, T. Y. Chou and I. S. Krull, *Anal. Chem.*, (1988) submitted for publication.
10 *Manual of Analytical Methods*, National Institute for Occupational Safety and Health, Cincinnati, OH, 3rd ed., 1984, Method No. P&CAM 221.
11 C. X. Gao and I. S. Krull, (1988) unpublished results.

Journal of Chromatography, 463 (1989) 201–206
Elsevier Science Publishers B.V., Amsterdam — Printed in The Netherlands

CHROM. 21 021

Note

Separation and assay of N-nitroso compounds by high-performance liquid chromatography with chemiluminescence detection

C. PINCHE, J. P. BILLARD, A. M. FRASEY, H. BARGNOUX, J. PETIT and J. A. BERGER
Laboratoire de Chimie analytique et Bromatologie de la Faculté de Pharmacie et Institut de la Viande des Universités, BP 38, 63001 Clermont-Ferrand Cédex (France)
and
B. DANG VU and J. YONGER
Laboratoire de Chimie analytique et Bromatologie, Faculté de Pharmacie, 4, Avenue de l'Observatoire, 75006 Paris (France)
(First received April 28th, 1988; revised manuscript received September 26th, 1988)

Assay of nitrite and total N-nitroso compounds can be carried out by chemiluminescence detection after chemical denitrosation and recovery of the liberated nitric oxide [1–4]. In addition, nitrite can be differentiated from N-nitroso compounds by carrying out an initial selective reduction of nitrite, which is thereby eliminated, enabling the N-nitroso compounds alone to be assayed[5–7]. We developed a method for separately assaying nitrite and total N-nitroso compounds based on these reactions that can be applied to various types of sample, liquid and solid, including foodstuffs and, in particular, pork products[8,9].

Concomitantly, we set out to improve further this method by its combination with high-performance liquid chromatography (HPLC). Such analysis by HPLC with denitrosation and chemiluminescence detection allows separate assay of individual N-nitroso compounds. The method was developed using mixtures of reference N-nitrosamines, according to the modified technique of Rühl and Reusch[10]. Evaluation of the method was satisfactory.

MATERIALS AND METHODS

General principle

The N-nitroso compounds were first separated by HPLC and then chemically denitrosated. The nitric oxide evolved was assayed in a chemiluminescence analyser. The study was performed on a mixture of four reference N-nitrosamines.

Apparatus (Fig. 1)

The apparatus consisted of an HPLC instrument, a chemical denitrosation reactor and attachments and a chemiluminescence detector + integrator + recorder.

Two chromatographs were used: a Waters instrument equipped with a Type 6000 A pump suitable for micro-flow-rates, and a Rheodyne Type 7125 injection loop (v = 20 μl); a Hewlett-Packard HP 1081 B equipped with a variable volume automat-

0021-9673/89/$03.50

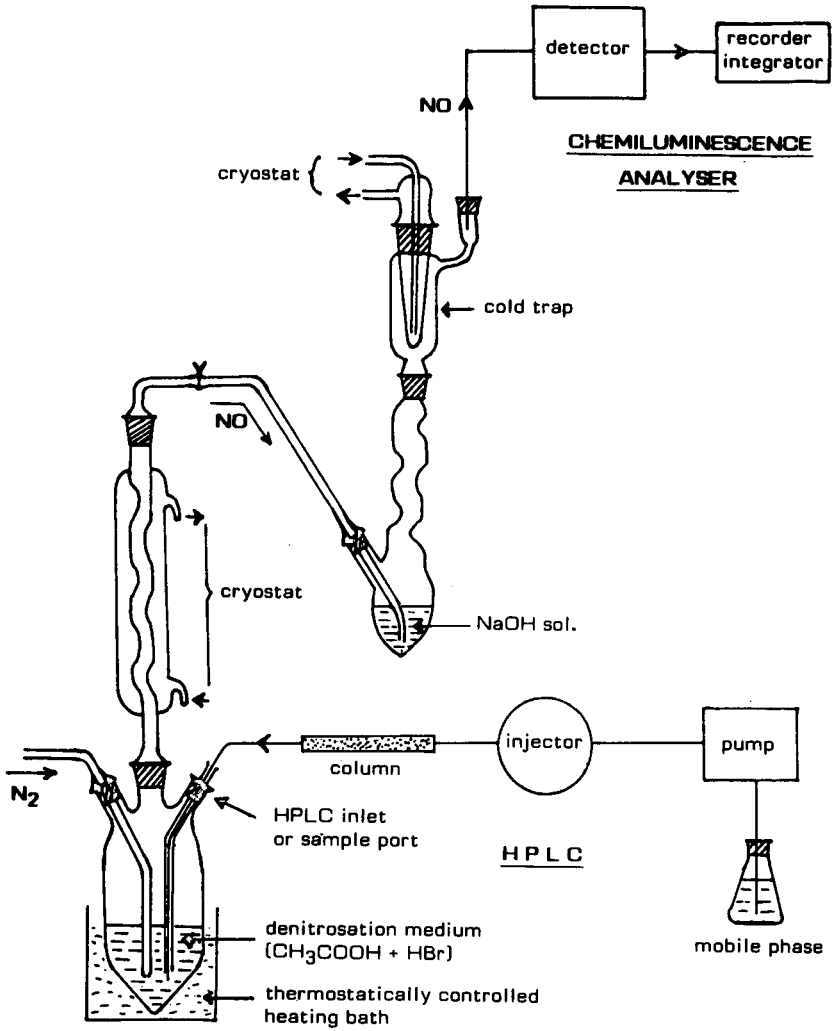

Fig. 1. Apparatus.

ic injector (79841 A). The column (250 mm × 2.1 mm) was packed with Spherisorb 5-μm silica. The column outlet was connected to the denitrosation reactor via a PTFE capillary inserted through a glass tube.

The eluate was led directly into the reaction medium of 15 ml of 48% hydrogen bromide solution in 100 ml acetic acid, kept at a constant temperature of 80°C in a three-necked flask immersed in a thermostatically regulated heating bath. Denitrosation was immediate, and the nitric oxide liberated was swept out of the flask by a stream of nitrogen through three traps designed to remove water and reactants. These were, successively, a condenser, a bubbler containing 33% (w/v) aqueous sodium hydroxide and a cold trap. The condenser and the cold trap were fed with ethanol–water (2:3) at −4°C from a cryostat.

A classical atmospheric nitrogen oxide detector was used "Topaze" (COSMA). The nitric oxide, carried by the nitrogen stream, was mixed with ozone and then drawn by a pump through calibrated capillary tubes fitted to flow regulators. The gas flow was then led to a reaction chamber kept under vacuum by a second pump. The oxidation of nitric oxide by ozone generates excited nitrogen dioxide which releases photons. These are captured by a photomultiplier.

$$NO + O_3 \rightarrow O_2 + NO_2^* \rightarrow NO_2 + h\nu$$

The signal was amplified and converted either into vpm (volumes per million) of NO after calibration with a reference gas mixture (79 vpm NO) or recorded on an integrator (HP 3393 A).

Reagents

Glacial acetic acid and 48% hydrogen bromide were of RPE ACS quality (Carlo-Erba). Hexane and isopropanol were of HPLC quality (Rathburn). Reference N-nitrosamines were obtained from Sigma; they were: N-nitrosodiphenylamine (NDPhA) powder in sealed ampoules (Isopac); N-nitrosomorpholine (NMor) powder in sealed ampoules (Isopac); N-nitrosodimethylamine (NDMA) liquid in sealed ampoules (Isopac); N-nitrosopyrrolidine (NPyr) liquid in sealed ampoules (Isopac).

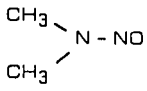

NDMA ($C_2H_6N_2O$) $m = 74.8$

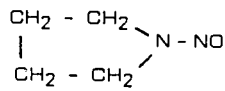

NPyr ($C_4H_8N_2O$) $m = 100.11$

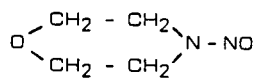

NMor ($C_4H_8N_2O_2$) $m = 116.11$

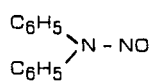

NDPhA ($C_{12}H_{10}N_2O$) $m = 198.2$

HPLC procedure

Stock solutions of N-nitrosamines were made up in the mobile phase: NDPhA, 3.48; NMor, 2.14; NDMA, 2.42; NPyr, 1.82 μmol/ml. The mobile phase was hexane–isopropanol (96.5:3.5), ultrasonically degassed. The flow-rate was 400 μl/min, and the volume injected was 20 μl.

RESULTS

Evaluation of the method

Specificity. Only substances that liberate nitric oxide, *i.e.*, nitrites and nitroso compounds under the operating conditions can be detected. Hence the method is absolutely specific to the N-nitrosamines studied.

Resolution. Under the HPLC conditions used, satisfactory separation of the four reference N-nitrosamines was achieved in 18 min (Fig. 2). The denitrosation reaction was rapid and did not affect the chromatographic resolution.

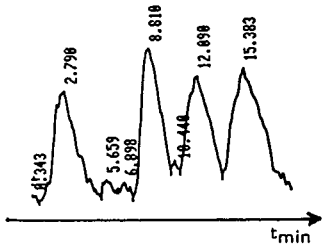

Fig. 2. HPLC chromatogram of a mixture of four N-nitrosamines (2 nmol injected). Mobile phase: hexane–isopropanol (96.5:3.5). Flow-rate: 400 μl/min. Retention times: NDPhA, 2.79; NMor, 8.81; NDMA, 12.09; NPyr, 15.38 min.

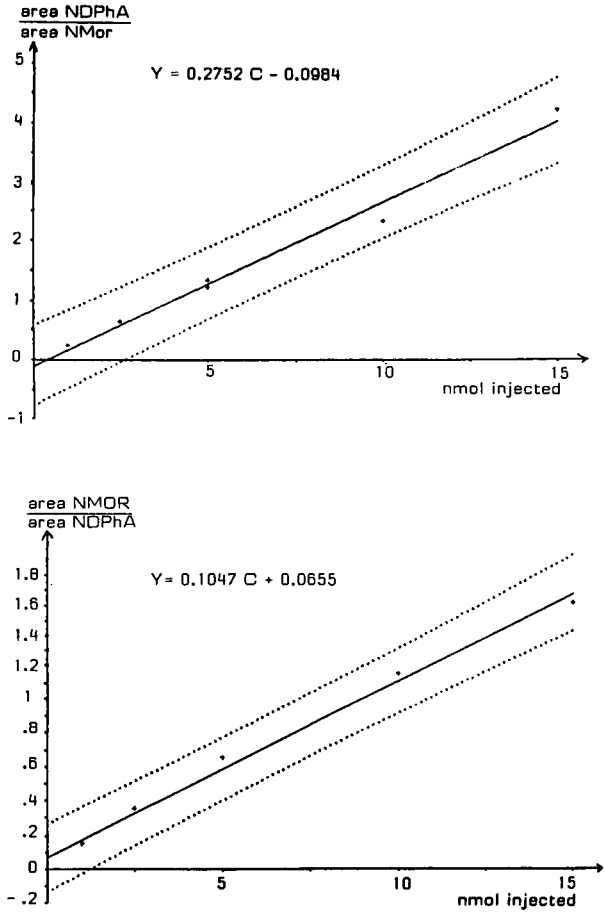

Fig. 3.

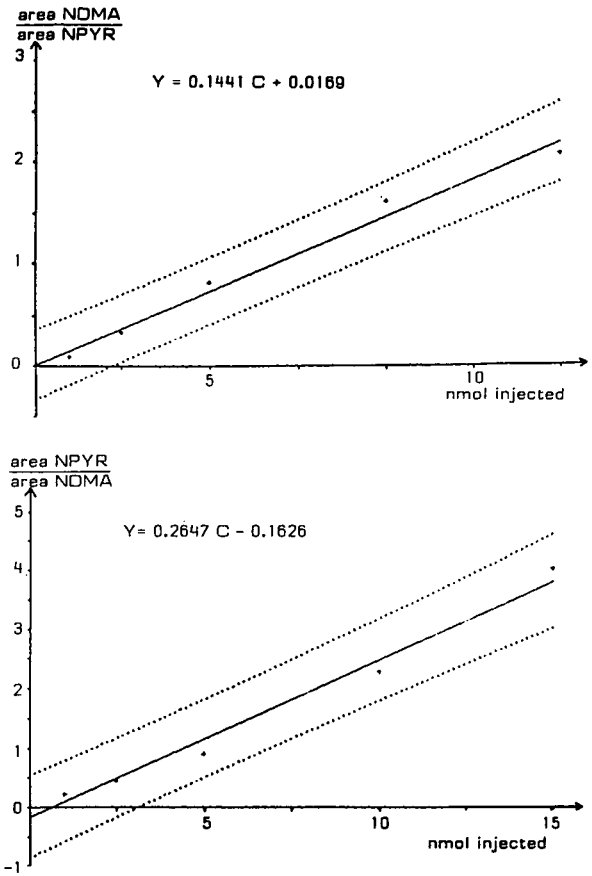

Fig. 3. Calibration graphs for the four N-nitrosamines used.

Linearity. Calibration curves for each N-nitrosamine were obtained over the range 0–15 nmol injected (0–0.75 μmol/ml), using one of the others as the internal standard (5 nmol). The detector response was linear over this range (Fig. 3). The correlation coefficients were: NDPhA, 0.992; NMor, 0.996; NDMA, 0.993; NPyr, 0.992.

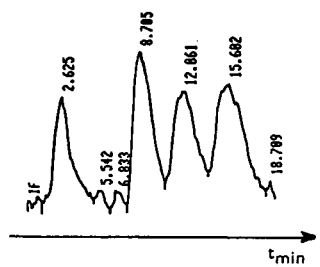

Fig. 4. Chromatogram of a pork product spiked with nitrosamines.

Precision. The repeatability and reproducibility were assessed using various dilutions of the stock solutions of N-nitrosamines in the HPLC mobile phase. The results are given in Table I.

Limits of detection. The detection threshold calculated from the mean value of the background noise ($n = 10$) plus three standard deviations ($\bar{M} + 3$) was of the order of 1 nmol injected: NDPhA, 0.6; NMor, 0.8; NDMA, 1.0; NPyr, 1.2 nmol.

Applications

This method was applied to the differential assay of N-nitrosamines in foodstuffs and especially in pork products. According to Klein and Debry[11], the extraction is performed with dichloromethane (2 × 5 ml) from a suspension of 1 g mixed sample previously homogenized with an Ultra Turrax in 3 ml distilled water. The pooled extracts are dried on anhydrous sodium sulphate and concentrated to 1 ml at 50°C in an evaporator Type Kuderna Danish before HPLC with chemiluminescence detection.

Fig. 4 shows a typical chromatogram of a dry cured ham spiked sample with 100 nmol/g of each N-nitrosamine studied. Their mean recovery is about 80%.

CONCLUSIONS

HPLC with denitrosation and chemiluminescence detection is applicable to the separation and individual assay of N-nitrosamines in solution. The method is specific to nitroso compounds, since it is based on their ability to release nitric oxide by chemical denitrosation. Evaluation of the resolution, linearity and reproducibility is satisfactory.

Therefore, this method can be applied to the differential assay of nitrosamines in pork products. Moreover, the application of this procedure to various kinds of samples including liquid and solid foodstuffs from animal or vegetal origin can be considered without major modifications.

ACKNOWLEDGEMENTS

This work was supported by the Ministry of Agriculture (Research contract No. 85/29 "06.12.85"). We also thank Mr. J. Queuille, glassblower at the Faculty of Pharmacy, Clermont-Ferrand, who made the glassware.

REFERENCES

1 T. Y. Fan, D. Fine and A. Lafleur, in P. N. Cheremisinoff and H. J. Perlis (Editors), *Analytical Measurements and Instrumentation for Process and Pollution Control,* Ann. Arbor Sci. Publ., Ann Arbor, MI, 1981, p. 273.
2 G. S. Drescher and C. W. Frank, *Anal. Chem.,* 50 (1978) 2118.
3 R. C. Massey, J. M. Baily, P. E. Key, D. J. McWeeny and M. E. Knowles, *Food Add. Contam.,* 1 (1984) 237.
4 N. P. Sen and S. J. Kubacki, *Food Add. Contam.,* 4 (1987) 357.
5 R. D. Cox, *Anal. Chem.,* 52 (1980) 332.
6 R. C. Doerr, J. B. Fox, L. Lakritz and W. Fiddler, *Anal. Chem.,* 53 (1981) 381.
7 C. L. Walters, P. N. Gillatt, R. C. Palmer and P. L. R. Smith, *Food Add. Contam.,* 4 (1987) 133.
8 B. Dang Vu, J. L. Paul, O. G. Ekindjian, J. Yonger, M. Gaudric and J. Guerre, *Clin. Chem.,* 29 (1983) 1860.
9 C. Pinche, J. P. Billard, A. M. Frasey, B. Dang Vu, J. Yonger, J. P. Poma, M. Saudan, H. Bargnoux, J. Petit and J. A. Berger, *Food Add. Contam.,* submitted for publication.
10 C. Rühl and J. Reusch, *J. Chromatogr.,* 328 (1985) 362.
11 D. Klein and G. Debry, *Ann. Nutr. Aliment.,* 34 (1980) 779.

Journal of Chromatography, 463 (1989) 207–211
Elsevier Science Publishers B.V., Amsterdam — Printed in The Netherlands

CHROM. 21 018

Note

Analysis of B_6 vitamers in foods using a modified high-performance liquid chromatographic method

ROLAND BITSCH* and JÖRG MÖLLER

University Paderborn, Department of Home Economics, Nutrition Section (FB 6), Warburger Str. 100, D-4790 Paderborn (F.R.G.)

(First received June 10th, 1988; revised manuscript received September 26th, 1988)

In recent years high-performance liquid chromatographic (HPLC) procedures, which are capable of separating and quantifying the various vitamin forms (vitamers), have been accepted as reliable, time sparing and sensitive methods for the determination of the pyridoxine content in foods and other biological materials. HPLC techniques have been presented by numerous authors and the detection limits are comparable to those of microbiological assays[1–15]. Nevertheless, the procedures described so far exhibit some disadvantages, summarized as follows:

(1) separation of the vitamers with the aid of ternary gradient elution techniques, which are poorly reproducible for routine work[1–3];

(2) elution with buffers of relatively high concentrations, *e.g.*, 0.5 *M* phosphate, which are not easy to handle and are able to crystallize within the columns and tubes[1,2,6];

(3) rather long retention times, $\geqslant$ 1 h (refs. 1, 2 and 5);

(4) incomplete separation of the several vitamers, mostly not including pyridoxic acid, which may be present in foods, though vitamin inactive[3,6,9,13,15].

Some procedures[4,5] are hardly reproducible[2]. Considering these problems we have developed a modified HPLC method for the separation of all B_6 vitamers including their phosphorylated metabolites (but without pyridoxine phosphate) as well as the inactive pyridoxic acid. The method is based on the procedure of Gregory and Feldstein[3] who employed reversed-phase chromatography with an ion-pair reagent. The most prominent modifications refer to the mode of elution, by means of a binary gradient, and the extraction medium using perchloric acid to extract also pyridoxic acid.

EXPERIMENTAL

Reagents

All chemicals, reagents and standards were of analytical or HPLC grade. 4-Pyridoxic acid (4-PA) and 4-desoxypyridoxine hydrochloride (DPN) were obtained from Sigma-Chemie (Deisenhofen, F.R.G.), alkaline phosphatase (specific activity 140 U/mg) from Boehringer (Ingelheim, F.R.G.), B_6 vitamers and all other chemicals from Merck (Darmstadt, F.R.G.).

0021-9673/89/$03.50

Chromatographic conditions

An LKB HPLC gradient system (Pharmacia LKB, Freiburg, F.R.G.) consisting of an HPLC pump, syringe-loading sample injector Rheodyne Model 7125 with an 100-μl loop and solvent conditioner for solvent degassing, HPLC controller, gradient mixer and mixing valve for low-pressure gradient mixing was utilized. For detection an Hitachi fluorescence detector Model F 1000 with a 40-μl flow cell (excitation 330 nm, emission 400 nm) was equipped with an Hitachi integrator Model D-2000 (Merck/Hitachi, Darmstadt, F.R.G.).

The analytical column was a LiChrospher RP-18, 5 μm, 125 mm × 4 mm (Merck LiChrocart No. 50943) with a guard column containing LiChrospher RP-18, 4 mm × 4 mm (Merck LiChrocart No. 50803). The separations were performed at 25°C. The mobile phase consisted of methanol (solvent A) and 0.03 *M* phosphate buffer pH 2.7 + 4 m*M* octanesulphonic acid (solvent B), delivered at a flow-rate of 1.5 ml/min. A binary gradient was formed as follows: 90% B and 10% A from 0 to 2 min; linear gradient from 90% B at 2 min to 60% B at 12 min; 60% B and 40% A from 12 to 17 min; 60% B from 17 min to 90% B at 19 min.

For post-column derivatization, 0.5 *M* phosphate buffer pH 7.5 was mixed with sodium hydrogensulphite (10 μl of a 37% aqueous solution per ml buffer) with a flow-rate of 0.07 ml/min. Desoxypyridoxine (DPN) served as an internal standard.

Sample preparation and extraction procedure

All steps for extraction of food samples must be conducted under subdued light and using brown glass vessels. A representative minced food sample, *e.g.*, 0.5–2.0 g, was mixed with 50 nmol DPN as an internal standard and homogenized in an ice-bath with 5 ml ice-cold 0.1–0.5 *M* perchloric acid (dependent on protein content) using an Ultra-Turrax homogenizer. After filtration or centrifugation, the supernatant was adjusted to pH 7.5 with 5 *M* and finally 0.1 *M* potassium hydroxide and kept in an ice-bath for another 10 min. After an additional filtration step, the clear filtrate was then adjusted to pH 4.0 with 0.1 *M* hydrochloric acid and filtered through a 0.45-μm pore size membrane filter (Minisart NML, Sartorius/Göttingen, F.R.G.).

For dephosphorylation of vitamers, 20 μl alkaline phosphatase suspension (10 mg/ml, 140 U/mg) were added to an aliquot of the solution taken after the last filtration step, followed by incubation for 30 min at 25°C. Adjustment to pH 4.0 and filtration through a membrane filter were performed as above.

An 100-μl volume of the clear filtrate before and after dephosphorylation were used for the HPLC analysis.

RESULTS AND DISCUSSION

The chromatographic procedure used enables rather good separations of all vitamers as well as pyridoxic acid (4-PA), but excluding pyridoxine phosphate, which occurs only in minute amounts in foods. The binary gradient employed for elution is well reproducible; separations are performed in a relatively short time of about 30 min.

The chromatogram of a standard mixture (100 n*M* solution in 0.1 *M* acetate buffer, pH 4.0, 400 n*M* DPN) is shown in Fig. 1. The lowest detectable amount of substances separated corresponds to 0.4–0.7 pmol. This is lower than the detection

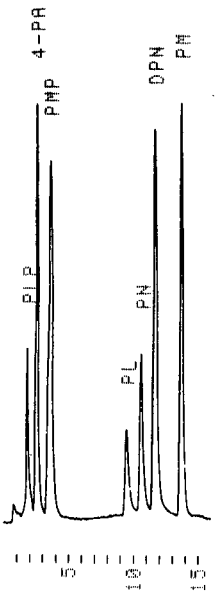

Fig. 1. Chromatogram of vitamin B_6 standard. Time scale in min.

limits reported to date, to the best at our knowledge. Linearity of the dose response between the peak height and the vitamer concentration is achieved up to at least 1 μM.

The within-day coefficients of variation determined for 100 nM solutions ranged from 1.1 (DPN) to 5.0% (PLP), those of the day-to-day variation from 6.2% (4-PA) to 10.3% pyridoxamine 5′-phosphate (PMP). When food samples are analyzed, however, the separation and resolution of PLP, being eluted first, may be inadequate since it is eluted very close to the elution front. For a suitable verification of peak identity, a duplicate of the food sample is treated with alkaline phosphatase. As shown for the case of raw pork liver, the peaks of the phosphorylated derivatives in the sample, PLP and PMP, have disappeared and the peaks of pyridoxal (PL) and pyridoxamine (PM) have increased (Fig. 2).

The technique of post-column derivatization with sodium hydrogensulphite as first described by Coburn and Mahuren[1,2] leads to an enhancement of the fluorescence intensity mainly of PLP and 4-PA. Additionally, the fluorescence of interfering matrix substances that might overlap the peaks of B_6 vitamers is minimized due to the simultaneous shift from an acidic to a weakly alkaline pH. Thus, particularly in food samples with a rather complex matrix, *e.g.*, pork liver, such interfering peaks rarely occur.

In Table I the concentration of the vitamers and of 4-PA in raw liver as well as in pasteurized milk is given. Noteworthy is the relatively high amount of the vitamin inactive 4-PA in milk that was also found by Coburn and Mahuren[1]. Regarding the total content of vitamin B_6, it appears that our own results calculated from the concentration of the single derivatives correspond to the mean value of 40–45 μg B_6/dl given in food tables only after addition of the inactive pyridoxic acid[16,17].

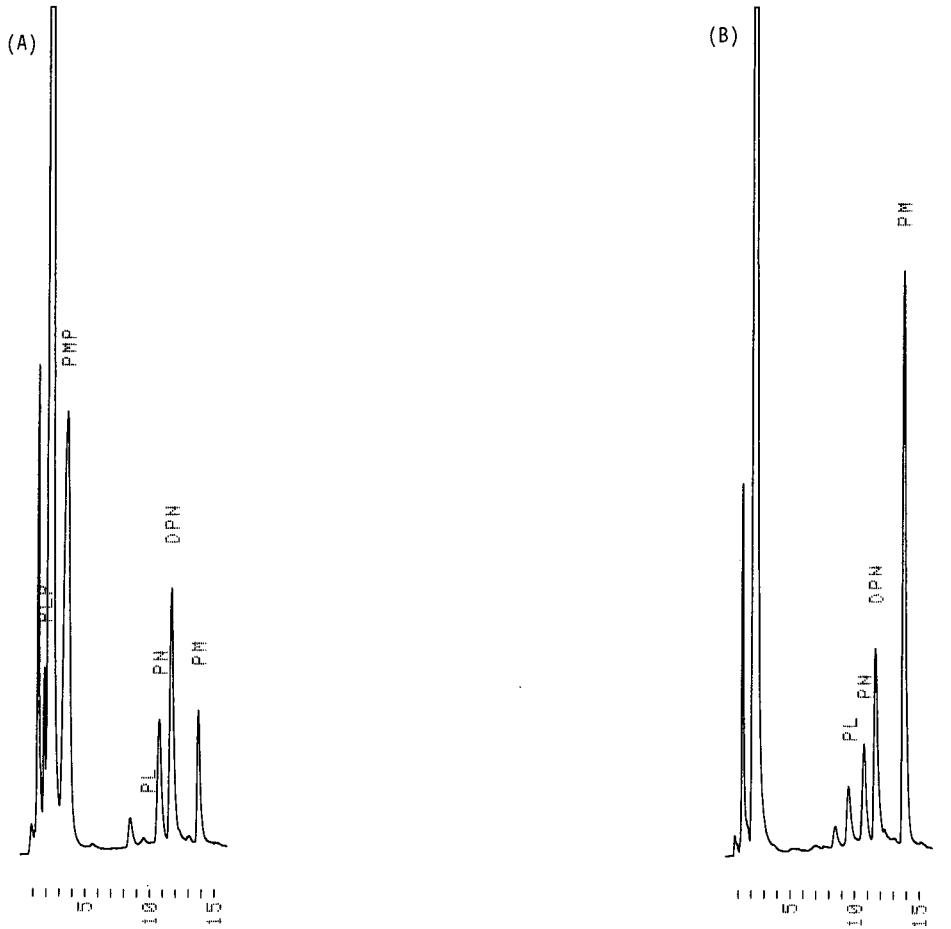

Fig. 2. (A) Separation of B_6 vitamers in a sample of raw pork liver. (B) Chromatogram of a sample of raw pork liver treated with alkaline phosphatase. Time scale in min.

TABLE I

CONTENT (nmol/g) OF B_6 VITAMERS IN RAW LIVER AND PASTEURIZED MILK

n.d. = Not detectable.

	PLP	*4-PA*	*PMP*	*PL*	*PN*	*PM*	*Σ*
Raw liver	7.2 ±0.7	n.d.	24.2 ±0.2	1.0 ±0.1	7.4±0.4	10.8 ±0.4	50.61≡850.3 μg/100 g
recovery (%)	89.2		96.0	95.8	101.8	96.3	
Pasteurized	0.35±0.06	0.65±0.03	0.19±0.01	1.18±0.02	n.d.	0.18±0.02	2.55≡ 43.5 μg/100 g
milk	94.9	101.4	96.8	95.3	96.2	92.4	
recovery (%)							

Recoveries were determined by spiking of representative food samples (0.5 g liver, 5.0 g milk) with vitamers (5 nmol) before extraction. Values for phosphorylated vitamers are given as their corresponding unphosphorylated compounds after treatment with phosphatase.

The results provide evidence of a reasonable reliability comparable to other HPLC methods.

ACKNOWLEDGEMENT

This research was supported by Deutsche Forschungsgemeinschaft, grant Bi 218/5-1.

REFERENCES

1 S. P. Coburn and J. D. Mahuren, *Anal. Biochem.*, 129 (1983) 310.
2 S. P. Coburn and J. D. Mahuren, *Methods Enzymol.*, 122 (1986) 102.
3 J. F. Gregory and D. Feldstein, *J. Agric. Food Chem.*, 33 (1985) 359.
4 J. T. Vanderslice and C. E. Maire, *J. Chromatogr.*, 196 (1980) 176.
5 J. T. Vanderslice, C. E. Maire, R. F. Doherty and G. R. Beecher, *J. Agric. Food Chem.*, 28 (1980) 1145.
6 A. K. Williams, *Methods Enzymol.*, 62 (1979) 415.
7 J. A. Pierotti, A. G. Dickinson, J. K. Palmer and J. A. Driskell, *J. Chromatogr.*, 306 (1984) 377.
8 L. A. Morrison and J. A. Driskell, *J. Chromatogr.*, 337 (1985) 249.
9 K. L. Lim, R. W. Young and J. A. Driskell, *J. Chromatogr.*, 188 (1980) 285.
10 J. F. Gregory, *Anal. Biochem.*, 102 (1980) 374.
11 A. Lui, L. Lumeng and T.-K. Li, *Am. J. Clin. Nutr.*, 41 (1985) 1236.
12 L. M. Bacon and D. E. Turk, *Nutr. Rep. Int.*, 35 (1987) 1035.
13 B. Bötticher and D. Bötticher, *Int. J. Vit. Nutr. Res.*, 57 (1987) 273.
14 A. Bognar, *Z. Lebensm.-Unters.-Forsch.*, 181 (1985) 200.
15 J. Schrijver, A. J. Speek and W. H. Schreurs, *Int. J. Vit. Nutr. Res.*, 51 (1981) 216.
16 S. W. Souci, W. Fachmann and H. Kraut, *Die Zusammensetzung der Lebensmittel-Nährwerttabellen*, Wiss. Verlagsgesellschaft, Stuttgart, 3rd ed., 1986/87.
17 A. A. Paul and D. A. T. Southgate, *McCane and Widdowson's The Composition of Foods*, Elsevier/North Holland Biomedical Press, Amsterdam, New York, Oxford, 4th ed., 1978.

Journal of Chromatography, 463 (1989) 212–215
Elsevier Science Publishers B.V., Amsterdam — Printed in The Netherlands

CHROM. 21 019

Note

Detection of proteolytic enzymes in fractions after liquid chromatography

IVO ŠAFAŘÍK
Laboratory of Analytical Chemistry, South Bohemian Biological Centre, Branišovská 31, 370 05 České Budějovice (Czechoslovakia)
(First received May 16th, 1988; revised manuscript received September 30th, 1988)

Proteinases are among the most intensively studied of enzymes. Many papers have been published about their chromatographic isolation and purification. During this process it is usually necessary to identify the fractions containing the desired proteolytic enzymes. Usually the standard assays for the determination of proteolytic activity are used for this purpose[1,2]. When a great number of fractions is to be tested, it may be time consuming and laborious.

A simple procedure for rapid detection of proteinases is described in this note. It is based on the hydrolysis of a very thin layer of proteinaceous insoluble chromolytic substrate (gelatin cross-linked with glutaraldehyde in the presence of a suitable dye[3,4]) by proteinases present in fractions after chromatography. Proteinase positive and negative fractions can clearly be distinguished in a short period of time.

EXPERIMENTAL

Materials

Gelatin for bacteriology, water-soluble nigrosin, test combination for the determination of trypsin activity and other chemicals were from Lachema (Czechoslovakia). Glutaraldehyde was from Fluka (Switzerland).

Trypsin (specific activity 35 nkat/mg using N-α-tosyl-L-arginine-4-nitroanilide as substrate) was obtained from Léčiva (Chechoslovakia). Alkaline bacterial proteinase produced by an alkalophilic strain of *Bacillus* sp. (declared specific activity 220 000 D.U. per g) was obtained from the Research Institute of Fat Industry, Rakovník, Czechoslovakia. Lysozyme from chicken egg white was from Drůbežářský průmysl (Czechoslovakia). GelBond film was from Marine Colloids Division, U.S.A.

The glass plates used for the preparation of gelatin plates were thoroughly washed in a detergent solution, rinsed with water and dried in a dust-proof chamber.

Preparation of gelatin plates

Gelatin (2 g) and water-soluble nigrosin (1 g) were dissolved in 100 ml of water with heating in a bath of boiling water. The warm solution was clarified by centrifugation and supernatant was poured on glass plates or hydrophilic plastic sheets (GelBond film). Usually 5 ml of solution were used to cover 8 cm × 8 cm plates or

0021-9673/89/$03.50

sheets. After approximately 30 min, the solution was poured off from the plates or sheets; only a very thin layer of the solution should remain on them. Plates were allowed to dry in a perfectly horizontal position at laboratory temperature overnight. Dry plates were immersed in 1–2% glutaraldehyde solution for 30–60 min to cross-link the gelatin molecules, thoroughly washed with water and dried at ambient temperature. The prepared gelatin plates can be stored at room temperature for at least 6 months without any damage.

Fast protein liquid chromatography

The fast protein liquid chromatography was performed on a FPLC system (Pharmacia, Sweden) equipped with a MONO S HR 5/5 column using 0.05 mol dm^{-3} phosphate buffer, pH 7.0, as a mobile phase A, and the same buffer containing 1 mol dm^{-3} sodium chloride as a mobile phase B. The flow-rate was 1 ml/min, and 0.5-ml fractions were collected. The distribution of total proteins in the effluent was monitored at 280 nm.

Detection of proteinases in eluted fractions

Two simple procedures can be used, depending on the pH of the effluent.

pH of effluent is close to the pH optimum of detected proteinase. A 10-μl volume of solution was taken from each fraction and pipetted onto the surface of a gelatin plate to form a small drop. The incubation was carried out at ambient temperature or in a thermostat for 10–20 min after the application of the last drop. The plate was then thoroughly rinsed with running water so that the gelatin fragments originating from the action of proteolytic enzymes were washed away. To speed up this procedure, hot (50–60°C) running water can be used without any risk. Colourless spots indicate the presence of proteinases.

pH of effluent is far away from the pH optimum of detected proteinase. First 10-μl drops of a suitable buffer were placed on the surface of a gelatin plate and then 10-μl aliquots from fractions were added to the buffer drops. The subsequent procedure was as described above.

RESULTS AND DISCUSSION

A 500-μl volume of a model mixture containing 0.5 mg of trypsin and 0.5 mg of lysozyme was used for chromatography on a column of cation exchanger. Fig. 1 shows the distribution of total proteins. Thirty fractions containing 0.5 ml of effluent were collected. The detection of proteolytic activity was performed as described in the Experimental; 10-μl aliquots were applied directly to the surface of a gelatin plate. Hydrolysis of the gelatin layer was observed in spots corresponding to fractions 12–14 (see Fig. 2). These fractions corresponded exactly to the trypsin peak (see Fig. 1, arrows indicate the presence of proteolytic activity).

The sensitivity of the detection was verified using standard solutions of trypsin and alkaline bacterial proteinase in 0.05 mol dm^{-3} Tris–HCl buffer, pH 8.5, containing 0.01 mol dm^{-3} calcium chloride. The properly prepared gelatin plates (thickness of gelatin layer measured by an optical microscope was 0.003–0.010 mm on different plates; on a single plate the layer was homogeneous) were hydrolyzed within 10–20 min

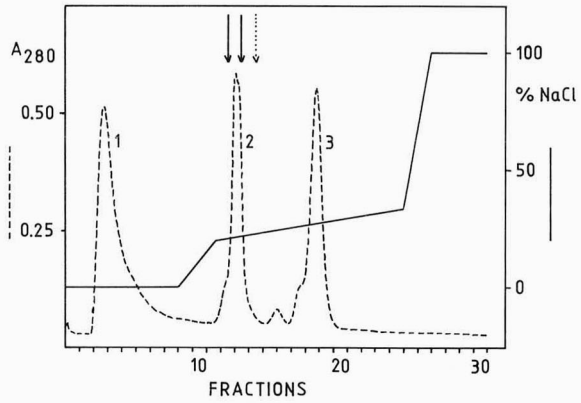

Fig. 1. Fast protein liquid chromatography of 500 μl of a model mixture containing 0.5 mg of trypsin and 0.5 mg of lysozyme on a MONO S HR 5/5 column. Buffers: A, 0.05 mol dm^{-3} phosphate buffer, pH 7.0; B, 0.05 mol dm^{-3} phosphate buffer, pH 7.0, and 1 mol dm^{-3} sodium chloride. Flow-rate 1 ml/min. --------- = Absorbance at 280 nm (protein content); ——— = gradient of sodium chloride; ——→ = presence of strong proteolytic activity; ·····→ = presence of weak proteolytic activity. Peaks: 1 = unidentified proteins; 2 = trypsin; 3 = lysozyme.

at ambient temperature by solutions containing 20 μg of trypsin per ml or 200 μg of bacterial alkaline proteinase per ml. The sensitivity depends, of course, on the thickness of the gelatin layer; the 0.070 mm thick gelatin layer (prepared only for comparison) was not hydrolyzed in 60 min by a solution containing 100 μg of trypsin

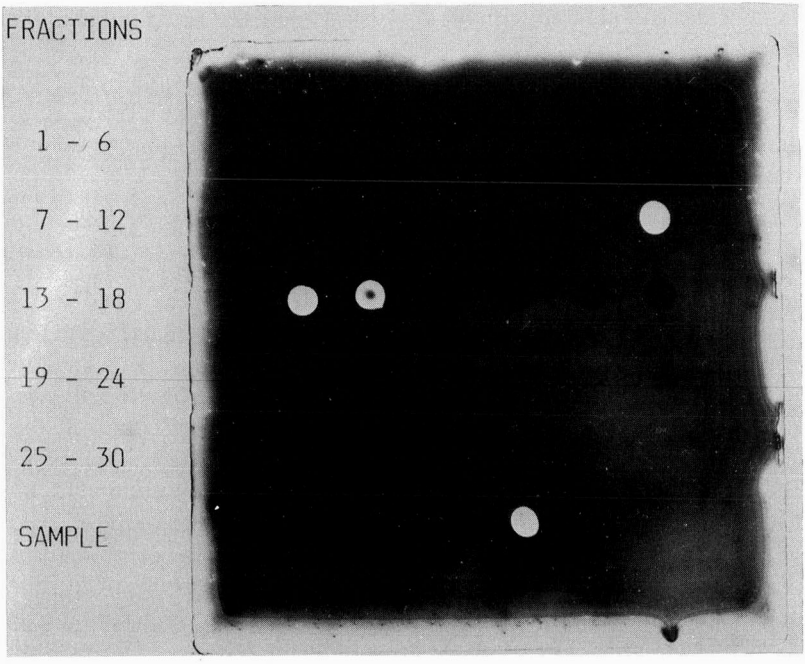

Fig. 2. Gelatin glass plate after detection of proteolytic activity in fractions. Trypsin is present in fractions 12–14.

per ml. No differences were observed between the properties of gelatin glass plates and gelatin plastic sheets.

Other proteinases, *e.g.*, chymotrypsin, various bacterial and mould extracellular proteinases hydrolyzed the gelatin layer and can be detected, too.

The pH of the effluent may play an important rôle in the detection of proteinases. When it is far away from the pH optimum of the detected proteinase, it can be adjusted to the appropriate value by mixing a drop of a suitable buffer with a drop of tested solution directly on the gelatin plate.

It is advisable to see first whether the sample to be separated contains proteinases which are capable of hydrolyzing the gelatin layer.

The procedure described can significantly shorten the time necessary for evaluation of fractions and thus speed up the whole separation process.

REFERENCES

1 P. Wunderwald, in H. U. Bergmeyer (Editor), *Methods of Enzymatic Analysis*, Vol. V, Verlag Chemie, Weinheim, 1984, p. 258.
2 L. Fukal and J. Káš, *Chem. Listy*, 78 (1984) 1176.
3 I. Šafařík, *J. Biochem. Biophys. Methods*, 14 (1987) 355.
4 I. Šafařík, *Biotechnol. Techniques*, 1 (1987) 135.

Journal of Chromatography, 463 (1989) 216–221
Elsevier Science Publishers B.V., Amsterdam — Printed in The Netherlands

CHROM. 21 072

Note

Determination of residual dimethyl sulphate in a lipophilic bulk drug by wide-bore capillary gas chromatography

MARK SEYMOUR
Control Division, Upjohn Ltd., Fleming Way, Crawley, West Sussex RH10 2NJ (U.K.)
(First received August 12th, 1988; revised manuscript received October 25th, 1988)

Dimethyl sulphate is widely used as a methylating agent for organic synthesis. It is volatile and readily hydrolysable so it seems unlikely that dimethyl sulphate would remain in any bulk drug substance after final processing. However, to verify that this potentially hazardous material[1] is not present, a routinely applicable gas chromatographic–flame ionization detection (GC–FID) method capable of detecting low levels was developed.

Previously published methods[2,3] both made use of packed-column GC with consequent high limits of detection and long analysis times. The method described below makes use of a J&W DB-1 Megabore, (30 m × 0.53 mm I.D., film thickness 5 μm) fused-silica wall-coated open-tubular (WCOT) wide-bore capillary column. This column was chosen because it is stable, inert and robust and is widely available. Normally, material like dimethyl sulphate would be chromatographed using a more polar stationary phase, but the inertness of the fused-silica column maintains good peak shape and the relatively thick film prevents column overload.

Hexane was chosen as the solvent because the drug is highly soluble in this solvent, it is inert to attack by dimethyl sulphate and its volatility is not excessive. The poor response of the flame ionization detector to dimethyl sulphate, due to the low carbon content and high oxidation state of the molecule, forced the use of a high concentration of drug in samples (approximately 10%, w/w) in order to achieve a sufficiently low limit of detection. Greater sensitivity may well be achievable using, say, a sulphur-specific detector although such detection systems may not be routinely available to all laboratories.

Matrix effects such as interfering peaks from the drug or trapping of the dimethyl sulphate by drug residues in the injector port were shown to be absent.

Loss of dimethyl sulphate from spiked samples of bulk drug was also investigated and losses (probably by volatilisation) were found to be marked when spiked drug was exposed to open atmosphere.

The method is linear, rapid (analysis time less than 5 min) and precise. It is suitable for use as a routine quantitative assay for dimethyl sulphate and is likely to be applicable to a variety of other bulk drug materials.

EXPERIMENTAL

Instrumentation

The chromatographic system consisted of a Hewlett-Packard 5890 gas chromatograph with a Hewlett-Packard 7673A auto-injector, a Hewlett-Packard split/splitless injector, a J&W DB-1 Megabore 30 m × 0.53 mm I.D. column, (5 μm film thickness), a Hewlett-Packard flame ionization detector and a Hewlett-Packard 3350A laboratory automation system for signal integration.

Conditions

Carrier gas: helium at 51 kPa (7.5 p.s.i.) producing a linear gas velocity of 59 cm s^{-1}. Injector: 140°C, splitless mode, purge after 30 s. Detector: 200°C, hydrogen at 150 kPa (22 p.s.i.), air at 250 kPa (37 p.s.i.). Injection volume: 2 μl. Oven temperature: 100°C. Split vent flow: 40 ml min^{-1}. Septum purge: 4 ml min^{-1}. Amplifier range: 2^5.

Materials

Hexane solvent (HPLC-grade) was obtained from FSA (Loughborough, U.K.). The dimethyl sulphate (99 + % Gold Label) was obtained from Aldrich (Gillingham, U.K.).

Preparation of standards

Standards were prepared in hexane at concentrations of 3–700 μg ml^{-1} dimethyl sulphate (nominally) with 5 nl ml^{-1} toluene as internal standard. Weighing of the dimethyl sulphate was carried out in a sealed syringe with the dimethyl sulphate being dispensed directly into the solvent after the weighing operation. This was done to prevent any loss by evaporation.

Preparation of samples

Samples were prepared by accurately weighing approximately 100 mg of the bulk drug into a suitable vial and adding 1.00 ml of an internal standard solution containing 5 nl ml^{-1} toluene in hexane. The vial was then sealed and the drug dissolved with gentle warming. A 2-μl volume of this solution was injected into the GC system using the conditions described above. All manipulations were carried out quickly and containers were kept closed with minimum headspace whenever possible in order to minimise evaporation as well as to reduce operator exposure to dimethyl sulphate.

RESULTS AND DISCUSSION

Linearity, precision and method performance

A typical chromatogram for a 100-μg ml^{-1} standard of dimethyl sulphate with toluene as internal standard is shown in Fig. 1. Linearity of response was established for solutions containing 3–700 μg ml^{-1} dimethyl sulphate with toluene as internal standard. The following regression line was calculated for the data:

$$\text{Response ratio} = 0.01027\,[(CH_3)_2SO_4]\ (\mu g\ ml^{-1}) - 0.01003$$

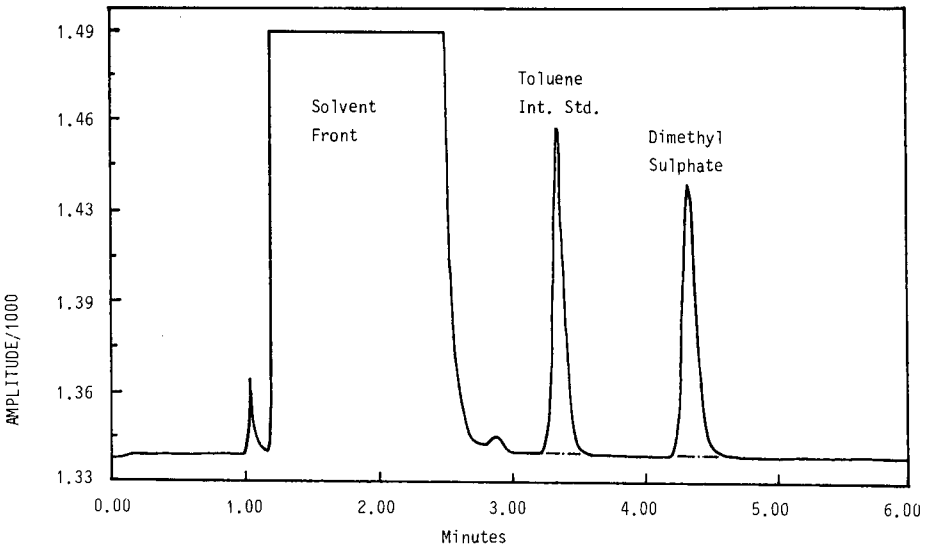

Fig. 1. Typical chromatogram for a 100-μg ml^{-1} dimethyl sulphate standard.

with a correlation coefficient (r) of 1.000. The probability that intercept is zero is 0.0497. The small negative intercept was probably due to the difficulty the integration system had in assigning an accurate baseline to the dimethyl sulphate peak in the low-concentration standards. This in turn was due to the digital noise seen in the signal recorded by the integrator (see Fig. 2 and also *Limit of detection* for further

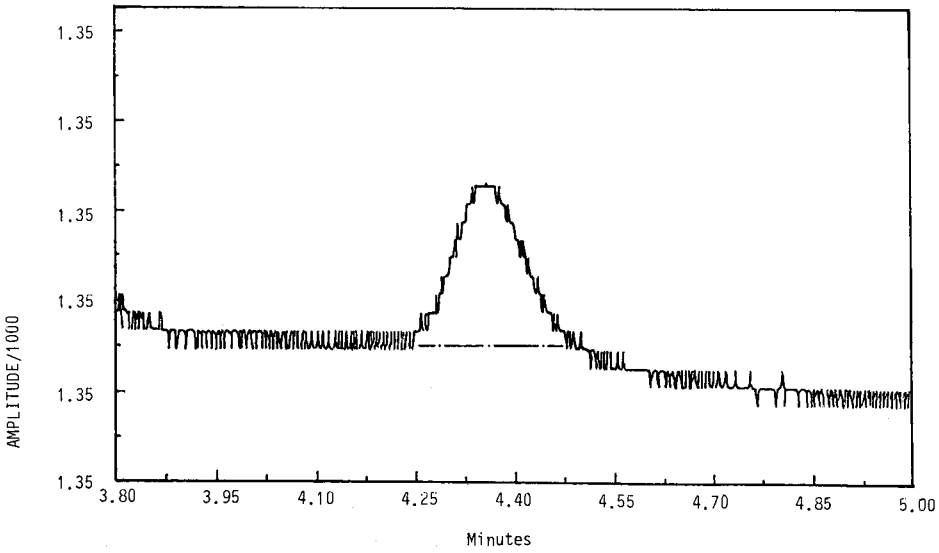

Fig. 2. Typical dimethyl sulphate peak for a 3-μg ml^{-1} standard. Note high baseline assignment.

discussion). The negative intercept would only be significant at low concentrations so quantitation is best carried out using at least bracketing standards when low levels are being determined.

The response ratios from six replicate injections of a 100 μg ml^{-1} standard containing 5 nl ml^{-1} toluene as internal standard gave a relative standard deviation (R.S.D.) of 0.52%, showing that the method exhibits good precision. Peak shape was found to be good, even at 700 μg ml^{-1}. However, chromatographic efficiency was quite poor for this type of system with only 4884 effective plates being generated for the 700 μg ml^{-1} dimethyl sulphate peak. This phenomenon may well be due, at least in part, to the use of a large volume (2 μl) injection in the splitless mode; a retention gap may help to alleviate this. It may also be that the mass-transfer kinetics are particularly slow for this material.

No interfering peaks were observed in the batch of hexane used. Furthermore, trapping of dimethyl sulphate by the bulk drug injected with the samples was shown to be absent: approximately 100 mg drug were added to 1.00 ml of the 70 μg ml^{-1} standard and the assay results obtained with and without added drug were not significantly different.

On account of the large amount of drug substance being injected, it is necessary to "bake out" the GC column every so often by raising the injector and detector temperatures to about 250°C and the column temperature to about 225°C for at least 1 h. It is also advisable to inject clean solvent to wash the injector port.

It was noted that using such a high concentration of bulk drug in the sample preparation could lead to the drug recrystallising from the sample solution after a few hours. This is unlikely to present a problem since the analysis time is so short and furthermore, the recrystallisation of the bulk drug is unlikely to affect the much lower concentration of dimethyl sulphate in the supernatant.

Limit of detection

The limit of detection was estimated by calculating the concentration of dimethyl sulphate at a signal-to-noise ratio of 3. This was done using a 3 μg ml^{-1} standard of dimethyl sulphate. The chromatogram is shown in Fig. 2 and from this, the limit of detection was estimated to be 1.2 μg ml^{-1} dimethyl sulphate which is equivalent to 12 μg g^{-1} dimethyl sulphate in bulk drug.

The limit of detection may be improved slightly by decreasing the "Range" setting on the HP 5890 amplifier but excessive amplification results in a noisy baseline and the gain in sensitivity achieved by this approach is limited.

Loss of dimethyl sulphate from bulk drug after spiking

Spiking of the bulk drug with a known level of dimethyl sulphate proved to be awkward on account of the ease with which dimethyl sulphate is lost on contact with open atmopshere. A primary objective in such an experiment is to ensure a homogeneous distribution of the spike throughout the bulk drug; the first attempt at achieving this centred around dissolving the drug in a solution of dimethyl sulphate in hexane and evaporating the hexane over a stream of nitrogen. Unfortunately, virtually all of the dimethyl sulphate was lost, probably by evaporation, using this approach.

The next approach taken was to melt the drug (1.9287 g) and add a known amount of dimethyl sulphate (9.8 mg) from a syringe directly to the melt in a stop-

TABLE I

LOSS OF DIMETHYL SULPHATE FROM SPIKED BULK DRUG STORED IN A CLOSED CONTAINER

Sampling time (h)	*Concentration dimethyl sulphate in bulk drug (%, w/w)*	*Percentage of initial concentration*
0	0.415	100.0
2	0.359	84.7
4	0.340	80.3
45	0.298	70.4
48	0.266	62.8

pered flask. The contents were then swirled vigorously. On cooling the spiked drug solidified and was then broken up using a spatula to give smaller pieces. This method was quite successful giving a recovery of 83.6% of the initial spiking level when analysed using the above method. This spiking process therefore resulted in a sample of bulk drug containing 0.424% (w/w) dimethyl sulphate. Good agreement between replicate analyses implied that the spiking was homogeneous.

Duplicate samples of the spiked drug were taken and assayed for dimethyl sulphate at intervals of 2, 4, 45 and 48 h. Between sampling, the spiked drug was kept in a tightly stoppered 50-ml conical flask. The results of the assays are shown in Table I. Approximately 4–10% of the dimethyl sulphate content was lost at each sampling regardless of the time between samples. This implies that the loss of the dimethyl sulphate is not due to degradation by reaction with the bulk drug and is probably caused by volatilisation on sampling. However degradation by, for example, moisture in the headspace has not been ruled out.

This loss was further investigated by placing the conical flask containing the spiked drug in a fume cupboard with the fan on and the flask stopper removed. Initial duplicate samples were taken and assayed as before followed by subsequent duplicate samples at 1, 2.5 and 5 h. The results, given in Table II, show that loss of the dimethyl sulphate is quite rapid despite the bulk drug existing as coarse aggregates. This sup-

TABLE II

LOSS OF DIMETHYL SULPHATE FROM SPIKED BULK DRUG STORED IN AN OPEN CONTAINER

Sampling time (h)	*Percentage of initial concentration*
0	100.0
1	56.6
2.5	48.7
5	15.5

ports the view that the dimethyl sulphate is lost on account of its exposure to the atmosphere and not because of any reaction with the bulk drug.

CONCLUSIONS

Dimethyl sulphate was chemically stable in the bulk drug but exposure to an open atmosphere results in significant loss of dimethyl sulphate. Sampling should, therefore, be carried out in such a way as to minimise exposure of the bulk drug to the atmosphere. On examination, none of the batches of bulk drug manufactured to date was found to contain any dimethyl sulphate at or above the limit of detection of 12 $\mu g\ g^{-1}$.

REFERENCES

1 M. Windholz (Editor), *The Merck Index*, Merck & Co., Rahway, NJ, 9th ed., 1976, p. 433, No. 3246.
2 N. M. Turkevich, S. I. Tereshchuk and O. M. Tereshchuk, *Farmatsiya (Moscow)*, 27 (1978) 79–80.
3 I. A. Zheltukhin, N. I. Glybochko, A. S. Sobolev and T. S. Maslakova, *Zavod. Lab.*, 50 (1984) 21.

Journal of Chromatography, 463 (1989) 222–226
Elsevier Science Publishers B.V., Amsterdam — Printed in The Netherlands

CHROM. 21 012

Note

Reversed-phase high-performance liquid chromatographic analysis of the reaction mixture occurring in the production of a synthetic diester lubricant

E. PAPP*
Research Group for Analytical Chemistry of Hungarian Academy of Sciences, P.O. Box 158, H-8201 Veszprém (Hungary)
and
I. NAGY
Institute of Hydrocarbon and Coal Processing, Veszprém University of Chemical Engineering, Veszprém (Hungary)
(First received June 22nd, 1988; revised manuscript received September 27th, 1988)

A simple, rapid reversed-phase liquid chromatographic method has been developed to study the kinetics of esterification in the production of the synthetic lubricant di(2-ethylhexyl)sebacate using an octylsilica stationary phase and methanol–aqueous phosphate buffer eluents. By the use of suitable eluent compositions and the quantity of raw materials (sebacic acid and 2-ethylhexanol), the intermediate monoester and di(2-ethylhexyl) sebacate can be determined.

In a reaction mixture containing diester, monoester, 2-ethylhexanol and sebacic acid, the concentration of the diester and the alcohol can be determined by gas chromatography (GC)[1] or by high-performance liquid chromatography (HPLC)[2,3], but the monoester and sebacic acid can be analysed only by GC after derivatization (esterification or silylation[4,5]). The advantage of the HPLC method developed is that no derivatization of the compounds is needed.

EXPERIMENTAL

The chromatographic system used consisted of a pump, Model 6000A, a differential refractometer detector (Varian LC 4010), a six-port injection valve (Model 7125, Rheodyne) with a 10-μl loop and a dual-channel recorder (Varian Model 9176).

The analytical column contained octylsilica (Nucleosil C_8), 150 mm × 4 mm I.D., 5 μm. The column temperature was maintained at 25 ± 0.5°C by means of a water-bath and a water-jacket.

The eluents were prepared as described[6] with an aqueous phosphate buffer of constant methanol concentration and sodium bromide concentration. The pH of the eluents was measured with a combined glass electrode calibrated with aqueous buffers.

The purity of the 2-ethylhexanol used for the preparation of the calibration graph was controlled by capillary GC (99.5%, w/w), and the sebacic acid was ana-

0021-9673/89/$03.50

lysed by LC (>99.5%, w/w). Standard diester [di(2-ethylhexyl)sebacate] was prepared by us and purified in several steps. Its composition was determined by capillary GC based on percentage areas: 94.5% (w/w) diester, 3.6% (w/w) 2-ethylhexanol. An HP5880A GC instrument with flame ionization detection (FID) and a chemically bonded, stationary phase, SE-54, were employed. For the determination of the diester and monoester in the reaction mixtures, the samples were dissolved in 85% (v/v) methanol–aqueous phosphate buffer eluent (5 m*M* sodium dihydrogenphosphate, 40 m*M* phosphoric acid, 20 m*M* sodium bromide). In order to analyse 2-ethylhexanol and sebacic acid, the samples were mixed with 70% (v/v) methanol–20 m*M* aqueous sodium bromide solution in a separation funnel. The diester cannot be dissolved in this solution (lower phase). The sebacic acid and the 2-ethylhexanol can be determined from the upper phase.

RESULTS AND DISCUSSION

In order to establish the optimum conditions for liquid chromatographic analysis, the retention of the compounds was studied as a function of the methanol concentration of the eluent (Fig. 1). The concentration of the sodium dihydrogenphosphate in the eluent was 5 or 25 m*M* and the concentration of the phosphoric acid was kept constant at 40 m*M*. The pH of the eluent was *ca.* 3.4. It was found that the retention of sebacic acid increased significantly by decreasing the pH of the eluent (pH 5 to 3.5). When the pH of the eluent was >4 the peak of sebacic acid appeared before the dead volume. The retention of the monoester, 2-ethylhexanol and the diester were independent of the eluent pH in range pH 3–5. The peak shapes of the monoester and diester improved slightly with the addition of the buffer. Fig. 1 shows that plots of log k' *vs.* methanol concentration are linear ($k' = V_R - V_0/V_0$ where $V_0 = 1.65$ cm^3). This suggests that the extent of retention can be controlled by the methanol concentration of the eluent. The slopes of the plots are significantly different.

The separation and determination of all the components could not be carried out with one particular eluent composition due to the large differences in polarity and solubility of the compounds. In order to decrease the retention of the diester (for a more rapid analysis), an eluent with a methanol concentration of 85% was applied. However, sebacic acid was eluted near the dead volume and was overlapped by the injection peak caused by dilution of the samples in methanol (Fig. 2).

The 85% methanol–aqueous phosphate buffer eluent (5 m*M* sodium dihydrogen phosphate–40 m*M* phosphoric acid–20 m*M* sodium bromide) was suitable for separation of the diester, monoester and 2-ethylhexanol, but not for the quantitation of 2-ethylhexanol because of its small retention volume (2.3 cm^3); it was eluted after the injection peak. In order to increase the retention of 2-ethylhexanol and sebacic acid, it is advisable to choose an eluent with a lower methanol concentration (<75%, v/v). By decreasing the methanol concentration to 70% (v/v) (25 m*M* sodium dihydrogenphosphate–40 m*M* phosphoric acid–20 m*M* sodium bromide) the peaks of 2-ethylhexanol and sebacic acid were satisfactory for their quantitation (Fig. 3). This eluent was not suitable for the analysis of the monoester because of the high retention of the latter. The samples were dissolved in 70% (v/v) methanol–aqueous 20 m*M* sodium bromide (instead of the eluent) for the preparation of the calibration graphs for sebacic acid and 2-ethylhexanol and for the investigation of the reaction mixture.

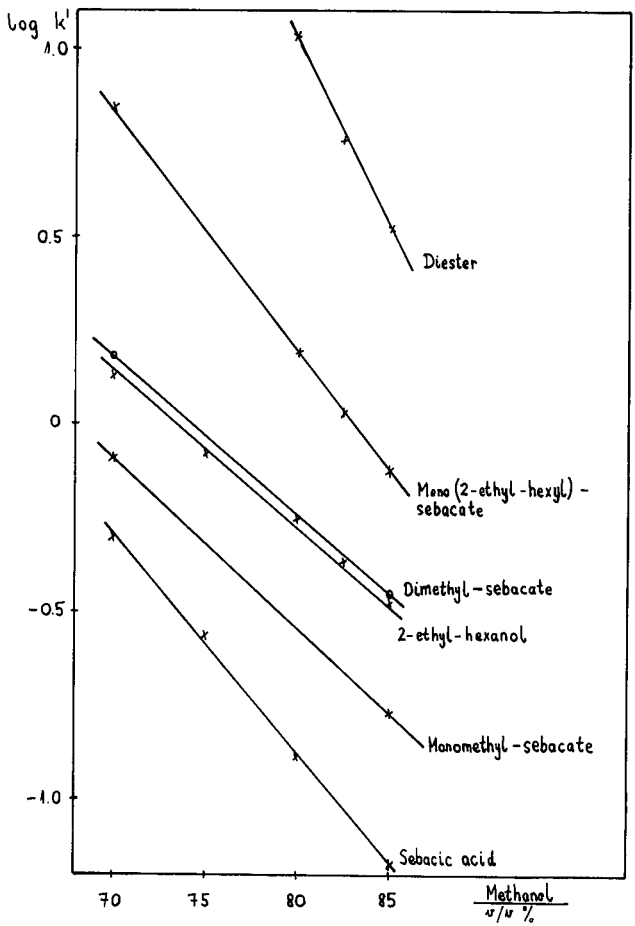

Fig. 1. Plots of log k' *vs.* methanol concentration of the eluent.

After a few days storage of the samples dissolved in the eluent, sebacic acid reacts with methanol forming monomethyl sebacate and dimethyl sebacate owing to acid catalysis of the esterification.

The elution curve of monomethyl sebacate is also shown in Fig. 3. The diester cannot be dissolved in 70% (v/v) methanol–aqueous mixture because it forms another phase. The two phases can be separated in a separation funnel. Standard solutions were used to demonstrate that sebacic acid and 2-ethylhexanol can be determined in the upper phase without any loss.

The determination of the concentration of the monoester in the reaction mixture was more difficult because no standard was available. In order to obtain a calibration graph for the monoester, a reaction mixture was prepared containing *ca.* 60% (w/w) monoester. The actual concentration of the monoester was calculated indirectly as follows:

$$\text{Monoester (\%, w/w)} = 100 - (\text{sebacic acid} + \text{2-ethylhexanol} + \text{diester})$$

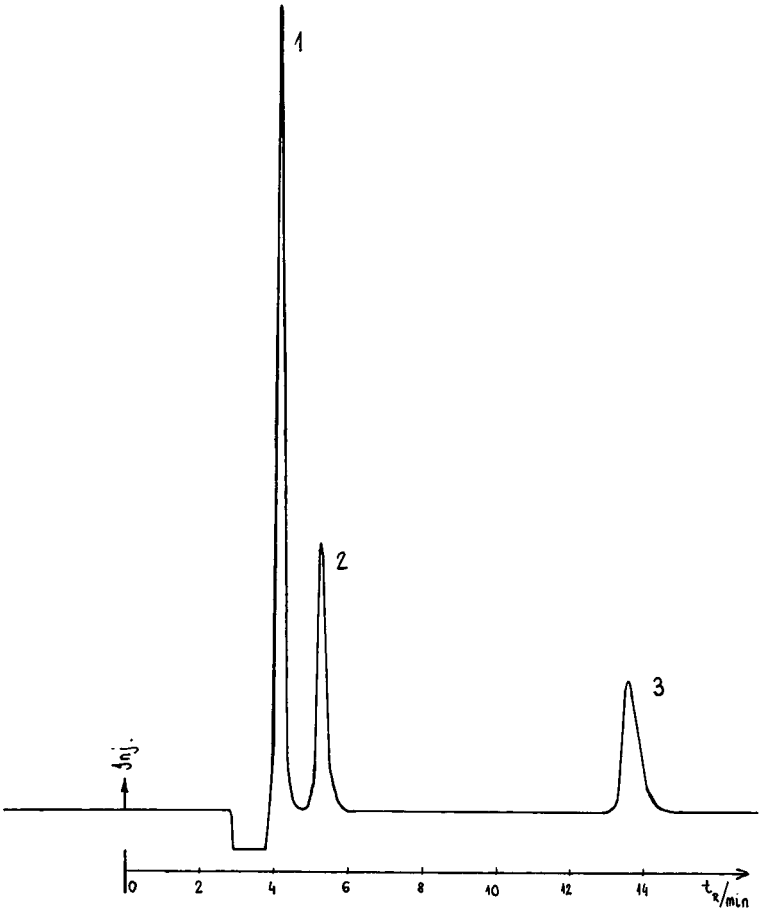

Fig. 2. Chromatogram of the reaction mixture. Eluent: 85% methanol–aqueous phosphate buffer (5 m*M* sodium dihydrogenphosphate, 40 m*M* phosphoric acid, 20 m*M* sodium bromide). Column: Nucleosil C_8 (150 mm × 4 mm). Detector: refractive index. Eluent flow-rate: 0.5 ml/min. Peaks: 1 = 2-ethylhexanol; 2 = mono(2-ethylhexyl)sebacate; 3 = di(2-ethylhexyl)sebacate.

The water formed in the esterification process was removed by azeotropic distillation. Traces amount of water were removed by sodium sulphate. The composition of this reaction mixture was: diester, 34.7 ± 0.1 (n = 11); sebacic acid, 1.2 ± 0.05 (n = 7); 2-ethylhexanol, 3.2 ± 0.1 (n = 7); monoester, 60.8 ± 0.1% (w/w) (n = 11). The calibration graph for the monoester was prepared by dilution of this reaction mixture. Data for the calibration were calculated from the peak areas of the compounds. The parameters of the calibration graphs for the four components are summarized in Table I.

The composition of the reaction mixtures was estimated using the equations corresponding to the calibration graphs shown in Table I. Based on the concentration data determined by this method, the optimum technological parameters were estimated. They will be discussed in detail in a subsequent paper.

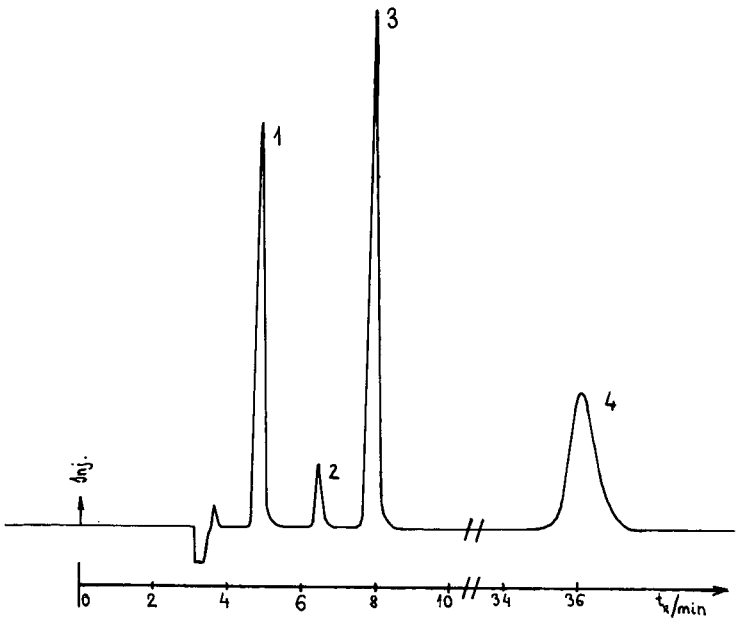

Fig. 3. Chromatogram of the reaction mixture. Eluent: 70% methanol–aqueous phosphate buffer (25 m*M* sodium dihydrogenphosphate, 40 m*M* phosphoric acid, 20 m*M* sodium bromide). Column: Nucleosil C_8 (150 mm × 4 mm). Detector: refractive index. Eluent flow-rate: 0.5 ml/min. Peaks: 1 = sebacic acid; 2 = monomethylsebacate; 3 = 2-ethylhexanol; 4 = mono(2-ethylhexyl)sebacate.

TABLE I

PARAMETERS OF THE CALIBRATION GRAPHS FOR SEBACIC ACID, 2-ETHYLHEXANOL, MONOESTER AND DIESTER

$A = a + bc$, where A is the peak area in mm^2, and c is the concentration of the injected sample in g/l (injection volume 10 μl).

Sample	*Range tested (g/l)*	*a*	*b*	*Regression coefficient*
Sebacic acid*	0–12	1.13	84.07	0.9999
2-Ethylhexanol*	0–12	−3.02	76.06	0.9998
Monoester**	0–15	2.13	82.83	0.9996
Diester**	0–24	11.88	97.81	0.9995

* Eluent: 70% methanol–aqueous phosphate buffer–sodium bromide.
** Eluent: 85% methanol–aqueous phosphate buffer–sodium bromide.

REFERENCES

1 A. Zeman, *Fresenius' Z. Anal. Chem.*, 310 (1982) 243.
2 F. E. Lockwood, L. J. Matienzo and B. Sprissler, *J. Chromatogr.*, 262 (1983) 397.
3 H. Hirata, K. Higuchi and S. Nakasato, *Yakugaku*, 33 (1984) 290.
4 J. Molnar-Perl, V. Fabian-Vonsik and M. Pinter-Szakacs, *Chromatographia*, 18 (1984) 637.
5 T. P. Mawhinney, R. S. R. Robinett, A. Atalay and M. A. Madson, *J. Chromatogr.*, 361 (1986) 117.
6 A. Bartha and G. Vigh, *J. Chromatogr.*, 260 (1983) 337.

Journal of Chromatography, 463 (1989) 227–228
Elsevier Science Publishers B.V., Amsterdam — Printed in The Netherlands

CHROM. 21 054

Note

Determination of the ophthalmic drug guaiazulene by high-performance liquid chromatography

E. VIDAL-OLLIVIER and G. SCHWADROHN
Laboratoires DULCIS, "Le Mercator", rue de l'Industrie, 98000 Monaco (Monaco)
R. ELIAS and G. BALANSARD*
Laboratoire de Pharmacognosie–Homéopathie, Faculté de Pharmacie, 27 Boulevard Jean Moulin, 13385 Marseille Cédex 05 (France)
and
A. BABADJAMIAN
ES IPSOI, Université d'Aix–Marseille III, Avenue Escadrille Normandie-Niemen, 13397 Marseille Cédex 13 (France)
(First received February 25th, 1988; revised manuscript received October 18th, 1988)

Guaiazulene (Fig. 1) is a sesquiterpene hydrocarbon used as an anti-inflammatory agent in numerous pharmaceutical preparations[1,2] and in particular in dermatology and ophthalmology, where it is used to treat conjunctivitis. As it is used therapeutically, it is important to possess specific methods for testing its purity and for its determination, especially as it is an unstable molecule.

Two high-performance liquid chromatographic (HPLC) methods have been used: reversed-phase HPLC on an octadecyl-bonded silica with a binary eluent [acetonitrile–water (77.5:22.5)[3]] and HPLC on a silica column with cyclohexane as eluent, the main peak containing guaiazulene being separated in a subsequent step by gas chromatography. A new HPLC procedure is described in this paper which makes possible the determination of guaiazulene in an eye-drop solution.

EXPERIMENTAL

A Waters Assoc. Model M 510 pump fitted with an U6K universal injector is used in combination with a UV 490 spectrophotometer. A Microinformatic digital data processor is used to calculate retention times and peak areas.

Separations are carried out under isocratic conditions using a μPorasil 10-μm column (30 cm × 4 mm I.D.) (Waters Assoc.). The mobile phase is *n*-hexane–ethyl acetate (98:2) at a flow-rate of 1 ml/min and detection is performed at 600 nm.

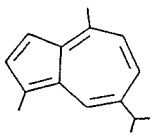

Fig. 1. Guaiazulene.

0021-9673/89/$03.50

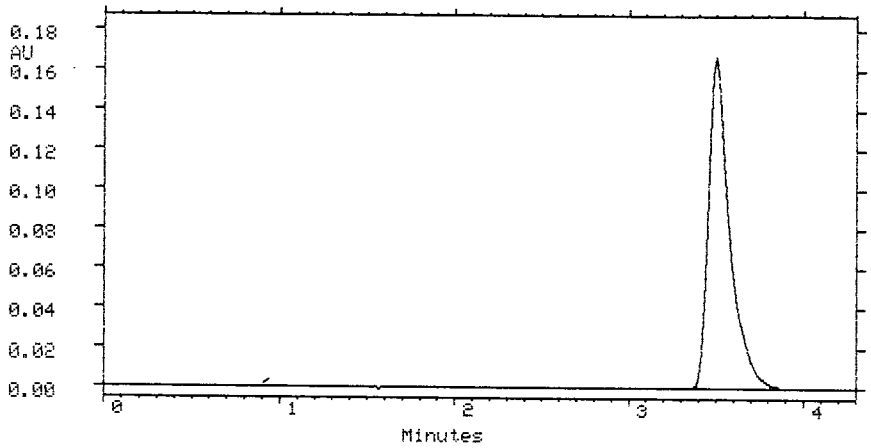

Fig 2. Typical chromatogram of eye-drop solution.

Standard

A 50-mg amount of guaiazulene (Merck, Ref. 4250) is dissolved in 100 ml of borate buffer prepared by dissolving 1.71 g of boric acid and 0.265 g of sodium borate in water and diluting to 100 ml. A 10-ml volume of the solution is extracted three times with 10 ml of light petroleum (b.p. 40–65°C) and the organic phases are filtered and evaporated to dryness. The residue is dissolved in 2 ml of ethyl acetate.

A 20-μl volume of 2.5 μg/ml solution of guaiazulene was injected.

Sample

A 10-ml sample of eye drops is extracted in the same way as for the standard. A 20-μl volume of sample solution is injected.

RESULTS AND DISCUSSION

The calibration graph is linear for guaiazulene concentrations in the range 0.125–2 mg/ml (n = 10) with a correlation coefficient of 0.9999. For the sample concentrations investigated the coefficients of variation are between 0.75 and 1.38%.

Fig. 2 shows that the peak for guaiazulene appears at 3.48 min. At the wavelength used (600 nm) there is no interference from other constituents.

The procedure is rapid, sensitive and reliable and is suitable for the routine determination of guaiazulene in eye-drop solutions.

REFERENCES

1 P. R. Rampal, J. L. Nono, R. Peterson, R. Barbaras and C. Cavenal, *Gaz. Med. Fr.*, 56 (1983) 2059.
2 Th. Saigot, *Med. Chir. Dig.*, 9 (1980) 651.
3 Ph. Morin, M. Caude, H. Richard and R. Rosset, *J. Chromatogr.*, 363 (1986) 57.
4 K. Grob, Jr., D. Fröhlich, B. Schilling, H. P. Neukom and P. Nägeli, *J. Chromatogr.*, 295 (1984) 55.

Journal of Chromatography, 463 (1989) 229–233
Elsevier Science Publishers B.V., Amsterdam — Printed in The Netherlands

CHROM. 21 092

Note

Spectrometric and thin-layer chromatographic quantification of sulfathiazole residues in honey

JOSEPH SHERMA*, WILLIAM BRETSCHNEIDER, MICHELLE DITTAMO, NICK DiBIASE and DAVID HUH

Department of Chemistry, Lafayette College, Easton, PA 18042 (U.S.A.)

and

DANIEL P. SCHWARTZ

Eastern Regional Research Center, Agricultural Research Service, U.S. Department of Agriculture, Philadelphia, PA 19118 (U.S.A.)

(First received September 5th, 1988; revised manuscript received November 9th, 1988)

Sulfathiazole (ST) is used for the prevention and treatment of the disease known as American foulbrood in honey bees. Although application of ST for this purpose is now regulated by the U.S. Food and Drug Administration, honey sold for human consumption may be contaminated if the product is imported into the U.S.A. or if bees were fed the drug illegally. A variety of methods for the detection and quantification of ST in honey have been reported, including colorimetry based on the Bratton-Marshall reaction[1], thin-layer chromatography (TLC)[2,3], and high-performance liquid chromatography (HPLC)[4,5]. In this paper, a previously described screening procedure[6] for residues of ST in honey, involving isolation of the drug on tandem alumina and anion-exchange columns and detection with Bratton-Marshall diazotization-coupling reagents, has been extended to provide quantification of ST by colorimetry at the 1-ppm level and by quantitative silica gel TLC in the concentration range 0.1–1 ppm.

EXPERIMENTAL

Stock solutions of ST and sulfaquinoxaline (SQO) (Sigma, St. Louis, MO, U.S.A.) (10.0 mg/ml) were prepared in 2 *M* hydrochloric acid, and dilutions of these solutions were made to prepare TLC standards containing 50, 100, 200, 400, 800 and 1200 ng ST/10 μl, each also containing 1000 ng SQO/10 μl. Spiking solutions of ST were prepared at 100–5000 ng/ml. A methanol solution containing 10 μg/ml of SQO internal standard was also prepared.

Bio-Rad (Richmond, CA, U.S.A.) AG MP-1 anion-exchange resin was prepared and converted to the bisulfate form as described earlier[6]. The upper column was composed of a glass chromatography tube, 13 cm × 1.5 cm, plugged loosely with glas wool, dry-packed with 7.5 g of neutral alumina (Alfa Products, Danvers, MA, U.S.A.), and topped with 1 cm of fine sand. The bottom column was prepared in a Fisher "large volume" pasteur pipet (No. 13-678-8). A 4-mm glass bead was dropped

0021-9673/89/$03.50

into the pipet, followed by a 5-mm layer of sand, 2 ml of well-stirred 0.2 g/ml resin slurry, and 5 mm of sand on top. A plastic funnel was attached via Tygon tubing to the top of the lower column to accept without loss the effluent from the upper column.

For colorimetry, honey (5.0 g) was weighed into a 100-ml beaker and dissolved in about 50 ml of distilled water. The solution was poured into the alumina column and the beaker rinsed several times with water. After the solution had percolated through both columns, the upper tube walls were washed down several times with water. After draining, the upper tube was removed, and the lower tube walls were washed down several times with water. After draining, the lower column was dried by drawing vacuum. A volume of 1 ml of 5% aqueous acetic acid was added to the lower column, and after draining, ST was eluted with 5 ml of 3.5 *M* hydrochloric acid collected in a 10-ml volumetric flask. One drop each of sodium nitrite, ammonium sulfamate, and N-1-(naphthyl)ethylenediamine dihydrochloride (NED) (Eastman-Kodak, Rochester, NY, U.S.A.) reagents, prepared as previously described[6], were added in order at 1-min intervals, with 10 s shaking after each addition. The solution was diluted to the line with distilled water. After standing in the dark for 15 min, absorbance was measured with a Varian DMS 90 spectrometer at 540 nm, the wavelength of maximum absorbance, and at 490 and 590 nm to correct for background absorbance.

For TLC, the same procedure was employed with the following changes: (i) 1 g of honey was weighed into a 50-ml beaker and dissolved in 25 ml of water; (ii) ST was eluted from the ion-exchange column with 5 ml of 4% trifluoroacetic acid in 95% ethanol collected in a tapered 5-ml silanized glass centrifuge tube. SQO internal standard solution (100 μl; 1 μg) was added, the tube was placed in a 60°C water bath, and the solution was evaporated just to dryness with a stream of nitrogen. The residue was reconstituted with about 75 μl of 2 *M* hydrochloric acid with 15 s of vortex mixing. The entire solution was spotted on the plate in small portions, with drying between applications.

TLC was performed on Whatman (Clifton, NJ, U.S.A.) LHPKD channeled, preadsorbent high-perfo mance silica gel plates. Samples and standards were applied by streaking onto the preadsorbent area with a Drummond microdispenser, and the layer was developed with 2-propanol–conc. ammonium hydroxide (8:2, v/v) in a paper-lined glass tank. The dried chromatogram was sprayed with 1% sodium nitrite in 1 *M* hydrochloric acid, air dried, sprayed with 0.8% aqueous ammonium sulfamate, air dried again, and sprayed with 0.3% NED in 1 *M* hydrochloric acid. The sodium nitrite solution was removed from a refrigerator just before spraying. The first two sprays were applied uniformly until the layer just began to become dark from excess moisture; the NED was sprayed only until the red/purple zones no longer became darker. ST and SQO zones were scanned in the transmission mode with either a Kontes Model K-49500 or Model 800 fiber optics densitometer. The K-49500 was equipped with a baseline corrector and strip chart recorder, and the 5-mm light beam and "longwave UV" source were used. The Model 800 was interfaced with an HP 3390A integrator/recorder, and the 8-mm light beam and white phosphor source (440 nm peak emission) were used. Densitometry attenuation was set to give *ca.* 80% full scale deflection for the internal standard peak on each chromatogram. Calibration curves were plots of ST/SQO peak area ratios *vs.* nanograms of ST spotted. Standard curve slope and intercept data were used to calculate the level of ST in spiked and incurred samples from ST/SQO area ratios.

Recovery studies were done using a variety of honey samples that differed in color and viscosity. Samples were spiked at 1.00 ppm (5 μg ST/5 g honey) for colorimetry. For TLC, honey that was prescreened[6] and found to contain <25 μg/kg of ST was used, and appropriate volumes of the spiking solutions were added to honey to prepare samples fortified at 0.1, 0.5 and 1 ppm (0.1–1 μg ST/1 g honey). Recovery for TLC samples was calculated by comparing the theoretical ST amount to the amount calculated from the ST/SQO area ratio of the sample. The recovery by colorimetry for the 1-ppm fortified samples was calculated by dividing the difference between the corrected absorbances of the fortified and unfortified samples by the corrected absorbance of a standard containing the theoretical amount of ST. Corrected absorbance was calculated as the absorbance at 540 nm minus half the sum of the absorbance at 490 nm and 590 nm.

RESULTS AND DISCUSSION

Colorimetry

Table I shows recovery and precision data for the 1-ppm fortified samples analyzed by the colorimetric method. The table shows that the minimum recovery was about 76% for the different types of honeys tested. The average value and standard deviation for the five analyses of the palmetto honey was 0.875 ± 0.015 ppm. No more than three separate analyses were performed for any of the other samples. It was reported earlier[6] that spike levels as low as 0.5 ppm could be determined accurately by colorimetry using a smaller alumina and ion-exchange column and volumetric flask. Concentrations below 1 ppm were not analyzed in the present study.

TABLE I

RECOVERY OF SULFATHIAZOLE FROM HONEY SAMPLES FORTIFIED AT 1 ppm USING COLORIMETRIC DETERMINATION

Honey samples were provided by L. W. Doner, U.S. Department of Agriculture, Eastern Regional Research Center, Philadelphia, PA. U.S.A.

Honey	*Recovery (ppm)*	*Honey*	*Recovery (ppm)*
Light color		*Dark color*	
Alfalfa-clover	0.881	Gallberry	0.758
	0.884		0.914
Clover	0.890		0.854
	0.847	Canada	0.775
Medium color			0.831
Island blend	0.798	Avocado	0.843
	0.788		0.872
Alfalfa	0.881	Soybean	0.853
	0.814		0.850
Goldenrod-clover	0.984	Palmetto	0.888
Cotton sage	0.923		0.856
	0.923		0.875
	0.931		0.891
			0.864

TLC

Development with 2-propanol–conc. ammonium hydroxide (8:2, v/v) separated SQO and ST with respective R_F values of 0.70 and 0.60. Drugs were detected as flat red-purple bands spread across the layer channels. Old sodium nitrite and ammonium sulfamate spray solutions resulted in faint zones and non-white backgrounds, respectively. NED purchased from Eastman-Kodak gave the best detection when compared with reagent purchased from other companies. The minimum level for precise scanning was 20 ng of ST, although about 5–10 ng could be detected visually. The calibration curve was linear (correlation coefficient value > 0.990) for the 50–1200 ng range of ST used in this study.

Table II shows recovery and precision data for the analysis of fortified honey samples that were produced and purchased locally. Duplicate samples were analyzed in each case except for the 0.50-ppm alfalfa honey spike, for which five samples were run. The mean for the five replicates was 0.424 ppm sulfathiazole with a standard deviation of 0.026 ppm. Percent recoveries ranged from 96 to 76%, with an overall average recovery of 85.6%. A blank sample was chromatographed with each series of honey spikes, and no ST was detected (Fig. 1).

SQO was chosen as the internal standard because it can be separated on the TLC plate from ST, and it can be assumed that any loss in the blow down, reconstitution, and spotting steps will be similar for the two drugs. The sensitivity of detection

TABLE II

RECOVERY OF SULFATHIAZOLE FROM FORTIFIED HONEY SAMPLES USING QUANTITATIVE TLC DETERMINATION

Honey	*Amount added (ppm)*	*Amount found (ppm)*
Orange blossom (light color)	1.0	0.922
		0.901
	0.50	0.444
		0.454
	0.10	0.086
		0.080
Clover (medium color)	1.0	0.979
		0.901
	0.50	0.431
		0.462
		0.407
		0.428
		0.394
	0.10	0.080
		0.111
Buckwheat (dark, viscous)	1.0	0.933
		0.884
	0.50	0.409
		0.384
	0.10	0.083
		0.077

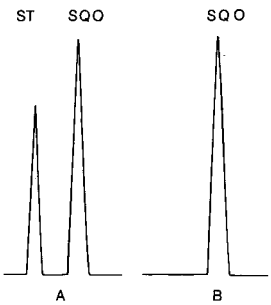

Fig. 1. Recorder tracings of TLC plate scans of (A) clover honey spiked with ST (R_F 0.60) at 0.5 ppm and (B) unfortified clover honey. SQO (R_F 0.70) internal standard was added to the column effluent before spotting. The peaks represent theoretical values of 500 ng for ST and 1000 ng for SQO. A Kontes K-49500 scanner with baseline corrector was used for measurement.

of SQO was about 30% lower than ST using the Bratton-Marshall reagent, based on relative scan areas of chromatograms containing equal weights of the two drugs.

An earlier quantitative TLC screening procedure for ST in honey was reported[3]. This method involved recovery of ST and added SQO by solvent extraction, followed by silica gel TLC, detection with fluorescamine, and scanning of induced fluorescence. A standard curve was prepared by spiking blank honey with ST and SQO and processing the standards the same way as samples. Spiked samples used for recovery studies were essentially identical to the spiked standards used to prepare the standard curve. The method described in this paper utilizes the Bratton-Marshall reagent, which is more selective for detection of ST and SQO than fluorescamine. In addition, the ion-exchange column was shown[6] to have specificity for only ST, SQO and sulfadimethoxine. Direct standards are employed rather than spiked standards, so that a blank honey is not required for each separate analysis, and a 1-g rather than 5-g honey sample is used. Internal standard was not added to the honey sample before being passed through the columns because exactly equal recoveries of ST and SQO could not be confirmed, and we did not want to have to process standards through the columns. The absolute recovery of ST was sufficiently adequate to preclude the need for addition of internal standard to the honey samples.

One dark and one light honey that tested positive during the earlier screening[6] of 110 samples were assayed for incurred residues by the TLC method. Duplicate analyses resulted in values of 0.515 ppm for the dark honey and 0.288 ppm for the light honey. These values were similar to the levels that could be visually estimated by the screening procedure with the use of permanent, artificial color standards[6].

REFERENCES

1 S. Bregha-Morris, *Laboratory Bulletin No. 165*, Health Protection Branch, Agriculture Canada, Scarborough, 1979.
2 A. Grandi, *Apidologie*, 6 (1975) 91.
3 E. Neidert, Z. Barniak and A. Sauve, *J. Assoc. Off. Anal. Chem.*, 69 (1986) 641.
4 F. Belliardo, *J. Apic. Res.*, 20 (1981) 44.
5 C. P. Barry and G. M. MacEachern, *J. Assoc. Off. Anal. Chem.*, 66 (1983) 4.
6 D. P. Schwartz and J. Sherma, *J. Assoc. Off. Anal. Chem.*, 69 (1986) 72.

PUBLICATION SCHEDULE FOR 1989

Journal of Chromatography and Journal of Chromatography, Biomedical Applications

MONTH	J	F	M	
Journal of Chromatography	461 462 463/1	463/2 464/1	The publication schedule for further issues will be published later	
Bibliography Section		486/1		
Biomedical Applications	487/1	487/2	488/1 488/2	

INFORMATION FOR AUTHORS

(Detailed *Instructions to Authors* were published in Vol. 445, pp. 453–456. A free reprint can be obtained by application to the publisher, Elsevier Science Publishers B.V., P.O. Box 330, 1000 AH Amsterdam, The Netherlands.)

Types of Contributions. The following types of papers are published in the *Journal of Chromatography* and the section on *Biomedical Applications:* Regular research papers (Full-length papers), Notes, Review articles and Letters to the Editor. Notes are usually descriptions of short investigations and reflect the same quality of research as Full-length papers, but should preferably not exceed six printed pages. Letters to the Editor can comment on (parts of) previously published articles, or they can report minor technical improvements of previously published procedures; they should preferably not exceed two printed pages. For review articles, see inside front cover under Submission of Papers.

Submission. Every paper must be accompanied by a letter from the senior author, stating that he is submitting the paper for publication in the *Journal of Chromatography*. Please do not send a letter signed by the director of the institute or the professor unless he is one of the authors.

Manuscripts. Manuscripts should be typed in double spacing on consecutively numbered pages of uniform size. The manuscript should be preceded by a sheet of manuscript paper carrying the title of the paper and the name and full postal address of the person to whom the proofs are to be sent. Authors of papers in French or German are requested to supply an English translation of the title of the paper. As a rule, papers should be divided into sections, headed by a caption (*e.g.*, Summary, Introduction, Experimental, Results, Discussion, etc.). All illustrations, photographs, tables, etc., should be on separate sheets.

Introduction. Every paper must have a concise introduction mentioning what has been done before on the topic described, and stating clearly what is new in the paper now submitted.

Summary. Full-length papers and Review articles should have a summary of 50–100 words which clearly and briefly indicates what is new, different and significant. In the case of French or German articles an additional summary in English, headed by an English translation of the title, should also be provided. (Notes and Letters to the Editor are published without a summary.)

Illustrations. The figures should be submitted in a form suitable for reproduction, drawn in Indian ink on drawing or tracing paper. Each illustration should have a legend, all the *legends* being typed (with double spacing) together on a *separate sheet.* If structures are given in the text, the original drawings should be supplied. Coloured illustrations are reproduced at the author's expense, the cost being determined by the number of pages and by the number of colours needed. The written permission of the author and publisher must be obtained for the use of any figure already published. Its source must be indicated in the legend.

References. References should be numbered in the order in which they are cited in the text, and listed in numerical sequence on a separate sheet at the end of the article. Please check a recent issue for the layout of the reference list. Abbreviations for the titles of journals should follow the system used by *Chemical Abstracts.* Articles not yet published should be given as "in press" (journal should be specified), "submitted for publication" (journal should be specified), "in preparation" or "personal communication".

Dispatch. Before sending the manuscript to the Editor please check that the envelope contains three copies of the paper complete with references, legends and figures. One of the sets of figures must be the originals suitable for direct reproduction. Please also ensure that permission to publish has been obtained from your institute.

Proofs. One set of proofs will be sent to the author to be carefully checked for printer's errors. Corrections must be restricted to instances in which the proof is at variance with the manuscript. "Extra corrections" will be inserted at the author's expense.

Reprints. Fifty reprints of Full-length papers, Notes and Letters to the Editor will be supplied free of charge. Additional reprints can be ordered by the authors. An order form containing price quotations will be sent to the authors together with the proofs of their article.

Advertisements. Advertisement rates are available from the publisher on request. The Editors of the journal accept no responsibility for the contents of the advertisements.

Quantitative Gas Chromatography for Laboratory Analyses and On-line Process Control

by G. GUIOCHON and C.L. GUILLEMIN

(Journal of Chromatography Library, 42)

This is a book which no chemical analyst should be without!

It explains how quantitative gas chromatography can - or should - be used for accurate and precise analysis. All the problems involved in the achievement of quantitative analysis by GC are covered, whether in the research lab, the routine analysis lab or in process control.

The discussion of the theoretical background is restricted to essentials. It is presented in a way that is simple enough to be understood by all analytical chemists, while being complete and up-to-date.

Extensive and detailed descriptions are given of the various steps involved in the derivation of precise and accurate data. This starts with the selection of the instrumentation and column, continues with the choice of optimum experimental conditions, then calibration and ends with the use of correct procedures for data acquisition and calculations.

Finally, there is almost always a way to reduce errors and an entire chapter deals with this single issue. Numerous examples are provided.

A lexicon explaining the most important chromatographic terms and a detailed index complete the book.

This is a book which should be on the library shelf of all universities, instrument companies and any laboratory and plant where gas chromatography is used.

1988 780 pages
US$ 165.75 / Dfl. 315.00
ISBN 0-444-42857-7

A brochure describing the contents of this book in detail is available on request from the publisher

Elsevier Science Publishers

P.O. Box 211, 1000 AE Amsterdam, The Netherlands
P.O. Box 1663, Grand Central Station, New York, NY 10163, USA